Storm Surge Barrier Eastern Scheldt

Evaluation of water movement studies for design and construction of the barrier

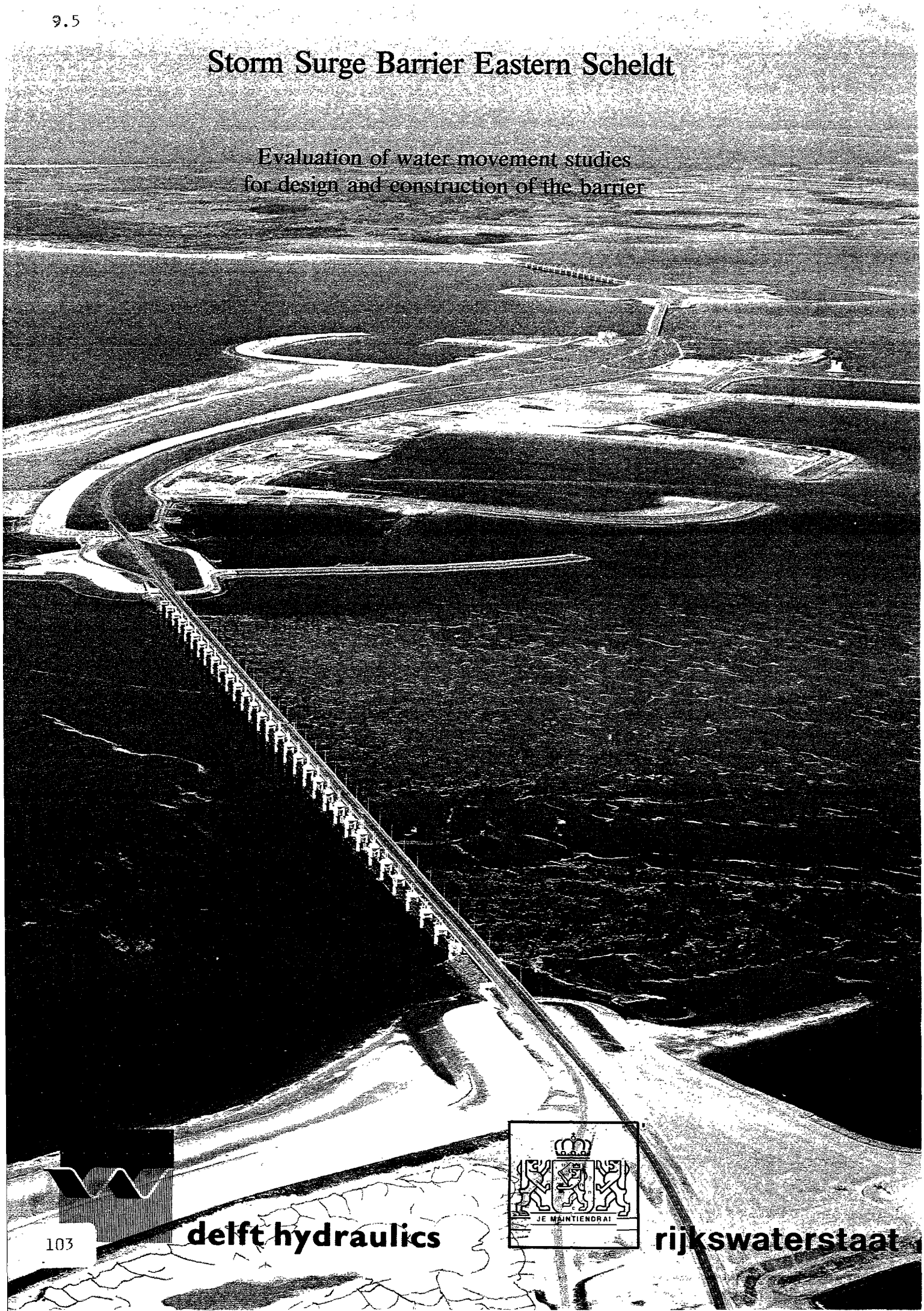

delft hydraulics

JE MAINTIENDRAI

rijkswaterstaat

Storm Surge Barrier Eastern Scheldt

Evaluation of water movement studies for design and construction of the barrier

July 1989

WL - code : Z 88
RWS - code : PEGESS-N-89011

CONTENTS

CONTENTS (continued)

CONTENTS (continued)

CONTENTS (continued)

List of Figures

List of Figures (continued)

List of Figures (continued)

Chapter 6

Chapter 7

List of Figures (continued)

Chapter 8

1. Introduction

1.1 Aim and scope of the evaluation study

The construction of the storm-surge barrier in the mouth of the Eastern Scheldt estuary completed the Dutch Delta works. These works were commenced after the flood disaster of February 1953, to provide reliable protection to the lowland delta area in the south-west of the country.
The Eastern Scheldt project is not only the final part of the Delta Works, it is also by far the largest and most spectacular achievement. In the initial plans, the mouth of the Eastern Scheldt was to be closed by a massive dam. In 1976, after considerations on environnemental aspects, the Dutch Government decided not to construct a massive dam but a hydraulic structure. The barrier will not interrupt the tidal movements in the estuary under normal circumstances, but will be closed in the event of severe storm floods. It took a little over ten years to realize this in many aspects unique structure. On October 4th, 1986, Her Majesty the Queen of the Netherlands inaugurated the Eastern Scheldt storm-surge barrier.

During these years, extensive hydraulic studies were carried out for the design and construction of all stages of the structure. The studies related to the water movement formed a substantial part of these hydraulics studies.
The study and also the design and the construction period, more or less coincided with the rapid development of the numerical flow models. These models became an indispensable tool in hydraulic studies in general, and hydrodynamic modelling in particular. This was strikingly illustrated by the use of water movement models during the study period. In the beginning, almost all investigations were performed in hydraulic scale models, while at the end of the study period most investigations were carried out by means of numerical models.

Hydraulic scale models and numerical models, both overall as well as detail-models, were constructed for the Eastern Scheldt estuary and also for the storm-surge barrier and surroundings (during various stages of construction). Most types of investigations were performed in more than one model. On the other hand several extensive field campaigns were carried out during the construction period of the barrier. The data were regularly used to re-verify the various models .
In this way, valuable sets of data, both from prototype and from the various models became available. Together with the experience, obtained from the

simultaneous operation of the different models, a unique opportunity was created for a comprehensive quantitative evaluation of water-movement models and their performance, related to specific types of investigations.

The water-movement studies were planned, conducted and evaluated in close collaboration between RIJKSWATERSTAAT (the Dutch Public Works Department) and DELFT HYDRAULICS.
All hydraulic scale model tests were performed by DELFT HYDRAULICS. As regards the numerical models, RIJKSWATERSTAAT conducted the one-dimensional overall model studies. Both partners, either separately or jointly, performed studies on both two-dimensional overall models and two-dimensional detail models. Similarly, the forecast system, using the input of not only results obtained from numerical models but also from scale models, was set up jointly. Therefore, both the evaluation study and the reporting, are joint efforts as well.

The main objectives of this evaluation study are:

1. To record and to report on the methodologies that were followed and the various types of models used: to account for experience, obtained from their application, performance and specific merits.
2. To set up an umbrella report, providing information on the main outlines and setup of the water movement studies, as well as their most important results and findings. In this way, the report serves as an entry and directory to the numerous (detail) study reports, produced during the 10-year study period. The report will be particularly important for the coming decades and for those who were not directly involved in the studies.
3. Another important purpose of the report is to provide a reliable inventory of the various types of models and their merits and shortcomings. Such a document will form a valuable basis for the near future to determine and to plan relevant (basic) research topics in this field.

Almost all the study reports have been written in Dutch. In order to make the experience and know-how, obtained from the water-movement studies for the Eastern Scheldt barrier available to fellow researchers abroad, it was decided to write this report in English. The authors are: Mr. J.C.M. Dijkzeul, Mr. H.E. Klatter of the Public Works Department, Mr. G. Hartsuiker and Mr. R.A.H. Thabet of DELFT HYDRAULICS.

Mr. H.N.C. Breusers, Dr. P. Kolkman and Dr. G.K. Verboom, all staff members of DELFT HYDRAULICS, have reviewed the report and provided many valuable suggestions, for which the authors wish to express their gratitude.

1.2 Setup of the report

For the reader who is not acquainted with the Eastern Scheldt Estuary or the Dutch Delta Plan in general and the storm-surge barrier in particular, a brief summary of these subjects is given in Chapter 2. The chapter includes some useful facts, dates and figures. In addition, the design concept and the method of the construction of the barrier are translated in a brief summary of (water movement) study requirements.

Chapter 3 begins with a brief introduction on tidal motion and long waves, followed by a short description of the various water-movement models, as applied in the period during which the studies were performed. Both types, i.e. hydraulic scale models and numerical models, as well as their manner of operation, are described. In addition, the forecast system for flow parameters used during various executional operations in the field, is briefly introduced.

In view of its important effects on tidal movements and the similarity of its applications in the various types of (numerical and scale) models, a separate chapter (4) is devoted to the simulation of the hydraulic characteristics of the barrier. Here the most important parameter is the discharge coefficient.

Chapter 5, 6 and 7 provide more detailed descriptions of the various models. Chapter 5 deals with hydraulic scale models, Chapter 6 with one-dimensional numerical models and Chapter 7 with two-dimensional models.
Except for the description of each model and its "construction" and operation, aspects like boundary conditions, calibration and verification are treated per model. Accuracy analyses and assessments are included. In these chapters only verification as a complementary activity next to calibration, is considered. Later verifications, carried out during the construction period of the barrier, are treated in Chapter 8. The verifications, in reality re-verifications, are treated in more detail in Chapter 8. They form the backbone of this report. The results are used to provide findings, conclusions and recommendations on the performance of the various models, their merits and shortcomings in general as well as for specific studies.
Finally, in Chapter 9 summaries and conclusions for each topic are given.

It is not required to read all chapters, or to go through the chapters in strict sequence because those readers, who are interested in the performance of the various model types and their capabilities, can suffice with reading Chapters 3, 8 and 9. The reader interested in the capabilities and performance of a certain type of model is advised to go trough Chapters 3, (5, 6 or 7) and 8. The reader who is mainly interested in the modelling of the flow characteristics of hydraulic structures, should read Chapters 4 and 8.
The reader whose time is limited, is advised to read, by way of "executive summary", either Chapters 3 and 9, or Chapter 3 and Section 1.3.

1.3 Main conclusions

1. Overall tidal scale models can be safely substituted by numerical models, either one- or two-dimensional (vertically averaged), depending on the geometry of the estuary and type and extent of results that are needed.
   When a two-dimensional flow simulation is sufficient it appears that a two-dimensional numerical model like WAQUA is as accurate as a detail scale model.

   A detail scale model is strictly needed only if three-dimensional phenomena play a significant role. For large structures, such as the storm-surge barrier, a combination of a scale model and a numerical two-dimensional model will provide an optimal study tool.

2. For the hydraulic studies of the Eastern Scheldt storm-surge barrier mainly three different combinations of models were used:
   - A combination of scale models; an overall tidal model at distorted scales and a detail model of the mouth of the estuary.
   - A set of two-dimensional depth-averaged numerical models; an overall coarse grid model and several nested detail models.
   - A one-dimensional numerical model with an additional "resistance model" to compute the lateral discharge distribution along the barrier axis.

   Scale models and two-dimensional numerical models were used for detailed design purposes. The one-dimensional model was mainly used for operational forecasts.

   The choice of above-mentioned combinations of models reflected the evolution of hydraulic study techniques during the time that the studies of the Eastern Scheldt storm-surge barrier were carried out.

3. To ensure optimal use of hydraulic research results for design and operational purposes, a careful selection of "governing" hydraulic parameters is very important. For the storm-surge barrier the following governing parameters were used:
   - discharge per main channel, Q.
   - averaged velocity per opening at the axis of the barrier, q/A.
   - head difference across the barrier, Δh.

   All the models that were used, either scale models, two-dimensional or one-dimensional numerical models, reproduced these parameters with more or less the same accuracy. The type of model that was chosen depended on the required application.
   - When only the basic parameters, Q, q/A, Δh and water levels are required, a one-dimensional model (together with the additional resistance model) is sufficient; providing that the discharge coefficients are known from scale models or two-dimensional numerical models.
   - When, in addition to the basic flow parameters, depth-averaged velocity distributions are of interest, two-dimensional numerical models can substitute scale models.
   - When three-dimensional aspects of the flow or flow-related phenomena such as stability of rubble stone or local scour are to be determined, an undistorted scale model is to be used.

4. The correct reproduction of the hydraulic characteristics of the storm-surge barrier was vitally important for the application of all models, both numerical and scale models. The hydraulic characteristics of the barrier were derived from flume tests. The discharge coefficients from the flume tests could be used directly for the schematization of barrier sections, for the scale models, both distorted and undistorted.

   The hydraulic characteristics of the barrier could be simulated correctly in two-dimensional (depth-averaged) numerical models by using the same discharge coeficients, determined from flume tests. For a correct reproduction of the water movement in the direct vicinity of the barrier, it appeared that the numerical solution at the place of the barrier had to be treated very carefully.

   For use in a one-dimensional numerical model, an overall discharge coefficient for the entire channel was used. This coefficient must be deter-

mined from either a scale model or through a two-dimensional numerical model.

5. The hydraulic studies concerning the storm-surge barrier showed that calibration and verification of the model, merely based on data of the initial situation, is not always sufficient. The behaviour of the model during the construction stages should be investigated as well. The original calibration of the fine-grid two-dimensional model, for example, was not suitable for several construction stages of the barrier.

2. Description of the estuarine system and hydraulic boundary conditions

2.1 Introduction

A large part of the Netherlands lies below mean sea level. It is protected from floods by dikes and dunes. The area that is situated below a storm-surge level of MSL.+5.0 m is indicated in Figure 2.1.

Figure 2.1 The Netherlands, without dikes (area below storm-surge level are shaded)

In times long gone by the protection against storm surges merely consisted of building dikes, but in this century programmes were performed to drastically shorten the coast line. This began in 1932 with the closure of the Zuiderzee. The plans to further shorten the coast line were speeded up, when in 1953 a catastrophic flood disaster struck the south-western part of the Netherlands. As a result of this flood, 1400 km^2 of land were inundated and more than 1800 people lost their lives (see Figure 2.2).

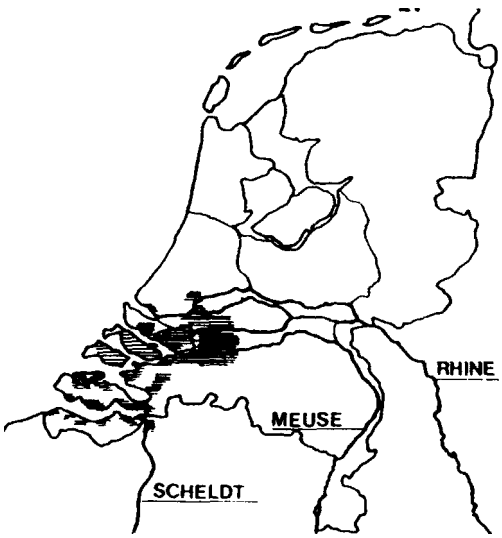

Figure 2.2 The Netherlands, situation flood February 1953 (flooded area shaded)

Immediately after the situation had been restored, the Delta Plan was drawn up to prevent future disasters. According to the plan all estuaries had to be closed, except for the entrances to the harbours of Rotterdam and Antwerp. All planned closures, except the one in the Eastern Scheldt, were performed between 1956 and 1972.

Contrary to the initial plan it was decided in 1976 to build a storm-surge barrier in the mouth of the Eastern Scheldt instead of a closing dam. The reason for this decision was that the Dutch people began to realize that the preservation of the unique environment of the Eastern Scheldt should be considered equally important as the safety requirements. With a barrier, which will be closed only during severe floods, the tidal movements in the estuary will be maintained almost all the time. A barrier solution will both guarantee safety and preserve the environment.

2.2 Eastern Scheldt estuary

The Eastern Scheldt estuary is a part of the Dutch delta. Its shape is caused by interaction of the rivers Rhine, Meuse and Scheldt and the North Sea during the past centuries. Man strongly influenced the development of the delta. During the last decades, the influence of man even dominated the development, by constructing a number of dams as a part of the Delta Plan.

The water motion in the Eastern Scheldt is dominated by tidal flow. The fresh water discharge into the estuary is negligible, since no major river is connected with the Eastern Scheldt estuary. So, strictly speaking, the Eastern Scheldt is rather a tidal basin than an estuary.

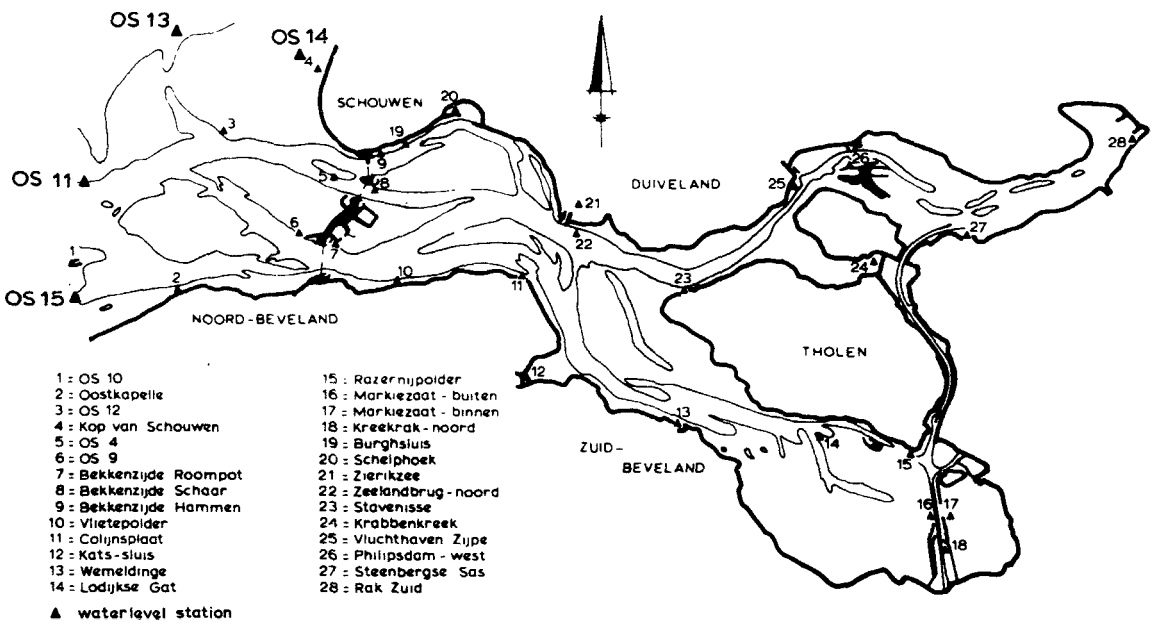

Figure 2.3 The Eastern Scheldt estuary with measuring stations

The Eastern Scheldt basin contains a great number of tidal flats and channels, with a depth of over 50 m locally. Three main channels connect the Eastern Scheldt with the sea: from north to south, the Hammen, the Schaar and the Roompot. The maximum depth of these channels at the location of the barrier is 35 m. The area of tidal flats and channels extends seawards.
The bed of the Eastern Scheldt consists of fine sands (grain size 150 - 200 μm). Since flow velocities of 1.0 to 1.5 m/s occur in the channels (average tide), the sandy bed is highly mobile.

Covering the entire Eastern Scheldt, a large number of permanent measuring stations is installed (Figure 2.3), to record a number of hydraulic parameters. Additional data are obtained during extensive measurement campaigns. The main characteristics of the water motion are given below:

- The tidal flow is dominated by the semi-diurnal component (M2);
- The tidal range varies from 2.3 m at neap tide to 3.1 m at spring tide in the mouth of the Eastern Scheldt;
- The mean tidal range is 2.8 m (Figure 2.4);
- The tidal range increases going east to about 3.5 m at Yerseke, for the situation without the barrier.

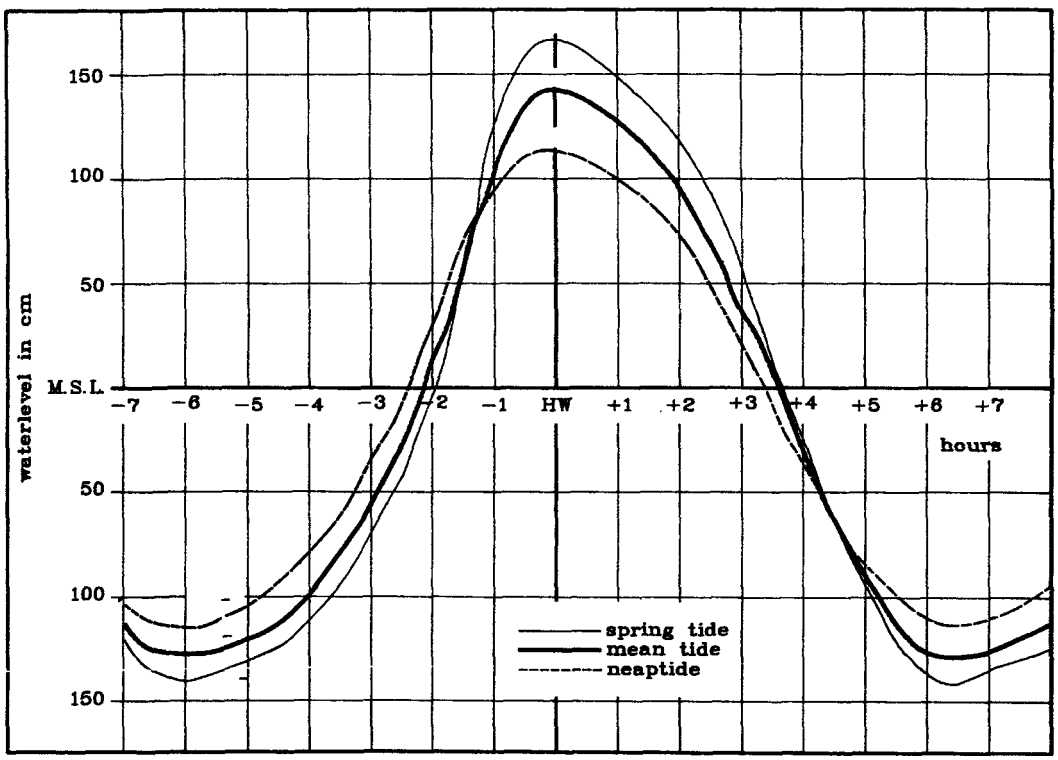

Figure 2.4 Water level curves in the mouth of the Eastern Scheldt (station OS4)

In the final situation a tidal range at Yerseke, of at least 2.7 m under mean tidal conditions, had to be maintained. To achieve this a flow opening of the barrier of 17600 m² (below mean sea level) was chosen in combination with a compartmentalisation of the estuary (Figure 2.5). This compartmentalisation reduces the tidal volume by about 30%. After finishing the construction of the barrier, a final figure based on observations can be given; the mean tidal range at Yerseke is 3.3 m.

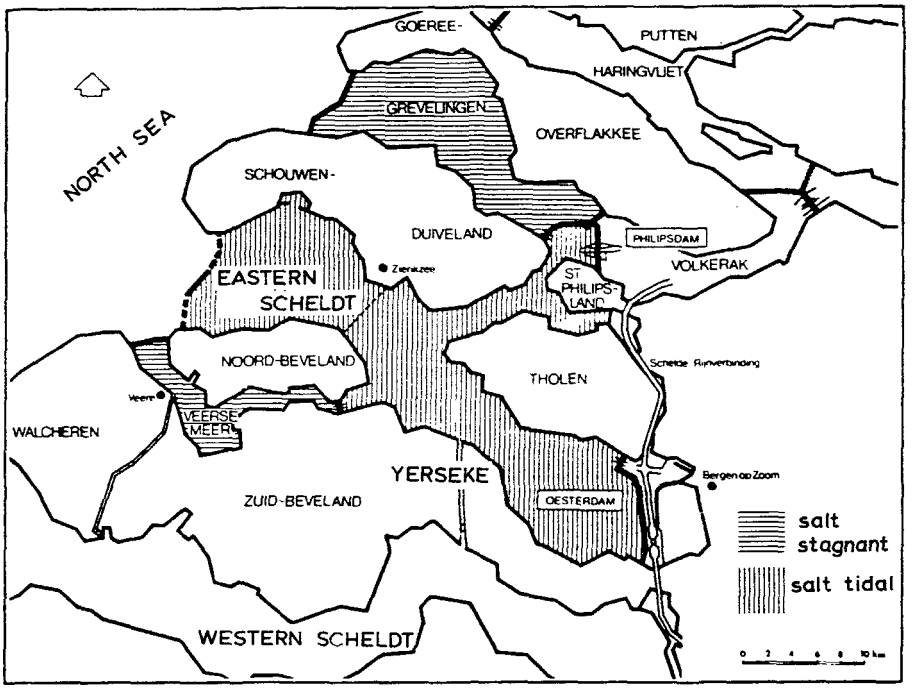

Figure 2.5 The Eastern Scheldt estuary after completion of works

2.3 **Storm-surge barrier**

The storm-surge barrier has been built across the three main tidal channels in the mouth of the Eastern Scheldt (Figure 2.6), from north to south, respectively the Hammen, the Schaar and the Roompot. The three barrier sections are interconnected by dams that have been constructed upon the shallow tidal flats between the main channels. The total length of the barrier and dam sections is about 9 km. The actual length of the barrier is about 3 km.

The construction of the barrier took place in the original channels, without a building pit. This construction method was chosen to minimize the effect of the construction activities on the tidal movements in the Eastern Scheldt. To enable such a construction method, prefabricated elements were used when and where possible.

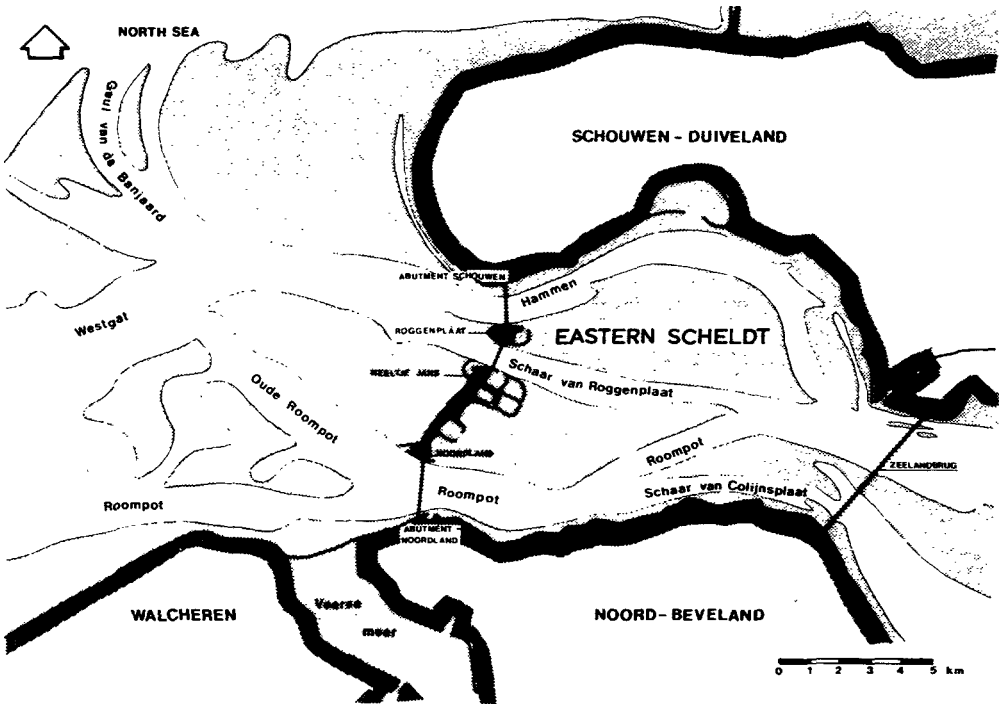

Figure 2.6 Location of the storm-surge barrier in the mouth of the Eastern Scheldt

The original sea bed served as a foundation. Firstly the upper layer was excavated and replaced by a layer of course sand, followed by a deep compaction of the sand bed. This was done by a specially designed compacting barge, the "Mytilus". The sand bed was then covered by large prefabricated foundation mats, 41 m wide and 200 m long. For this the "Cardium" pontoon was used. Upon the mats prefabricated piers were placed by the pier-lifting vessel "Ostrea". These piers were huge monolitic concrete structures, being 20 m wide and 50 m long at the base, with heights up to 40 m. The distance from pier to pier is 45 m. The barrier consists of a total of 62 of these basic sections of 45 m. The piers were packed by a rubble sill, that was built up in layers. The top layer had been designed to resist the extreme velocities that might occur when a gate fails to close. A concrete sill beam and an upper beam frame the actual flow opening, which can be closed by a gate. This gate is operated by hydraulic cilinders which are placed on top of the piers. Finally, a concrete bridge girder was positioned upon the piers. All these elements were placed between, and upon the piers by a large floating crane. Most critical of these operations was the placement of the sill beams, which had to be positioned accurately between the piers, metres below sea level, during a short period around slack water. After the positioning of the sill beams, a rubble side-fill was put in place. This had to be done very carefully, because the concrete beams should not be damaged by the large rubble stones. A specially constructed crane, placed on a pontoon, positioned the rubble stones in small portions.

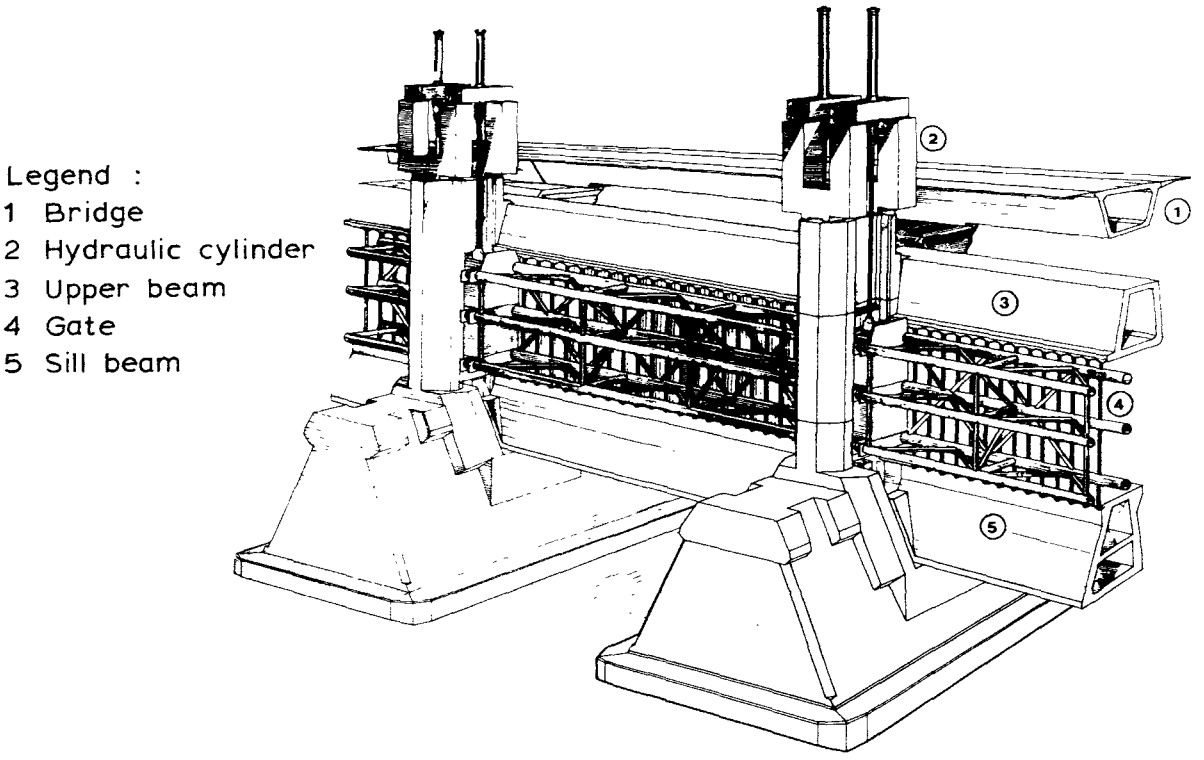

Figure 2.7 Perspective view of the structural elements of the storm-surge barrier (the rubble sill is not shown)

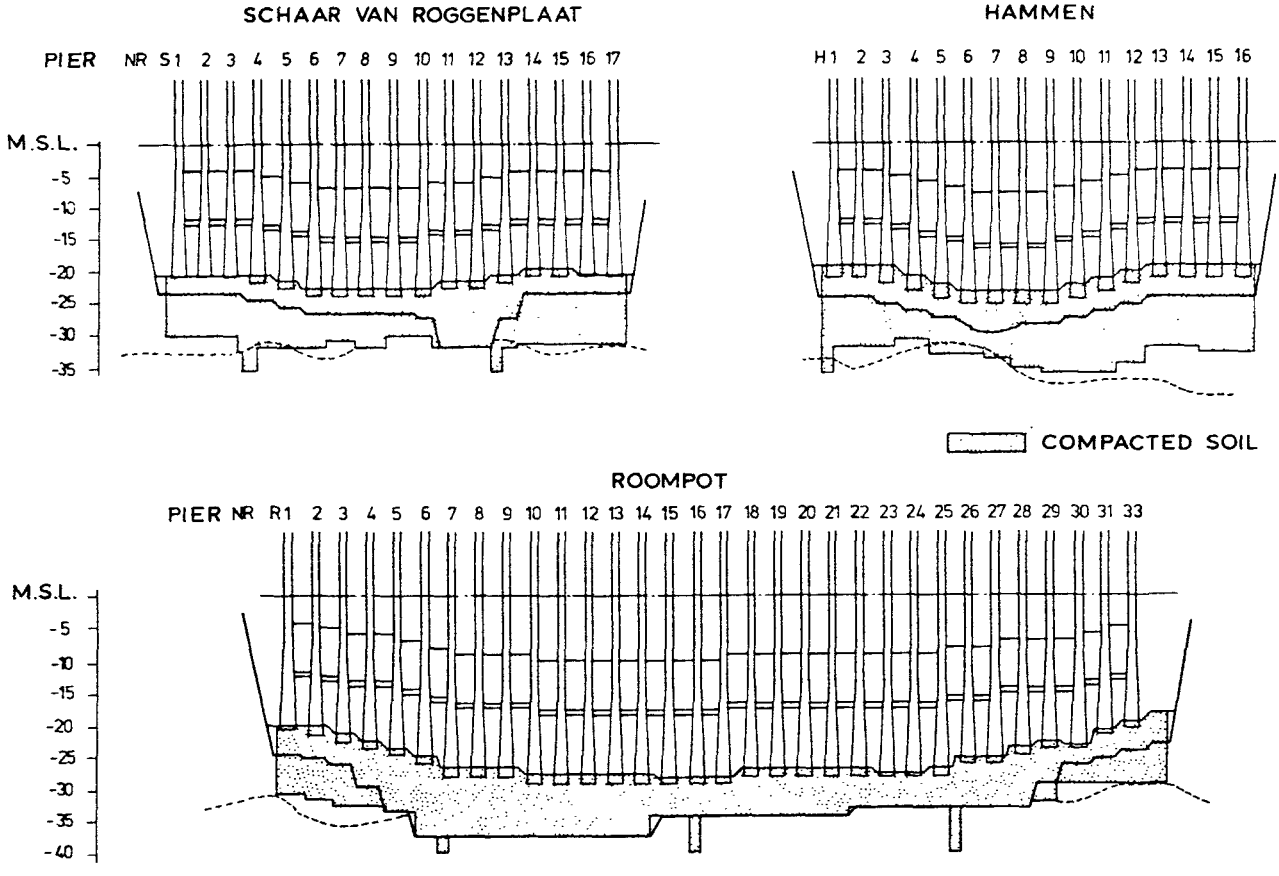

Figure 2.8 Cross-section of the channels at the location of the storm-surge barrier (distorted scale)

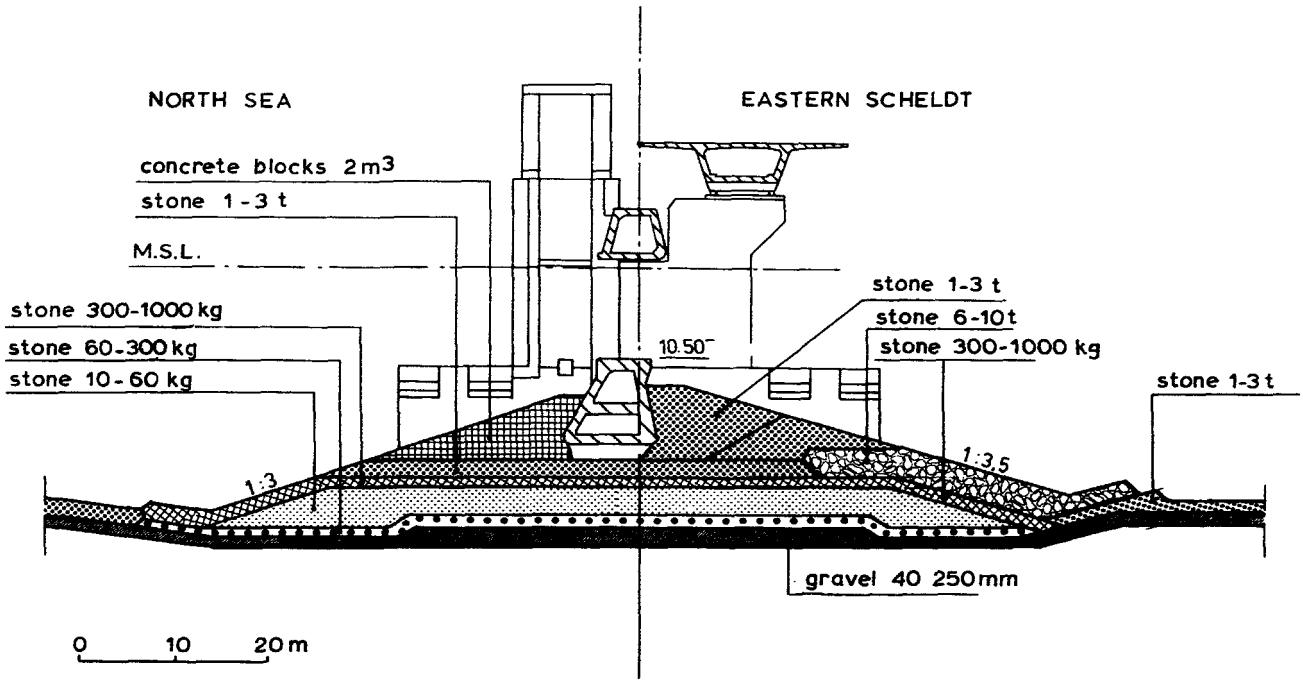

Figure 2.9 Rubble sill construction at pier location Roompot 12

The Figures 2.7 through 2.9 give an impression of the structure and the construction of the barrier (see also [2-1]).

The type of structure as well as the construction method, implied a number of major hydraulic problems that had to be solved:

- At the location of the barrier the flow-velocities increased, caused by the narrowing of the flow opening (up to 5 m/s under normal tidal conditions, with the barrier completed). To prevent scour of the sand directly downstream the barrier, a bed protection was required (Figure 2.10). The required length of the bed protection is governed by the rate of development of the scour holes at the end of the bed protection. Thus an accurate prediction of the scour was needed.
- All operations that were carried out under open sea conditions, positioning of mats, piers, etc, called for an accurate prediction of the hydraulic boundary conditions.
- The stability of the rubble stone structures, both during construction and for the completed barrier, had to be investigated.
- The impact of the construction of the barrier on the morphology and the environment had to be predicted.

Thus a prediction of the hydraulic boundary conditions for these phenomena was essential.

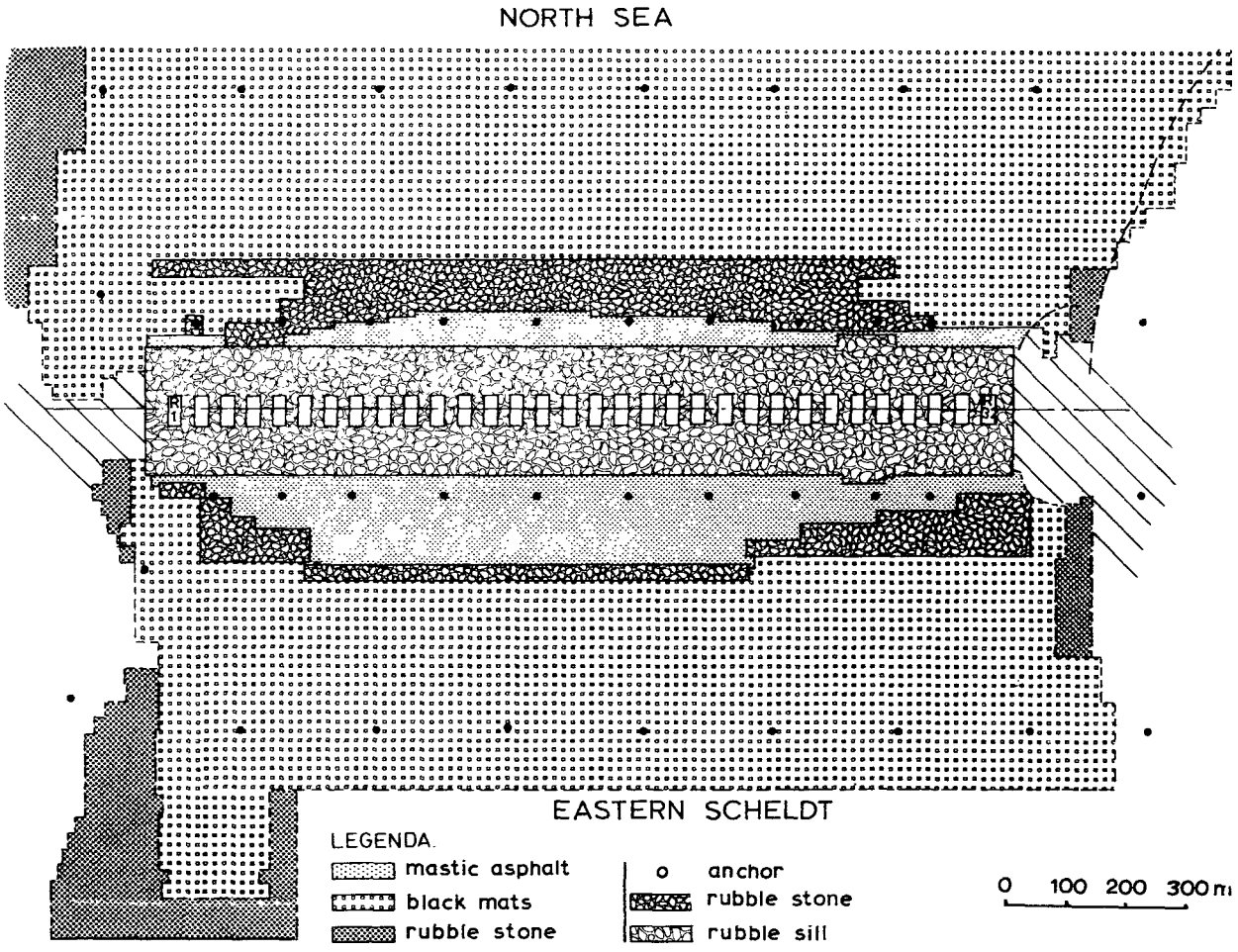

Figure 2.10 Bottom protection in the Roompot channel

2.4 Flow conditions

The complexity of the flow pattern and the numerous possible geometries of the barrier under construction, made a flexible prediction system for the flow conditions necessary. This could be accomplished by choosing a selected number of hydraulic parameters, which:

- govern the processes related to the hydraulic problems
- can be predicted with reasonable accuracy

For the impact of the barrier on the large scale flow, the discharge characteristics of the barrier are the governing parameters. These are expressed by the value of μA, the effective flow opening of the barrier.
The sum of the effective flow openings of the entire barrier determines the magnitude of the tidal range (for example at Yerseke). The distribution of μA over the main channels governes the flow pattern in the mouth of the Eastern Scheldt.

To represent the flow conditions in the vicinity of the barrier the following basic hydraulic parameters were selected:

Q	=	discharge through a main channel	(m^3/s)
Δh	=	head diffence over the barrier	(m)
q/A	=	average velocity at the axis of the barrier, defined as: discharge per barrier section/wet cross section	(m/s)

For example, the hydrodynamic loads on the construction equipment could be related to q/A at the work location.
In Table 2.1 some more examples are given of the flow parameters that were used as "governing parameters" for the hydraulic problems encountered.
With this approach the flow parameters that had to be predicted, depended only on the global geometry of the barrier under construction. Details of the flow pattern were incorporated in the "translation" from basic flow parameter to hydrodynamic loads or stability criteria. Thus changes in the construction order of the barrier did only influence the flow parameters but not the stability relations. On the other hand, changes in details of the design of the barrier did only affect the stability relations.

aspect	hydraulic parameter
environmental aspects	sum of μA of the barrier
morphology at the mouth of the Eastern Scheldt	distribution of μA over main channels
stability of rubble sill: during construction	q/A
at final situation	Δh
hydrodynamic loads on the large structural elements (piers, sill beams, upper beams, gates) during positioning	q/A
stability of bed protection	Δh and barrier geometry
scouring	Q and barrier geometry

Table 2.1 Relation between various aspects and the hydraulic parameters.

The prediction of the flow parameters can be divided in several stages, depending on their application. The following applications will be discussed:

- flow parameters as design parameters
- flow parameters for the planning of the construction activities
- flow parameters for operational control of the construction activities

Design parameters:

For the Eastern Scheldt storm-surge barrier the flow conditions were crucial design parameters. For design purposes the statistics of the flow parameters were needed, mainly of maximum values and extreme values. For example, of Q, Δh and q/A at maximum ebb flow and maximum flood flow.

Planning of construction activities:

For the planning of the construction activities, which took place in open sea, forecasts of time series of the hydraulic parameters were used. These forecasts were based on a forecast of the water motion under astronomical tide conditions.

Operational control of construction activities:

For operational support, short-term forecasts were used. These forecasts were based on both the astronomical tide and the predicted meteorological effects. For the most critical operations like positioning of the mats, piers and sill beams, the predicted hydraulic parameters were recorded on line to verify and if necessary, to correct the forecast on the spot.

In this report the models which were used to obtain the required flow information will be described. The results that were obtained from the application of these models to the storm-surge barrier will be presented, following the approach outlined above.

Reference of Chapter 2

[2-1] Rijkswaterstaat
Design report storm-surge barrier Eastern Scheldt, Part 1, Total design, 1987 (in Dutch)

3. Modelling tidal flow

3.1 Introduction

The hydraulic studies for the initially planned closure of the Eastern Scheldt started already in 1965. The used research methods were based on the experience of preceding investigations on other closure works of the Delta Plan. The research for the design of the closure dam merely consisted of scale model tests. At that time, one-dimensional numerical models were already available, but their operational use was limited. Two-dimensional numerical models were still in the development stage.
In the course of the studies for the storm-surge barrier, numerical flow models developed rapidly. In the beginning of the seventies the first operational one-dimensional numerical model of the Eastern Scheldt became available.
Two-dimensional numerical models were applied for the first time in the studies for the Eastern Scheldt to determine the impact of the planned closure on the water levels in the adjacent part of the North Sea. At that time, these models were not available in the Netherlands; the computations were done at the Rand Corporation, United States of America (see Chapter 7). From the time when two-dimensional models for the Eastern Scheldt became available in the Netherlands, the development progressed rapidly. In 1983, the overall tidal scale model (distorted scale) was dismantled, since it could be replaced by the available numerical models. At that time not a single pier had been placed yet in the Eastern Scheldt.

In this chapter the methods and the models that were used for the hydraulic studies for the Eastern Scheldt storm-surge barrier are described in general. Details will be described in the following chapters.

3.2 Basic equations

The equations on which the simulations are based are the hydrodynamic basic equations for an incompressible fluid with a constant density (Navier-Stokes equations).

For computations of tidal flow, a number of assumptions must be made. The most important is that vertical velocities and vertical accelerations are negligible. The result of this assumption is that the pressure distribution is always hydrostatic.

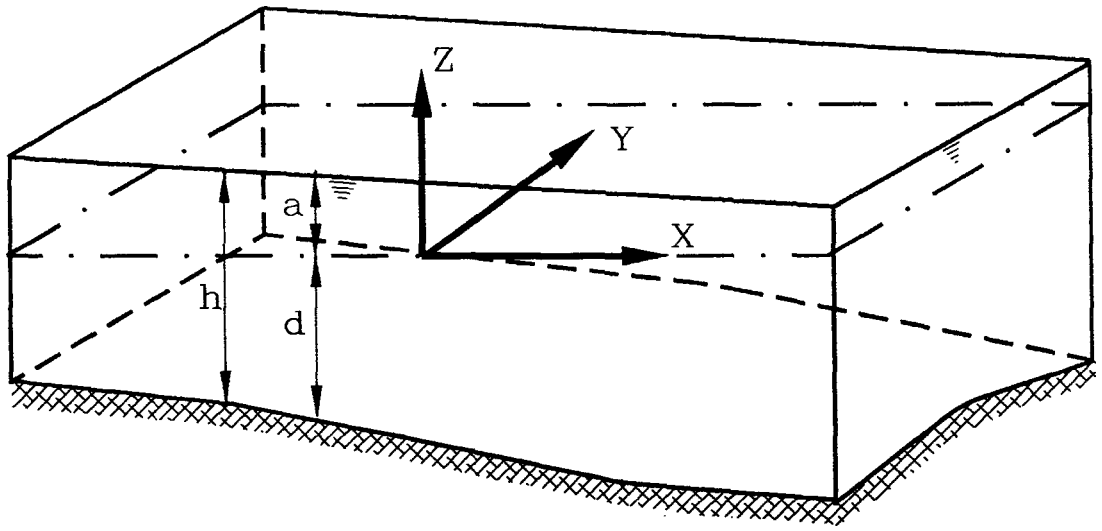

Figure 3.1 Parameters two-dimensional long-wave equations

The assumptions leading to the so-named "long wave" approximation are described in detail in [3-1]. The resulting depth-integrated continuity equation is given by (see also Figure 3.1):

$$\frac{\partial(hU)}{\partial x} + \frac{\partial(hV)}{\partial y} + \frac{\partial h}{\partial t} = 0 \qquad (3.1)$$

The depth integrated momentum equations are given by Equations 3.2 and 3.3:

$$\frac{\partial U}{\partial t} + U\frac{\partial U}{\partial x} + V\frac{\partial U}{\partial y} = fV + \nu_t\left(\frac{\partial^2 U}{\partial x^2} + \frac{\partial^2 U}{\partial y^2}\right) - g\frac{\partial a}{\partial x} - \frac{g\,U\sqrt{U^2+V^2}}{C^2\,h} + \frac{\rho_a C_D\,W^2\cos\phi}{h\,\rho_w} \qquad (3.2)$$

$$\frac{\partial V}{\partial t} + U\frac{\partial V}{\partial x} + V\frac{\partial V}{\partial y} = -fU + \nu_t\left(\frac{\partial^2 V}{\partial x^2} + \frac{\partial^2 V}{\partial y^2}\right) - g\frac{\partial a}{\partial y} - \frac{g\,V\sqrt{U^2+V^2}}{C^2\,h} + \frac{\rho_a C_D\,W^2\sin\phi}{h\,\rho_w} \qquad (3.3)$$

where:

U	= depth-averaged velocity in x direction	(m/s)
V	= depth-averaged velocity in y direction	(m/s)
d	= distance from the bottom to the reference plane	(m)
a	= water elevation relative to the reference plane	(m)
h	= water depth (= d + a)	(m)
ν_t	= eddy-viscosity coefficient for horizontal momentum exchange	(m^2/s)
C	= Chézy coefficient for bottom friction	($m^{\frac{1}{2}}/s$)
f	= Coriolis parameter = $2\omega \sin\psi$	(s^{-1})

ω	= angular speed of rotation of the earth = 0.73 * 10^{-4}	(s^{-1})
ψ	= geographic latitude	(deg.)
g	= acceleration caused by gravity	(m/s^2)
C_D	= coefficient for wind shear stress	(-)
W	= wind speed	(m/s)
ϕ	= angle between wind direction and x direction	(deg.)
ρ_w	= density of water	(kg/m^3)
ρ_a	= density of air	kg/m^3)

Equations 3.1, 3.2 and 3.3 schematize the tidal flow as a two-dimensional depth-averaged flow. A further simplification can be made by integrating the equations not only in vertical direction but also in the horizontal direction perpendicular to the main flow direction. Thus, the one-dimensional long-wave equations 3.4 and 3.5 can be obtained, see [3-2] and Figure 3.2.

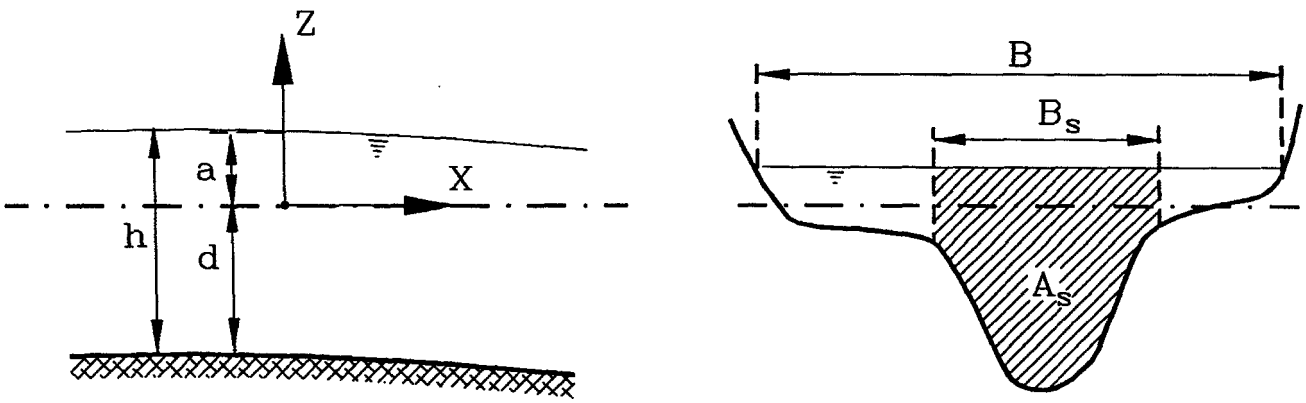

Figure 3.2 Parameters one-dimensional long-wave equations

One-dimensional continuity equation:

$$\frac{\partial A}{\partial t} + \frac{\partial Q}{\partial x} = 0 \qquad (3.4)$$

One-dimensional momentum equation:

$$\frac{\partial Q}{\partial t} + \frac{\partial}{\partial x}\left(\frac{Q^2}{A_s}\right) + gA_s \frac{\partial a}{\partial x} + \frac{gQ|Q|}{C^2 RA_s} - \frac{\rho_a C_D B_s W^2 \cos\phi}{\rho_w h} = 0 \qquad (3.5)$$

where:

Q	= discharge	(m^3/s)
B	= width at the water surface	(m)
B_s	= width of the flow area at the surface	(m)
A	= total area = $\int_{-d}^{z} B\, dz$	(m^2)

A_s = flow area = $\int_{-d}^{z} B_s \, dz$ (m^2)

R = hydraulic radius (m)

remaining parameters like (3.2) and (3.3)

3.3 Tidal models

The simulation techniques that were applied in the storm-surge barrier studies can be divided into three types, following the historical development:

- Hydraulic scale models
- One-dimensional numerical models
- Two-dimensional numerical models

For the simulation of water movements in hydraulic scale models, use is made of the same physical principles as those governing the water movement at full scale in nature. To ensure that the scaled physical phenomena are reproduced correctly by the scale model, the correct application of scale laws is of vital importance. The scale laws are discussed further in Chapter 5.

For the Eastern Scheldt estuary two large scale models were built (see Chapter 5):

- An overall tidal model (DELFT HYDRAULICS project M1000);
  A distorted model, vertical scale 1:100 and horizontal scale 1:400. The model covered the entire estuary of the Eastern Scheldt.
- A detail model of the mouth of the Eastern Scheldt (DELFT HYDRAULICS project M1001):
  An undistorted model, scale 1:80. The model is a steady state model. The boundary conditions were derived from the overall model M1000.

One-dimensional numerical models are based on the numerical solution of the one-dimensional long-wave equations i.e. Equations 3.4 and 3.5. Using such a model (IMPLIC, see Chapter 6), the Eastern Scheldt had to be schematized into a network of tidal channels.
In addition to the one-dimensional model, the so-named "R1495" model was available to compute the lateral distribution of the discharge along the barrier axis.

Two-dimensional numerical models are based on the numerical solution of two-dimensional long-wave equations, i.e. Equations 3.1, 3.2 and 3.3. For solving these equations the WAQUA program system was used. For the Eastern Scheldt several models were used (see Chapter 7, Figure 7.2):

- An overall model, OOST3;
  This model covered the entire Eastern Scheldt with a grid size of 400 m.
- A detail model of the mouth of the Eastern Scheldt, DOOS1;
  The DOOS1 model covered an area 20 km long and 10 km wide with a grid size of 100 m. The boundary conditions for this model were derived from the overall model, OOST3.
- A set of small detail models in the vicinity of the barrier;
  Two 90 m grid size models (MOOS-N AND MOOS-Z), that were nested in the OOST3 model, provided boundary conditions for three 45 m grid size models (HAMMEN, SCHAAR and ROOMPOT). The three 45 m grid size models were rotated in such a way that the barrier was parallel to one of the axes of the model. The grid size of 45 m corresponded to a basic section of the barrier; 45 m is the distance from pier to pier.
- In addition to the WAQUA models for the storm-surge barrier, several WAQUA models were also used for the compartmentalisation works (see Section 2.2). In this report, the models used for the storm-surge barrier only are discussed. The compartmentalisation models are discussed in [3-3].

The type of model to be used depends on several factors.
In general, no single model will solve all problems. If such a model would exist, it would probably not be economical in use. Each type of model therefore will have its own applications. Some general remarks regarding the different types of models will be given hereafter.

Scale models provide the most detailed information. These are the only models that are fully three-dimensional (except the distorted model). Obtaining information by measurements is unfortunately time-consuming and expensive. All data not recorded are lost after the test. An advantage of scale models is the possibility to investigate phenomena like stability of rubble stone, scouring, etc. directly in the model. A major disadvantage is the fixed geometry of the model. Alteration of the bottom geometry and especially of the boundaries of the model are very time-consuming and expensive.

Numerical models (one-dimensional and two-dimensional) provide less details of the flow pattern than scale models. Numerical models compute no more than what they are built for. Additional information on aspects such as stone stability, is not available. The results of all computed data can, however, be stored and hence made available at a later stage.
A great advantage of the numerical models is their flexibility. The bottom geometry and the location and type of the boundaries are much more flexible

than in scale models.
Two-dimensional numerical models give more details than one-dimensional models; the run time of the two-dimensional models is, however, substantially longer than that of a one-dimensional model.

3.4 Input data

For all models discussed above a set of input data is neccessary. These input data consist of:

- Boundary geometry and bottom bathymetry
- Boundary conditions
- Data for calibration and verification.
- Schematization of the barrier

The information required is basically the same for all types of model (scale model, as well as numerical model). The way the data are applied in the model is, however, completely different for each model. Below, the required data will be described briefly. Details will be given in the following chapters.

Boundary geometry and bottom bathymetry

The boundary geometry and bottom bathymetry must be known accurately. Also the roughness of the bottom must be represented correctly in the model. Changes in bottom geometry at the site have to be taken into account in the model. The accuracy of the results of the model tests or of the computations depends directly on the accuracy of the geometry in the model. The schematization of the bottom geometry will be discussed in Chapters 5, 6 and 7 for each model.

Boundary conditions and initial state conditions

To solve tidal problems, boundary conditions are required. These conditions may be either of the water level type, velocity type or discharge type. The boundary conditions can be derived from site measurements, or can be obtained from another (scale or numerical) model. The choice of the boundaries and the boundary conditions is discussed for the models applied in Chapters 5, 6 and 7 Besides the above described conditions, the initial conditions are also necessary for this type of problems. However, after a certain running-in period, the initial state is no longer important. A correct set of initial state conditions can substantially reduce the run-in time of model tests or computations.

Calibration and verification

A thorough calibration and verification of the model must be an essential part

of any research program. For the calibration and verification of tidal models, site measurements are used. For the Eastern Scheldt these measurements comprised observed water levels from the fixed stations (Figure 2.3), velocities and transport rates obtained during measurement campaigns. A special type of verification is the comparison of different models such as scale models and numerical models.

Schematization of the storm-surge barrier

A geometrically complex structure like the storm-surge barrier has to be schematized to a certain extent, if modelled in a tidal model.
For relatively large hydraulic scale models only small-scale details have to be schematized. For distorted scale models and even more for numerical models, a structure must be schematized much more. For the storm-surge barrier, this schematization was based on flume tests. The schematization is further described in Chapter 4.

3.5 Application of tidal models to the Eastern Scheldt

In Chapter 2 the following governing hydraulic parameters for the storm surge barrier were selected:

Q	=	discharge through a main channel	(m^3/s)
Δh	=	head difference over the barrier	(m)
q/A	=	average velocity at the axis of the barrier, defined as: discharge per barrier section / wet cross section	(m/s)

These parameters had to be predicted as design parameters and also for planning and controlling of the construction activities. For these predictions scale models as well as numerical models were available. As for the storm-surge barrier, three different combinations of models were used. These three "main tracks" were:

1) scale models only
2) one-dimensional numerical models with input from scale models
3) two-dimensional numerical models

@1) Scale models (M1000 - M1001; Chapter 5)
This is the classical track, that had been used for the former hydraulic research for the closure works of the Delta Plan. For the Eastern Scheldt the overall tidal model M1000 delivered the overall tidal motion and the boundary conditions for the detail model, M1001. In addition to the flow parameters,

M1001 also provided relations between these flow parameters and scour, stability of rubble stone, etc.

@2) One-dimensional numerical models (IMPLIC - R1495; Chapter 6)
The one-dimensional tidal model IMPLIC computes water levels and discharges. From these data the R1495 model computes q/A along the barrier.
The accuracy of these models, in particular the R1495 model, depends strongly on the input from scale model results (M1000 and M1001). This track can therefore be regarded as a mixed track of numerical models and scale models. Because of the short run time of the one-dimensional models, these models were suitable for the operational forecasts. The forecast system is described in Section 3.6.

@3) Two-dimensional numerical models (Chapter 7)
Two-dimensional models can compute the flow parameters, without input from the scale models M1000 and M1001.

However, for the schematization of the barrier in the two-dimensional numerical models, input from scale model tests was needed. For this, the same flume tests were used, as those used for the schematization of the barrier in M1000 and in M1001.

For the storm-surge barrier the following allocation of duties between the three "model tracks" can be distinguished:

- The IMPLIC-R1495 track was used for operational forecasts and for computation of design flow parameters.

- The M1000-M1001 track was used to determine the discharge characteristics of the barrier for IMPLIC and the two-dimensional models and for the calibration of the R1495 model. Further M1001 provided relations between hydraulic parameters and stability of rubble stone, scour and loads on structural elements and equipment.

- The two-dimensional numerical models were used to check the one-dimensional model, particularly for construction stages of the barrier, when a flow pattern was expected that differed from the pattern for which the model was calibrated. Furthermore, the impact of possible changes in the morphology of the mouth of the Eastern Scheldt could be investigated effectively. The two-dimensional models replaced the scale models M1000-M1001 for several

applications. For design purposes, however, the computations of the flow in the vicinity of the barrier were not performed by the two-dimensional models. At that time these models were not used for these applications as insufficient experience was then available.

3.6 **Setup of the forecast system**

Considering the total number of simulations that were made, most were performed by the models IMPLIC-R1495 to compute the basic hydraulic parameters Δh, Q and q/A. These parameters were used as design parameters and for operational forecasts.
The difference between the computation of design criteria and operational forecasts is the input of the models. Both applications will be described briefly. Figure 3.3 shows a diagram of the forecast system, the input from the scale models and from the two-dimensional numerical models.

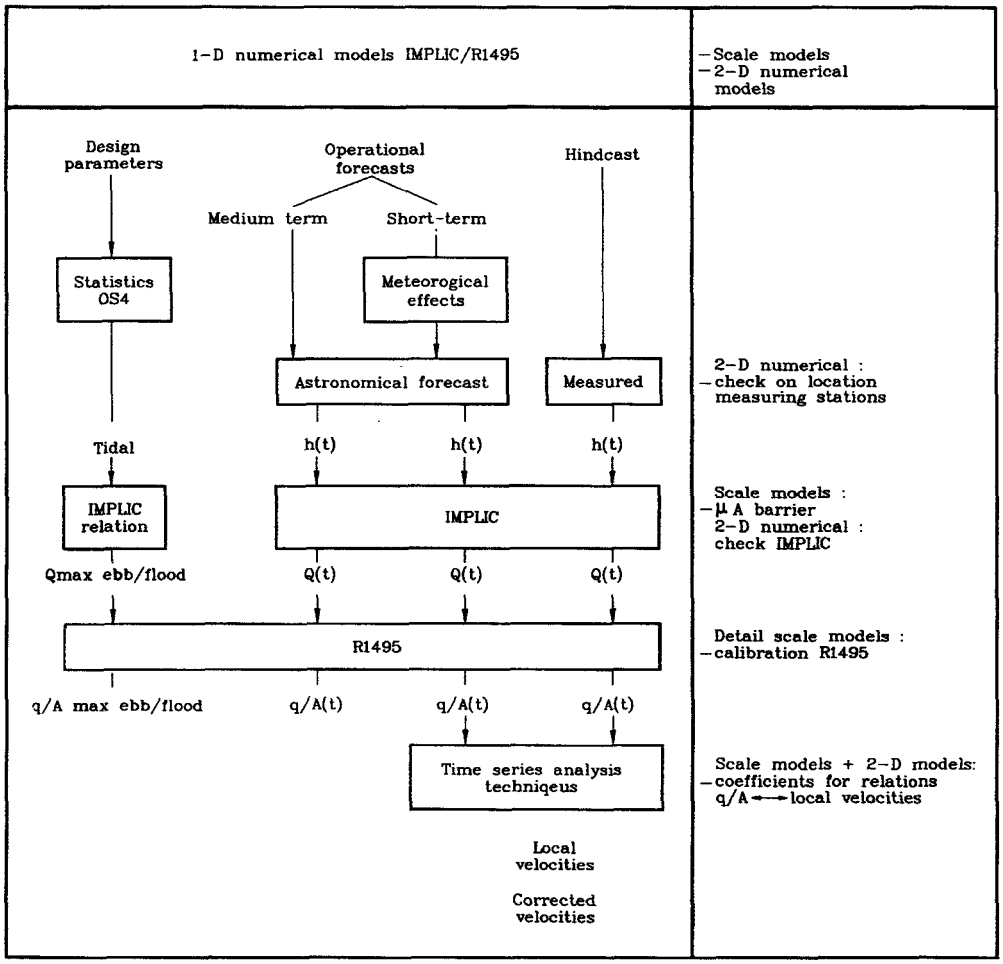

Figure 3.3 Scheme of forecast system

Design parameters:

As design parameters, the statistics of Q, q/A and Δh at maximum ebb flow and maximum flood flow were computed for various construction phases of the barrier. Both for average tidal conditions and for extreme tidal conditions, with one year return period. The computation of these statistics was based on the observed statistics of the tidal motion (without influence of the barrier). For this purpose, station OS4 (see Figure 2.3) was used. The influence of the barrier on this station was acceptably small, and also over 10 years of data collection were available.

The tidal motion was characterized by the tidal range at station OS4. The statistics of the tidal range at OS4 could be transformed into statistics of discharge at maximum ebb/flood flow in the three main channels. This transformation was performed by using a linear relation between maximum discharge and tidal range, computed with the one-dimensional model, IMPLIC. An example of such a computed relation is shown by Figure 3.4.

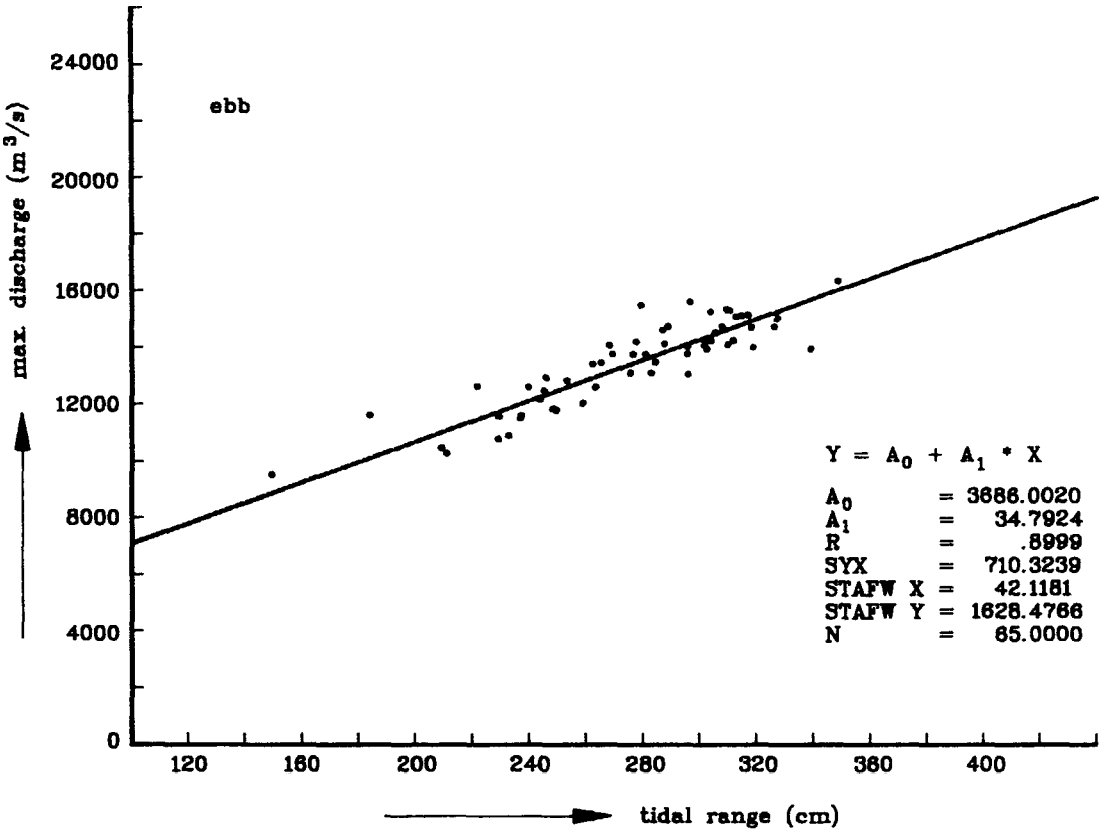

Figure 3.4 Linear regression maximum ebb discharge through Hammen channel and tidal range at station OS4 (computed with IMPLIC)

The computed relation is a function of the combination of the hydraulic resistance of the channels:

$$Q = f(\mu A_{Roompot}, \mu A_{Schaar}, \mu A_{Hammen}) \qquad (3.11)$$

where:

$\mu A_{Roompot}$ is the hydraulic resistance of the Roompot
μA_{Schaar} is the hydraulic resistance of the Schaar
μA_{Hammen} is the hydraulic resistance of the Hammen

For a limited number of combinations of μA (occurring during the construction stages) the relations between maximum discharge and tidal range were computed for ebb and flood flow. For other construction stages these relations could be interpolated.
With the approach outlined above the statistics of the maximum discharges through the barrier were determined. Using the maximum discharge Q_{max}, the water level at Q_{max} and the geometry of the barrier, the average velocities, q/A, through the barrier at maximum flow could be computed with the R1495 model.
A similar approach as used for the discharges could also be used for the statistics of the head differences, Δh. As for the Eastern Scheldt, this was only done for the situation when the barrier was completed. For other construction stages, the head differences were deduced from the computed discharges using the discharge coefficient, μ.

Operational forecasts:

For operational forecasts, time series of the discharge, average velocity through the barrier and head difference were computed with the integrated IMPLIC-R1495 model (see Section 6.4). Additionally, local velocities were computed from q/A using time series analysis techniques.

For a period of several months ahead, a forecast of the above quantities based on predicted astronomical conditions was made. In this case the model was driven by astronomical (water level) boundary conditions.

For the short-term forecast, the above procedure was repeated, taking into account, however, the meteorological effect on the boundary conditions (set-up/set-down).
Afterwards a hindcast was made on routine basis as a check on the forecast.

References of Chapter 3

[3-1] RAND Corporation and Leendertse J.J.
Aspects of a computational model for long-period water-wave propagation, RM-5294-PR, May 1967

[3-2] Cunge, Holley, Verweij
Practical aspects of computational river hydraulics, Pitman Publishing Limited, ISBN 0 273 08442 9, London, 1980

[3-3] Rijkswaterstaat
Hydraulic research for the design of the compartmentalisation dams, sandfill closures, Driemaandelijks Bericht nr. 119, pages 463-469, February 1987 (in Dutch)

4. Simulation of the Storm-Surge barrier

4.1 Introduction

Hydraulic structures, be they a weir, a barrage or a simple bridge, form a discontinuity in the water flow. Besides changes in the flow field in the direct vicinity of the structure, a head difference will build up across the structure, the extent of both being dependent on magnitude and distribution of the "resistance" as well as on the characteristics of the flow.
Here the term "resistance" denotes the accumulated effect of frictional and form losses experienced by the flow when passing the structure. Frictional losses at floor and side walls are usually (very) small relative to the form losses. The latter are mainly caused by flow deceleration downstream of the structure and associated phenomena such as flow separation, energy conversion by (excessive) turbulence, momentum transfer and generation of eddies, etc.

The resistance of the structure may modify the tidal motion in the entire estuary. Therefore, it is essential that the abovementioned hydraulic characteristics of the structure are correctly simulated in the model. To which extent, depends on the type of model used. In a one-dimensional model for example, it is sufficient to express a singular quantity describing the accumulated effect.
A useful tool in this respect is the well-known concept of "coefficient of discharge", describing the empirical relationship between the discharge through the structure and the head difference across it. In a two-dimensional model, the lateral varation of the discharge characteristics has to be expressed as well, while in a three-dimensional model all relevant phenomena and their space variations should be simulated. In these cases the (two, respectively three-dimensional) flow field in the vicinity of the structure is also reproduced by the model.
It should be noted here that although the nominations one, two and three-dimensional formally apply only to numerical models, a similar classification holds true for scale models. A highly distorted scale model resembles the one-dimensional case, a slightly distorted one the two-dimensional case, while an undistorted model is capable of simulating the three-dimensional flow field. Hydraulic scale models are further discussed in Chapter 5 and the numerical models in Chapters 6 and 7.

In this chapter the various definitions of the coefficient of discharge and their inter-relations are discussed in Section 4.2. The following section (4.3) elaborates on the investigations to determine the discharge coefficient of the various designs on the one hand, and on their application in scale and numerical models on the other hand.

4.2 The coefficient of discharge

4.2.1 Theoretical considerations

First consider the case of a uniform channel and a uniform structure, both of infinite width. This is the two-dimensional (vertical) case, which we here denote 2DV, classically described by applying Bernoulli's principle (no energy loss between sections 1 and 2, see Figure 4.1), yielding:

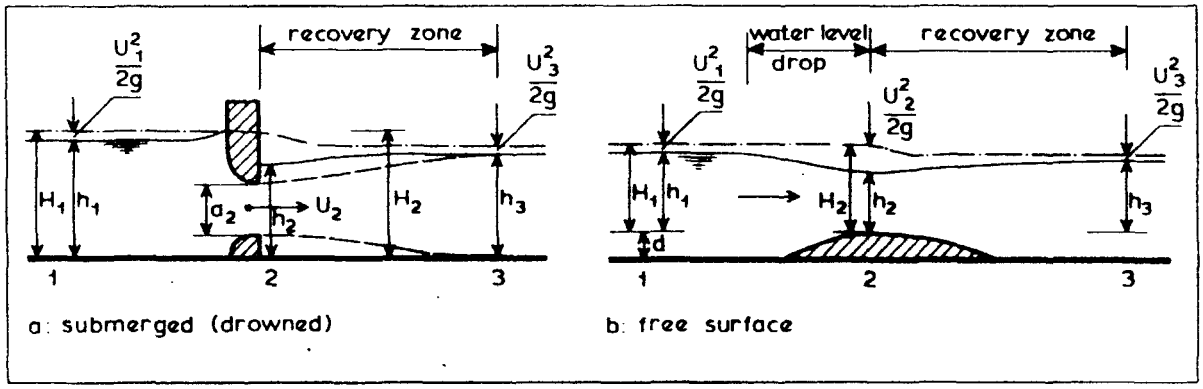

Figure 4.1 Flow regime at the structure, 2DV case

$$q = U_2 \cdot a_2 = a_2\sqrt{2g(H_1-h_2)} \qquad (4.1)$$

where:

q	=	discharge per unit (lateral) width	(m^2/s)
g	=	gravitational acceleration = 9.81	(m/s^2)

For other quantities, reference is made to Figure 4.1.

Between Sections 2 and 3, the energy loss can sometimes be approximated by applying the momentum law and continuity condition, which yields, when substituted in equation (4.1), a lengthy implicit expression.
This expression is an approximation only. Excepting that upstream and frictional losses are neglected, the application of the momentum law requires knowledge of the pressure distribution. Only in an eddy or in a nearly hori-

zontal flow it is correct to assume the pressure distribution to be approximately hydrostatic. Therefore, in civil engineering practice a much simpler expression was adopted. The simplification comprises replacing h_2 by h_3 in equation (4.1) (meaning no recovery in the water level between Sections 2 and 3, which usually is a good approximation of real situations) and multiplying with a coefficient μ, being a correction factor to adjust for approximations and/or simplifications.

$$q = \mu_2 \cdot a_2\sqrt{2g \cdot \Delta H} \qquad (4.2)$$

where $\Delta H = H_1 - h_3$ (m)

The coefficient μ, called coefficient of discharge, can only be obtained through measurements on a scale model of the structure. The suffix 2 is added to denote a 2DV case.
The above simplification is not the sole reason for the need of model tests; as the complicated processes taking place in the vicinity of a structure cannot (yet) be fully evaluated, scale model tests will be necessary anyway.

So far we have considered an "ideal" situation. In reality the channel and the structure have a finite width and, usually, a non-uniform cross-section. Obviously, a three-dimensional flow field corresponds to such a three-dimensional geometry, which we assign the notation 3D (see Figure 4.2).

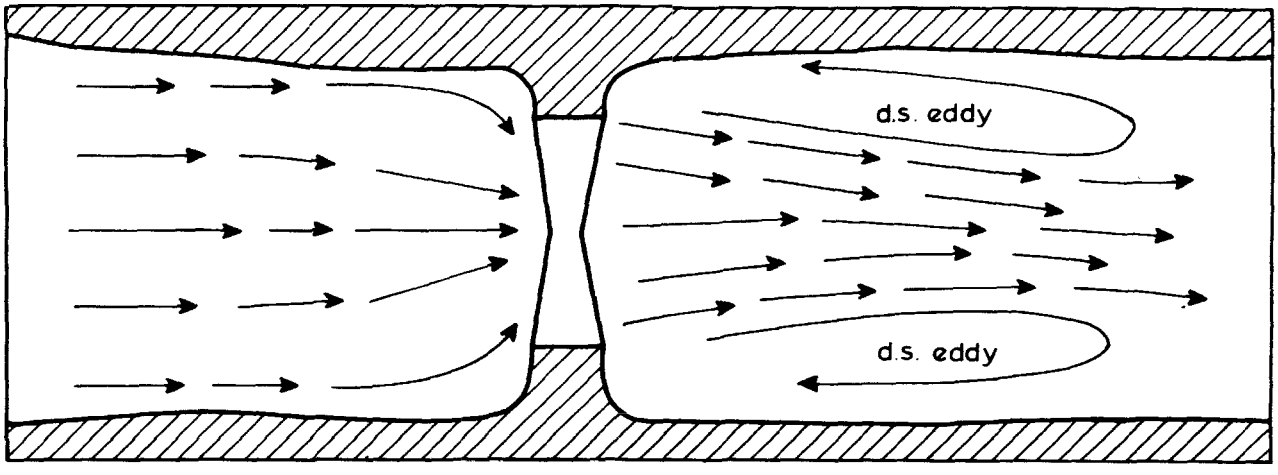

Figure 4.2 Flow regime at the structure, 3D case (plan view)

The larger the lateral variations in water depth and/or "resistance" of the structure are, the more pronounced the three-dimensional effects will be, causing lateral current components which may differ in intensity as a function of location and depth. As a consequence, the water-surface elevation will also

vary both in the longitudinal and lateral direction.
Moreover, flow separation will take place downstream of wall abutments, leading, if sufficiently intruding in the unobstructed flow, to the formation of eddies (with vertical axes, see Figure 4.2). More in general, widening of the flow section downstream of the structure will lead to significant deviations from the 2DV case. Nevertheless the above simplified expression can still be used to describe the characteristics of the structure in the 3D case:

$$Q = \mu_3 \cdot A\sqrt{2g \cdot \Delta h} \qquad (4.3)$$

where:

Q	=	discharge through the structure	(m^3/s)
A	=	wet cross-sectional area of the (throat of the) structure	(m^2)
μ_3	=	discharge coefficient of the structure as a whole	(-)
Δh	=	head difference over the structure, being the difference in water elevation between a point on the upstream and a point on the downstream side of the structure, both usually taken along one of the banks	(m)

Besides the correction effects mentioned in the 2DV case, the μ_3 takes also into acount the effects introduced by the three-dimensional character of the flow field and the water surface. Note also the difference in definition of the head difference in the 2DV and 3D expressions ($H_1 - h_3$ and $h_1 - h_3$, respectively).
In addition, practice - both from field and model data - shows that μ_3 may also vary with the downstream water elevation and/or the discharge. Summarizing (see also [4-2]):

μ_3 = f (structure's geometry, structure's roughness, locations of measurement of Δh, location/definition of A and downstream water level, discharge)

(4.4)

4.2.2 Relation between μ_2 and μ_3

From the above it might be clear that the magnitude of μ_3 cannot be predicted in a straightforward way when the value of μ_2 is known for the various sections of the structure, e.g. via flume - i.e. 2DV - tests. In other words:

$$\mu_3 A \neq \sum_{i=1}^{n} \mu_{2,i} \cdot A_i \qquad (4.5)$$

with suffix i = 1 to n denoting the different sections, corresponding to different depths in the cross-section and/or to different geometries of the structure's profile (see also [4-3] and [4-4]).

This means that a model test of the entire structure in its (future) surroundings is a must if the discharge characteristics are to be predicted beforehand. In fact this is the practice for (large) hydraulic structures all over the world.

These model investigations are further discussed in Section 4.3. Prior to that let us examine the inequality of equation (4.5) more closely.
We shall do this through the schematized structure shown in Figure 4.3, built in a channel of uniform cross-section.

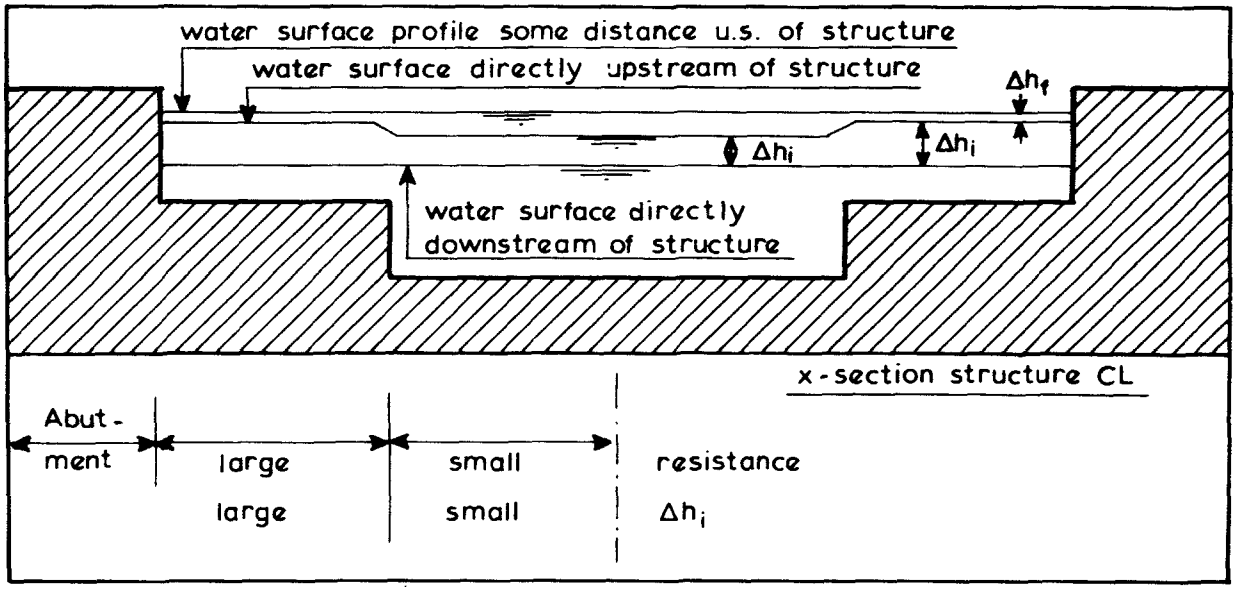

Figure 4.3 Lateral variation of the head difference

Some distance upstream of the structure, the water surface across the channel cross-section is more or less horizontal; the water flow has not yet "felt" the structure. The lateral difference in discharge capacity, caused by the lateral variation in structure's "resistance" (which need not be abrupt as in the case considered here), causes differences in approach velocity and hence a surface profile directly upstream of the structure as sketched in Figure 4.3. Thus a "depression" of some length in the flow direction forms upstream of the low-resistance part of the structure.
In contrast the water surface downstream of the structure shows much less lateral variations. In fact it is rather horizontal, even close to the structure.

Therefore, the actual head difference over the structure is not constant, but varies laterally as shown in Figure 4.3. To account for this, equation (4.5) should be modified as follows:

$$\mu_3 \, A\sqrt{2g \, . \, \Delta h} = \sum_{i=1}^{n} \mu_{2,i} \, . \, A_i \sqrt{2g \, . \, \Delta h_i} \qquad (4.6)$$

However, in general the above equation is not valid either. Inequality results from the discharge capacity of some parts of the structure being reduced (relative to the 2DV case) by flow skewly approaching, by formation of large eddies directly upstream or downstream of the structure, by sharp depth variations, etc; in short, by pronounced three-dimensional effects.
Equation (4.5) will approach an equality only in case the lateral distribution of the structure's discharge capacity equals the approach discharge distribution (which more or less equals that in the undisturbed situation). In such a case, which is usually associated with the absence of large eddies, the "local" head difference is uniformly distributed across the channel.

If the measuring points of Δh are located "rather far" from the structure, the measured Δh would include a part which is actually caused by bed friction in the unaffected part of the flow (Δh_f in Figure 4.3). The effect is particularly pronounced in case the structure's resistance is relatively small.

The righthand side of equation (4.5) can be replaced by: $\bar{\mu}_2 . A$

where:

$$\bar{\mu}_2 = \left(\sum_{i=1}^{n} \mu_{2,i} \, . \, A_i \right) / A \qquad (4.7)$$

which represents "the averaged cumulative two-dimensional coefficient of discharge of the structure".
The ratio $\mu_3/\bar{\mu}_2$ provides a measure to judge the existence and extent of three-dimensional effects through their influence on the magnitude of the coefficient of discharge. In the present study the above ratio has also been used as a tool to judge in a correct way the ability of (vertically averaged) two-dimensional numerical models to reproduce discharge characteristics of composite wide structures as the storm-surge barrier in the mouth of the Eastern Scheldt estuary.

4.2.3 Other conditions

The discussions in Section 4.2.1 and 4.2.2 were restricted to the case of drowned flow under steady-state conditions.
In free surface flow, drowned flow conditions remain as long as the Froude number, defined as $F_r = U_2/\sqrt{gh_2}$ (where U_2 and h_2 are at structure site) remains well below a critical value of about 1. If the critical value is exceeded, supercritical flow conditions are obtained, with the discharge being dependent on the upstream water level only. For 2DV condition:

$$q = \frac{2}{3} m_2 \sqrt{\frac{2}{3} g H_1^3} \qquad (4.8)$$

(broad-crested structure)

where m_2 = discharge coefficient for modular (= supercritical) flow conditions, its value depends on the geometry of the structure and is comparable to μ_2 in a drowned flow case.

The transition to modular conditions takes place when a disturbance on the downstream side of the structure cannot propagate to its upstream side against the high current-velocity at the throat, which defines the critical condition of $F_r = 1$ (see [4-2]).

Under unsteady conditions inertia effects influence the water flow. In long waves the effect of inertia is small most of the time, relative to gravity, convective and frictional effects. However, it cannot be neglected around slack water; then acceleration effects are of the same order of magnitude as gravity and other forces. In other words, equations (4.3) and (4.4) remain valid under tidal conditions, except for a limited period around slack water. The larger the resistance of the structure is, the shorter this period will be.
In view of dependence of μ_3 on the structure's geometry and the location of the measurement at the reference point for the downstream water level, the discharge coefficient for flood flow could vary significantly from that for ebb flow, particularly in the case of asymmetrical structures. In addition to this, μ may further vary as a function of the level of downstream water level.

4.3 Model investigations on discharge characteristics of the barrier

4.3.1 Need and setup of investigations

The discharge characteristics of the storm-surge barrier are an important design parameter. The coefficient of discharge influences directly the required wet cross-sectional area of the structure. The flow field in the direct vicinity is an important input for appurtenances such as bed and bank protection works.

Particularly because from the start onwards unconventional design concepts were considered, flume tests to determine μ_2 of various alternatives were conducted already in the early design stages of the barrier. The results, and for some alternatives also the results of detail models, formed an important input to arrive at reliable cost estimates and profound judgement of the design.

Once the present design concept was decided upon, flume tests to determine μ_2, and its variation as a function of water level and Δh, were conducted for some typical locations in the cross-section of the three main channels (see further Section 4.3.2). The results were needed for the following objectives:

a. To enable the design of a barrier model for application in the distorted overall model of the estuary (M1000) and a barrier model for application in the undistorted detail model of the mouth area (M1001). Both models needed a barrier simulation which at each location (with its local sill height and varying water levels) had the correct discharge characteristics, in spite of the distortion in the case of M1000 or the simplification of the (complex) geometry in the case of M1001. See further Section 4.3.3.

b. As input for mathematical models. Originally the results had to be applied only for the one-dimensional model describing the lateral distribution of the discharge through the barrier (R1495). Later, however, another application emerged, namely in the two-dimensional overall models and detail models (WAQUA). See further Section 4.3.4.

For the one-dimensional numerical model of the estuary (IMPLIC), it is obvious that μ_3 should be applied to describe the discharge characteristics of the barrier, both for the various construction stages and for the final situation. The corresponding values have been provided from the results of the scale

models M1000 and M1001. If these models were not available, μ_3-values might have been provided by the two-dimensional detail models WAQUA (see further Section 4.3.4).

The setup described above and relations between the different models are shown graphically in Figure 4.4.

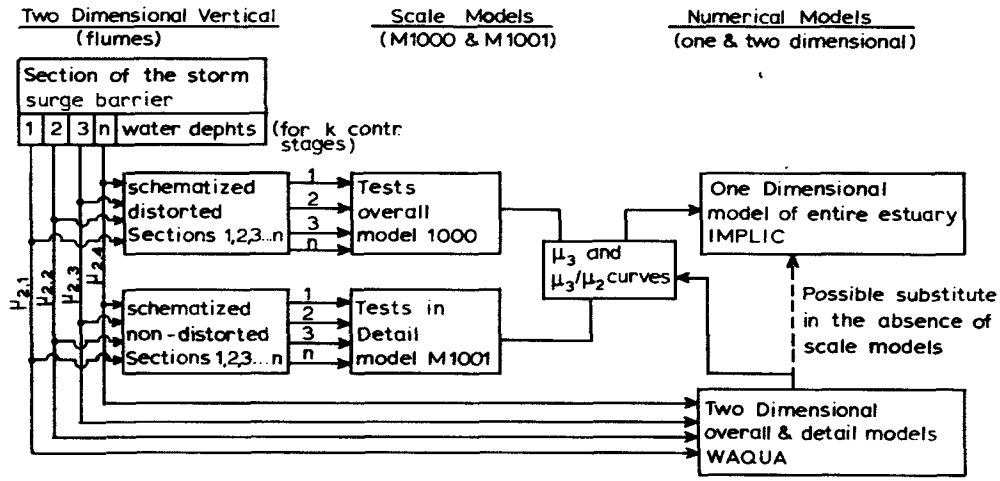

Figure 4.4 Setup and relations on discharge characteristics of the barrier

In view of the method of construction adopted (prefabricated elements, see Chapter 2), the flume tests were conducted for a number k of the consecutive construction stages for each of the selected locations (water depth), see further Section 4.3.2.
From the results of tests in the scale models (M1000 and M1001) a set of curves giving $\mu_3/\bar{\mu}_2$ values as a function of $\bar{\mu}_2 A$ have been constructed. They proved to be a valuable tool for the operation of the IMPLIC and R1495 models, which were continuously used to provide flow data for the various operations on work sites.

4.3.2 Flume tests

To determine the two-dimensional coefficient of discharge μ_2, flume tests are conducted on a representative section of the structure. In the case of the storm-surge barrier, the representative section runs from the centre-line of a compartment to the centre-line of an adjacent compartment, i.e. with the pre-

fabricated pier in the centre of the section. Depending on the flume width and chosen scale, the test section can of course be composed of any integer number of the representative section.

The flow at a hydraulic structure with free-water surface, is mainly governed by inertia and gravity forces, which is the typical case for applying Froude's Law of similarity (see standard text books and Chapter 5 of this report):
$Fr_{model} = Fr_{prototype}$, where F_r = Froude number

Geometrical similitude is essential; therefore distorted models are unacceptable. In addition, the length scale should be chosen in such a way that flow forces caused by the other phenomena, which were not considered when deriving Froude's law of similitude and therefore are reproduced on different scales in the models, do not cause significant variations in the force balance and hence do not introduce errors known as scale effects.

The most important elements for scale effects in such models as for the storm-surge barrier are:

- viscous forces: as in all other scale models, the flow in the model must be turbulent; requirement: Reynolds Number > a critical value
- forces associated with the development of shear layers at the various (horizontal, vertical and skew) edges of the structure; requirement: Reynolds Number > a critical value and correct roughness
- frictional forces; requirement: correct reproduction of roughness
- surface tension forces in the model must have no influence as is the case in the field, which is particularly important in the case of flow on the limit of flow separation with air-inclusion; requirement: Weber Number > a critical value.

Except for the first (general) requirement of turbulent flow in the model, no quantitative data on the above-discussed minimum requirements are given in literature. In fact on the one hand they depend to a large extent on (details of) the geometry and material(s) of the structure and on the absolute dimensions of the model on the other hand. Therefore, experience plays an important role in the selection of the scale; there are some options to adjust the results for possible scale effects; see e.g. [4-5]. As it is a 2DV case, in the field the flume results cannot be checked in a straightforward manner (since only μ_3 can be determined from field data).

For the storm-surge barrier, a linear scale of 1:40 has been chosen, based on experience with similar structures on the one hand, and on the other hand on the size of available flumes, accuracy of measurements and requirements on the reproduction of the rubble sill. One 45 m-section, from compartment centre line to adjacent compartment centre-line, has been built to that scale, including the rubble top layers of the sill (see Figure 4.5). Simulation of the top layer of the sill according to the linear scale was required for a correct reproduction of bed friction.

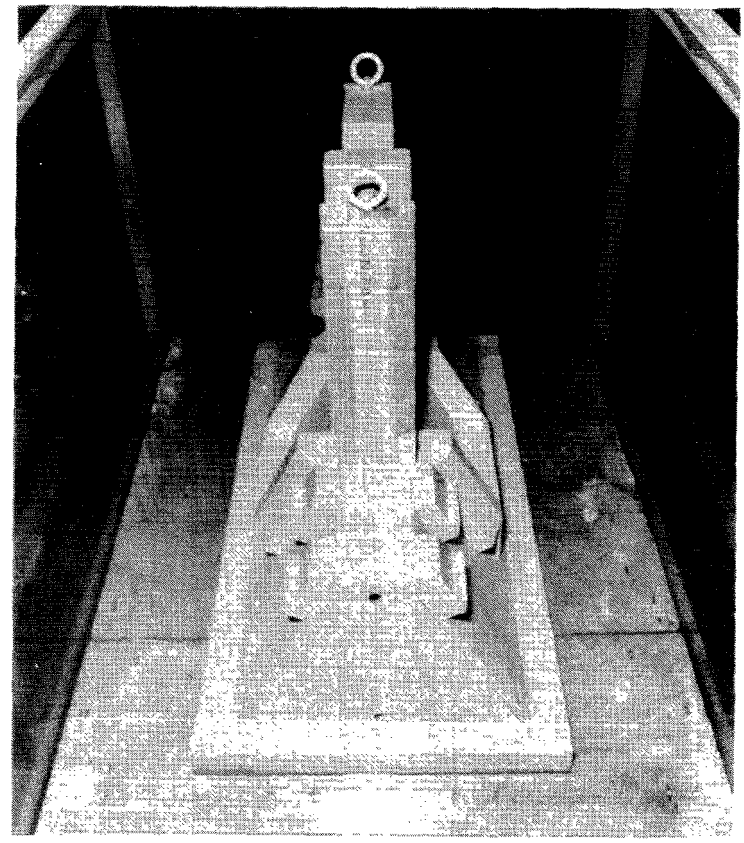

Figure 4.5 Geometrically similar model, scale 1:40, of a representative section of the storm-surge barrier; setup in the flume for placed pier.

For the flume tests three typical locations were selected, representing different water depths in the three channels and associated differences in the longitudinal bed section at pier-foundation level (dredged, natural or heightened). On the other side of the matrix, three characteristic construction stages were chosen for the flume tests, namely: pier placed on a foundation mat, sill construction completed and sill beam placed (see Figure 4.6). The selection was made in view of anticipated extensive investigations for the construction stages of the barrier.

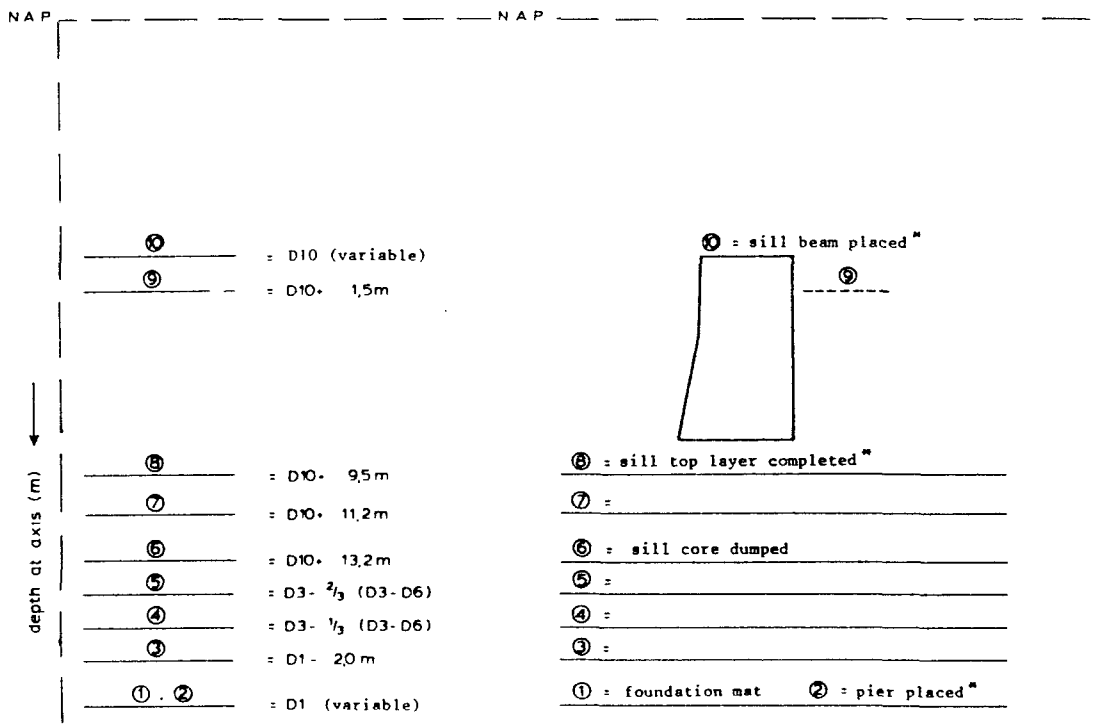

Figure 4.6 Selected construction stages per site for flume tests (*) and schematization in the scale and numerical models (1 through 10)

The results of the above-described nine test series are summarized in Figure 4.7. Each point represents an extensive test programme, comprising tests for ebb and flood directions with stepwise variation of downstream water level and head difference (see Equation 4.4) as well as repeatability tests.
The discharge coefficient μ_2 has been determined, taking the head difference as the difference between the water surface level upstream and the water surface level downstream of the structure, which is different from the definition derived in equation (4.2). This in view of the envisaged application in numerical models and comparison of $\bar{\mu}_2$ and μ_3 (see Section 4.2.2). The upstream water level was measured 40 m upstream of the barrier axis, the downstream water level 200 m downstream of the axis. The downstream point was directly beyond the recovery zone of the downstream water level (see Figure 4.1). The test results have been corrected for the wall roughness of the flume, which does not exist in a 2DV case, applying Einsteins's approach (see e.g. [4-1]). The inaccuracy of μ_2 thus determined, has been assessed to fall within ± 5% (± 2 times the standard deviation, [4-6]).

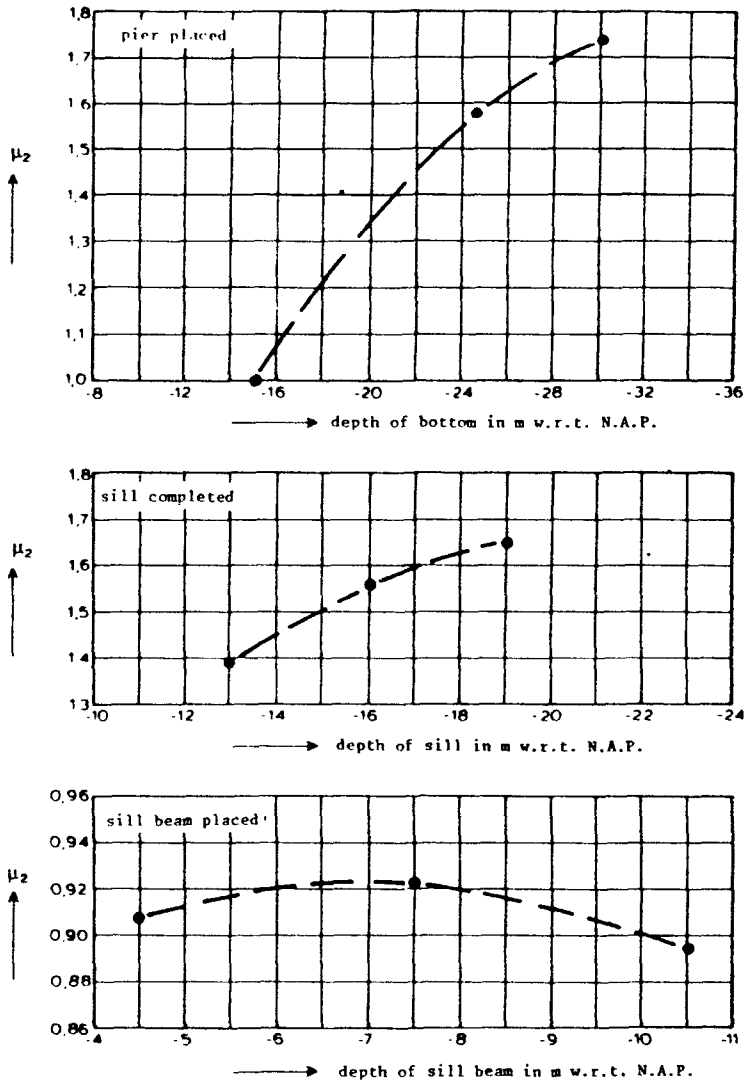

Figure 4.7 Basic values of μ_2

Within the range of expected downstream water levels, the discharge coefficient μ_2 hardly varied as a function of the downstream water level, and was very nearly equal for ebb and flood directions. The variation as a function of the head difference Δh was, however, appreciable (up to about 20%). This effect, and corresponding variations in μ_2 were only investigated at one of the three typical locations; larger variations are not impossible. The values given in Figure 4.7 correspond to the expected (range of) head difference(s) at the construction stages in question.

4.3.3 Scale models

As mentioned in Chapter 3, two scale models were used in the Eastern Scheldt studies:

a. The distorted overall model of the entire estuary (project M1000); horizontal scale 1:400, vertical scale 1:100.

b. The undistorted detail model of the mouth area of the estuary where the storm-surge barrier was being built (project M1001); scale 1:80.

An essential requirement for the simulation of the storm-surge barrier in these models is the correct reproduction of the discharge characteristics for the various construction stages and different boundary conditions. In other words both the cross-sectional area A and the discharge coefficient μ must be reproduced to scale. Note that from applying Froude's law to equation (4.3), it follows that the scale of μ should be 1:1, i.e. $\mu_{model} = \mu_{prototype}$.

To obtain this for the overall model M1000, a schematized structure, having the same A and the same μ_2 as a function of construction stage, has been designed and tested in a (smaller) flume, see Figure 4.8. To avoid large deviations caused by scale distortion (of 4), the distortion was reduced by 50% by having the horizontal scale of the structure 1:200 in the flow direction. In this way differences in the length-width ratio of the compartments and in side slopes could be reduced.

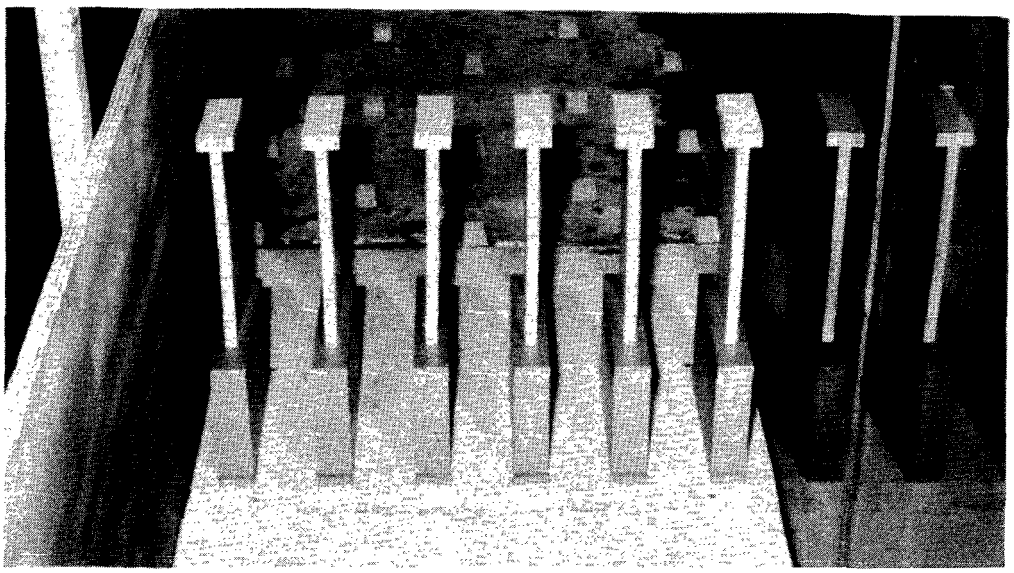

Figure 4.8 Model of the storm-surge barrier for the 1:100/400 overall distorted model; setup in flume for placed piers

In principle, a geometrically similar model of the storm-surge barrier is required for the undistorted detail model M1001. However, building such a model would be too expensive and take too much time in view of the complex geometry and the large number (65) of the piers and sill beams. Moreover, scale effects

could even emerge due to many small-size protrusions on the pier. Therefore, a similar approach has been followed as for M1000 but - of course - with the model piers having much more resemblance to the real ones and without the need to change the scale locally (see Figure 4.9 and compare it with Figure 4.8).

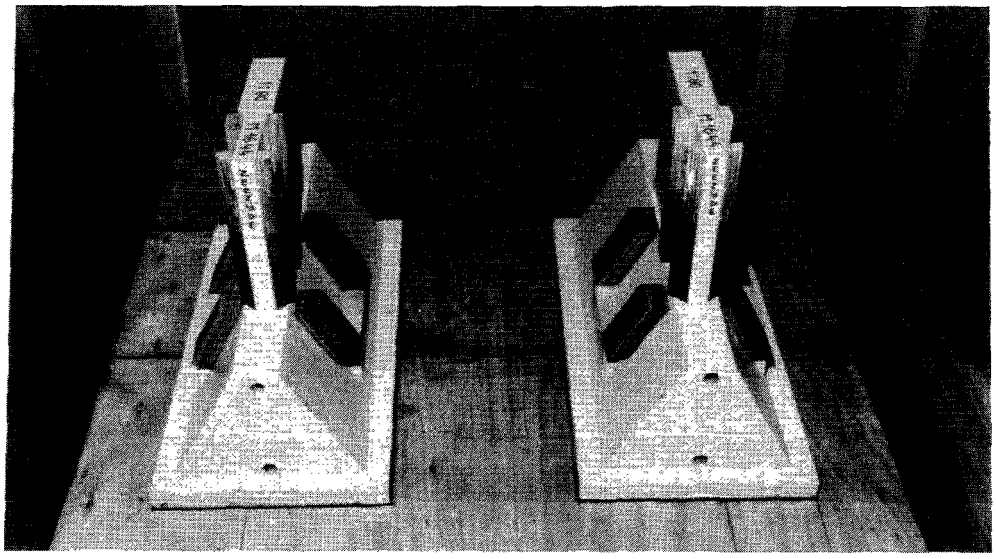

Figure 4.9 Model of the storm-surge barrier for the 1:80 detail model; setup in the flume for placed piers

In a model, or in the field, the value of μ_3 is found by substituting known or measured values of A, Q and Δh in equation (4.3). Procedures followed in the scale models of the Eastern Scheldt are discussed further in Sections 5.3.2. and 5.6.2.

Except for some deviations in the relation between μ and Δh, particularly in the case of the undistorted model, the schematized sections of the storm-surge barrier for both models reproduced the two-dimensional discharge characteristics (μ_2) of the structure, as determined through the flume tests described in section 4.3.2, within an inaccuracy range of ± 5%. Assuming mutual independency of inaccuracies (this and that of determining μ_2 through the flume tests which also amounts to ± 5%, see Section 4.3.2), the schematized sections of the barrier would reproduce $\bar{\mu}_2$ of the "real structure" within an inaccuracy range of ± 7%.

Consequently, one can expect that the discharge characteristics of the structure as a whole (μ_3) will be equally or slightly less accurately reproduced, any how by the undistorted (detail) model. From experience with similar cases in the past and from the results of a systematic research programme [4-7], no serious deviations were expected in the value of μ_3 determined from the dis-

torted overall model (with a distortion factor 4). Indeed, this was the case. Even for construction stages with large abrupt lateral changes in resistance (stages of sill beam installation), the differences in μ_3 between distorted and undistorted model remained within a margin of ± 5% [4-8]. That is to say, well within the inaccuracy range of determining μ_3 from measurements in such models. Note that (Δh and Q) measurement inaccuracies add to make the inaccuracy range of determining μ_3 from the model larger than that of reproducing the hydraulic characteristics in that model.

A given value of μ corresponds to a certain definition of Δh. For the storm-surge barrier, the water-level stations were installed in the work harbours located on both (sea and inner) sides of the structure in the three channels, see Figure 4.10. This was not only practical and equivalent to field locations, it also ensured that under no circumstances the water-level stations will be located in the turbulent high-velocity flow downstream of the barrier. A test series in the detail model (Roompot channel) did not reveal any systematic difference between Δh determined from observations in the work harbours and Δh determined from water-level observations in the channel [4-9].

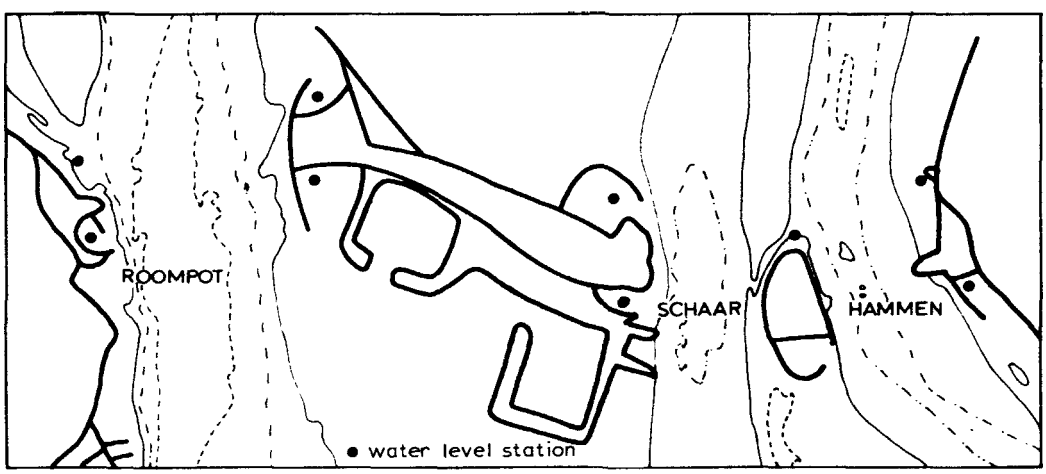

Figure 4.10 Location of water-level stations

As mentioned in Section 4.3.1, the results of both scale models have been used to construct Figures 4.11 through 4.13, giving $\mu_3/\bar{\mu}_2$ as function of $\bar{\mu}_2$ A for the three channel sites (Roompot, Schaar and Hammen), both for flood and ebb current. The same results are presented in Figures 4.14 through 4.16, now giving (the absolute value of) μ_3 as function of $\bar{\mu}_2$ A. Inspection of these figures shows that indeed the differences in μ_3 (or $\mu_3/\bar{\mu}_2$) between distorted and undistorted model are relatively small. The utilization of these figures is discussed in Section 4.3.4, together with a further analysis of the results.

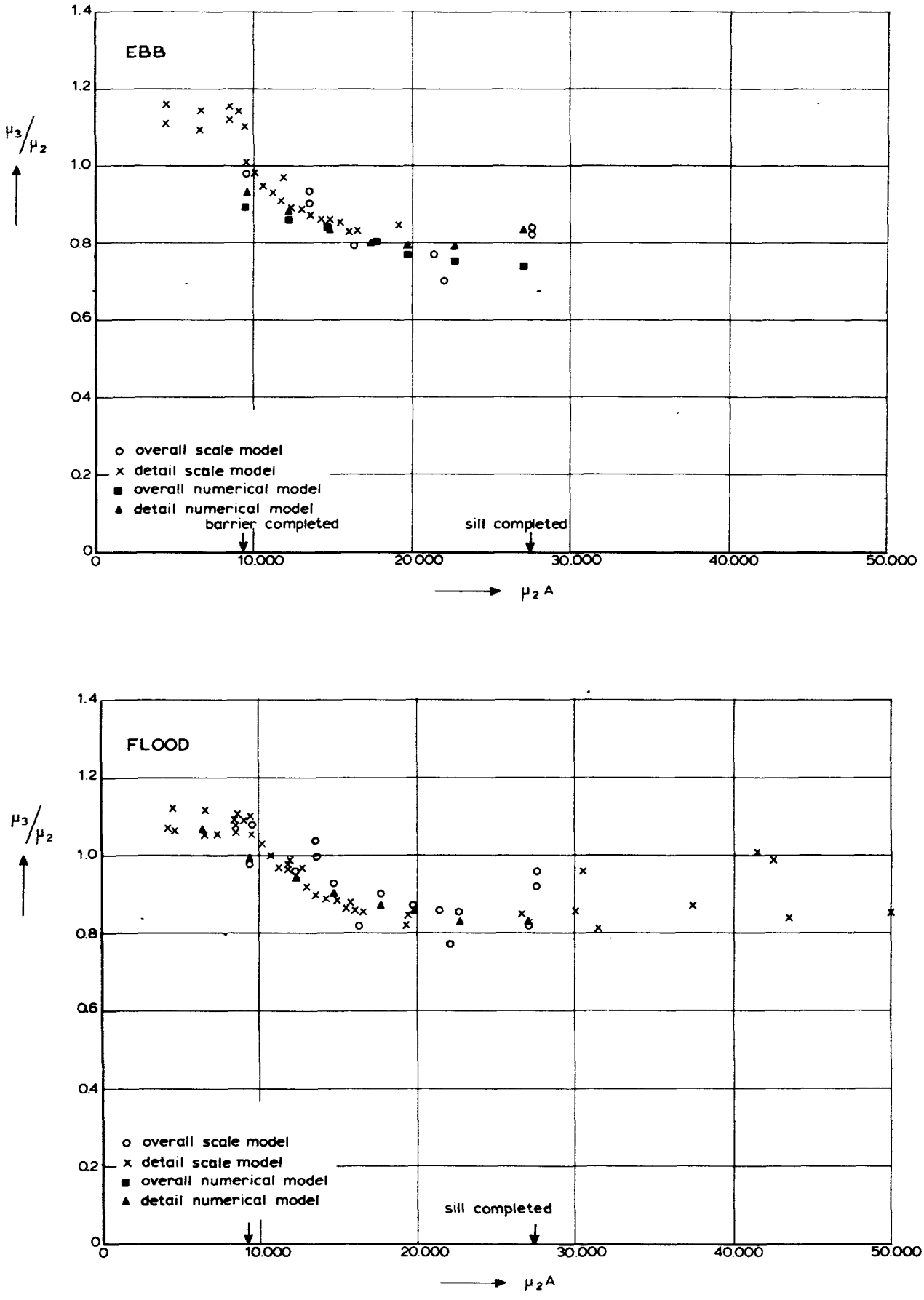

Figure 4.11 $\mu_3/\bar{\mu}_2$ as a function of $\bar{\mu}_2$ A, Roompot Channel

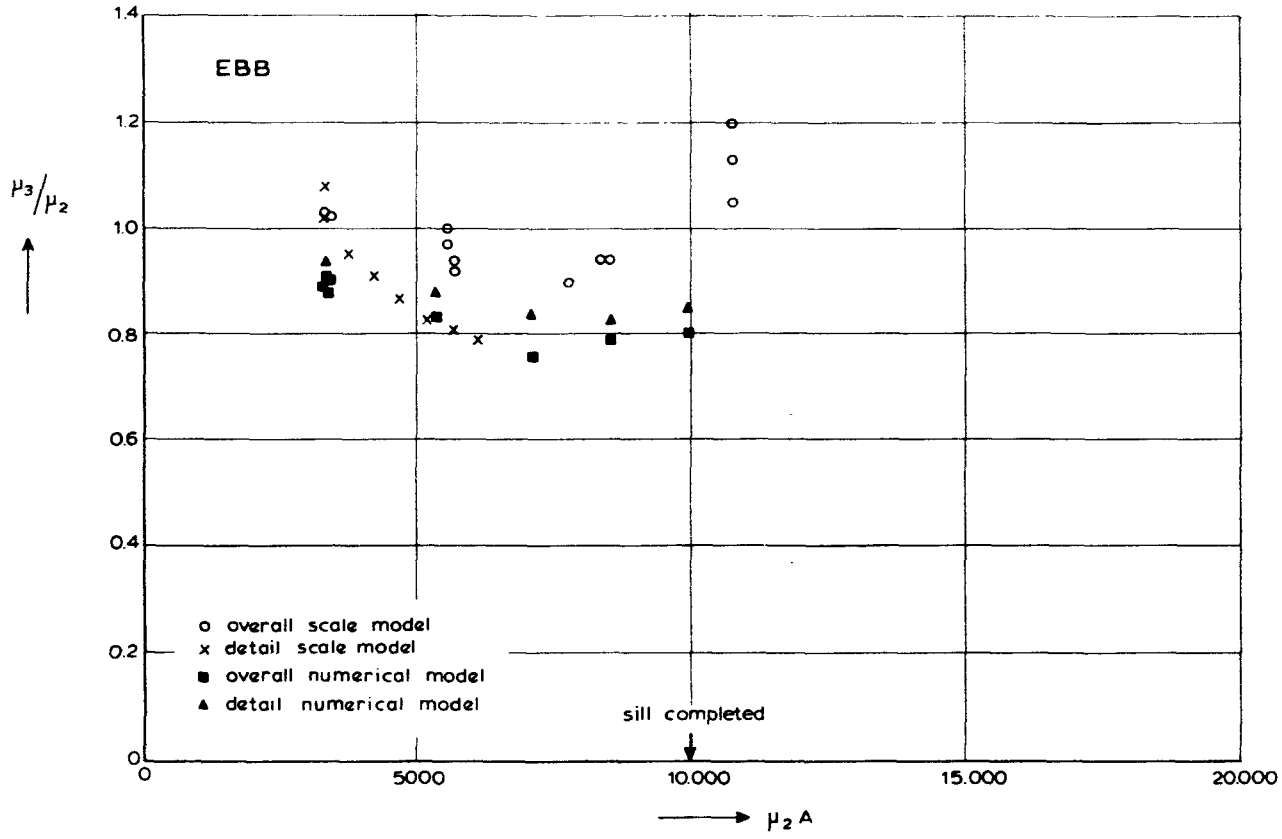

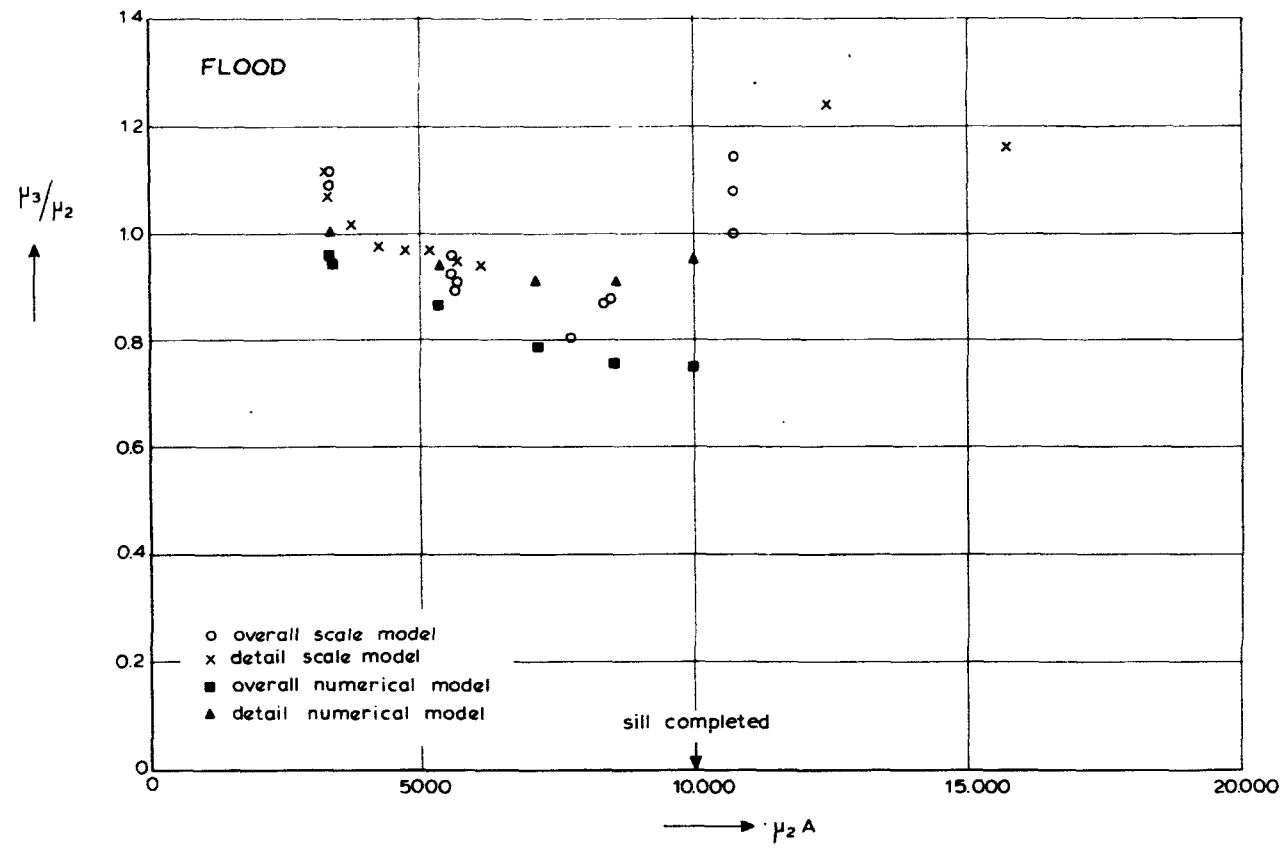

Figure 4.12 $\mu_3/\bar{\mu}_2$ as a function of $\bar{\mu}_2$ A, Schaar Channel

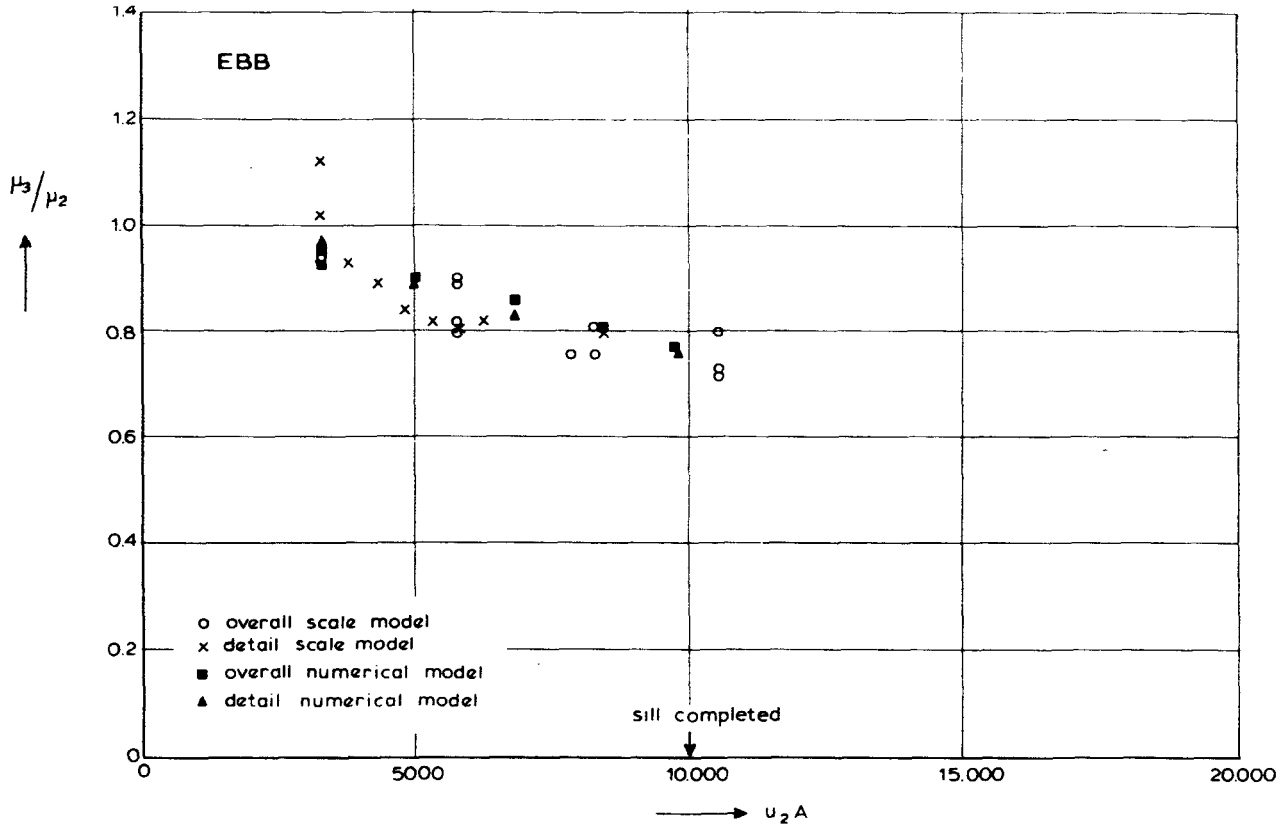

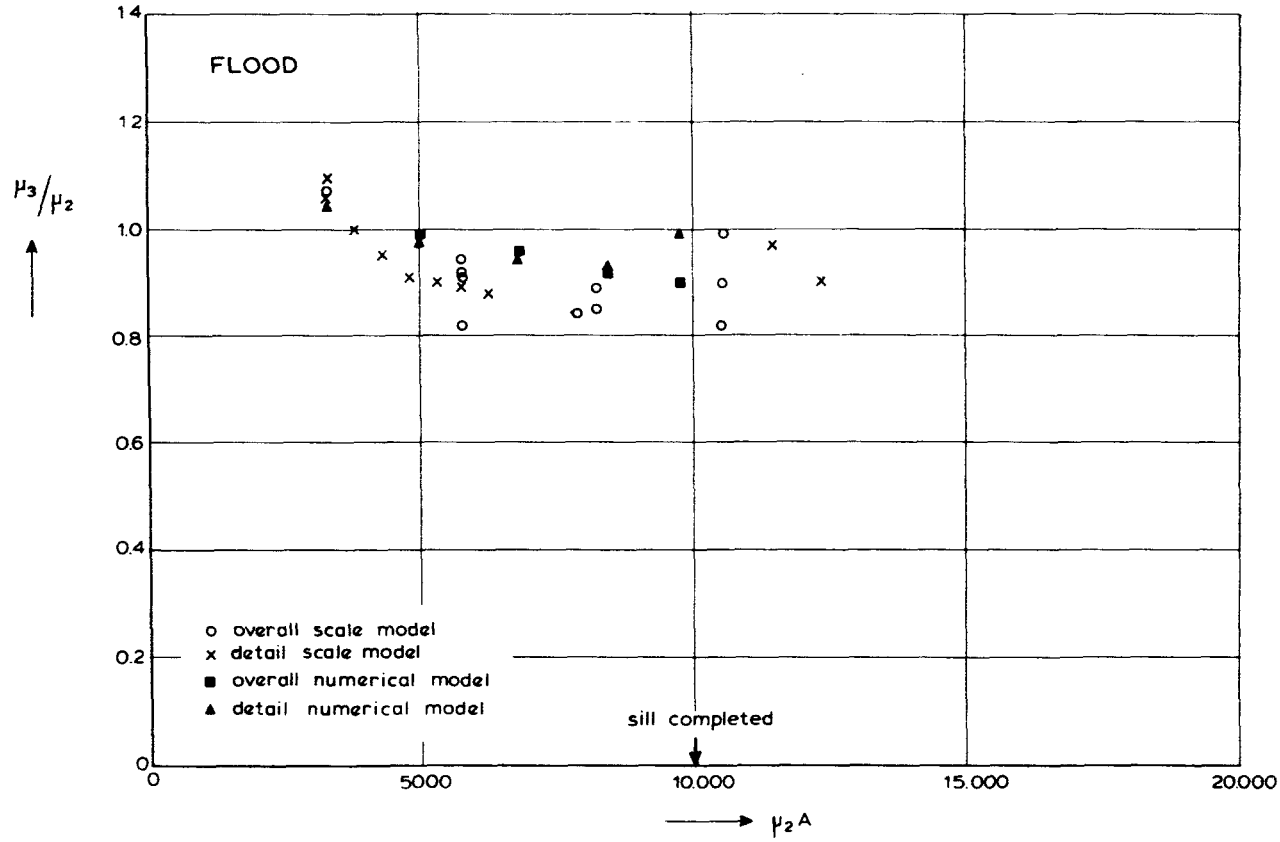

Figure 4.13 $\mu_3/\bar{\mu}_2$ as a function of $\bar{\mu}_2$ A, Hammen Channel

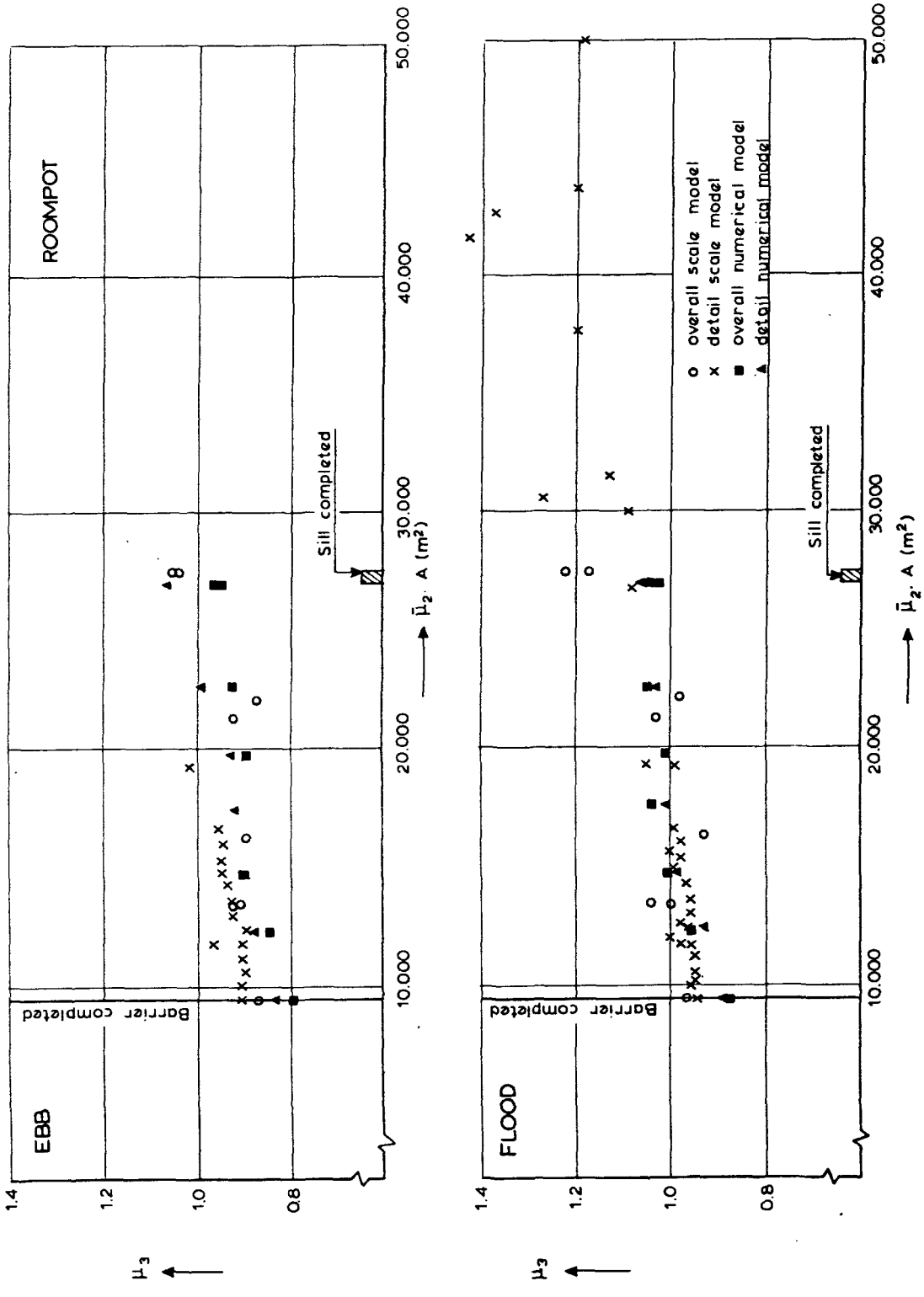

Figure 4.14 μ_3 as a function of $\bar{\mu}_2$ A, Roompot Channel

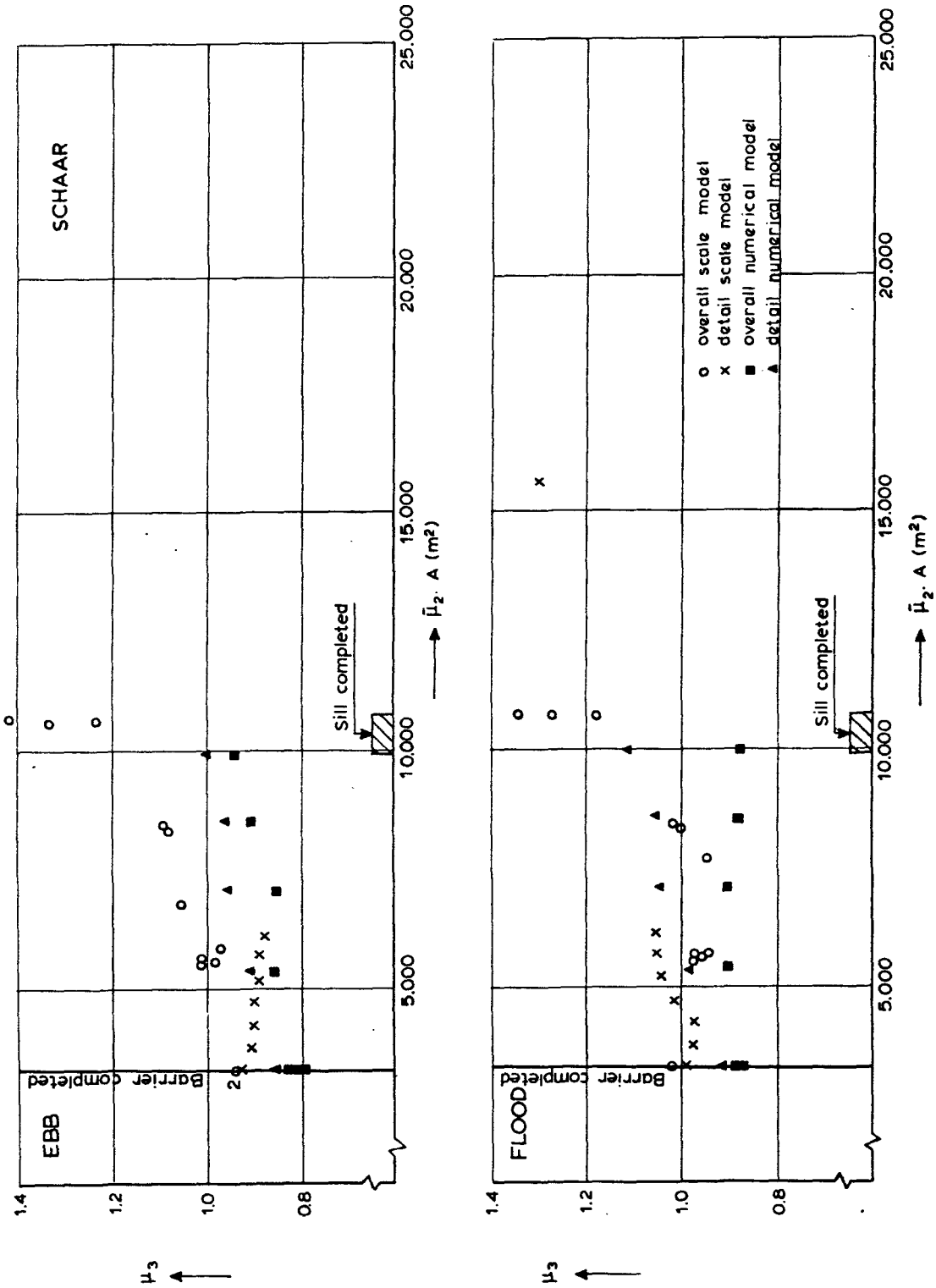

Figure 4.15 μ_3 as a function of $\bar{\mu}_2$ A, Schaar Channel

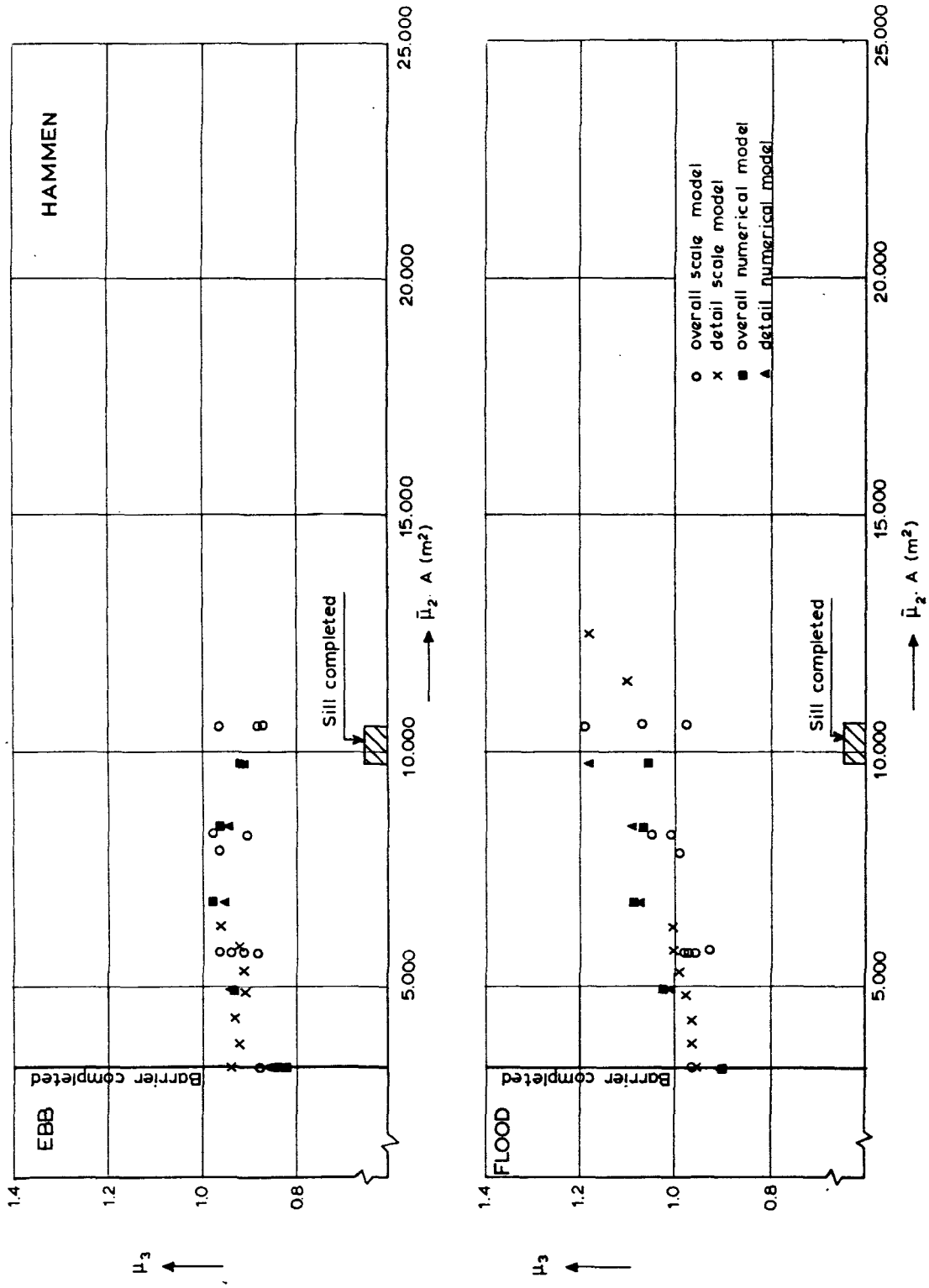

Figure 4.16 μ_3 as a function of $\bar{\mu}_2$ A, Hammen Channel

4.3.4 Numerical models

The value (definition) of the coefficient of discharge μ to be applied in a numerical model depends on the type of the model.
For one-dimensional models, where flow through a channel is represented by a single quantity Q, it is obvious that the three-dimensional coefficient of discharge μ_3 must be used (notwithstanding the unfortunate combination of the words one-dimensional and three-dimensional). For operational application of the one-dimensional model IMPLIC, use has been made of Figures 4.11 through 4.13 to assess the values of μ_3 for a given situation (for which $\sum \mu_{2,i} \cdot A_i = \bar{\mu}_2 A$ can be computed straightforwardly). This procedure has worked satisfactorily throughout the construction period of the storm-surge barrier, however with the quantitative value of the relations being adapted a few times as more results of model investigations and/or field data became available. Figures 4.11 through 4.13 give the final version.

An important adaptation concerned the value of μ_2 for the construction phase sill completed. Comparisons between the detail numerical and scale models (phases of sill beam installation) on the one hand, and between the two-dimensional overall numerical model and the prototype (phase sill completed) on the other hand, both indicated that the μ_2 value applied in the numerical models for construction phase sill completed should be reduced by 20%. The original value, derived from the flume tests (see Figure 4.7), and which was used as input for schematization of the barrier model for the scale model, proved to be too large for the numerical model! A closely reasoned explanation for this inconsistency has not yet been found. Possibly skewly approaching flow conditions and/or differences in approach velocity could be partly held responsible. Without the (detail) scale model and frequent verification of the models through extensive field campaigns, this discrepancy would not have been discovered in time. It might have been avoided if more extensive flume tests were carried out to determine μ_2 for more construction phases and at more locations (water depths) in the cross-section.

For two-dimensional (horizontal) models, where the structure occupies a relatively large number of grid cells (say more than about 8), one can expect that μ_2 values should be applied. Indeed, this proved to be the case for the two-dimensional models MOOS-N, MOOS-Z (grid size 90 m), ROOMPOT, SCHAAR, HAMMEN (grid size 45 m) and DOOS-1 (grid size 100 m). This has been verified through Figures 4.11 through 4.13 (see [4-10]).

This becomes questionable when the structure occupies only few grid cells, as it is the case with the overall model OOST-3, with the barrier in the Roompot occupying 4 cells, and in the Schaar and Hammen 2 cells each. However, experiments have shown that even then μ_2 values (averaged over the sections forming a grid cell) must be applied [4-10]. This conclusion was based on verification via the $\mu_3/\bar{\mu}_2$ relations (Figures 4.11 through 4.13) and reduction of tidal motion in the estuary as a function of the resistance in the mouth, see Figure 4.17. In this figure, the reduction of tidal motion is represented by the term $Q_{t,cs}/Q_{t,os}$, where:

$Q_{t,cs}$ = Maximum total discharge through the mouth for a given construction stage

$Q_{t,os}$ = Maximum total discharge through the mouth in the original situation

The results of M1000 are also given in the figure.

From the discussion in Section 4.2.2, it can be expected that low values of $\mu_3/\bar{\mu}_2$ occur when pronounced three-dimensional effects are present. Inspection of Figures 4.11 through 4.13 shows that indeed low(est) values of $\mu_3/\bar{\mu}_2$ are obtained during placing phases of the sill beams.
However, low values of $\mu_3/\bar{\mu}_2$ are also encountered for the case when the sill is completed in the entire channel, which in fact is a case of minimum three dimensional effects.
This "discrepancy" can be attributed to the definition of Δh. As the water levels are measured in the work harbours (some 600 m from the structure), energy losses due to bed friction (Δh_f in Figure 4.3) form an appreciable part of Δh during the early stages of construction (large Q and small head difference over the structure), resulting in an apparently low μ_3 and $\mu_3/\bar{\mu}_2$. The construction stage sill completed is such a case, e.g. in Figure 4.18 , $(\Delta h - \Delta h_f)/\Delta h$ amounts from 0.55 to 0.60, its square root (≈ 0.76) is a measure of $\mu_3/\bar{\mu}_2$. On the other hand, the bed-friction effect is negligible during construction stages with small Q and large head difference over the structure. Advanced phases of sill beam placing are such a case, see Figure 4.19.

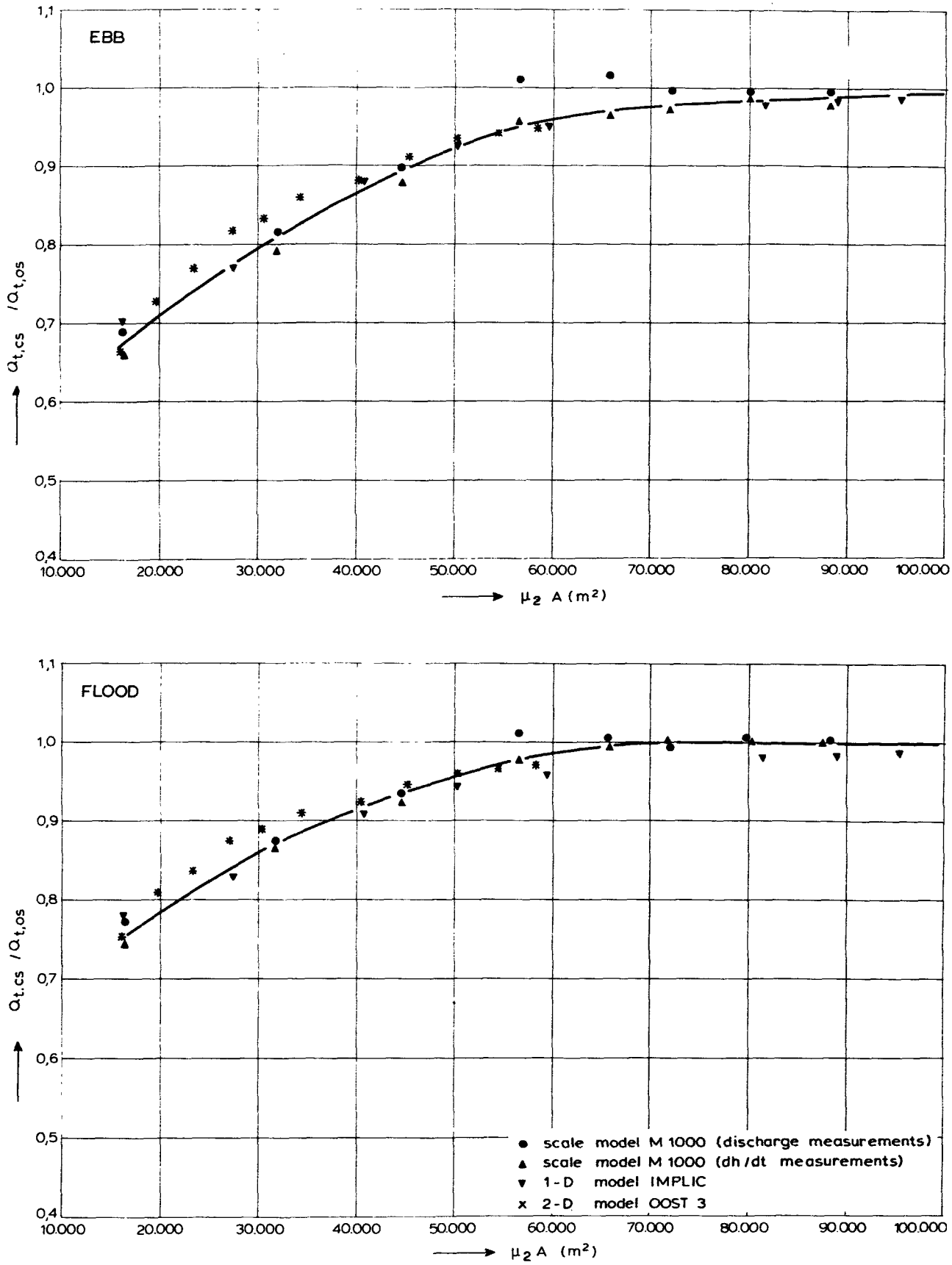

Figure 4.17 Reduction of tidal motion as a function of the resistance in the mouth

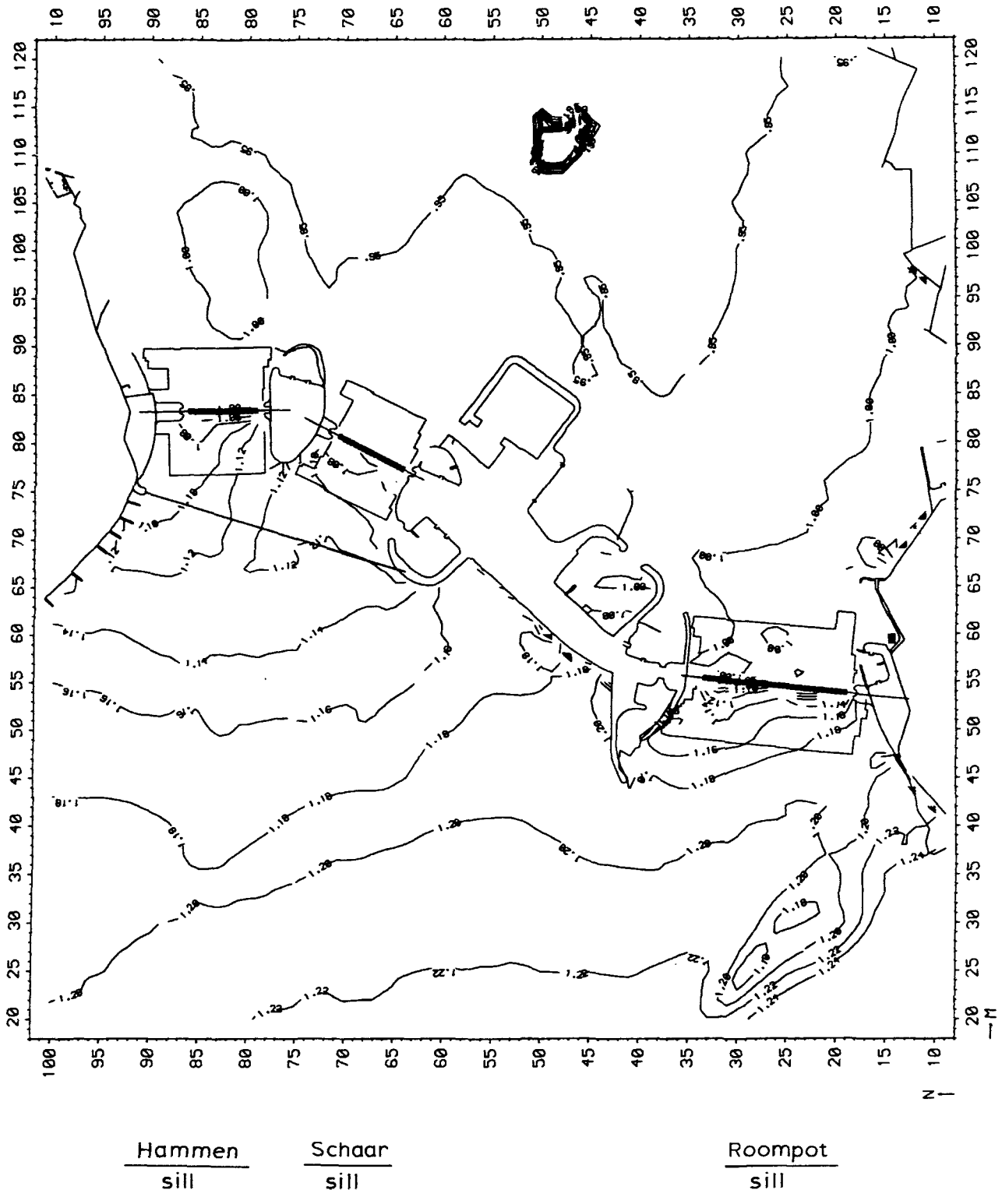

Figure 4.18 Water levels at maximum flood flow, construction phase: sill completed at all three channels

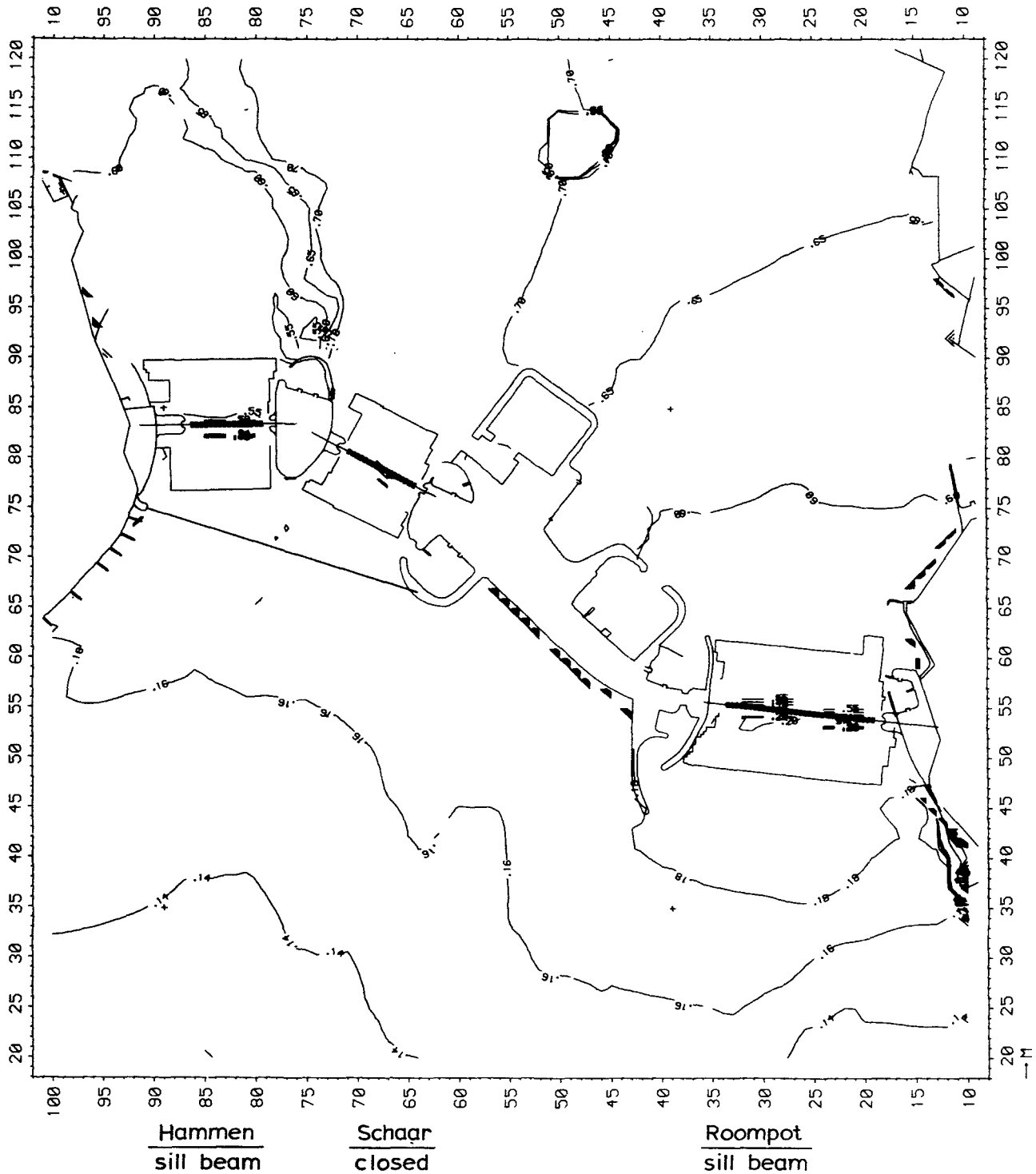

Figure 4.19 Water levels at maximum ebb flow, construction phase: sill beams installed at all channels and gates at Schaar channel closed

References of Chapter 4

[4-1] VEN TE CHOW
Open-channel hydraulics, McGraw-Hill, 1955.

[4-2] Rijkswaterstaat
Final Report Storm Surge Barrier Eastern Scheldt, Investigation on the feasibility of closure of the Eastern Scheldt by means of a partially prefabricated structure. Report part 2: Hydraulic Aspects, The Hague, December 1984 (in Dutch).

[4-3] Demmerle, D.
Discharge Capacity of Low Head Barrages, IAHR Symposium on scale effects in modelling hydraulic structures, Esslingen am Neckar, West Germany, September 1984.

[4-4] Bernhart, H. and Bakowies, F.
Discrepancies in Test Results of Two- and Three- Dimensional Investigations for a Weir Structure, IAHR Symposium on scale effects in modelling hydraulic structures, Esslingen am Neckar, West Germany, September 1984.

[4-5] Kolkman, P.A.
Considerations about the accuracy of discharge relations of hydraulic structures and the use of scale models for their calibration, IAHR Symposium on scale effects in modelling hydraulic structures, Esslingen am Neckar, West Germany, September 1984.

[4-6] DELFT HYDRAULICS and Graauw, A.F. de
Schematization of the piers for the detail model and the tidal model of the Eastern Scheldt, M 1644, April 1981 (in Dutch).

[4-7] DELFT HYDRAULICS and Rees, A. van
Discharge coefficients of closure gaps in distorted models,
M711-XIV, 1972 (in Dutch)

[4-8] DELFT HYDRAULICS and Hartsuiker, G.
Eastern Scheldt Storm Surge Barrier, Overall tidal model, Flow boundary conditions construction stages, Summary of water levels and head differences, M1696-XIII, February 1982 (in Dutch).

References of Chapter 4 (continued)

[4-9] DELFT HYDRAULICS and Hartsuiker, G.
Eastern Scheldt Storm Surge Barrier, Detail model, Current pattern for last phases of sill beam installation, M 2135, November 1985, (in Dutch).

[4-10] DELFT HYDRAULICS and Hartsuiker, G.
Two-dimensional models of the Eastern Scheldt mouth, computation of current pattern during placing of sill beams, R 2094-03, February 1986 (in Dutch).

[4-11] Klatter H.E., Thabet R.A.H. and Hartsuiker G.,
Modelling hydraulic structures in numerical and scale models, 22th IAHR Congress, Lausanne, 1987.

5. Hydraulic scale models

5.1 Introduction

At location "De Voorst" of Delft Hydraulics two hydraulic scale models of the Eastern Scheldt, called M1000 and M1001, were used for investigations concerning the construction of the storm-surge barrier.

The model M1000 represented the entire Eastern Scheldt estuary and an adjacent part of the sea. The model had originally been built in 1969 to investigate the total closure of the Eastern Scheldt.
The main objectives of the studies in this model were:

- study of the overall tidal movement, providing information on discharges and water levels
- determination of mutual influence of the closure gaps and, based on this, the recommendable sequence of the building stages
- determination of boundary conditions for detail model(s)

The model was in operation from 1970 until 1983; after that period, the previously mentioned data were computed by using two-dimensional numerical models (see Chapter 7).

The model M1001 represented the mouth of the Eastern Scheldt with its three main channels. The model had also been built to investigate the total closure of the Eastern Scheldt.
The main objective of studies in this model was:

- determination of the scour holes and from this the total length and lay-out of the bed-protection works

In addition, the following items could also be investigated in this detail model:

- determination of flow pattern, detailed information on current-velocities and directions in the vicinity of the barrier
- determination of effective cross-sectional area of the barrier
- determination of stability of rubble-stone material

The model was in operation from 1970 up to 1986; the model could (up to that time) not be replaced by a numerical model because of the three-dimensional flow effects near the barrier.

In the Sections 5.2 through 5.4 aspects related to the overall model M1000 will be discussed, the Sections 5.5 through 5.7 deal with the detail model M1001.

5.2 Setup of overall scale model M1000

In this model the basic terms of the continuity equation and the (simplified) momentum equation in x, y and z direction are represented in a fundamentally proper way. Forces such as friction and the Coriolis-force are additionally modelled; forces caused by wind are not taken into account (only wind set-up as a part of the boundary conditions)
An essential condition is that all terms of the equations are reproduced on the same scale. Via a proper selection of the scales this goal can be achieved. In Section 5.2.1 the selection of the scales will be discussed.
Figures 5.1 and 5.2 give an impression of the model (see also [5-1]).

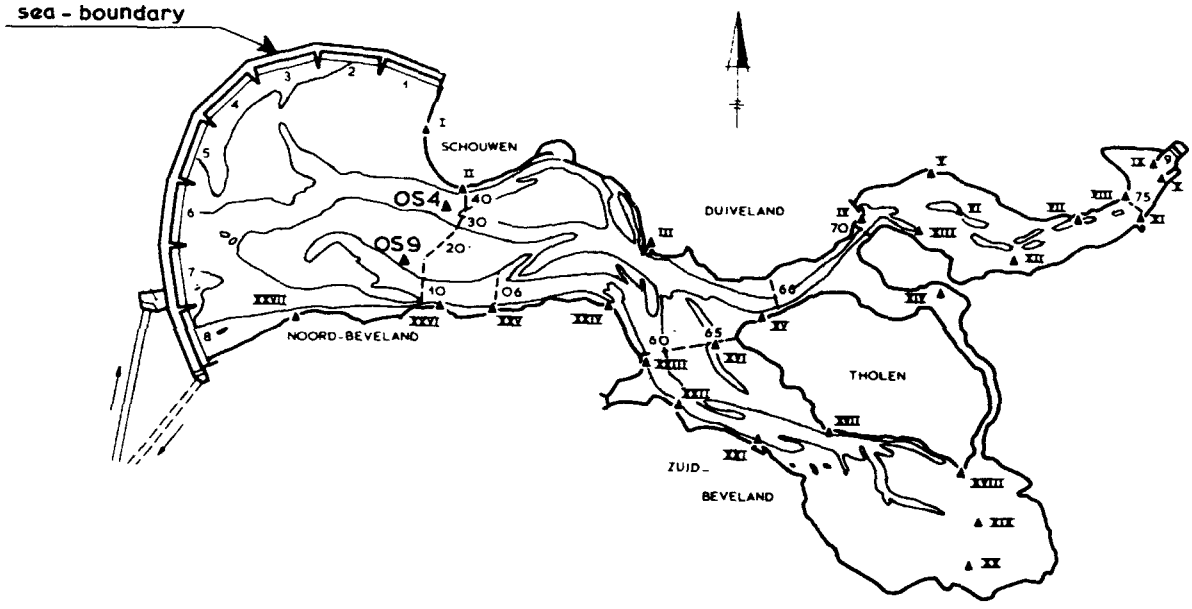

Figure 5.1 Lay-out of tidal model M1000

5.2.1 Selection of scales

Models for investigation of flows in open channels are usually built on the so called Froude-scale. This is related to the requirement that, in order to obtain a complete reproduction of the flow situation, horizontal velocities should be scaled on the scale of the celirity of tidal waves. In a more general sense, the assumption is made that inertia and gravity forces are re-

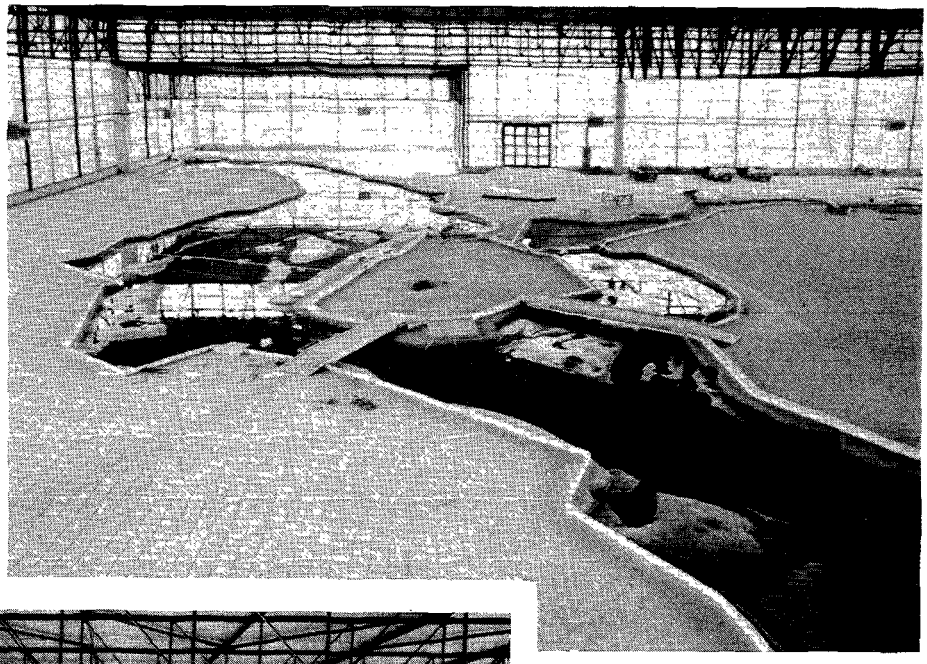

View of model
in north-eastern
direction

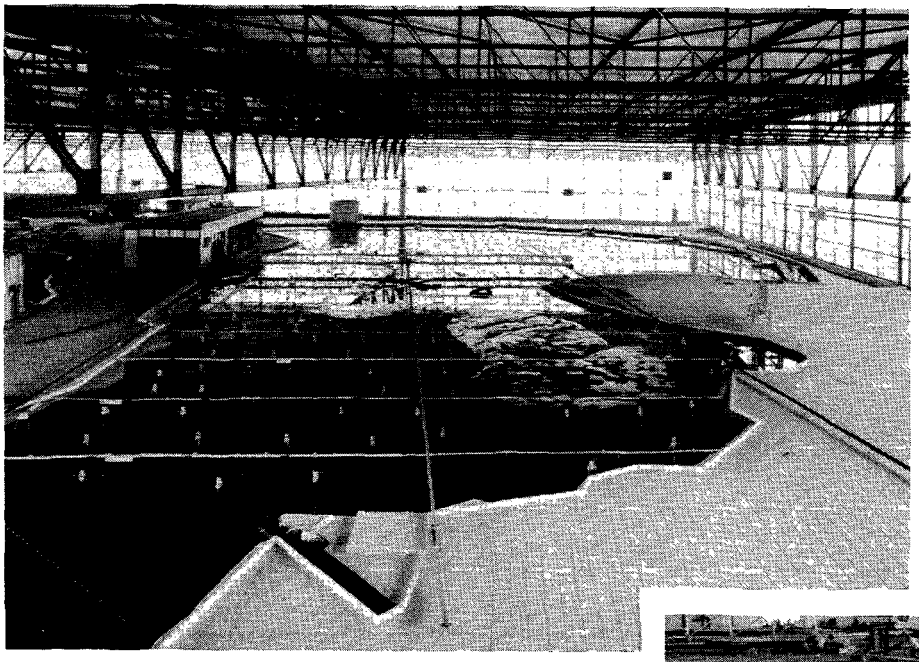

View of model
west of Zierikzee

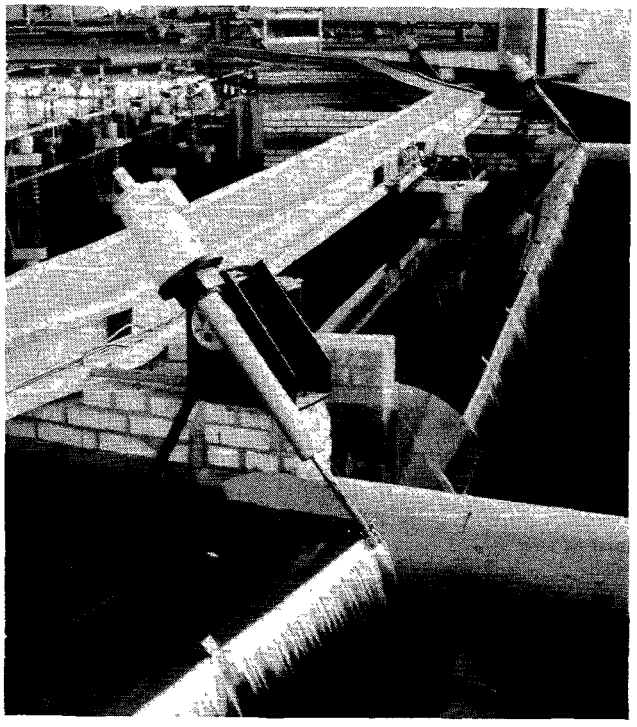

Tidal boundary of model

Fig. 5.2 Impression of overall tidal model M 1000

produced on the same scale, meaning that the Froude-number is the same for model and prototype. The definition of the Froude-number is:

$$Fr = u/\sqrt{g.h} \qquad (5.1)$$

with:

Fr	= Froude-number	(-)
u	= representative velocity	(m/s)
h	= representative waterdepth	(m)
g	= acceleration due to gravity	(m/s)

From this requirement and the requirement that the ratio between all other terms of the momentum equation (see Section 3.2) is the same for model and prototype, the following scale rules can be deducted (use is made of a scale factor n_α with n_α = value of α in prototype/value of α in model; α is a specific parameter such as length, velocity, etc.):

$$n_t = n_l/n_u \qquad (5.2)$$

$$n_u^2 = n_h \cdot n_g \qquad (5.3)$$

$$n_C^2 = n_g.n_l/n_h \qquad (5.4)$$

In equations (5.2) through (5.4) the following scale factors are used:

n_u = scale factor for velocity
n_t = scale factor for time
n_l = scale factor for length (horizontal scale factor)
n_h = scale factor for height (vertical scale factor)
n_C = scale factor for friction (C= Chézy-coefficient)
n_g = scale factor for gravity = 1

When vertical velocities can be neglected, one can consider the application of distorted models. A model with a larger horizontal scale factor than its vertical one gives not only a model with smaller horizontal dimensions, but at the same time a larger value for n_C (see equation 5.4). The Chézy-value in the model becomes smaller if the ratio n_l/n_h is larger. In such a case the hydraulic roughness of the model has to be artificially increased. This has three advantages. First, the viscosity being too large in the model would cause a risk of producing a too low C-value in the model, for which no correction

would be possible. Now the C-value should be (much) lower and with extra roughness one can always adjust the roughness until the correct value of C is reached. The second advantage is the reduction of the time scale, meaning that many more testing in a model can be done. The third advantage is that with a model on a reduced horizontal scale one can produce higher Reynolds numbers and a reduced error by surface tension (capillary effects). As a consequence on the distortion the vertical profiles of the (horizontal) velocity are slightly disturbed. The mean velocities, however, will still be correct. This means that such a model no longer fully represents the momentum equations in x, y and z directions, but only the equations in x and y directions.

The selection of the vertical scale is mainly governed by the requirement that, just as in the prototype, the flow has to be turbulent and the requirement that the water movement and water levels can be measured properly. The turbulence of the flow is assured when the Reynolds-number (Re= u.h/ν) is larger than 1000 to 2000. For the model of the Eastern Scheldt this requirement can be satisfied for most of the tidal cycle if the vertical scale is selected as:

$$n_h = 100$$

However, on the tidal flats in the model the Reynolds-number is generally too small. Therefore velocity measurements on the tidal flats are not quite reliable. Nevertheless, the storage capacity of the tidal flats can be reproduced properly, meaning that their effect on the flow in the channels is correct.

Selection of the horizontal scale $n_l = 100$ still gives a very large model. If the selected horizontal and vertical scales are not the same ($n_h \neq n_l$) , then the model is said to be distorted. The ratio of n_l to n_h is the distortion factor. When the model is too distorted, it becomes less accurate, especially when three-dimensional effects are important as in the case of flow across dams and around abutments. On the basis of systematic investigations it was concluded that a distortion factor of 4 was acceptable for the Eastern Scheldt, see [5-2]. From this the horizontal scale is derived:

$$n_l = 400$$

At a distortion factor of 4 the flow is, in fact, not correctly represented for situations with large vertical narrowing where eddies and vortices with horizontal axes occur. In a distorted model one should have, at one single

time scale, different scales of vertical and horizontal velocities; however, eddies and vorticies have only one length scale and one velocity scale. An elongated, elliptically shaped eddy cannot exist and at best it will fall apart in a series of vortices with alternately turning directions. Since M1000 had originally been built to investigate the total closure of the Eastern Scheldt, the disadvantage of distortion was accepted. For the investigations concerning the storm-surge barrier this means that, for situations with a significant vertical narrowing, problems will arise with the interpretation of the flow-patterns downstream of the barrier. This only takes place at the final stage of the barrier and at building stages concerning the placing of the sill beams. At building stages up to the completion of the rubble sill, no problems would arise with flow patterns downstream of the barrier.

By selecting $n_l = 400$ and $n_h = 100$ the other scale factors can easily be determined by using equations (5.2), (5.3) and (5.4):

$$n_u = 10$$

$$n_t = 40$$

$$n_c = 2$$

Reproducing the Coriolis-force gives the following scale rules, concerning the speed of axial rotation of the Earth:

$$n_\omega = n_h/n_l . n_u = 1/40$$

This means that the model has to rotate 40 times faster than the Earth. This can be achieved by placing the whole model on a rotating-table. However, for a model like M1000 this is impossible. For the reproduction of the Coriolis-force in the model the so-called Coriolis-tops are used (see Figure 5.3), by which the Magnus-effect causes a lift force proportional to the velocity, and simulates the Coriolis force, see [5-3]. These tops are placed only in those parts of the model where the Coriolis-force gives a measureable transverse slope to the main direction of the current. This results in the use of the Coriolis-tops west of the line Zierikzee-Colijnsplaat (see Figure 5.1).

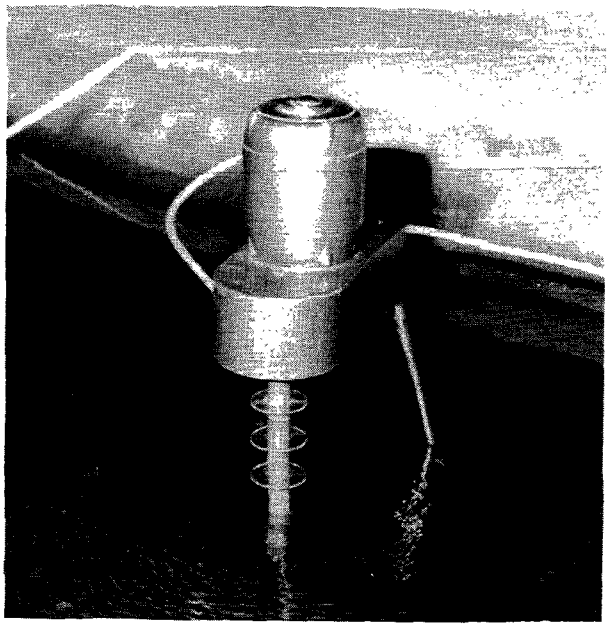

Figure 5.3 Coriolis-top

5.2.2 Schematization of the bathymetry

The bed topography of the model, representing the entire Eastern Scheldt and an adjacent part of the North Sea, was based on bathymetric surveys of the Dutch Public Works Department (Rijkswaterstaat). The model was originally based on soundings carried out in 1967. By implementing changes into the bed, large parts of the model were adjusted to the continuous changes of the bathymetry in nature.

The bed of the model was made of concrete. The profiling of the bed was carried out by using almost every available sounding cross-section from the prototype (distance apart varying from 100 to 200 m). The characteristic points in a cross-section were positioned in the model line by line. The accuracy that could be achieved is approximately 0.2 m in the vertical position and 5.0 m in the horizontal position (prototype measures).

The roughness coefficient of the bed in the model had to be twice as large as in the prototype due to the distortion (see Section 5.2.1). In the channels this was realized by fixing concrete blocks in a certain pattern and at a certain concentration on the model floor. The number of blocks in the pattern was related to the water depth (increasing depth gives increasing number of blocks). In the shallow parts of the model the extra roughness was achieved by applying gravel at a certain concentration on the model floor.

5.2.3 Boundary conditions

The position of the boundary at sea was selected in such a way that the tide at that place would hardly be influenced by the hydraulic structure to be investigated. The selection of the boundary location of the tidal model had been made by using the results of a 2D-mathematical model of the North Sea.
Figure 5.1 shows the selected boundary of the model.
The sea-boundary consisted of eight gates which could operate independently. In this way a realistic approximation of the spatial variation of phase and amplitude of the vertical tide could be achieved.
A problem was that at the location of the sea-boundary no information concerning the tide levels was available. The nearest measuring stations were, at first instance, only Vlietepolder and Burghsluis; later the stations OS 9 and OS 4 (about 1 km offshore the location of the dam; see Figure 5.1) became available.
For the adjustment of boundary conditions first an approximation was made for the water levels at the boundary site by extrapolation of the observations to the locations of the boundary. In an iterative process the definite boundary conditions were determined by an adjustment, more or less based on trial and error, in such a way that in the entire model a correct reproduction of vertical and horizontal tide was achieved.

5.2.4 Calibration and verification

The calibration of the tidal model had been carried out on basis of the prototype measurements performed on 11th september 1968. On this day extensive measurements of the currents and the water levels were carried out. The tidal range gave a good representation of the mean tidal range. Figures 5.4 through 5.6 show some results (discharges and water levels) of the calibration on the tide of 11-09-1968. In [5-4] an extensive presentation of the results is given. The good reproduction of the prototype measurements could be achieved by optimization of the boundary conditions at the gates of the model and locally adjusting the roughness.
In the course of the lifetime of the model several verifications (or re-calibrations) had been carried out. The verifications were necessary so as to investigate how the model performs at different tides (such as spring-tide and neap-tide). Moreover verifications were necessary out because the bathymetry of the Eastern Scheldt changed continuously. On the other hand, dam sections were constructed which influence the tidal movement in the Eastern Scheldt.

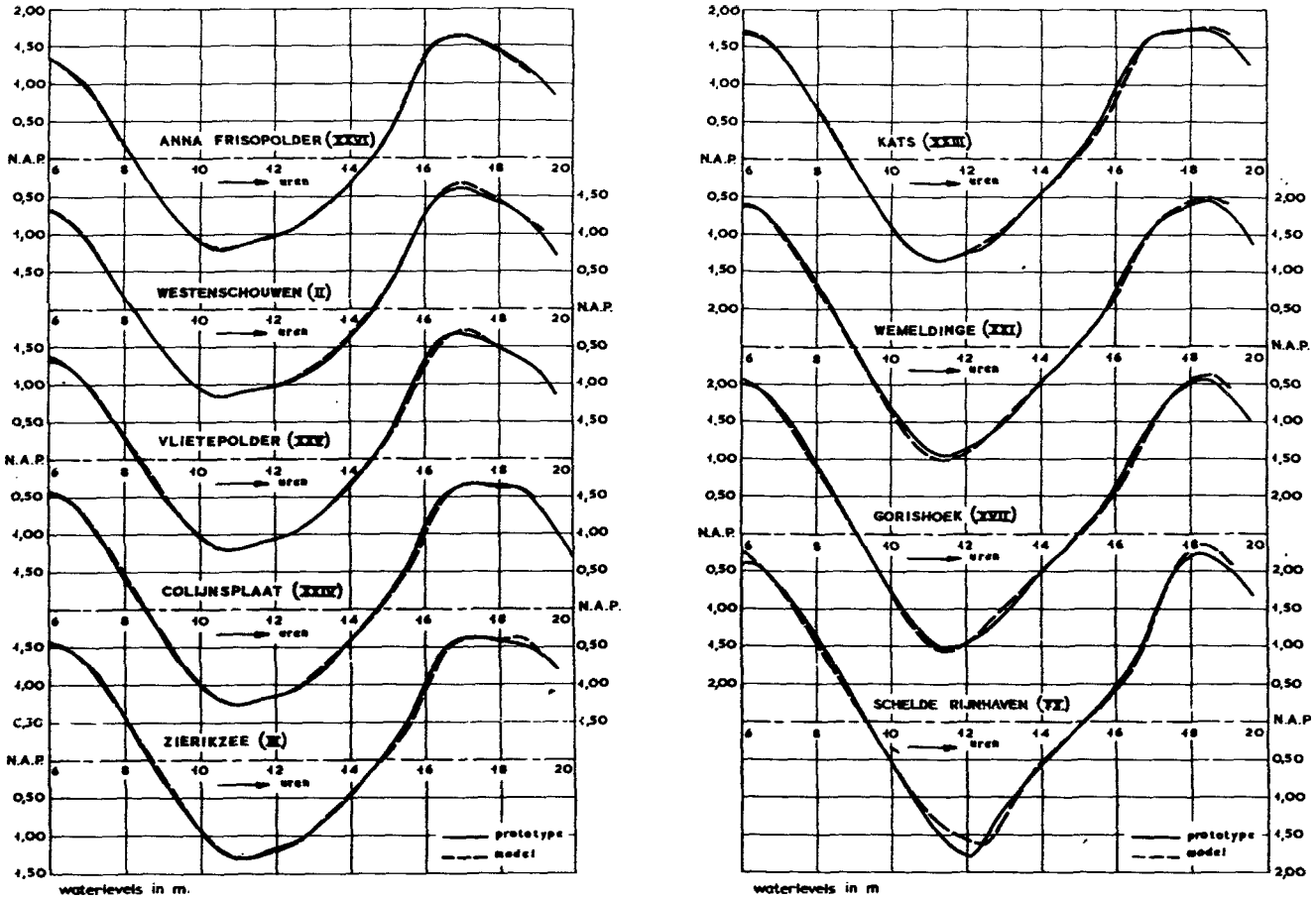

Figure 5.4 Results of calibration on tide 11-09-68; water levels

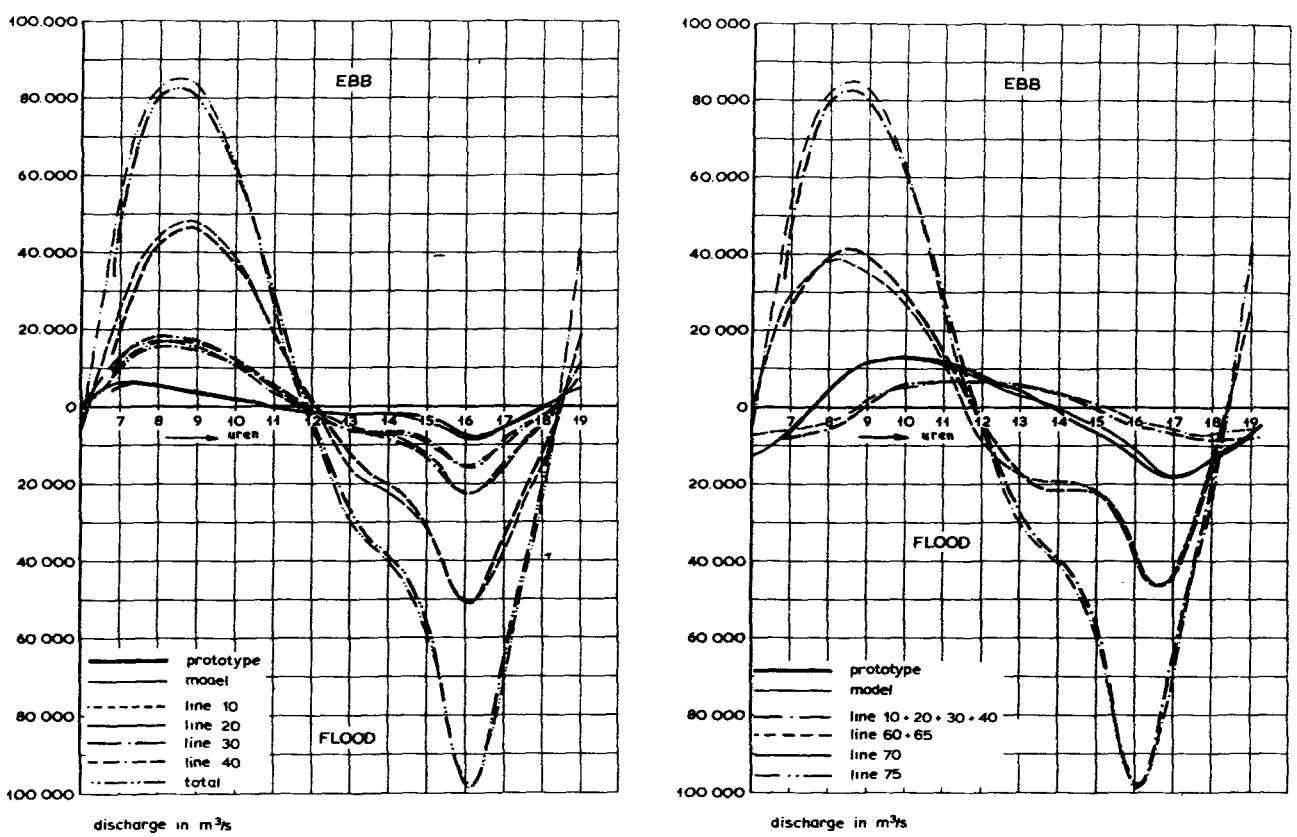

Figure 5.5 Results of calibration on tide 11-09-68; discharges

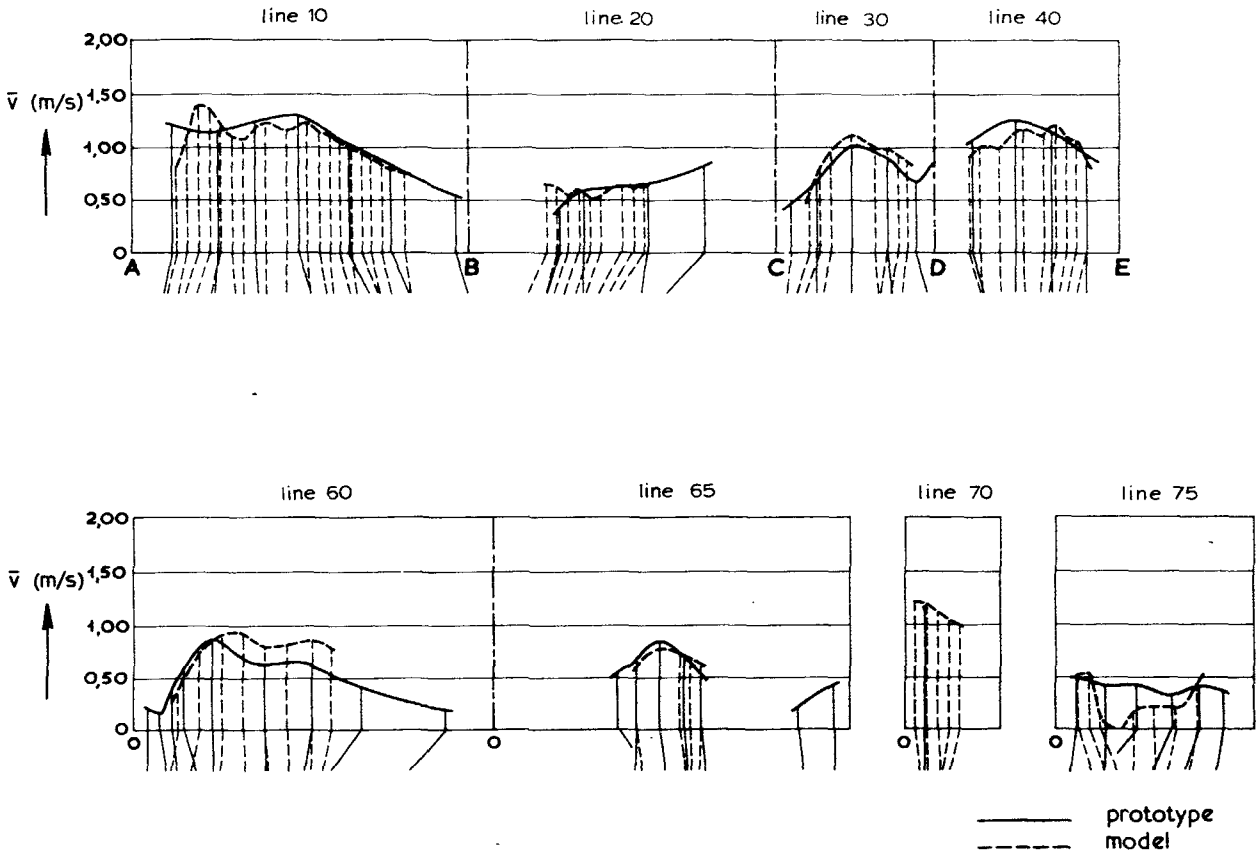

Figure 5.6 Results of calibration on tide 11-09-68; velocity distribution flood

With the reproduction of more recent prototype measurements the actual building stage was represented and eventually also the change in the bathymetry. Figure 5.7 shows some results of a verification for the tide of 27-07-81. An extensive representation of verification results is given in [5-5], [5-6] and [5-7].

From the results of the calibration and the verification, the following figures related to the achieved accuracy (standard deviation) were derived:

- water levels: accuracy in amplitude better than 2% and in phase better than 5 minutes;
- discharges: accuracy in amplitude better than 5% and in phase better than 10 minutes;
- velocity distribution: accuracy better than 0.15 m/s (maximum velocities were in the order of 1.5 m/s).

5.2.5 Available tides

As mentioned in the preceding section, the model was calibrated on the basis of measurements in nature. The tide during these measurements was used afterwards as a boundary condition for further investigations. A disadvantage of such a tide is that the absolute value of the results was strictly limited to

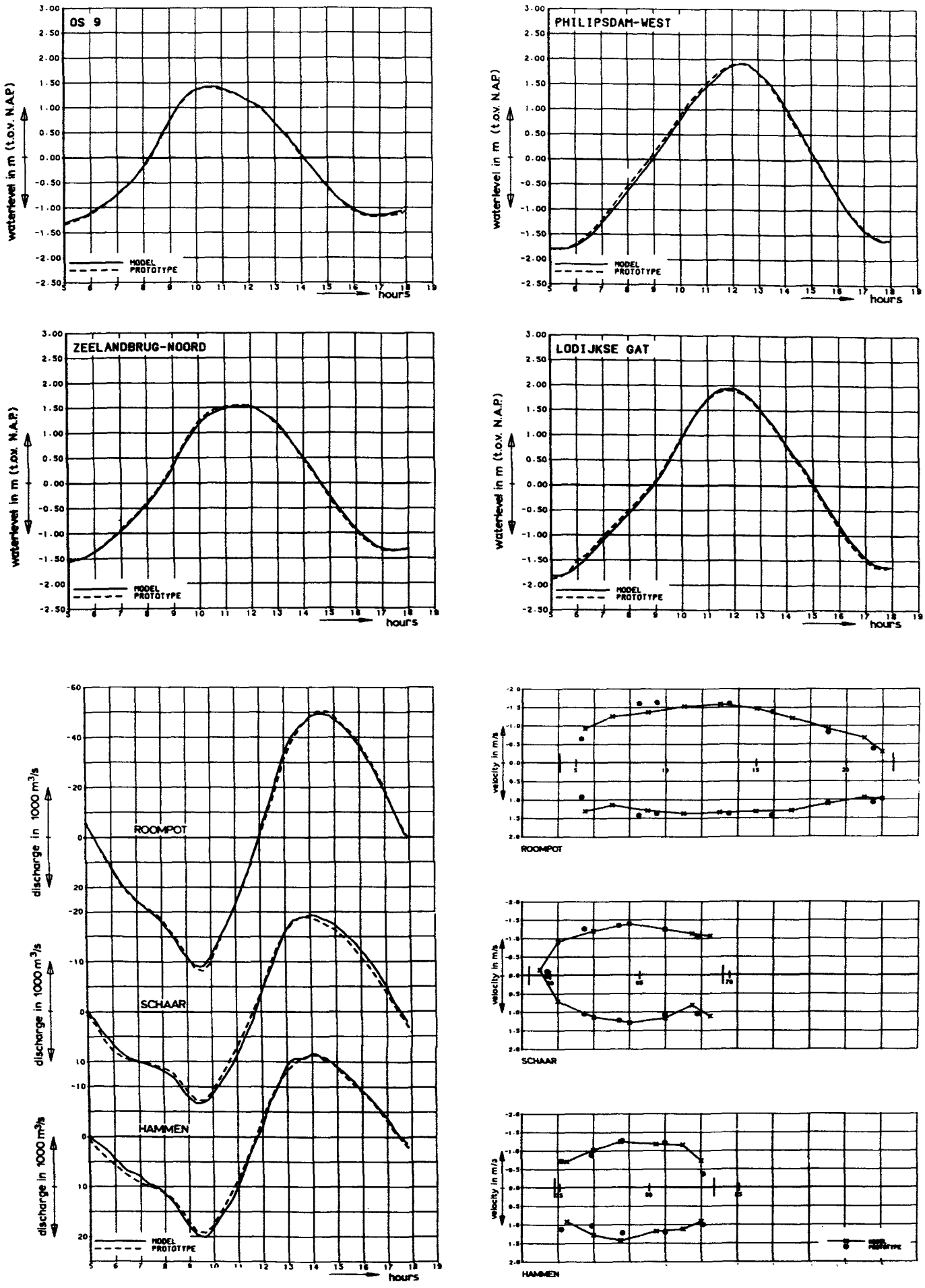

Figure 5.7 Results of verification on tide 27-07-81
water levels, discharges and velocity distributions

a single tide with specific characteristics which occured in the past.
For certain applications the use of natural tides is not useful because the stochastic element is unknown. This is the reason why sometimes use was made of a "representative average" of mean tides. Generation of such an average tide in the model gives problems in view of the absence of a set of results from measurements (only averaged water-level curves are available).
The same problem arises with the adjustment of a storm surge. The reproduction of a storm is only possible by using (historical) recordings of water levels. For the adjustment of a (design) superstorm, water levels are not available, so in this case fictive boundary conditions had to be applied.
As a result of the calibration and verification of the tidal model and later the adjustment of other tides, boundary conditions were available for a number of tides. In Table 5.1 an overview of the available tides is given.

kind of tide	date	remarks
observed tide	11-09-68	mean tide
	15-04-70	neap tide
	07-10-71	spring tide
	10-08-74	mean tide
	04-09-75	mean-spring tide
	27-07-81	mean-neap tide
	31-07-81	mean-spring tide
	11-01-82	strong spring tide
average	1961.0	average of mean tide 1951-1960
	1971.0	average of mean tide 1961-1970
storm	07-04-43	
	superstorm	fictive storm with design H.W.

Table 5.1 Available tides

5.3 **Execution of the investigations in model M1000**

5.3.1 Instruments and measurements

With specially constructed probes the following parameters were measured in the model:
- water level with a water-level follower (WAVO)
- current-velocity and direction with a combined instrument (SRM)

The 'WAVO' was of the type 'pointe vibrante' and the instrument was able to measure the water level with an accuracy of 0.1 mm, which means 0.01 m on the selected vertical scale. Figure 5.8 shows the instrument and the measuring probe.

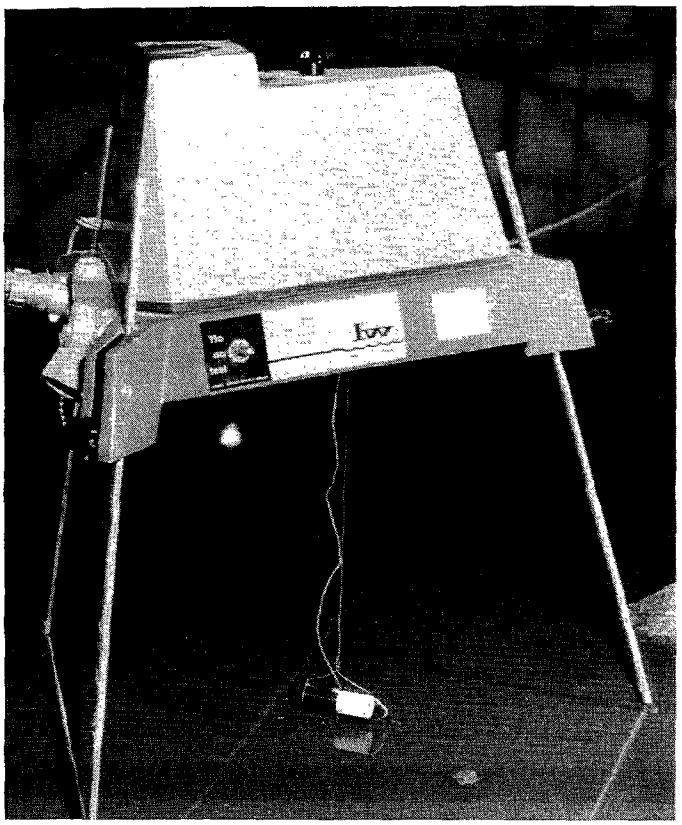

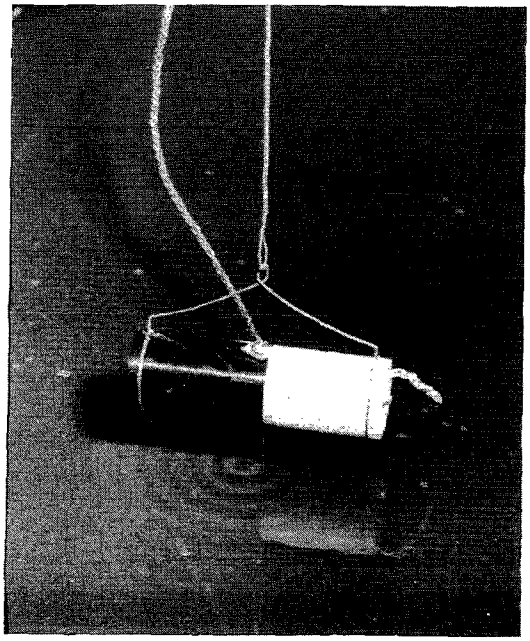

detail of measuring probe

Figure 5.8 Waterlevel follower (WAVO)

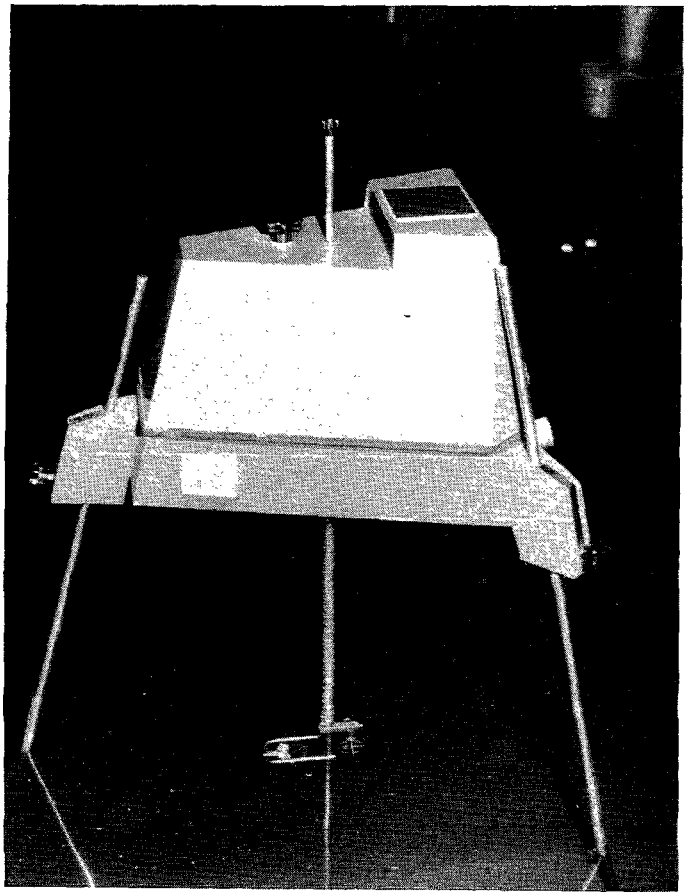

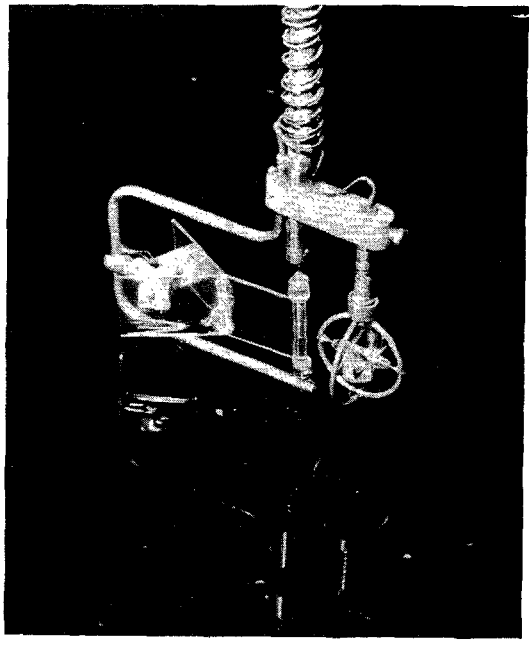

detail of measuring probe

Figure 5.9 Current velocity and direction recorder (SRM)

The 'SRM' consisted of a vane and a micro propeller (see Figure 5.9). The vane adjusts itself in the direction of the current and at the same time the micro-propeller is kept in the proper posititon according to the direction of the current (axis of the propeller parallel to the direction). The inaccuracy range of the measured velocity is approximately 5%. Due to the selected vertical scale and the dimensions of the 'SRM' the velocities cannot be measured in those parts of the model with a water depth less than approximately 6.0 m.

Recording of the flow pattern can be made by using photo cameras and plastic floats. In this way the current-velocities in the shallow parts of the model can be traced. For that purpose several remote-controlled cameras were fastened to suspension points onto the roof.

The setup of the measurements in the model was basically the same as in the prototype. For every water level or current-velocity and direction station a measuring instrument was required. The determination of the discharge in a channel could only be done by measuring the current-velocity and direction in an acceptable number of points. An essential difference with the prototype, however, is the option of repeating a specific tide in the model as often as necessary. As a consequence of this, the number of measuring points for specific tides and specific building stages is basically independent of the number of available probes. However, a good selection of the measuring points remains essential so as to reduce the time of the investigation for a given situation. Figure 5.10 gives an impression of some measurements in the model.

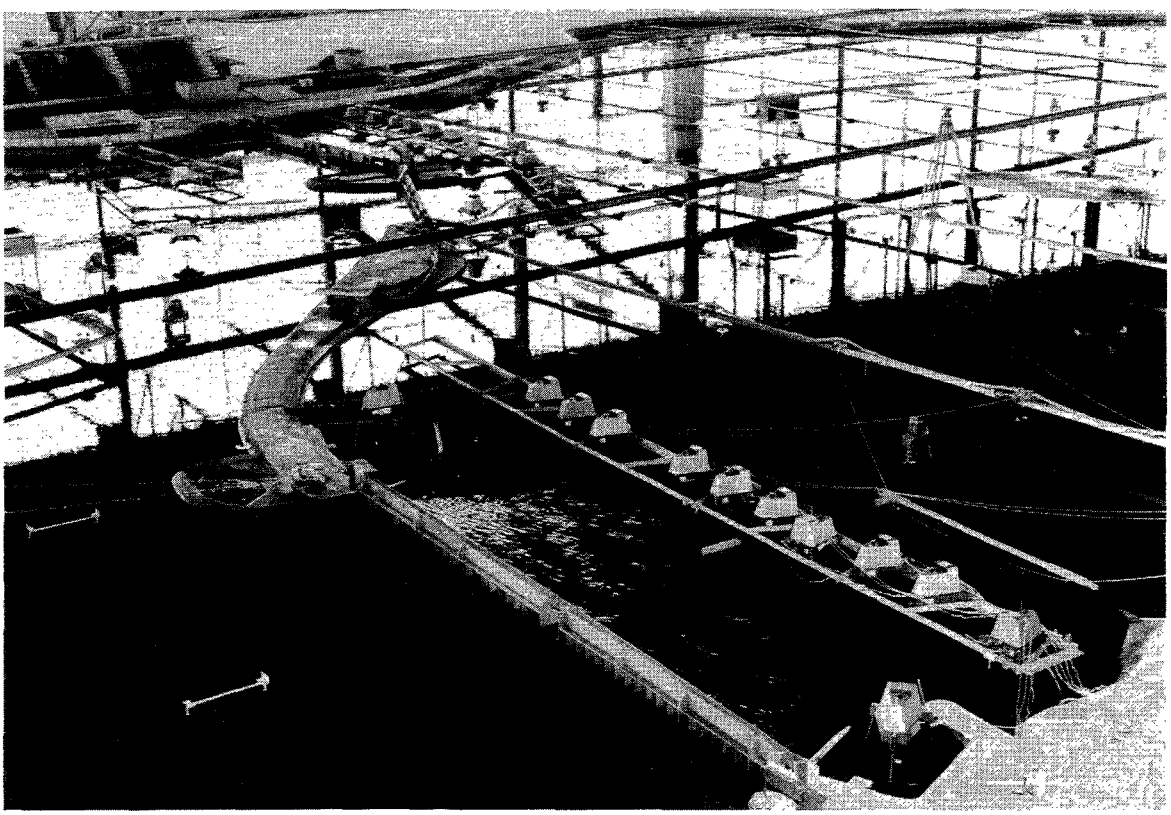

Figure 5.10 Impression of measurements in overall tidal model; water levels in working harbours and velocities in the three main channels

5.3.2 Schematization of building stages

To investigate a specific building stage of the barrier it was essential that the same building stage was built in the tidal model. For a number of reasons the representation of the barrier on the scales of the model gives some problems. In fact, an exact rebuilding on scale was hardly feasible and moreover, due to the scale distortion, gave no guarantee that the discharge characteristics of the barrier were correctly reproduced (this is the reason why it is necessary to design simplified elements; with these simplified elements any arbitrary building stage can be represented in a model).
The dimensions of the model barrier in the vertical direction and in the direction across the channel were according to the vertical scale and horizontal scale respectively. In the direction of the channel axis the dimensions were not in accordance with the horizontal scale; this resulted in a barrier which was somewhat too wide compared to a purely geometric scaling. This had to be done because otherwise the discharge characteristics could not be reproduced in a proper way. This schematization meant that in the tidal model measurements in the direct vicinity of the barrier were not useful.
For further considerations on this subject, refer to Section 4.3.3.

5.4 Results of the tests in model M1000

5.4.1 Velocities and discharges

From the results of the measurements of current-velocities and directions in points along a cross-section, several parameters could be determined, such as:
- local velocities
- velocity- and discharge distributions in a cross-section
- total discharge in a channel.

For all these parameters the variation during the tide is available.
The inaccuracy range of these measurements in the tidal model were estimated as follows:
- current-velocity 0.10 to 0.15 m/s
- current-direction 5 to 10°
- discharge 5%

This means that the velocity distributions and the discharges were a good approximation of comparable parameters in the prototype.
A few remarks concerning the velocity distribution in the vicinity of the barrier have to be made; these remarks relate to the scales of the model and the

schematization of the barrier:

- Upstream of the barrier the measured velocity distributions in the horizontal plane were a good representation of the prototype. For positions in the direct vicinity of the barrier (up to appr. 150 m off the axis), however, the distance from the axis could not directly be translated to field conditions, due to the schematization (barrier was too wide; see Section 5.3.2).

- Downstream of the barrier the measured velocity distributions in strongly narrowed situations (in vertical direction) were not fully representative for the prototype. The spreading of the flow after a vertical narrowing would behave in accordance with the vertical scale and thus interact with the 'wrong' geometry, which was reproduced at the horizontal scale.

- The discharge, determined from measured velocity distributions upstream and downstream the barrier were not affected by eventual deviations in the velocity distributions since the continuity condition was fullfilled in the model.

5.4.2 Water levels and head differences

Measuring the water levels in a number of measuring points provided information on the following parameters (variation during the tide included):

- local water level and tidal range
- head difference between measuring points (such as: head difference across the barrier and head difference across a tidal flat)

The inaccuracy range of these measurements in the tidal model could be estimated as follows:

- water level 0.03 to 0.05 m
- head loss 0.06 to 0.10 m

In connection with the distortion of the model a problem would arise downstream of the barrier, related to the interpretation of the location of the measuring point. The curvature of the surface of the water downstream the barrier was mainly determined by the vertical scale. So the location of the measuring points in the tidal model differed somewhat from the location in the prototype. This problem arose especially at building stages with a considerable vertical constriction.

5.4.3 Effective cross-sectional area

The effective cross-sectional area of the barrier could be computed from the measured discharges, water levels and head differences as follows:

$$\mu_3 A = Q/\sqrt{2g.\Delta h}$$

in which:

$\mu_3 A$	= effective cross-sectional area	(m^2)
Q	= discharge	(m^3/s)
g	= accelaration of gravity	(m/s^2)
Δh	= head difference	(m)

The computation was carried out by using values (every half hour) of discharge and head difference. This gave instantaneous values of the effective cross-sectional area. The head differences, which were used for the computation of $\mu_3 A$ were usually based on the water levels measured in the working harbours.
The computed values were related to the downstream water level and by using a least square method, the effective cross-section at N.A.P. was determined. The function: $\mu_3 A$ = F (downstream water level) was usually approximated by a straight line, if necessary separately for ebb- and flood-current.

5.5 Setup of detail scale model M1001

The M1001 model was equipped as a steady-state model and in this the terms of the continuity equation and the momentum equation in x, y and z direction were represented (except for time dependency).
With a good selection of the scales, the requirements related to the different objectives of the study can be met. In Section 5.5.1 the selection of the scales will be discussed.
Figure 5.11 gives an impression of the model.

5.5.1 Selection of scales

Since the detail model had to serve several objectives, this led to a number of, sometimes conflicting, scale-rules. Operating the model for the determination of flow patterns, etc. means the applicability of the Froude scale (see Section 5.2.1):

$$n_t = n_l / n_u$$

$$n_u^2 = n_h \cdot n_g$$

$$n_c^2 = n_l \cdot n_g / n_u$$

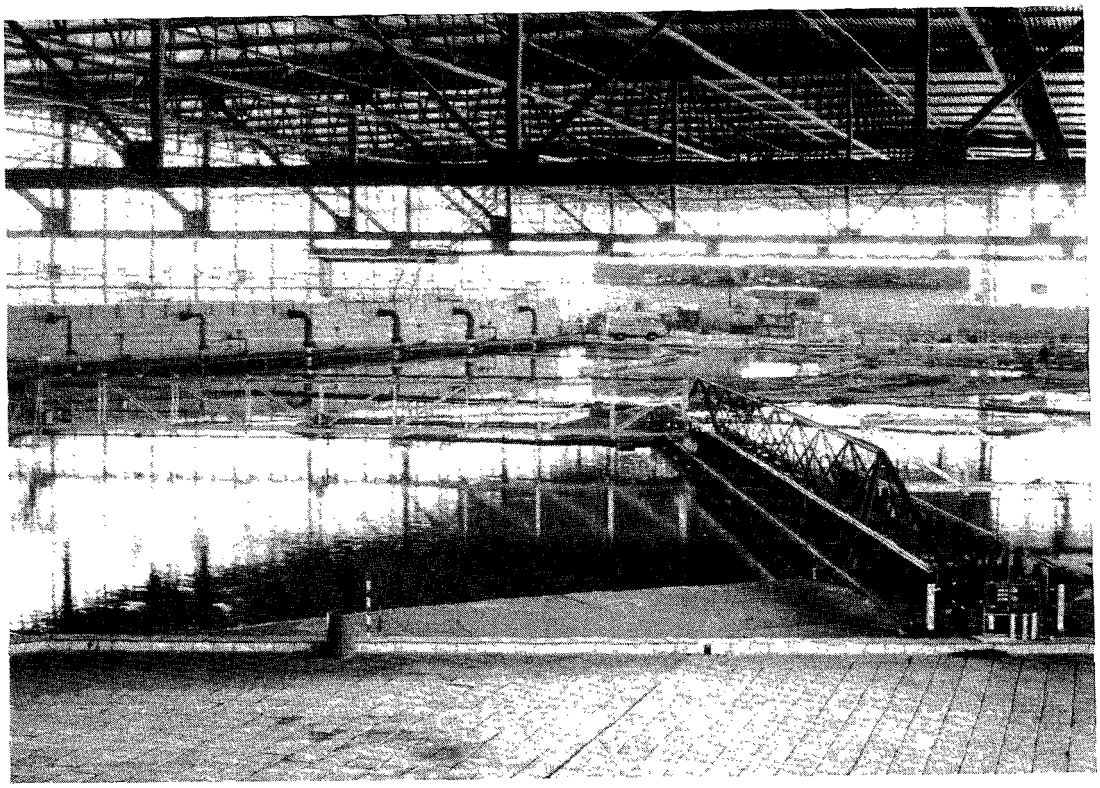

View of model in northern direction

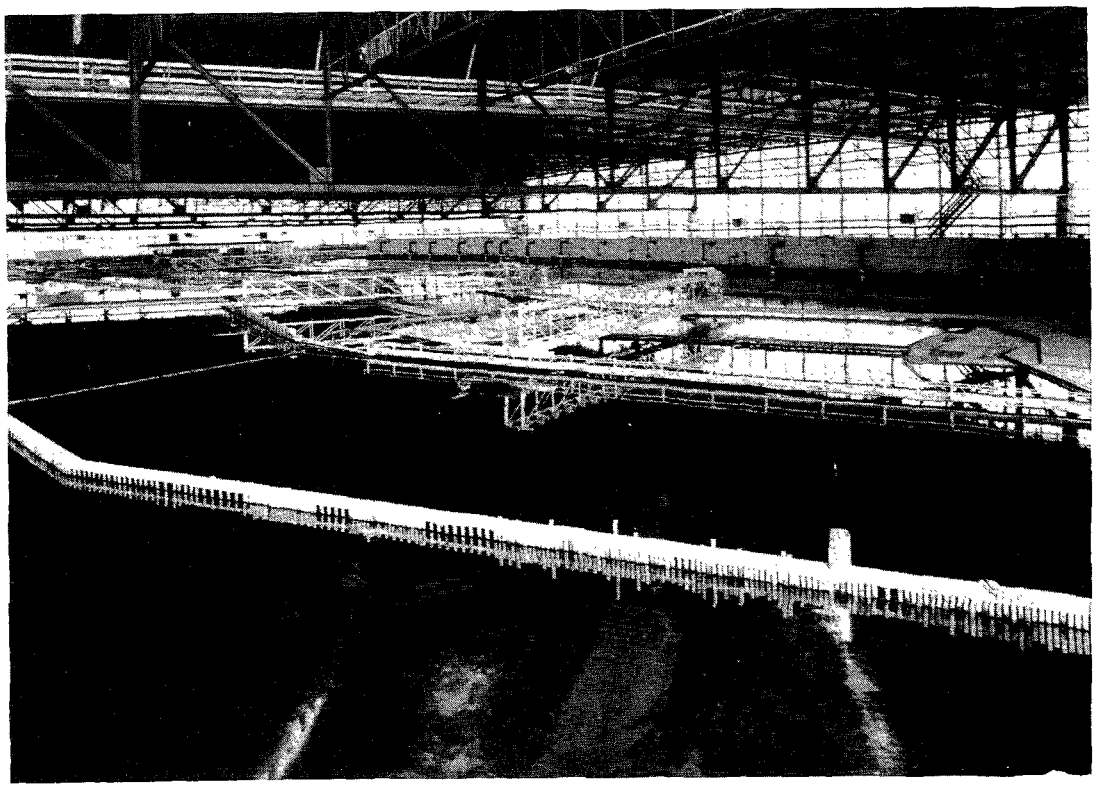

View of model in south-western direction

Figure 5.11 Impression of detail model M 1001

Investigations on local scour required a non-distorted model ($n_l = n_h$), particularly in view of correct simulation of the turbulence structure, plus that the stone diameter of the rubble cover on the bed protection which was investigated had to be representative for the bed roughness. The same requirement followed for the investigations related to the stability of rubble stone material and related to the 3-dimensional flow pattern in the vicinity of the barrier.
The selection of the vertical and horizontal scale was mainly determined by the requirement that the flow had to be sufficiently turbulent, the requirement that a scour test should fall within a working day and the requirement that the water movement, water height and scour depth could be measured accurately. On the other hand the horizontal dimensions of the model ought to be restricted so as to get a manageable size of the model.
The selected scale was:

$$n_l = n_h = 80$$

With this scale stone diameters larger than 4 mm in the model could be investigated without any scale effects (= 3.2 cm prototype); in this case viscous forces become negligible.

The execution of scour tests and the investigations on the stability of rubble gave also some supplementary restrictions and/or requirements such as:
- density and dimensions of the scouring material
- density, shape and dimensions of the rubble

Extensive discussion on this subject is beyond the scope of this report. For further information on this subject reference is made to [5-1].

5.5.2 Schematization of bathymetry

The bed topography of the model, representing an area of approximately 2.5 to 3.0 km on both sides of the barrier, was based on bathymetric surveys by the Dutch Public Works Department. The model was originally based on soundings carried out in 1967. By carrying out adjustments of the bed of the model, large parts of the model were adjusted to changes of the bathymetry in nature. For the investigations of future building stages, the bed was partly based on predictions of the future development of the bathymetry.
The bed of the model was built of concrete. The profilation of the bed was carried out by using almost every available sounding cross-section from the prototype (distance apart varying from 100 to 200 m). The characteristic

points in a cross-section were positioned in the model line by line. During building it was necessary to use 1 or 2 lines inbetween so as to achieve a satisfactory accuracy of approximately 0.2 m in the vertical position and 1.0 m in the horizontal position.
No additional roughness elements were applied in this model. Since the model was not distorted, this meant that the scale factor concerning the friction is near n_c = 1. The possible differences in effective roughness between a concrete bottom and a sandy bottom were judged to be of minor importance for the investigations.
On both sides of the bed protection works in the main channels the bottom was represented by a movable bed. The movable bed consisted of polystyrene grains which were stored in deepened parts of the model floor. The depth of these parts in the model was approximately 0.3 m (= 24.0 m in reality) below the original level of the bed, so this gave also the maximum scour depth. The length was 550 m (perpendicular to the axis of the barrier). When no scour tests were performed, the movable bed parts were covered by (ballasted) cloths yielding a completely fixed bed model.

5.5.3 Boundary conditions

The boundaries of the detail model M1001 were formed by the coastal lines of Noord-Beveland and Schouwen and by two boundaries with a series of adjustable gates almost perpendicular to the coast. The position of the gates was approximately 2.5 to 3.0 km east and west of the axis of the barrier. Figure 5.12 shows the model with the selected boundaries.

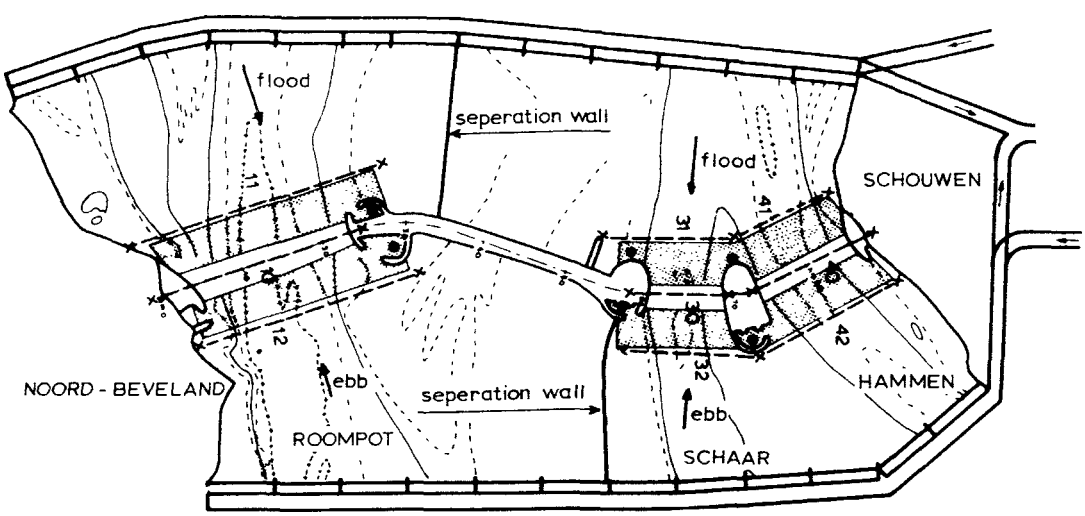

Figure 5.12 Lay-out of detail model M 1001

The model was equipped as a steady-state flow model. Both gated boundaries of the model could be used for the inflow of water (control of discharge) or for the outflow of water (control of water level). The western boundary consisted of thirteen sections and the eastern boundary of twelve sections. Each section could be controlled independently of the others. In this way it was possible to reproduce in the model ebb or flood flows alternately.
The boundary conditions were derived from the measurements in the tidal model M1000, from a test with an identical building stage of the barrier.
Usually the flow conditions at maximum ebb and/or maximum flood were selected for the investigations in the detail model.
For the inflow boundary a discharge-distribution was prescribed. The water-level in the model was controlled by the gates of the outflow boundary. Moreover, the required velocity-distribution in a cross-section near the inflow boundary could be reproduced by adjusting a grating downstream of that boundary.

5.5.4 Calibration

The detail model did not have to be calibrated in the same manner as with the tidal model. The original situation was not reproduced but the tests in the model started with the investigation of a situation with completed working harbours and a completed dam in the shallow parts.
In fact, every test in the detail model started with a reproduction of the velocity distributions and water levels (measured from the tidal model). It was expected that the flow pattern in the relatively short model would be highly dominated by the prescribed boundary conditions, but it turned out that the reproduction of the velocity distributions was rather difficult. The cause of the problems was the absence of the dynamic effects (with its influence of filling and emptying of the tidal flats) and probably differences in the roughness of the bed (too smooth). By means of a grating directly downstream of the inflow boundary (see also Section 5.5.3) this problem could be solved satisfactorily.

5.6 **Execution of the investigations in the model M1001**

5.6.1 Instruments and measurements

In the model the following parameters were measured with specially constructed probes:

- water level with a water-level follower (WAVO) and/or a point gauge
- current-velocity and -direction with a combined instrument (SRM) and/or an OTT-current meter

- scouring depth with a profile follower (PROVO)

The description of the WAVO and SRM is already given in Section 5.3.1. In this Section only the other instruments will be discussed.

The use of point gauges for the determination of the water level was restricted to a number of fixed measuring points (mostly in the working harbours) and was in first instance necessary to control the water level in the model. Additionally, these gauges could provide the head difference across the barrier. The accuracy of the water-level gauges was approximately 0.1 mm, meaning 0.01 m on the selected vertical scale.

Measurements with an OTT-current meter were usually carried out only to control the adjustment of the boundary conditions. For this application the measurements of the current-velocity were mostly restricted to one characteristic height in the vertical, at 0.4 times the depth from the bottom which approximated the average velocity in a (well-developed) vertical.

The 'PROVO' consisted of a measuring rod with an electrode (see Figure 5.13). With a servo-mechanism this rod was kept at a small distance above the polystyrene bed. The 'PROVO' was mounted on a moving carriage.

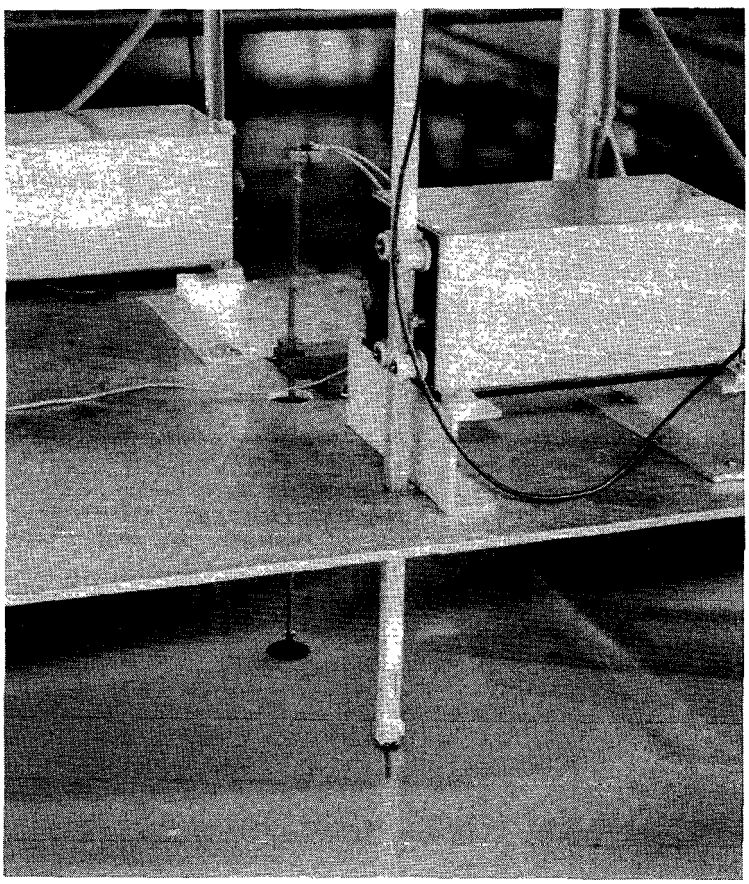

Figure 5.13 Profile follower (PROVO)

Measurements of the bed level took place in lines perpendicular to the axis of the barrier. The accuracy of the measured bed level (or scouring depth) was approximately 0.1 m (prototype value).

In the detail model the surface flow pattern could be recorded with photographic cameras. From the photographs the current-velocities could be determined and a general impression was obtained of separation points and the location of eddies.

The setup of the measurements of current-velocity and -direction were, just as in the tidal model, basically the same as in the prototype. However, the selection of the measuring points differed from the tidal model. In the detail model most information were gathered in the direct vicinity of the barrier (and in the compartments between two piers). Figure 5.14 gives an overall view of measurements in the vicinity of the (model) barrier.

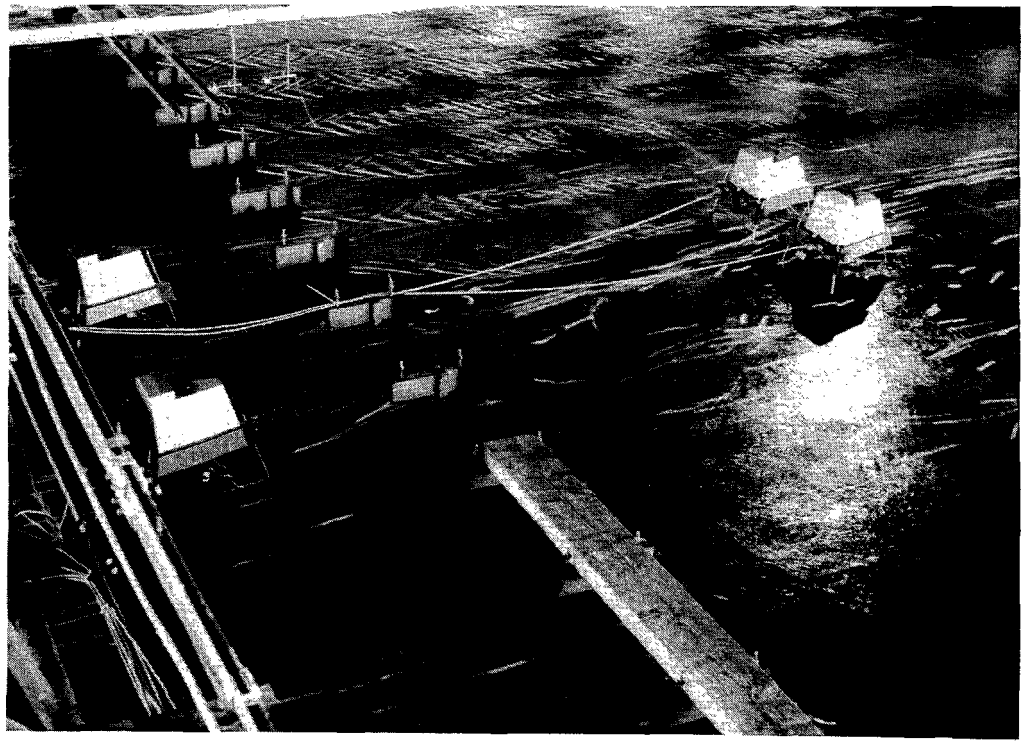

Figure 5.14 Impression of measurements in the detail model, water levels in vicinity of barrier

The execution of scour and stability tests was quite different. However, a discussion of these tests is beyond the scope of this report.

5.6.2 Schematization of building stages

Just as for the tidal model, schematized elements of the barrier had been designed for use in the detail model. In connection with the scale of the model it was hardly possible to construct the numerous elements of the barrier in full detail on that scale (see also Section 5.3.2).
On the basis of the results of the investigations on the discharge coefficient, simplified elements were built for all locations in the closure gaps. With these elements any arbitrary building stage could be represented in the model. For further information, refer to Section 4.3.3. Figure 5.15 gives an impression of a building stage in the model (piers placed and rubble sill partly completed).

Figure 5.15 View of building stage in the model; placed piers and rubble sill partly completed

5.7 Results of the tests in model M1001

5.7.1 Velocities and discharges

From the results of measurements of current-velocities and -directions in points along a profile (and in the vertical), some derived parameters could be determined, such as: local velocities, horizontal velocity-distributions and vertical velocity-profiles. Figures 5.16 and 5.17 show some examples of the

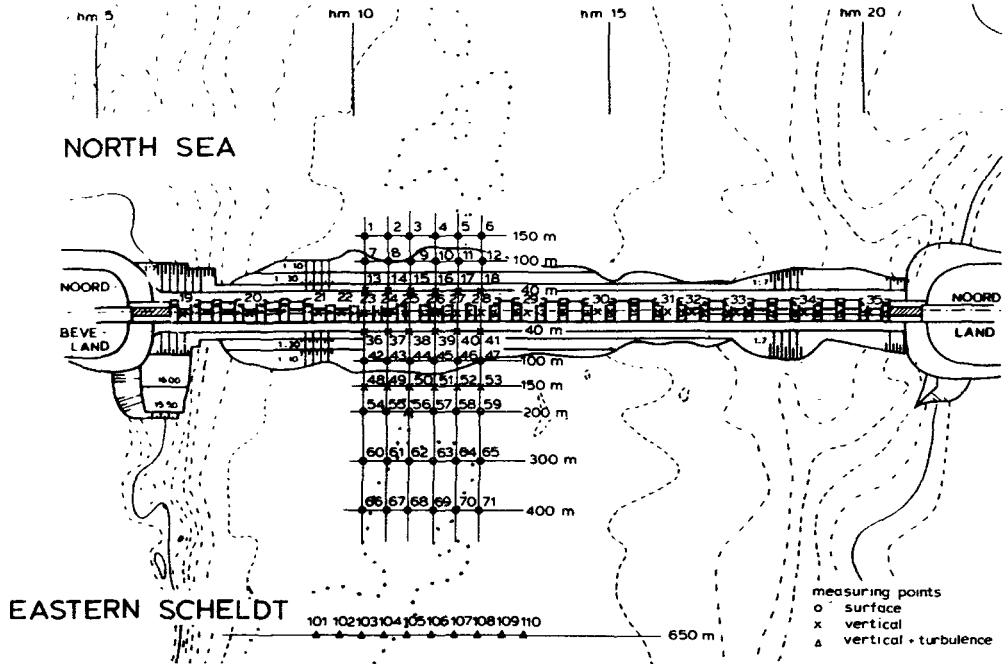

MEASURING SCHEME

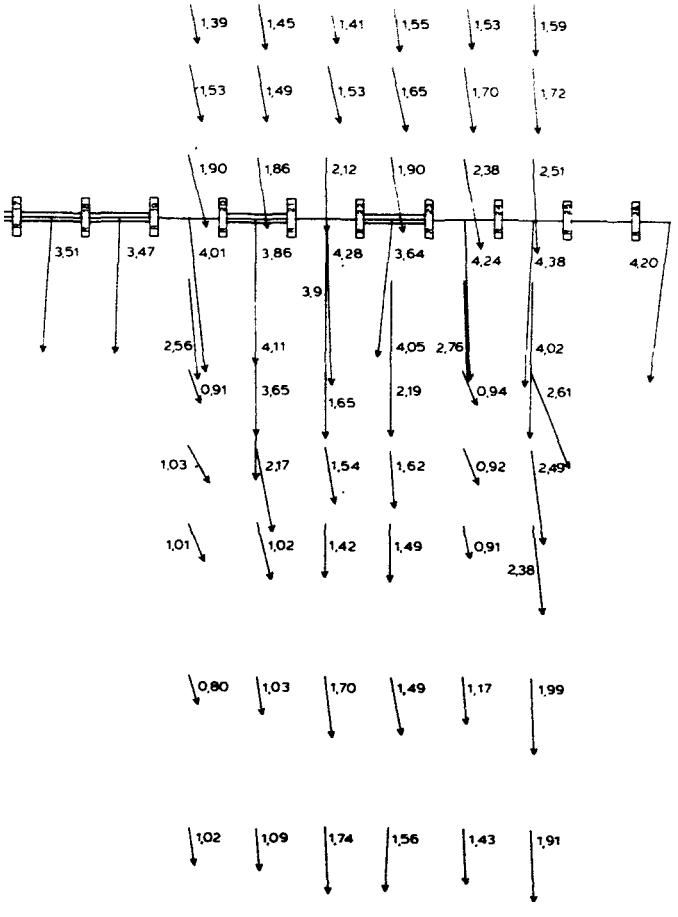

VELOCITIES AT SURFACE

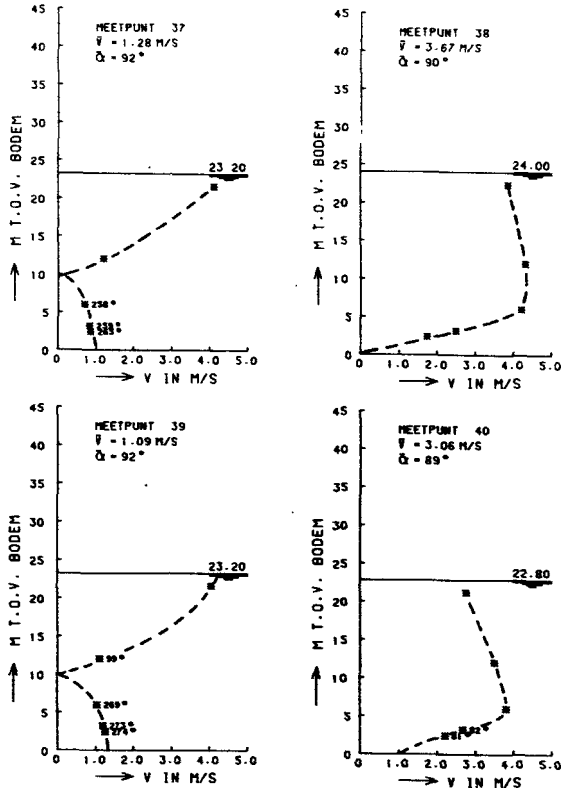

VELOCITY PROFILES

Figure 5.16 Results of velocity measurements in Roompot channel near a construction front (building stage with rubble sill completed and 19 sill beams installed)

results of the measurements. The determination of the discharge in a main channel did only make sense as a control of the velocity measurement; the discharge itself was imposed as a boundary condition.
Furthermore the measurements of the velocities could provide information about the turbulence characteristics of the flow.

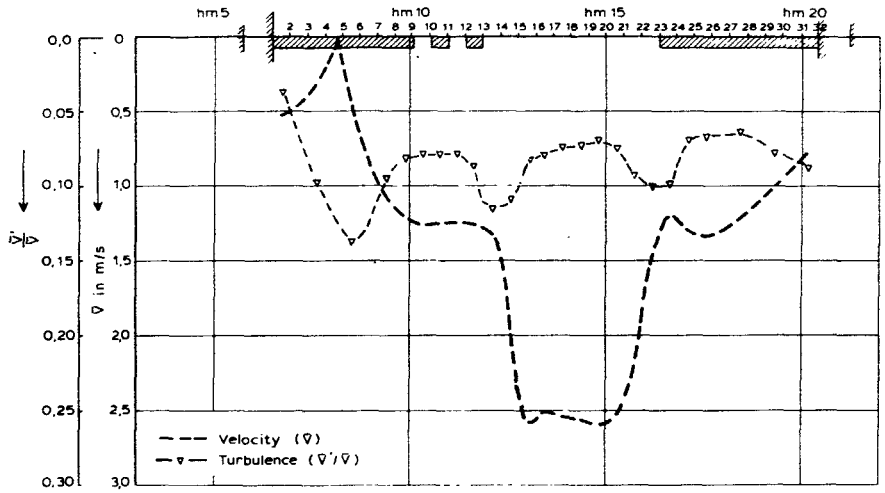

Figure 5.17 Distribution of velocity and turbulence intensity at end of the bed protection works in Roompot channel (building stage with 21 sill beams installed)

5.7.2 Water levels and head differences

Measuring the water levels in a number of points resulted in information about the following parameters:

- local water level
- local slopes of water level (eventually between the piers)
- head loss

In this detail model of the barrier the curvature of the water level in the vicinity of the barrier was a very realistic approximation of the prototype since the model was not distorted.

5.7.3 Effective cross-sectional area

The effective cross-sectional area of the barrier could be computed by using the measured discharges, water levels and head differences (see Section 5.4.3). The computation was, of course, only carried out for maximum ebb and maximum flood.

From these results the effective cross-sectional area at N.A.P. was determined, assuming that μ_3 does not change with a (slight) change of the downstream waterlevel.

5.7.4 Scour depth and stability of materials

Measuring the scour depth several times during a test and in a number of longitudinal sections gives as a result the relation of scour depth versus time. From the results of the tests and some additional information (see [5-8] and [5-9]) the scour in the model can be translated into the scour in reality. The obtained time-scour lines for the various sections are the basis for prediction of expected scour in a specific building stage.

The stability tests give information on the critical velocity or critical head difference for specific parts of the designed rubble stone structure (particularly the top layer) and the bed-protection works. It can be judged to what extent the measured critical head difference does meet the design criterion. The stability tests in the detail model were carried out to get an overall view of the rubble stability in the entire closure gap. Furthermore stability tests were carried out for situations and locations with an expected influence from bottom topography and/or geometry of the closure gap. Figure 5.18 illustrates the flow during stability tests for the compartment between the first pier and the abutment.

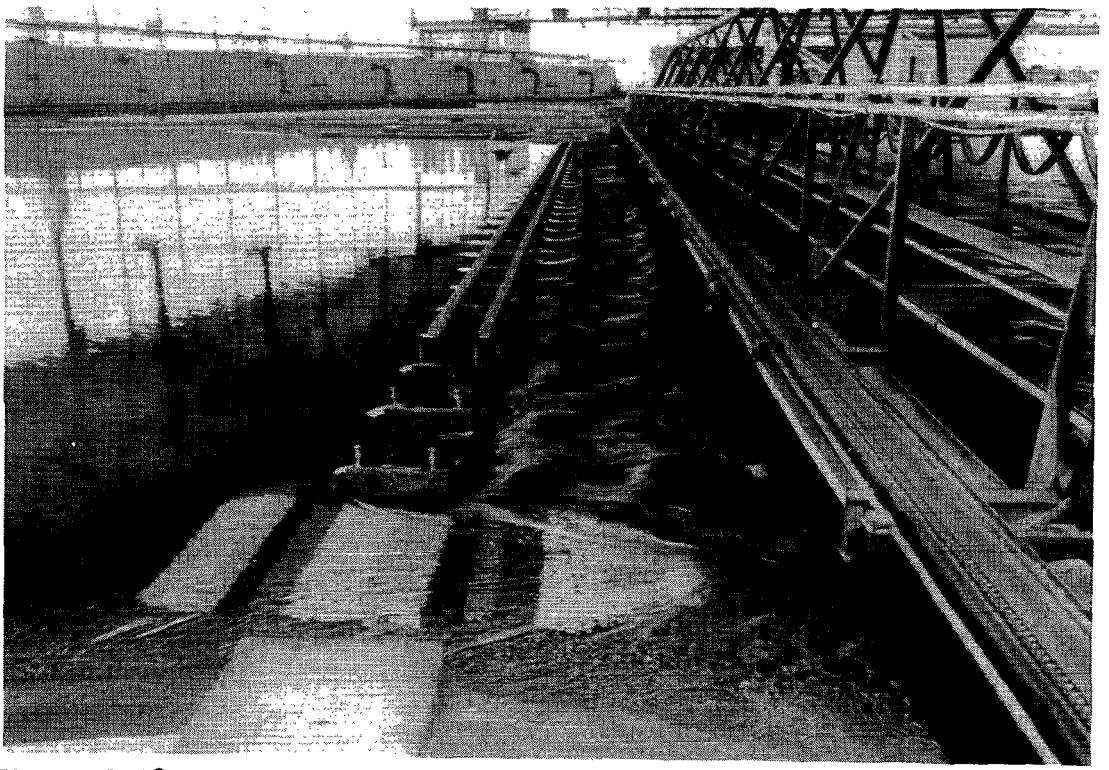

Figure 5.18 Flow pattern at stability test for compartment between first pier and abutment

References of Chapter 5

[5-1] DELFT HYDRAULICS and Warnaar H.S. and Derks H.
Enclosure Eastern Scheldt, Tidal model Eastern Scheldt and detail model closure gaps, Design and building of models, M1000/M1001 part I, June 1971 (in Dutch)

[5-2] DELFT HYDRAULICS and Rees A. van
Discharge coefficients of closure gaps in distorted models, M711-XIV, 1972 (in Dutch)

[5-3] DELFT HYDRAULICS
The magnus-effect at cylindrical tops with discs and the application in hydraulic model, M1000, 1970 (in Dutch)

[5-4] DELFT HYDRAULICS and Roode F.C. and Wijngaarden N.J. van
Enclosure Eastern Scheldt, Tidal model Eastern Scheldt, Calibration of model, M1000-II, November 1971 (in Dutch)

[5-5] DELFT HYDRAULICS and Wijngaarden N.J. van and Hartsuiker, G.
Enclosure Eastern Scheldt, Tidal model Eastern Scheldt, Reproduction of model, M1000-VI, December 1981 (in Dutch)

[5-6] DELFT HYDRAULICS and Hartsuiker, G.
Storm surge barrier Eastern Scheldt, Tidal model Eastern Scheldt, Reproduction of tide of 4th September 1975, M1000 part 14, September 1980 (in Dutch)

[5-7] DELFT HYDRAULICS and Hartsuiker, G.
Storm surge barrier Eastern Scheldt, Tidal model Eastern Scheldt, Reproduction of prototype tides, M1855, December 1982 (in Dutch)

[5-8] Rijkswaterstaat
Investigations on the possibility of enclosure of Eastern Scheldt with a partly prefabricated storm surge barrier, Final report part 2, Hydraulic aspects, December 1984, (in Dutch)

[5-9] DELFT HYDRAULICS and Driegen J.
Storm surge barrier Eastern Scheldt, Review of methods for prediction and monitoring of scour at the end of the bed protection, Evaluation scouring investigations, Q635, January 1988 (in Dutch).

6. One-dimensional models; IMPLIC-R1495

6.1 Introduction

The Eastern Scheldt estuary was modelled by a one-dimensional model, based on Rijkswaterstaat's computer program IMPLIC. Of all mathematical models, this one-dimensional model was used most during the construction of the storm-surge barrier, since it was suitable for operational forecasts, because of its fast operation speed. The main function of the IMPLIC model was to compute the water levels in the Eastern Scheldt, the head differences over the barrier and the discharges through the three main channels in which the barrier was being built.
In addition to the one-dimensional model, a model was available to compute the lateral distribution of the transport rate along the barrier. This so-called R1495 model makes use of on the distribution of the hydraulic resistance along the barrier.

With the combination of IMPLIC and R1495 the average velocity per barrier gate (q/A) could be computed. The parameter q/A was one of the basic hydraulic parameters for the design and construction of the storm-surge barrier, see Section 2.3. During the construction of the barrier most design parameters for the construction phases were computed with the models IMPLIC and R1495. After placement of the piers also all operational forecasts were computed with these models. The more sophisticated, and thus more time consuming and expensive, models such as the scale models M1000 and M1001, and the two-dimensional WAQUA models, were mainly used for calibration and verification of IMPLIC-R1495 and to obtain functional relations between, for example, local velocities and average velocity or between stability of rubble layers of the sill and average velocity or head difference (scale model M1001).
Throughout all construction stages of the barrier good results were obtained with the IMPLIC-R1495 system (see Section 8.1).

In this chapter a description is given of the models IMPLIC (Section 6.2) and R1495 (Section 6.3) and of the integrated model that was used for the forecasts (Section 6.4).

6.2 One-dimensional tidal model IMPLIC

6.2.1 Model description

The one-dimensional tidal model IMPLIC is based on a numerical solution of the one-dimensional long-wave equations; equations 6.1 and 6.2 (see Chapter 3 and Figure 6.1):

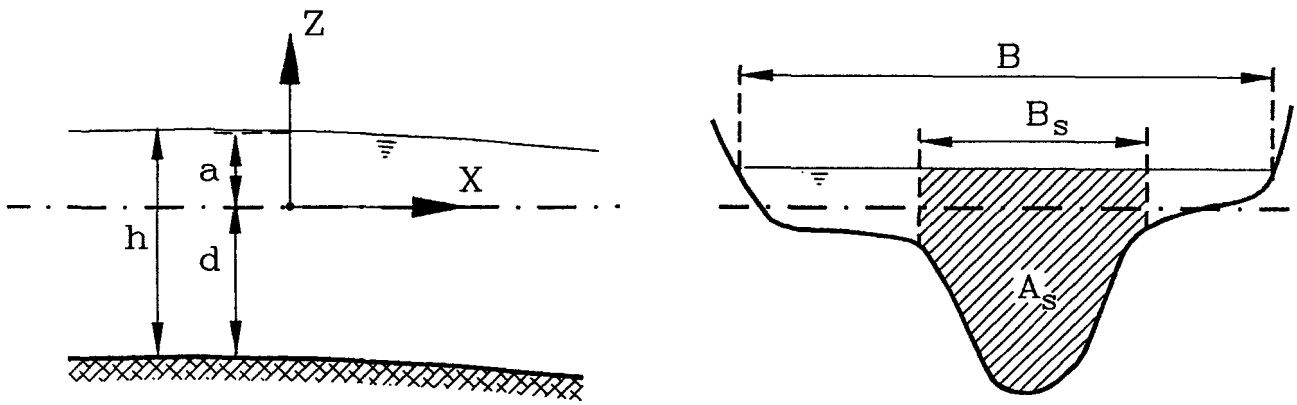

Figure 6.1 Parameters one-dimensional long-wave equations

$$\frac{\partial A}{\partial t} + \frac{\partial Q}{\partial x} = 0 \qquad (6.1)$$

$$\frac{\partial Q}{\partial t} + \frac{\partial}{\partial x}\left(\frac{Q^2}{A_s}\right) + gA_s\frac{\partial a}{\partial x} + g\frac{Q|Q|}{C^2RA_s} - \frac{\rho_a C_D B_s W^2 \cos\phi}{\rho_w} = 0 \qquad (6.2)$$

where:

Q	=	discharge	(m^3/s)
B	=	width at the watersurface	(m)
B_s	=	width of the flow area at the surface	(m)
d	=	distance from the bottom to the reference plane	(m)
a	=	water elevation relative to the reference plane	(m)
h	=	water depth (= d + a)	(m)
A	=	total area = $\int_{-d}^{z} B\,dz$	(m^2)
A_s	=	flow area = $\int_{-d}^{z} B_s\,dz$	(m^2)
C	=	Chézy coefficient for bottom friction	($m^{1/2}/s$)
g	=	acceleration due to gravity	(m/s^2)
R	=	hydraulic radius	(m)

C_D	= coefficient for wind-shear stress	(-)
W	= wind speed	(m/s)
ϕ	= angle between wind direction and channel axis	(°)
ρ_w	= density of water	(kg/m³)
ρ_a	= density of air	(kg/m³)

The equations 6.1 and 6.2 are solved with an implicit method, described in [6-1], [6-2].

The model is based on a number of assumptions, which are the basis for the one-dimensional long-wave equations (St-Venant hypotheses):

1. Velocity distribution, perpendicular to the main flow direction, is uniform.
2. Water surface, perpendicular to the main flow direction, is horizontal.
3. Vertical accelerations and vertical curvatures of stream lines are negligible.
4. Energy losses are conform a stationary approach (Chézy formula).
5. Very gentle bottom slopes; cosines of these slopes are close to one.

The consequences of these approximations are extensively discussed in [6-2]. Abovementioned assumptions were not fullfilled at the location of the barrier, here a set of modified equations had to be used (see Section 6.2.3 and Chapter 4).

6.2.2 Bottom geometry

For a one-dimensional model as IMPLIC, the Eastern Scheldt had to be schematized as a system of channels and nodes. The location of these channels and nodes was clearly defined for areas with pronounced channels separated by relatively high tidal flats. The Eastern Scheldt east of the line Zierikzee-Colijnsplaat (see Figure 2.4) was such an area. For the area seawards (west) of the storm-surge barrier, the locations of the channels and the nodes were not well defined. However, on the basis of the flow patterns, already known from the overall tidal scale model, a one-dimensional schematization could be made. When a basically two-dimensional area is schematized as a one-dimensional network on the basis of the flow pattern, special attention must be paid to situations where the flow pattern will change due to the construction activities. Such a change in the flow pattern was induced by the construction sequence of the barrier from north to south. This resulted in a change in the distribution of the hydraulic resistance over the main channels in which the barrier was under construction. For these situations a check was made with the two-dimensional WAQUA models.

The IMPLIC schematisation of the Eastern Scheldt is based on bathymetric surveys by the Dutch Public Works. Originally the schematization was based on data from around 1970. At the end of 1982 large parts of the schematization were revised, based on the results of more recent surveys from around 1980. In 1984 the area seawards of the storm-surge barrier was revised. Here special attention was paid to the expected changes in the flow pattern, caused by the construction scheme of the barrier. In addition to these major revisions a number of small modifications were made.

The number of revisions illustrated the importance of a flexible geometry simualtion, especially for a highly movable bed as in the Eastern Scheldt estuary. This was one of the major advantages of a numerical model. The final schematization comprised 230 channel sections and 171 nodes (see Figure 6.2 and [6-2]).

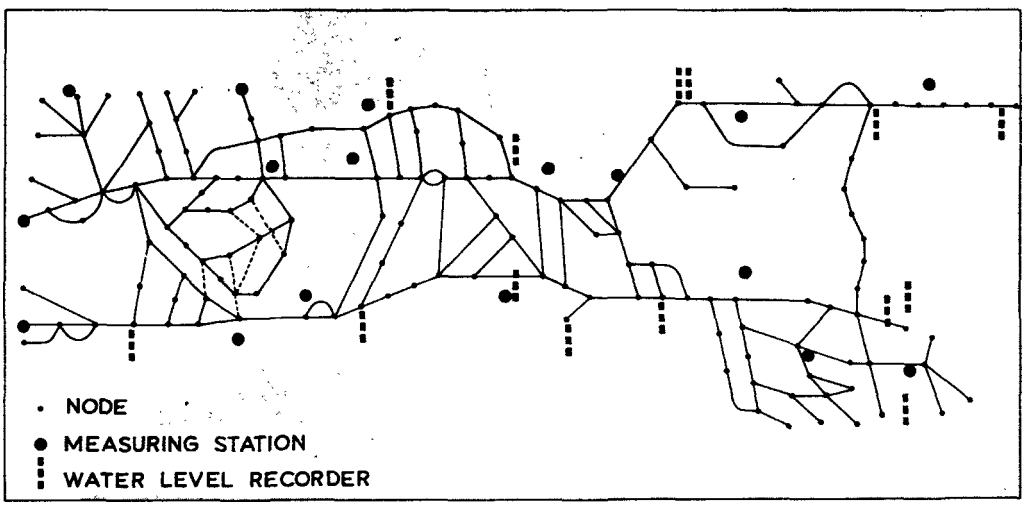

Figure 6.2 One-dimensional schematization of the Eastern Scheldt

The bottom friction was modelled by the Chézy formula. For the IMPLIC model the Chézy value was not directly derived from field data or from theoretical considerations. The procedure was as follows:

- Field data and theory gave the limits for the Chézy values.
- Within these limits the Chézy values were varied to calibrate the model.
- For the Eastern Scheldt this led to Chézy values ranging from 30 to 50 $m^{\frac{1}{2}}/s$ (see [6-2]).

The schematization procedure was, to some extent, subjective in character and therefore had to be done by experienced people. The location of the channels

and the nodes, and even the length of a channel between two nodes were all more or less subjective choices. A risk in this approach is that errors in the schematization are later camouflaged during the calibration of the model, for example by adjusting the roughness. The result would be a model that could react physically unrealistic in situations different from the situation for which the model was calibrated. To minimize this risk checks were made with the two-dimensional models.

6.2.3 Geometry of the barrier

At the location of the barrier the assumptions upon which the long-wave approach are based were no longer fullfilled. At this site the long-wave equation was replaced by a discharge relation. This approach is described in detail in Chapter 4. The discharge relation for subcritical flow is:

$$Q = \mu_3 A \sqrt{2g\Delta h} \qquad (6.3)$$

where:

Q	=	transport rate	(m^3/s)
μ_3	=	three-dimensional discharge coefficient	(-)
A	=	wett cross-sectional area	(m^2)
g	=	acceleration of gravity	(m/s^2)
Δh	=	head difference over the barrier	(m)

The coefficient μ_3 was determined in the scale models M1000 and M1001 for various construction stages of the barrier for subcritical free-surface-flow conditions. The IMPLIC model includes a routine that modifies equation 6.3, and the value of μ_3, to the situation of subcritical flow and to supercritical flow. Including the equations that are used for the transition between the different flow conditions, seven situations are distinguished. Furthermore, different coefficients were used for ebb and flood flow directions.

6.2.4 Boundary conditions

At the seaward boundary water level (tide) curves were used as boundary conditions. The seaward boundary was located at a location some distance from the barrier where the influence of the barrier on the tide curve becomes negligible. The water levels at the boundary were derived from four permanent field stations, OS11, OS13, OS14 and OS15 (see Figure 2.4). The inner boundaries were chosen at the end of the estuary ($Q = 0\ m^3/s$).
In addition wind velocity and wind direction could be specified as boundary conditions.

6.2.5 Calibration and verification

For the calibration and verification of the model, the data obtained from the permanent field stations and the results from the measuring campaigns were used. The field stations provided water levels throughout the entire Eastern Scheldt (see Chapter 2). During the measurement campaigns the discharges of several sections were obtained. For example the discharges in the three main channels where the storm-surge barrier was projected.

The calibrated model was verified with (of course) a different set of field conditions than those that had been used for the calibration. The verification showed that the inaccuracy range of the model in the vicinity of the barrier was as follows (see [6-2] and Figures 6.3 and 6.4):

- maximum transport rates at the location of the barrier: less than 10%
- time of slack water at the location of the barrier: less than 5 minutes
- water levels in the vicinity of the barrier: maximum 5 cm.

Because the calibration and verification were performed before the construction of the barrier had started, these results were, strictly speaking only valid for the original situation without the barrier. Therefore, the accuracy of IMPLIC was checked on a routine basis during the entire construction period of the barrier. The results of this verification will be presented in Section 8.1.

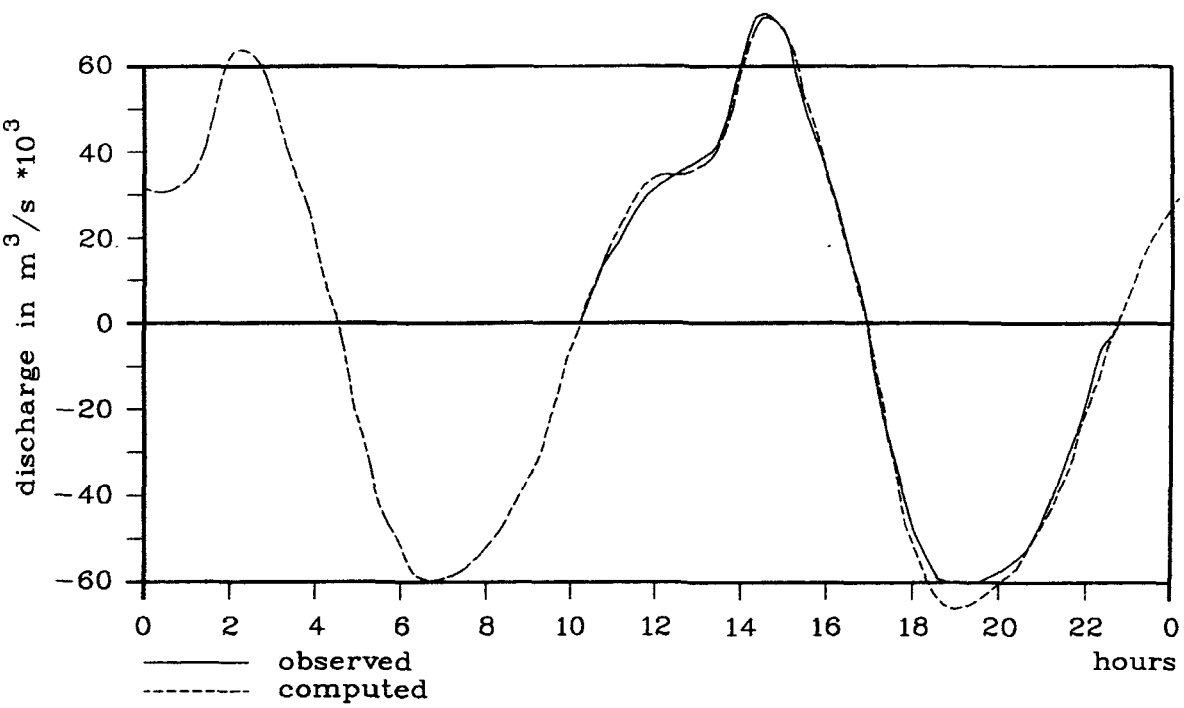

Figure 6.3 Results of verification IMPLIC model, Roompot discharge (11-01-82)

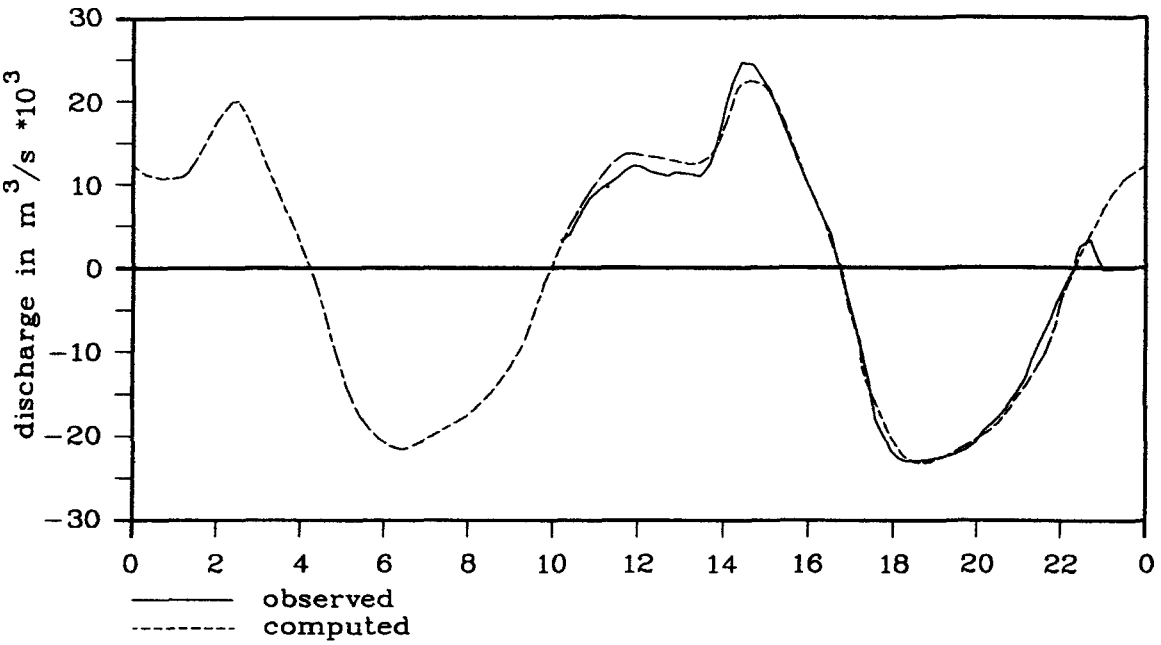

Figure 6.4 Results of verification IMPLIC model, Schaar discharge (11-01-82)

6.3 Lateral discharge distribution along the barrier: R1495

6.3.1 Model description

The so-called "R1495" model, named after the code number of the study that produced the model, computed the lateral discharge distribution along the barrier ([6-3], [6-4]). The basis for this computation was the assumption of a fixed lateral discharge distribution proportional to the lateral distribution of the hydraulic resistance along the barrier (where necessary, with an additional correction). The hydraulic resistance was represented by the value of $\mu_2 A$ per barrier section, where:

μ_2 = two-dimensional discharge coefficient (see Section 4.2.1) (-)
A = wet cross-sectional area, related to the down stream water level (m^2)

The discharge per barrier section i, q_i, is determined simply by the ratio of $(\mu_2 A)_i$ multiplied with a correction coefficient B_i:

$$q_i = B_i \frac{(\mu_2 A)_i}{\sum_{i=1}^{n} (\mu_2 A)_i} Q \qquad (6.4)$$

where:

Q = discharge through the entire channel (m^3/s)

(remaining parameters as described above)

Equation 6.4 can be derived from the equations that were used in chapter 4 to describe the discharge characteristics of the barrier.
The discharge rate through a single barrier section is given by equation 6.5:

$$q_i = (\mu_2 A)_i \sqrt{2g\ \Delta h_i} \tag{6.5}$$

The discharge through the entire channel is given by equation 6.6:

$$Q = \mu_3 A \sqrt{2g\ \Delta h} \tag{6.6}$$

When three-dimensional effects are absent, $\bar{\mu}_2$ will be equal to μ_3 (see Section 4.2.2) and the head difference over the single sections will be equal to the head difference over the entire barrier. In other words, there is no lateral exchange between the "stream tubes" through the various barrier openings. This leads to:

$$\mu_3 A = \sum_{i=1}^{n} (\mu_2 A)_i \tag{6.7}$$

$$Q = \sum_{i=1}^{n} q_i \tag{6.8}$$

$$\Delta h_i = \Delta h \tag{6.9}$$

Combining equations 6.7, 6.8 and 6.9 with equations 6.5 and 6.6 resulted in equation 6.4 with B = 1. Thus, the correction coefficient B could be seen as a correction for the influence of three-dimensional effects. These three-dimensional effects are caused by the influence of bottom geometry, abutments, lateral variation in the hydraulic resistance, etc.

The core of the R1495 model was the simple equation 6.4. Additionally the model provided an administration of the geometry of the barrier sections, the discharge coefficients and the correction coefficients. The construction of the storm-surge barrier was schematized into ten different construction stages for the main sections (Figure 6.5) and seven for the border sections. The geometry of the sections was characterized by the wet cross-section at the reference level NAP (A_{NAP}), and the width at the water surface. The hydraulic

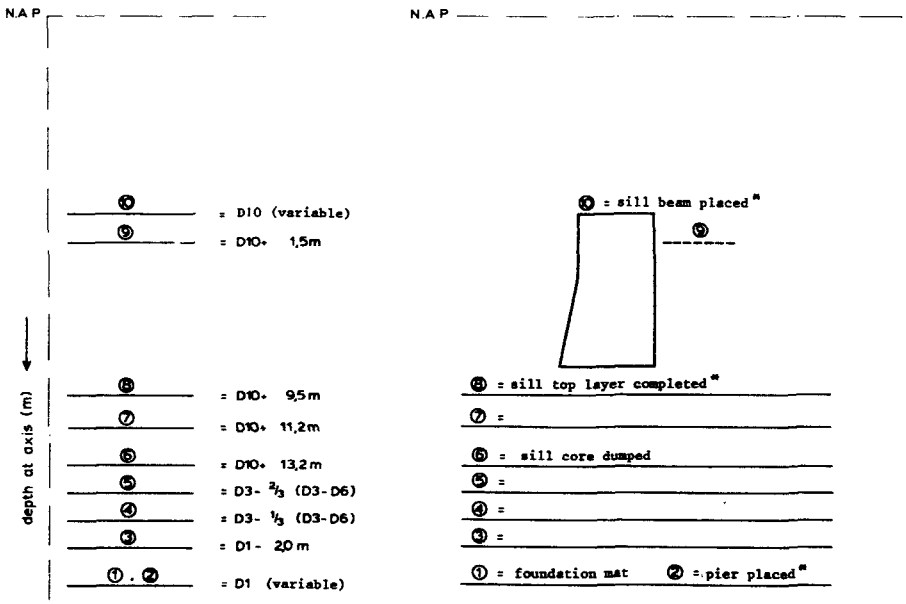

Figure 6.5 Selected construction stages per site for flume (tests(*) and schematization in the scale and numerical models

resistance was given by the discharge coefficient μ_2. The values of μ_2 have been determined through flume tests (see Section 4.3.2).

The value of the correction coefficient B was originally determined by a calibration of the R1495 model based on the results of the M1001 model (detail model of the mouth of the Eastern Scheldt, see Chapter 5). During the construction of the storm-surge barrier the set of B-values were verified with field data and modified where necesary. In the initial calibration of B the following effects were accounted for ([6-3], [6-4]):

- Bottom geometry in the vicinity of the barrier:
  This influence was dominant at the start of the building process and the hydraulic resistance of the barrier was small. The approximation of the barrier equation was too rough, in fact.

- Side abutments:
  The side abutments caused local contraction of the flow. This effect was schematized by a simple non-dimensional correction function on the discharge distribution in the vicinity of the side abutments. The influence of the abutments gradually diminished as the hydraulic resistance of the barrier increased.

- Skew inflow:
  The discharge coefficient, μ_2, was derived for a flow direction perpendicular to the axis of the barrier. For oblique flow the value of μ_2 was no longer correct and a correction was applied, based on experimental results from the scale model M1001. This is particularly the case in the vicinity of construction fronts, for example at the transition of sections with and without the rubble sill.

- Lateral variation of the head difference along the barrier:
  An abrupt lateral variation of the discharge capacity along the barrier caused a lateral variation of the head difference. In this case the assumption was no longer valid, that the lateral variation of the head difference, Δh, was negligible (see also Section 4.1.2). This effect was most pronounced for a structure consisting of sections with the sill beam installed as well as sections without the sill beam. Here an empirical correction based on scale model tests (M1001) was applied.

The approach outlined above, enabled the use of the results of the scale model tests much more effectively: The results of a scale model test were only valid for the specific geometry that had been tested. By calibrating the R1495 model to the scale model (the M1001 model) through a set of correction coefficients, the results of other geometries could be predicted without further scale model tests.

6.3.2 Boundary conditions

The boundary conditions for the R1495 model were the discharge through a main channel, Q, and the downstream water level.
These boundary conditions could either be constant values, or time series. Constant values were generally used to represent maxima, for design purposes (the steady state model M1001 fitted in this scheme). Time series were used for operational control.

6.3.3 Verification

After the initial calibration of the R1495 model on the basis of scale model tests in M1001, additional scale model tests (that were conducted for other purposes, for example tests on the stability of the bed protection) were consequentely used as a verification for the R1495 model. These verifications enabled an estimate of the accuracy of R1495 (see [6-5], [6-6]). The error in q/A was estimated to be 10% (standard deviation) for a random location and

construction stage. Combined with an error in the predicted transport rate computed with IMPLIC, this resulted in an overall error of 15% in q/A (standard deviation, errors in IMPLIC and R1495 being assumed to be mutually uncorrelated).
During the construction of the barrier a systematic verification of the models IMPLIC-R1495 was conducted on basis of field data, see Section 8.1. The overall inaccuracy of q/A turned out to be 12% (standard deviation).

6.4 Integrated model IMPLIC-R1495

Near the end of the construction activities (1986), the R1495 model was, for operational use, integrated in the IMPLIC schematisation. Each gate opening of the barrier was represented by a barrier section (see 6.2.3) in the IMPLIC model. The schematization was thus expanded with 68 sections; 62 representing normal sections and six border sections. The advantage of an integrated model was that all pre- and post-processing facilities of the IMPLIC system were also directly available for the barrier sections. Additionally, the facilities of the IMPLIC barrier routine, such as accounting for different flow conditions and the use of triggers for the gate movements, also became available for the barrier sections.

For use in IMPLIC the values of $(B\mu_2 A)_i$, computed by R1495, could not be used directly. For the IMPLIC model the sum of the effective cross-sectional areas of the sections, had to be equal to the value of $\mu_3 A$ of the barrier in the considered channel. Thus, besides B and μ_2, also μ_3 had to be incorperated.
Introducing an average value $B\bar{\mu}2$, defined as:

$$B\bar{\mu}_2 = \left(\sum_{i=1}^{n} (B\mu_2 A)_i\right)/A \qquad (6.10)$$

In the IMPLIC model the overall discharge coefficient μ_3 was used for the entire structure in a channel. The discharge coefficients for the sections had to be corrected in such a way that the average discharge coefficient for a channel was equal to μ_3. The corrected value of the discharge coefficient of a section was:

$$\mu_{i\text{-IMPLIC}} = (B\mu_2)_i * (\mu_3/B\bar{\mu}_2) \qquad (6.11)$$

Substitution of 6.10 in 6.11 gives:

$$\mu_{i\text{-IMPLIC}} = (B\mu_2)_i * \left(\frac{\mu_3 A}{\sum_{i=1}^{n} (B\mu_2 A)_i}\right) \qquad (6.12)$$

The values of the discharge coefficients (resulting from equation 6.12), the average depth of the sill and the width at the water surface per gate section (resulting from R1495) were directly used in IMPLIC. Compared to the original schematization, each channel was now represented by a number of parallel barrier sections, corresponding to the number of openings in the channel, instead of a single barrier section.

The integrated model, IMPLIC-R1495, ran on a Hewlett Packard computer system, HP1000F. The runtime was about three minutes for 24 hours simulation.

Even an extensively calibrated and verified model would not exactly reproduce all details of the prototype. For a final correction several routines, based on time-series analysis techniques, were developed to correct the forecasts for these errors. Such a final correction was specially important for the control of the more difficult operations. For example, installing of the concrete sill beams was guided by velocity measurements. These velocity measurements were also used to improve the velocity forecasts, by applying a correction based on the comparison of the computed and measured velocity [6-7]. In general, the most simple correction, by a constant factor for each flow direction, worked out well. An evaluation of the accuracy of the results of the forecasts will be given in Section 8.1.

References of Chapter 6

[6-1] DELFT HYDRAULICS and Stelling G.S.
Accuracy aspects of IMPLIC, R1484-I, 1979 (in Dutch)

[6-2] Rijkswaterstaat and Langerak A.
Revision one-dimensional tidal model Eastern Scheldt, Nota DDWT-84.024, November 1984 (in Dutch)

[6-3] DELFT HYDRAULICS and Hartsuiker G.
Computation of discharge distribution closure gaps, R1495/M1696/M1757, January 1982 (in Dutch)

[6-4] DELFT HYDRAULICS and Hartsuiker G.
Revision computational model R1495, May 1983 (in Dutch)

[6-5] Rijkswaterstaat
Flow information for the final construction stages of the storm surge barrier, BESTRO-M-84.338/SOOCOO-M-84.508, December 1984 (in Dutch)

[6-6] Thabet R.A.H. and Vlasblom H.P.L.
Forecasting current velocity on routine bases, Proceedings International Conferences on Numerical and Hydraulic Modelling of Ports and Harbours, Birmingham, England, April, 1985.

7. Two-dimensional numerical tidal models

7.1 Introduction

This chapter describes the application of two-dimensional mathematical (WAQUA) models for the computation of flow patterns in the Eastern Scheldt estuary and in the vicinity of the construction sites of the storm-surge barrier. It was the first time in the Netherlands that numerical models were used on this scale and for such detailed flow simulations.
For the computation of the flow pattern, a series of off-line nested models with a decreasing grid size, were used. In this way an increasing detail of the flow pattern could be achieved; the smallest detail, however, was equal to the dimensions of the applied grid size.
The main function of the two-dimensional models was to compute:

- the overall tidal movement (discharge and water levels)
- the mutual influence of closure gaps (asymmetric building stages)
- the flow pattern in the vicinity of the barrier (velocity- and discharge distributions upstream and downstream of the barrier and at the barrier axis).

The first application of the two-dimensional models for the Eastern Scheldt started in 1974 and after an extensive testing period it was decided in 1983 to use these models instead of the hydraulic scale model M1000.

In Section 7.2 a description is given of the WAQUA program system which is used for the computations.
A general description of the WAQUA-models used for the Eastern Scheldt, is presented in Section 7.3.
Sections 7.4 through 7.6 describe the schematization, calibration and verification of the series of models, namely the overall model of the entire Eastern Scheldt estuary, a more detailed model of the mouth of the Eastern Scheldt and the set of small-scale models in the direct vicinity of the barrier.
Finally, Section 7.7 gives a description of the operational experience with the models.

7.2 The WAQUA-system

WAQUA is a system of interlocking computer programs for the two-dimensional depth-averaged simulation of hydrodynamics and water quality in well-mixed estuaries, coastal seas, harbours and inland waters. The system can simulate the hydrodynamics in complex geographical areas and the land-water boundary is

determined by the model during simulation. The system accounts for sources of discharges, for tidal flats, for islands and dams, time-varying or constant flow restrictions in which sub- or super-critical flow occurs, and those generated by openings in dams, sluices or storm-surge barriers. The system is designed for planning, design and carrying out of engineering works and for the assessment of their impact. The input and the results of simulations can be presented in printed reports and graphical displays (time-histories, velocity and transport-vector plots, isolines of water levels and concentrations, etc.).
The system had originally been designed by J.J.Leendertse at the Rand Corporation in Santa Monica USA and had its origin in a program for computation of long-period waves [7-1]. Alongside ongoing engineering investigations, particularly for the Dutch Rijkswaterstaat (Delta Department), the system of programs was developed. Further program and system development was also done at Rijkswaterstaat, Data Processing Division and DELFT HYDRAULICS.

The partial differential equations used in the system are the two-dimensional shallow-water equations: equations 7.1, 7.2 and 7.3 (see also Section 3.2):

$$\frac{\partial(hU)}{\partial x} + \frac{\partial(hV)}{\partial y} + \frac{\partial h}{\partial t} = 0 \qquad (7.1)$$

The depth integrated momentum equations are given by Equations 7.2 and 7.3:

$$\frac{\partial U}{\partial t} + U\frac{\partial U}{\partial x} + V\frac{\partial U}{\partial y} = fV + \nu_t\left(\frac{\partial^2 U}{\partial x^2} + \frac{\partial^2 U}{\partial y^2}\right) - g\frac{\partial a}{\partial x} - \frac{g\,U\sqrt{U^2+V^2}}{C^2\,h} + \frac{\rho_a C_D\,W^2\cos\phi}{h\,\rho_w} \qquad (7.2)$$

$$\frac{\partial V}{\partial t} + U\frac{\partial V}{\partial x} + V\frac{\partial V}{\partial y} = -fU + \nu_t\left(\frac{\partial^2 V}{\partial x^2} + \frac{\partial^2 V}{\partial y^2}\right) - g\frac{\partial a}{\partial y} - \frac{g\,V\sqrt{U^2+V^2}}{C^2\,h} + \frac{\rho_a C_D\,W^2\sin\phi}{h\,\rho_w} \qquad (7.3)$$

These equations are numerically solved on a staggered grid using an ADI-method. The numerical scheme is unconditionally stable for flows without special structures such as barriers. The original numerical method, developed by J.J.Leendertse, was improved by G.S.Stelling [7-2]. Already mentioned previously are the special features in the system to account for energy-losses, caused by the storm-surge barrier, and to represent the process of drying and flooding of tidal flats.

A set of data, specifying all the input necessary to run a simulation for a particular area, is called a WAQUA-model. Part of the WAQUA-system is the Input Data Processor which checks and reports the given model-input. Graphic

display programs for visualizing input data and simulation results have been used for many illustrations in this report. Other post-processing programs are used e.g. for the computation of discharge coefficients.

7.3 General description of the WAQUA-models used

The development of the WAQUA program system was strongly stimulated by the applications required by the Delta Department. A model for the Haringvliet was followed by the general model for the coastal area and the estuaries in the Delta, RANDDELTA-2 (see Figure 7.1). In this model the influence of the closure of the Eastern Scheldt (and later the construction of the storm-surge barrier) on the adjacent sea area, could be investigated [7-7] and [7-8]. Although computed water levels were in good agreement with observed water levels, the grid size of 800 m in this model was too coarse to reproduce the transport rates in the entrances of the Eastern- and Western-Scheldt estuaries. So the 400 m grid model SCHELDES was built (see Figure 7.1). To make

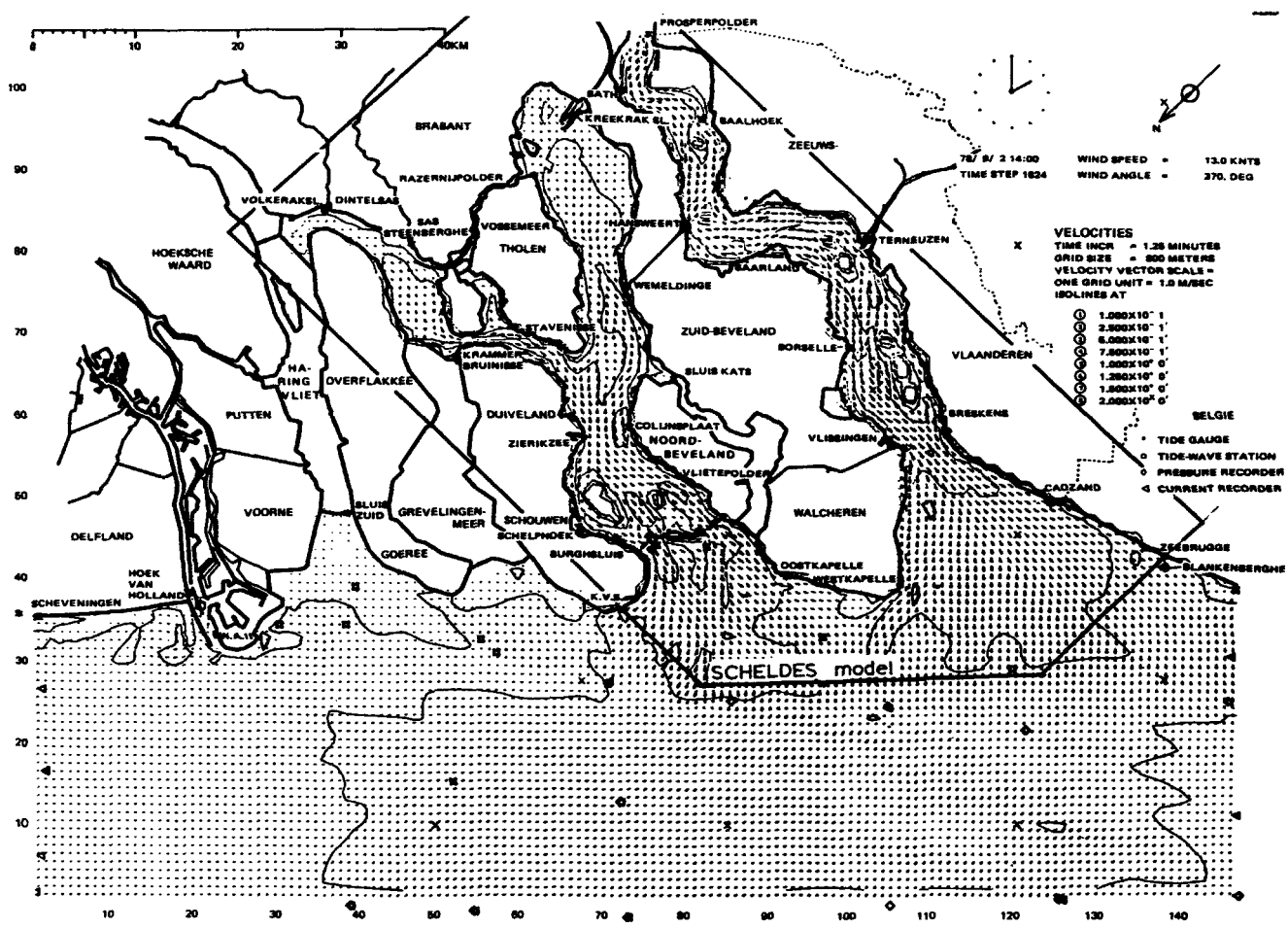

Figure 7.1 RANDDELTA-2 model (800 m grid) and nested SCHELDES model (400 m grid)

the calibration of these models easier and to reduce computer time, these models were divided into several 800 and 400 m submodels. An overview of these models can be found in [7-3].
One of the 400 m submodels was the overall model of the Eastern Scheldt OOST-2. A comparison of this mathematical model with the hydraulic scale model of the same area, M1000, showed that both models gave equivalent results [7-4]. A seaward extension of the model resulted in the frequently used model OOST-3 [7-6](see Figure 7.2), described in Section 7.4.

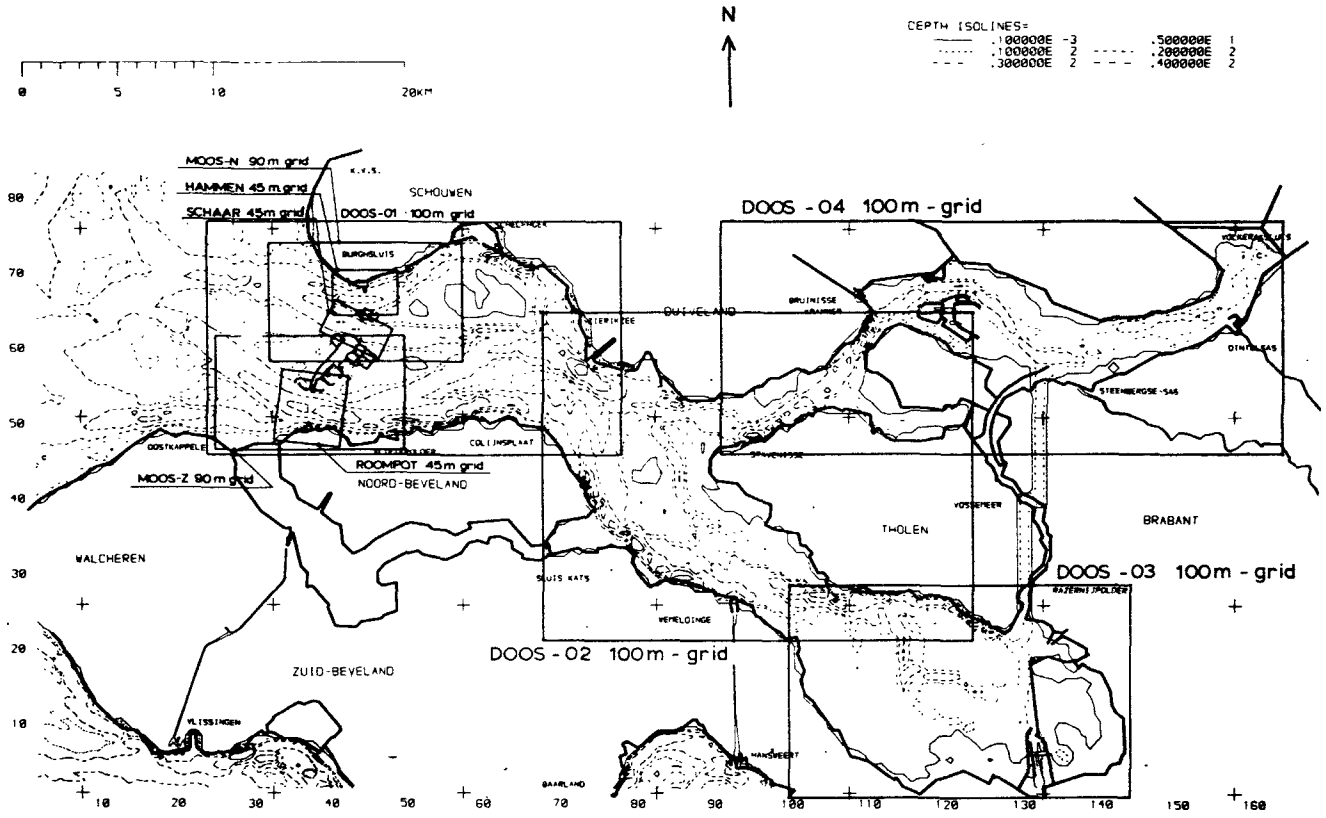

Figure 7.2 OOST-3 model (400 m grid) and nested 100 m, 90 m and 45 m models

Until 1983 computations with these models were only possible at the RAND Corporation, because of the size of the models exceeding the maximum number of 8000 grid points, which were possible for the WAQUA-version on the Rijkswaterstaat's UNIVAC computer at that time. Simulations with these models on the UNIVAC became possible after the implementation of the improved numerical scheme, designed by G.S.Stelling [7-2], in a redesigned version of the simulation program.

The pier-to-pier distance in the storm-surge barrier is 45 metres and to be able to compute transports through each separate opening, models with a grid

size of 45 m had to be built. However, the design of these small-scale models had to be based on the already mentioned limitation of 8000 grid points, to allow for computations on the Rijkswaterstaat's computer. Three 45 m grid-size models HAMMEN, SCHAAR and ROOMPOT were built for the direct vicinity of the storm-surge barrier in the three main channels. The two 90 m grid-size models MOOS-N and MOOS-Z for the northern and southern part of the storm-surge barrier, appeared to be necessary as intermediate models to provide accurate boundary conditions for these 45 m grid-size models (see Figure 7.2 and Section 7.6). At first the 90 m models received their boundary conditions from OOST-2, later on from OOST-3.

For an accurate computation of flow patterns in an estuary such as the Eastern Scheldt, a grid size of 400 m in the OOST-2 and OOST-3 model was too large. The topography of this area contained many important gullies and tidal flats on the same scale as this grid size, so they were difficult to schematize in the numerical grid. However, the velocity distributions in the Eastern Scheldt were very important for sediment transport and for environmental interests (fisheries). Also more detailed models were needed for the compartmentalisation works and the detail models for the closure of the secondary dams. Four 100 m detail models, together covering the entire Eastern Scheldt (see Figure 7.2), have been built since 1984. One of them is the DOOS-1 model of the mouth of the estuary (see Section 7.5).

During the development stage of these models many tests have been performed by the RAND Corporation and the Delta Department. For the different construction stages of the storm-surge barrier, many computations were performed by DELFT HYDRAULICS. All these computations yielded a considerrably better understanding of the behaviour of both the prototype system and its numerical equivalent.

A very important aspect of the use of numerical models is the interpretation of the results. The assumptions, used in the basic equations and the numerical aspects of the solution method, must always be kept in mind. An example is the interpretation of computed (vertically avaraged) flow velocities in the overall models (coarse grid): direct comparison with measured (local) velocities is hardly feasible since the computed velocities are an average value for one grid. Only in the most detailed models a good agreement can be expected and has also been found.

In Sections 7.3.1, 7.3.2 and 7.3.3 a general description of the most important components of the input data for the simulation program (i.e. a WAQUA-model)

are given, i.e. the data determining the geometry of the model, the data describing the storm-surge barrier and the initial- and boundary conditions driving the model.

7.3.1 Schematization of the geometry

The setting up of a WAQUA-model begins with the selection of the geographical area to be modelled. For this the desired grid size, number of grid points and orientation of the grid should be considered, together with the positioning of open and closed boundaries. The area represented by the model should be selected in such a way that the distance from the open boundaries to the area of interest is as large as possible to avoid that changes in the storm-surge barrier affect the open boundaries of the model and hence new boundary may conditions may become necessary. However, if a larger model is available, the results of such a model can be used (see Section 7.3.3).

The computer time used depends on the number of grid points and the time-step. It is an important factor in the design of a model because the WAQUA simulation program, as is the case for all programs for hydraulic computations, is a very extensive user of computer time and in practice only a limited amount of computer time for a simulation is acceptable.

The next important part of the geometry of the model is the bottom topography of the selected area. A schematic representation must be made on a discrete grid with a certain grid size. In every grid point a depth had to be selected manually (at that time) by drawing the grid on available survey charts and selecting a representative depth. This process is not straightforward and sometimes it is highly subjective too. The amount of work depends highly on the grid size used because the larger the grid the more attention must be given to obtain an accurate representation of gullies and tidal flats in the numerical bottom schematization.

It should be noted that all models had different bottom topographies because for each model the (at that time) most recent charts available were used. These differences in topography could cause differences in the results of the numerical and physical models and the prototype. Drying and flooding of the tidal flats in these models were influenced by the schematization of the bottom topography. In the small-scale models only the local velocity distributions in the shallow areas were affected but in the large-scale models the transport distributions in the channels could be affected.

With the help of contourline data (boundary outlines) the geometry of the closed boundaries was brought into the model. An extra check was done for the cross-sections at the site of the storm-surge barrier because they were important for a good representation of the transport distributions in the models.

7.3.2 Schematization of the storm-surge barrier

The storm-surge barrier has an enormous effect on both the large-scale water movement in the Eastern Scheldt and on the small-scale flow distributions in the vicinity of the barrier where turbulence causes energy losses that had to be accounted for in the models. For this the simulation program was provided with a facility (barriers) to model energy losses for (time-varying) flow restrictions (gates) in which sub- or supercritical flow occurs. A barrier restricted the flow in one direction and was seen, in the program, as an open boundary on both sides with a different treatment, and which were connected again locally using a relation between discharge and head difference [7-5]. These weir formulae contain discharge coefficients, barrier widths, sill depths and gate heights and are explained in more detail in Chapter 4.

In the beginning none of the models for the Eastern Scheldt had barriers because first a calibration and verification had to be carried out for actual situations in the prototype and, at that time, the construction of the storm-surge barrier had not yet begun.
Barriers were used for the first time by the RAND Corporation and the Delta Department in the OOST-2 and HAMMEN models, to investigate whether the effect on flow distributions by construction stages of the storm-surge barrier could be studied in these numerical models (see [7-5]).

After that DELFT HYDRAULICS applied these models for a large number of computations for different construction stages. For this DELFT HYDRAULICS studied different aspects of the use of the barriers in the simulation program and it appeared to be necessary to also try alternative formulations for modeling energy losses at the barrier sites, e.g. by replacing the barrier by a locally adapted bottom roughness and depth (more detail in Section 7.7). The representation of the barrier in the detailed models appeared to be essential for a good reproduction of actual flow patterns.

With grid sizes of 400 m in OOST-2 and OOST-3, 100 m in DOOS-1 and 90 m in MOOS-N and MOOS-Z, some adaptions in the model barriers had to be made in view of a pier distance in the storm-surge barrier of 45 m and an orientation of

the barrier which did not correspond with the model grids. Thus, barrier dimensions and barrier characteristics had to be transformed to barriers in the 400, 100, and 90 m grids (see Section 7.7).

7.3.3 Boundary conditions

As they are driving the model, boundary conditions are essential for an accurate computation of the flow field in the inner area. If an actual situation has to be reproduced in a model (e.g. for calibration or verification, see Sections 7.4.2, 7.5.2, 7.6.2), boundary conditions can be derived from overall models, which use measured data and in turn can produce boundary conditions for the detail models. Future situations can be simulated with predicted boundary conditions, but this was not necessary for the study of the effects of the construction of the storm-surge barrier. Here the available boundary conditions of an overall model could be used because they were hardly affected by the construction ([7-7] and [7-8]). Methods have been developed for composing the boundary conditions for the various models.

Observed water levels from measuring stations in the seaward direction of the storm-surge barrier were transformed into boundary conditions for the overall 400 m model OOST-2, or were used directly for its extended version OOST-3 (see Section 7.4). The option of using water levels, predicted for the astronomical tide, was only applied for the one-dimensional model IMPLIC.

Another technique (called nesting) is the extraction of results from a larger model and use them as boundary conditions for more detailed models. With this method good results were obtained. It appeared that the more detailed the model, described in detail in [7-14], the better was the agreement between computed and measured velocities.

The use of data from the 400 m model for the boundary conditions of the 45 m HAMMEN was tested but this step appeared not to work, so the 90 m models MOOS-N and MOOS-Z were built as an intermediate step. The 400 m models produced the boundary conditions for the 90 m models and these produced the boundary conditions for the 45 m models.

When water levels from the 400 m model were used as the only boundary conditions, the flow distributions along the open boundaries of the more detailed model were not correct, as well as the computed flow distribution in the model. The only way to ensure a correct transport distribution along the open

boundary was to use velocity-boundaries (discharge boundaries were not available in the WAQUA-version of Rijkswaterstaat at that time) and a small water level boundary to control the water level in the model, and to compensate for small differences in transports through the velocity-boundaries.

As velocities gave different transport rates in models with different grid sizes and bottom topographies, the transport rates in the larger model through sections coinciding with the boundary of the nested model and water levels were transformed to velocities with help of depths in the nested model, to ensure a correct transport distribution through the boundaries of the nested model. In this way also rotated nested models (SCHAAR and ROOMPOT) could be provided with boundary conditions. This technique, developed at the RAND Corporation, was incorporated in a special program, which was also used for the DOOS-1 model (see [7-14]).

The position of the open boundaries of the detail models, with respect to the area of interest (i.e. the storm-surge barrier), was such that changes could have an area of influence reaching over the open boundary. This meant that new boundary conditions should be generated through the overall model if it was expected that they were being affected by changes in the inner area of the model. The same procedure was applied in case the overall motion in the estuary was affected, e.g. due to progress in the blockage of the channels by the storm-surge barrier.

The starting conditions of all the models were a zero velocity field and a constant water level throughout the model, preferably the water level at high water slack to reduce the initial period of the model.

7.4 OOST-3

Two general models with the Eastern- and Western Scheldt estuaries and the adjacent sea area were available: the RANDDELTA-2 model with a grid size of 800 m and the SCHELDES model with a grid size of 400 m [7-7]. Several 800 and 400 m models were derived from these models to make the calibration process of separate parts easier [7-3]. With the 800 m model OOST of the Eastern Scheldt many computations have been made to investigate the influence of the numerical techniques used in WAQUA and the behaviour of the estuarine swystem, depending on system parameters (see [7-9], [7-10], [7-11], [7-12] and [7-13]).
A more detailed model was the 400 m model of the Eastern Scheldt OOST-2 [7-4]. The RANDDELTA-2 model had shown that the water levels at the location of the

OOST-2 boundary were hardly influenced by the barrier construction [7-8]. However, the construction of boundary conditions for the OOST-2 model was a complicated process because of the absence of measured data at the locaton of the boundary. The boundary conditions could be derived with help of cross-spectral analysis, transfer functions, results of the two general models and water-level records of five stations near the boundary. This technique was only available at the RAND Corporation. A more detailed description can be found in [7-4].

Prototype data were available, on a routine basis at a number of fixed tide gauges at some distance of the boundary of OOST-2. Therefore, the model area was extended in seaward direction. The new 400 m model was called OOST-3 and a description can be found in [7-6]. The model had its open boundaries close to the four measuring stations OS-11, OS-13, OS-14 and OS-15 making it possible to run the model directly with accurately measured water levels, with a 10 minute interval. This ensured a good transport distribution over the three main channels, which is strongly affected by mean sea-level variations along the open boundaries.

Both the OOST-2 and the OOST-3 model were used for the generation of boundary conditions for sub-models DOOS-1, MOOS-N and MOOS-Z. Errors in the overall models were directly transferred into errors in the computed flow of sub-models; a good calibration and verification of these models was very important.

7.4.1 Schematization

Generation of boundary conditions for the OOST-3 model was fairly simple. Prototype measurements of water levels could be used directly as boundary conditions. The same had been done for the one-dimensional IMPLIC model (see Section 6.2.4). During the simulation, the 10-minute values were interpolated linearly in time and along the open boundary.

The schematizations of the bottom topography of the OOST-2 and OOST-3 model were taken from the SCHELDES model and were based upon survey charts of 1976. An adjustment had been made to the situation of 1981 for the area around the construction sites of the storm-surge barrier. The schematization of the bottom of the Eastern Scheldt, with its gullies and tidal flats, in a 400 m grid was a far from straightforward process. Extreme care had to be taken to ensure that all cross-sections through the depth points of the model matched the cross- sections of the original charts [7-4].

For the situations during the different construction stages of the storm-surge barrier, barriers have been used in the 400 m grid to model the effect approximately.

7.4.2 Calibration and verification

The OOST-2 model was calibrated for the period 1 to 6 September 1976 with computed water levels from the RANDDELTA-2 model as boundary conditions. A verification of the OOST-2 model was done for the period 10-11 January 1982 [7-4]. A comparison between the resulting transport rates through Hammen, Schaar and Roompot in OOST-2 with the measured transport rates, is given in Figure 7.3. A comparison of water levels in different parts of the Eastern Scheldt is also given in Figure 7.3 (see also results of M1000; Figure 5.7).

Because the OOST-3 model is an extended version of the OOST-2 model, calibration (for the period 10-11 January 1982) was hardly necessary. The tides on 19 and 26 July 1983, 6 November and 29 December 1983 were used for verification of the model [7-6].
A comparison between computed transport rates through Hammen, Schaar and Roompot in OOST-3 to the measured transport rates for the period 19 July 1983 is given in Figure 7.4.

The calibration of the 400 m models was done by locally adjusting the bottom-friction coefficient, taken from the RANDDELTA-2 model. The boundary conditions had not been adjusted or modified, because the model was supposed to work also for other periods than the one used for calibration.

From the calibraton and verification of the model the following figures, related to the inaccuracy range of the results, were achieved:
- water levels: amplitude 2% and phase 5 minutes
- discharges: amplitude 5% and phase 10 minutes

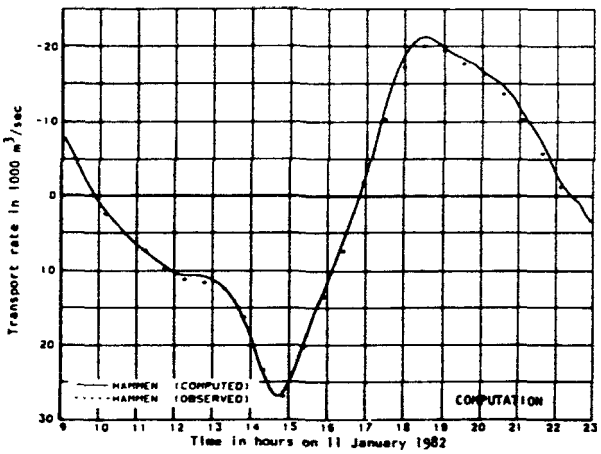

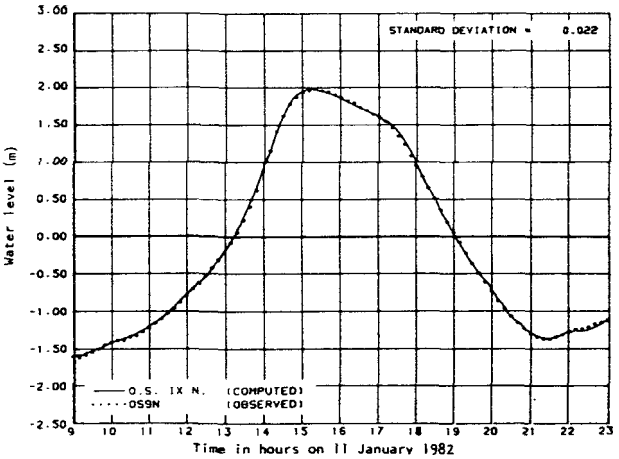

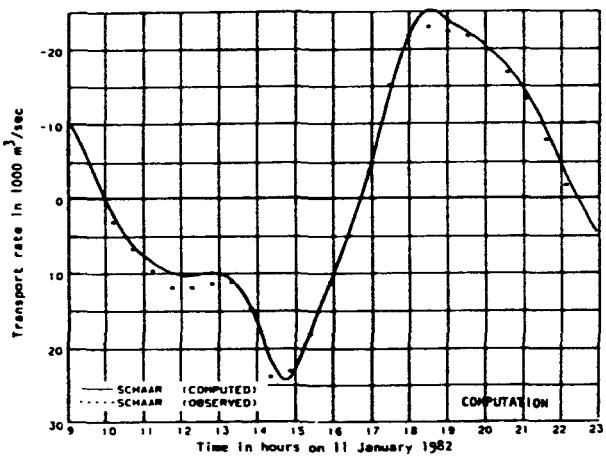

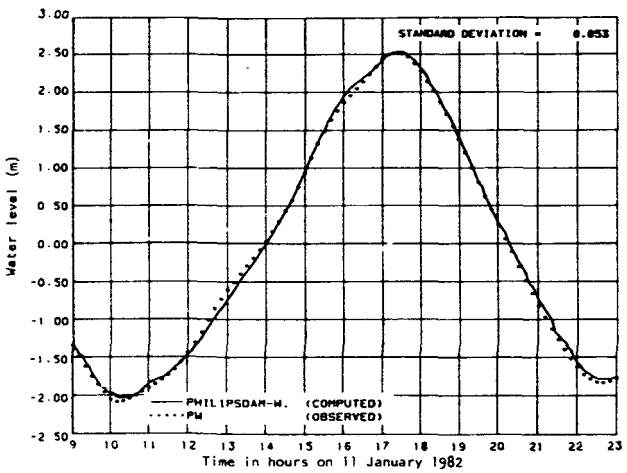

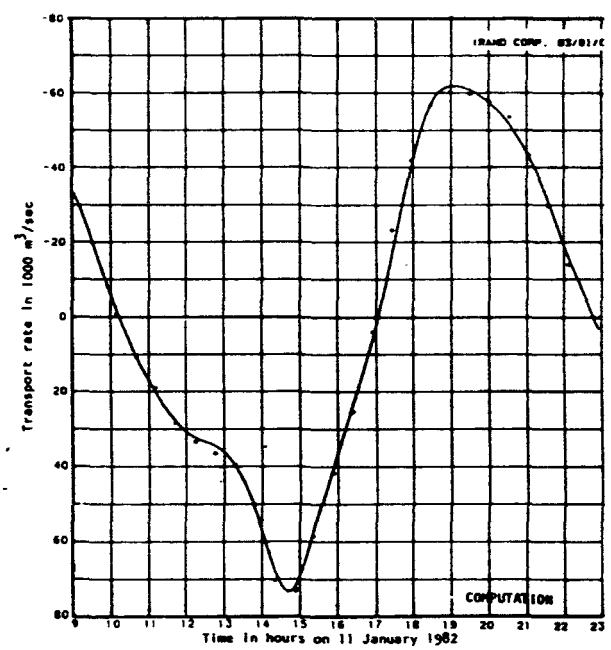

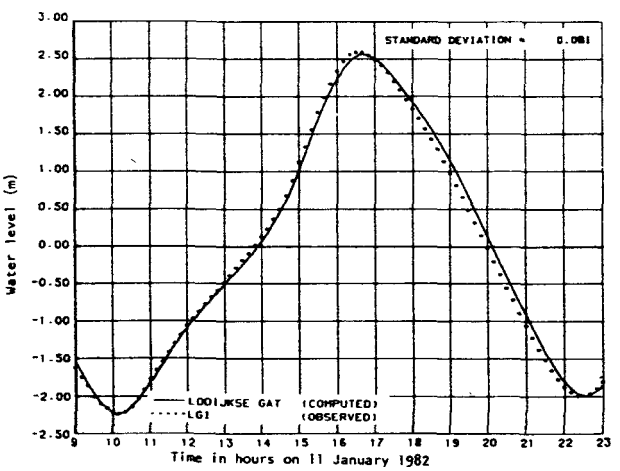

Figure 7.3 Results of calibration on tide 11-01-82;
transport rates and waterlevels

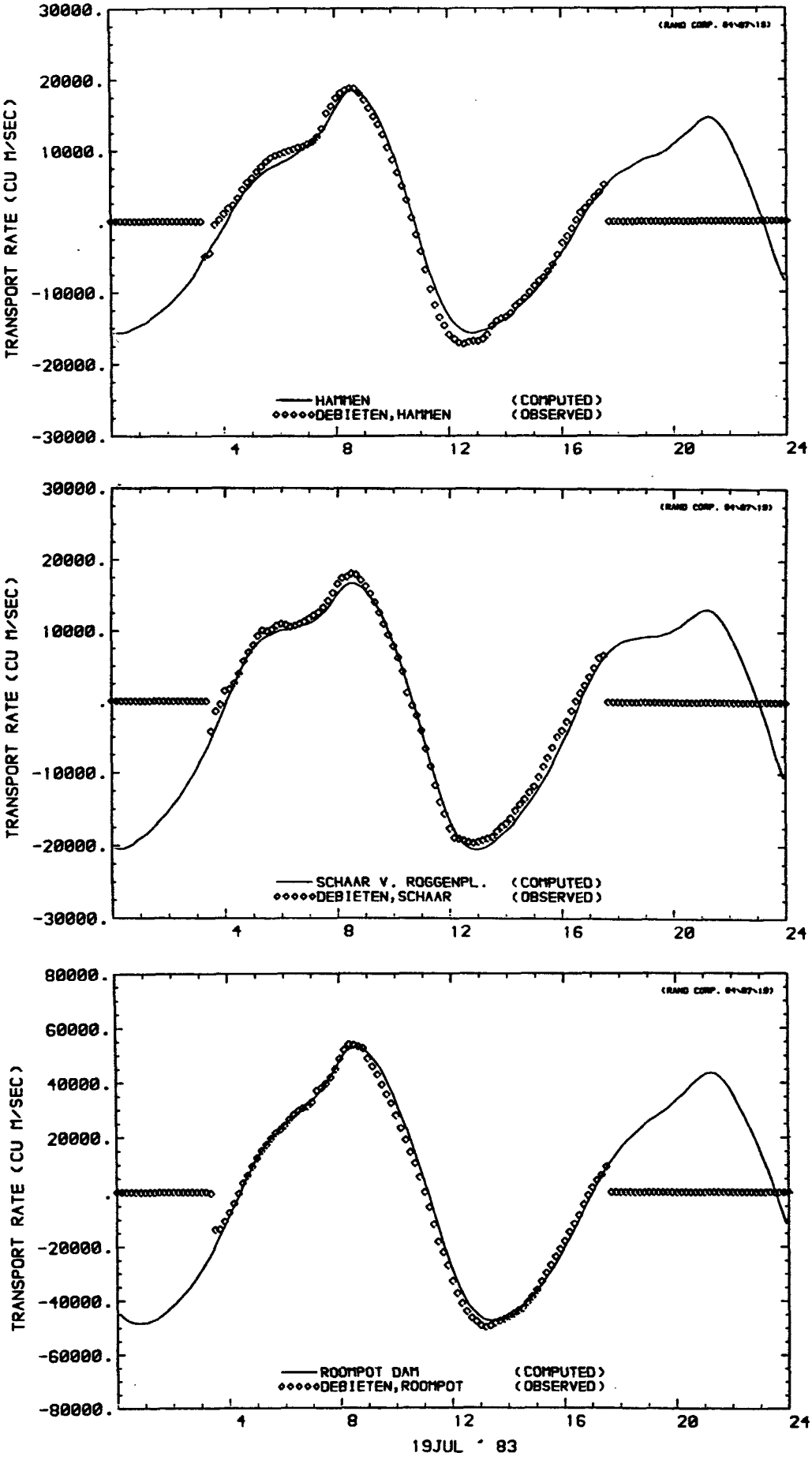

Figure 7.4 Results of verification on tide 19-07-83; transport rates

7.5 DOOS-1

Four 100 m models, together covering the entire estuary, were built. One of them was the DOOS-1 model of the mouth of the Eastern Scheldt (see Figure 7.5), built by the Delta Department and used by DELFT HYDRAULICS to investigate the effects of asymmetric (with respect to resistance or blockage ratio) construction stages. In these situations there was a change in transport distributions among the three main channels and the resulting water levels gave rise to changes in current-velocities in secondary channels and across the tidal flats. With a grid size of 100 m an accurate computation of these effects was possible (see Section 7.7).

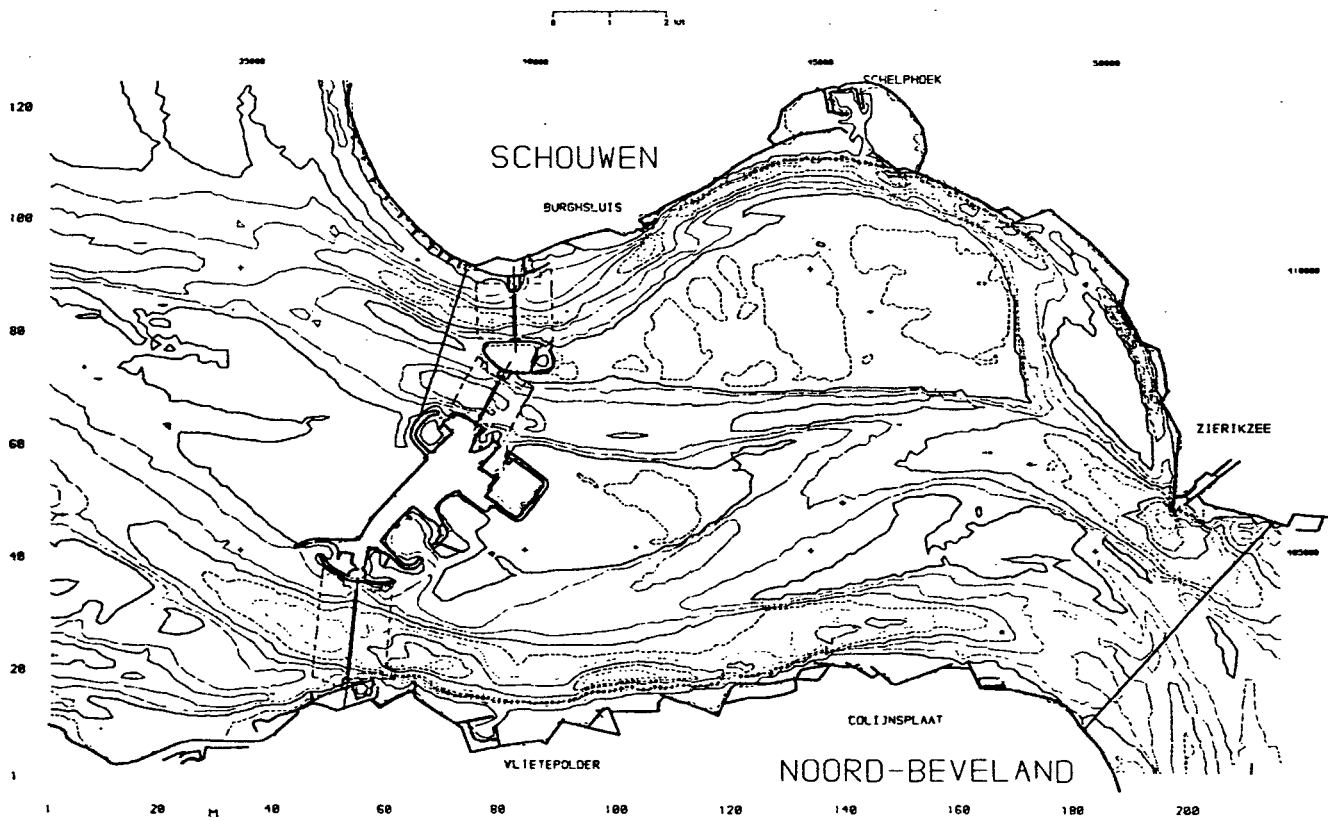

Figure 7.5 DOOS-1 model (100 m grid)

7.5.1 Schematization

With a grid size of 100 m the resulting grid had 16 times more grid points than a 400 m grid. This made the schematization of the bottom topography for the DOOS-1 model with its gullies and tidal flats less complicated. However, there always remained gullies with dimensions that made them difficult to schematize in the grid, but on this scale the contribution of these details with respect to the total tidal movement was of minor importance.

For the depths mostly survey charts of 1981 and 1982 had been used. For the tidal flat Roggenplaat and the adjacent secondary channel Kortsluitgeul, the most recent survey charts of 1983 and 1984 had been used, because this was essential for the investigation of the effect of asymmetric closures of the storm-surge barrier. Older survey charts had been used for various tidal flats.

For the calibration of the DOOS-1 model boundary conditions were taken from the OOST-2 model. For the investigations of the construction stages of the storm-surge barrier the boundary conditions were taken from the OOST-3 model. Like all nested models the open boundary of the DOOS-1 model consisted to a large extent of velocity-boundaries and only a small water-level boundary (in the northern section).

As mentioned in Section 7.3.2, barriers had been used in DOOS-1 to model the storm-surge barrier in the 100 m grid (see also Section 7.7).

7.5.2 Calibration and verification

The DOOS-1 model had been calibrated for 11 January 1982 only by adjusting the overall bottom friction (Manning) and the eddy viscosity. Also the choice of open boundary definitions (water level- and velocity boundaries) had been tested so as to achieve the best velocity distribution at the boundaries of the model, using results from the 400 m model.

In Figure 7.6 it is shown that the representation of the transport rates in the three main channels in DOOS-1 is of the same quality as in the 400 meter OOST-2 model (see Figure 7.3), as can be expected because OOST-2 provided the boundary conditions for DOOS-1.

A verification of the model had been done by DELFT HYDRAULICS for the measurements on 30-07-84 and 01-08-84.

7.6 90 m and 45 m models

To provide detailed information about the transport distribution through the storm-surge barrier, several 45 and 90 m models were built. The first 45 m detail model built was the HAMMEN model and with this one it was found that results of a 400 m model could not be used as boundary conditions for a 45 m model. With the special procedure, described in Sections 7.3.3 and 7.6.1,

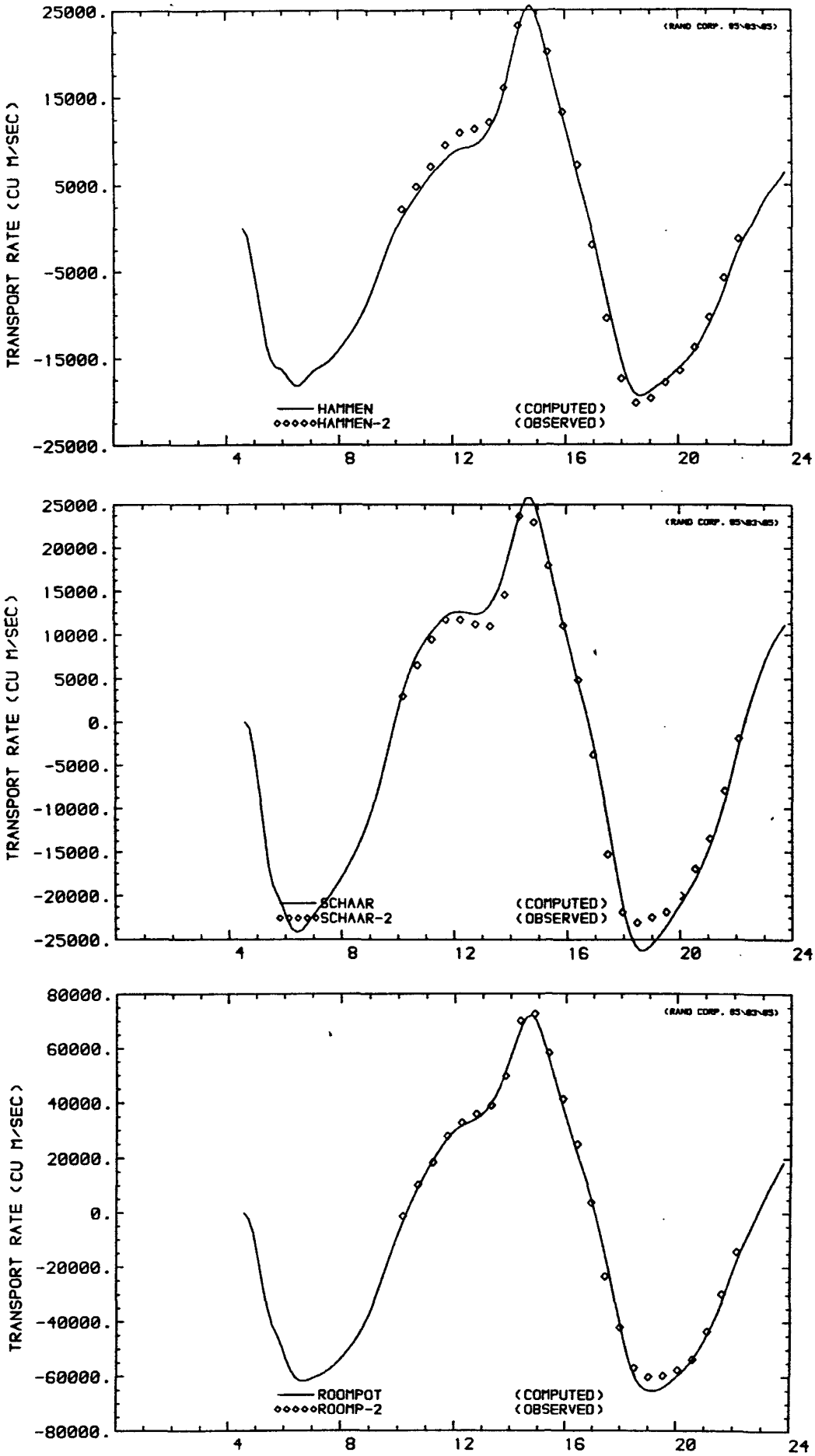

Figure 7.6 Results of calibration on tide 11-01-82; transport rates

transport rates and water levels computed in the 400 m model OOST-2 (or OOST-3), could be used as boundary conditions for the intermediate 90 m model MOOS-N of the northern part of the storm-surge barrier. The results of this model were used to produce boundary conditions for the HAMMEN model.

The technique of nesting models in larger models had been developed, improved and tested in many computations in the MOOS-N and HAMMEN model [7-14]. After this the 45 m model SCHAAR was built, oriented in the direction of the barrier and thus rotated in the MOOS-N model, followed by the 90 m model MOOS-Z of the southern part and its nested 45 m model ROOMPOT. All the 90 and 45 m detail models were designed with the mentioned limitation of 8000 grid points.

7.6.1 Schematization

For the schematization of the bed topography of the MOOS-N model and its nested models HAMMEN and SCHAAR, survey charts of 1978 and 1979 were used for the first versions (used in the stages of development), later on they had been corrected to the situation of 1981. For the MOOS-Z model and its nested model ROOMPOT charts of 1981 had been used.

Changes in construction stages of the storm-surge barrier especially affected the schematizations of models with grid sizes of 90 and 45 m. Not only the boundaries and the bed topography in the vicinity of the barrier, but also the schematization of the barrier itself changed during the construction, so all these models had to be changed many times during the studies.

7.6.2 Calibration and verification

The results in the 90 and 45 m models were highly dependent on the quality of their boundary conditions and their bed topography: they determined the resulting flow patterns in the area. This meant that a calibration of these models was hardly possible and the usual parameters for friction and eddy viscosity were used.

The same date as for OOST-3, 11 January 1982, had been used for verification, because data like transport rates through the main channels and velocities in various points in the centre of the models were available. The results showed a good agreement between computed and measured velocities and transport rates. In Figures 7.7 and 7.8, the current-pattern in the 90 m model MOOS-Z and the 45 m model ROOMPOT at maximum ebb is given. In Figures 7.9 and 7.10, the

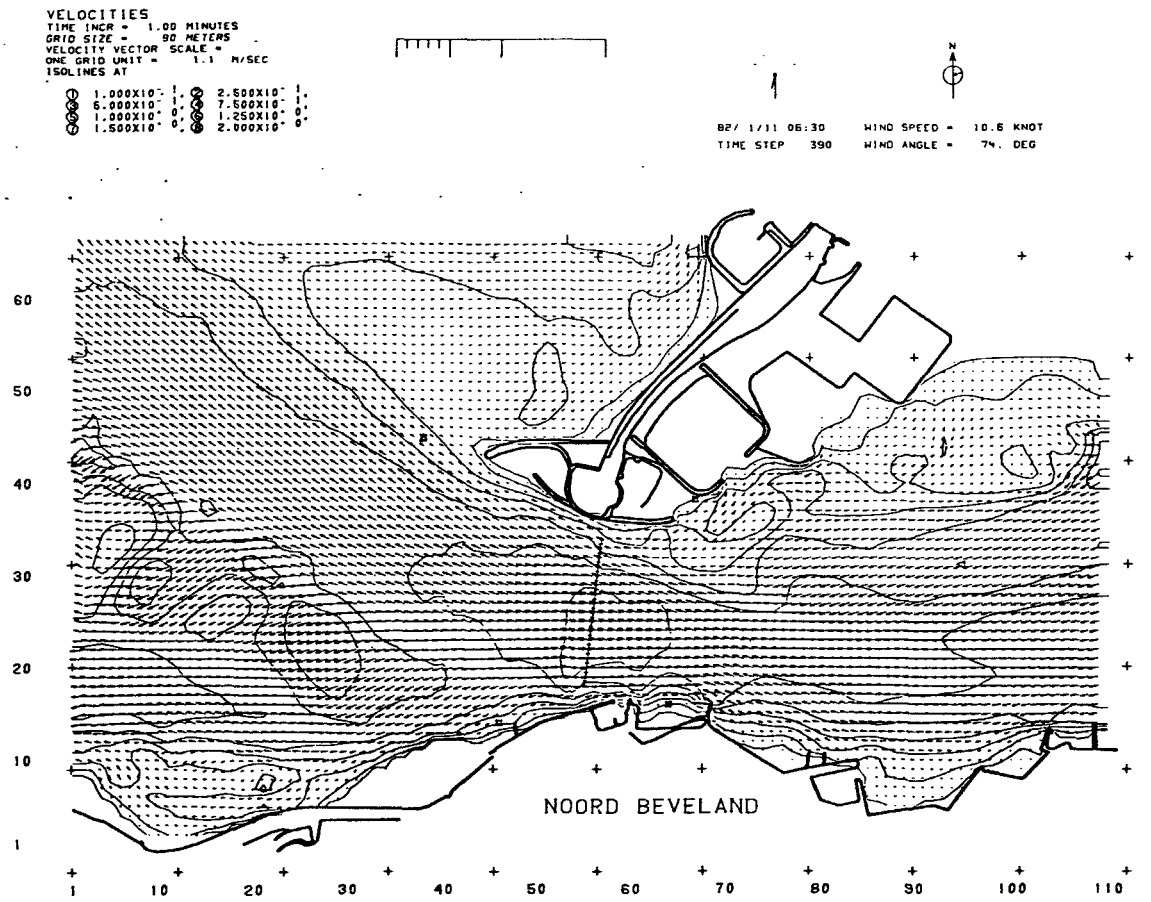

Figure 7.7 Flow pattern in MOOS-Z model (90 m grid)

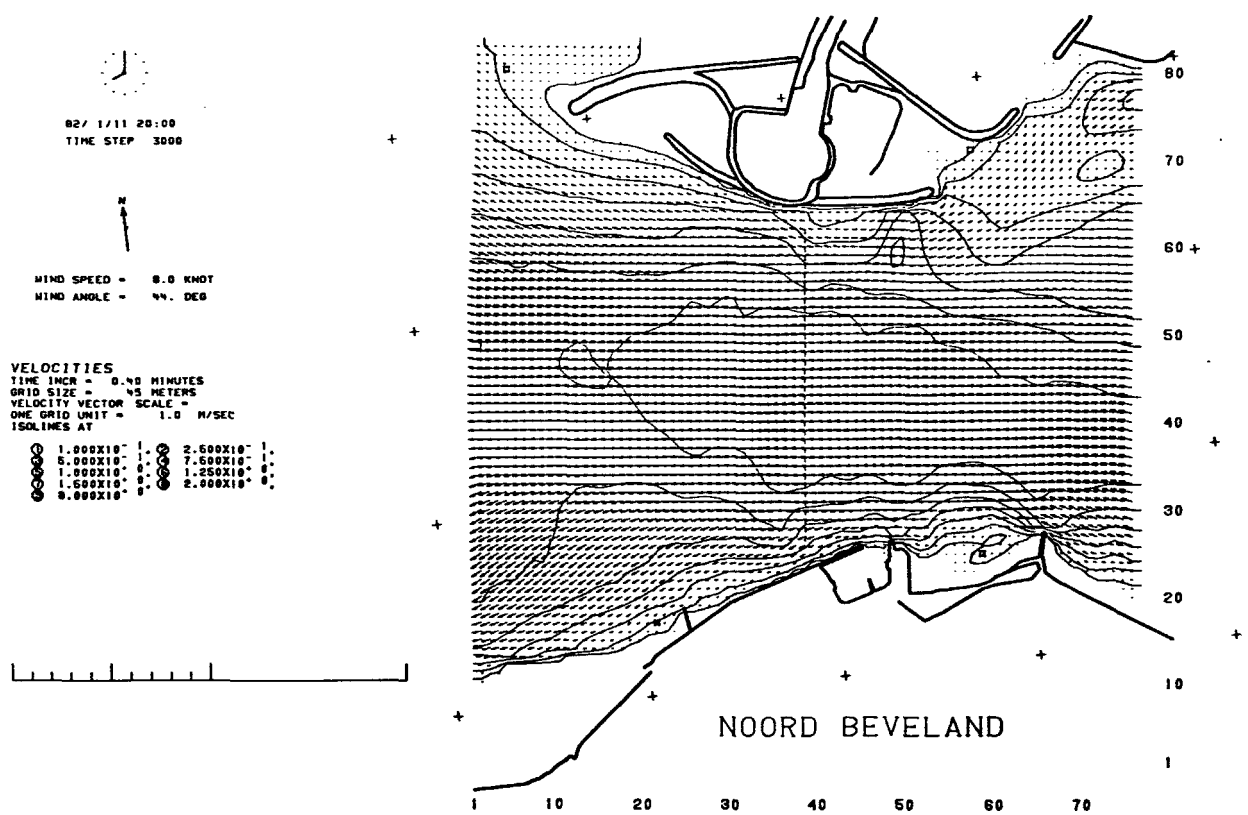

Figure 7.8 Flow pattern in ROOMPOT model (45 m grid)

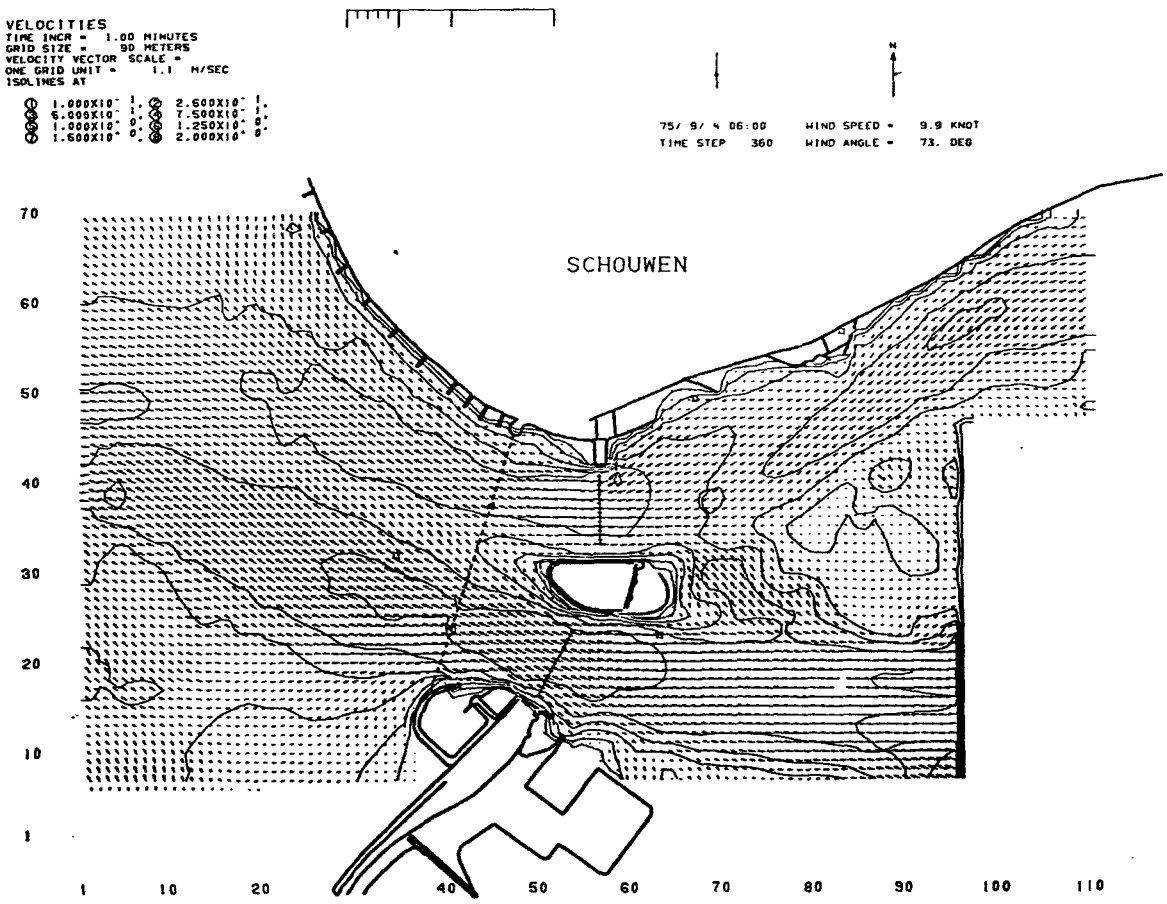

Figure 7.9 Flow pattern in MOOS-N model (90 m grid)

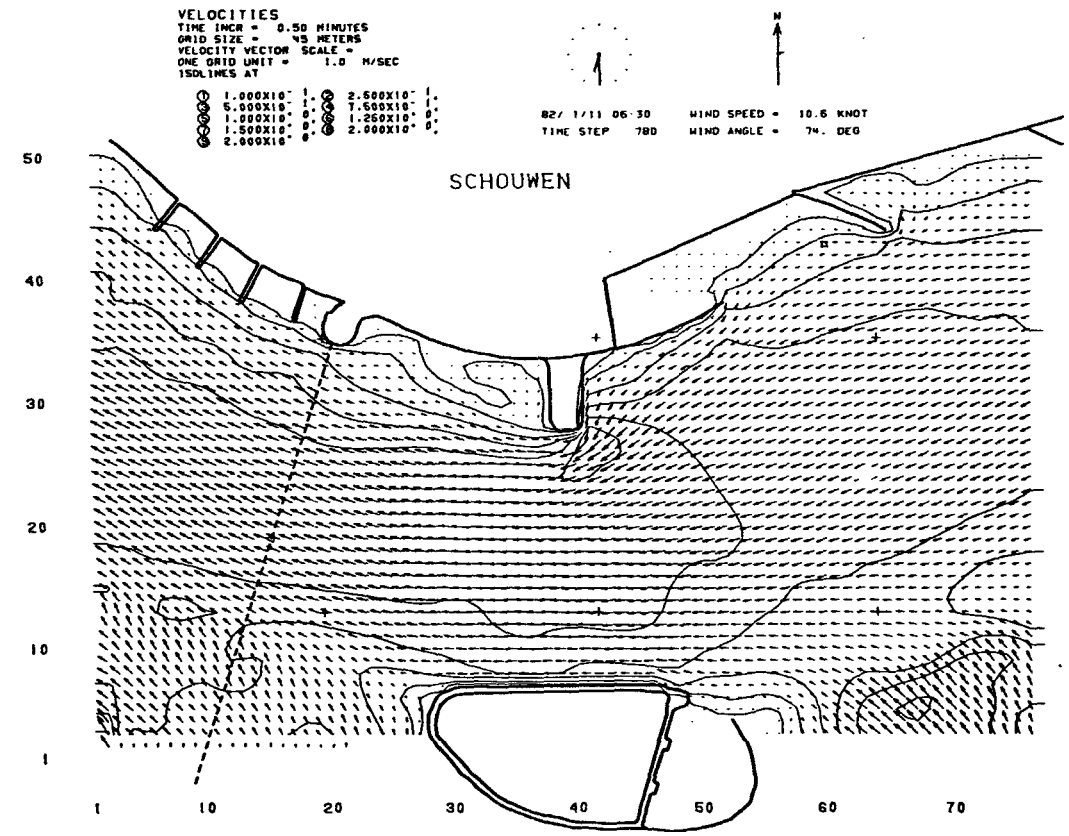

Figure 7.10 Flow pattern in HAMMEN model (45 m grid)

current-pattern is given in the 90 m model MOOS-N and the 45 m sub-model HAMMEN at maximum ebb. A comparison of computed (vertically averaged) velocities and (local) velocities, measured by two vessels on 11 January 1982, is presented in Figure 7.11.

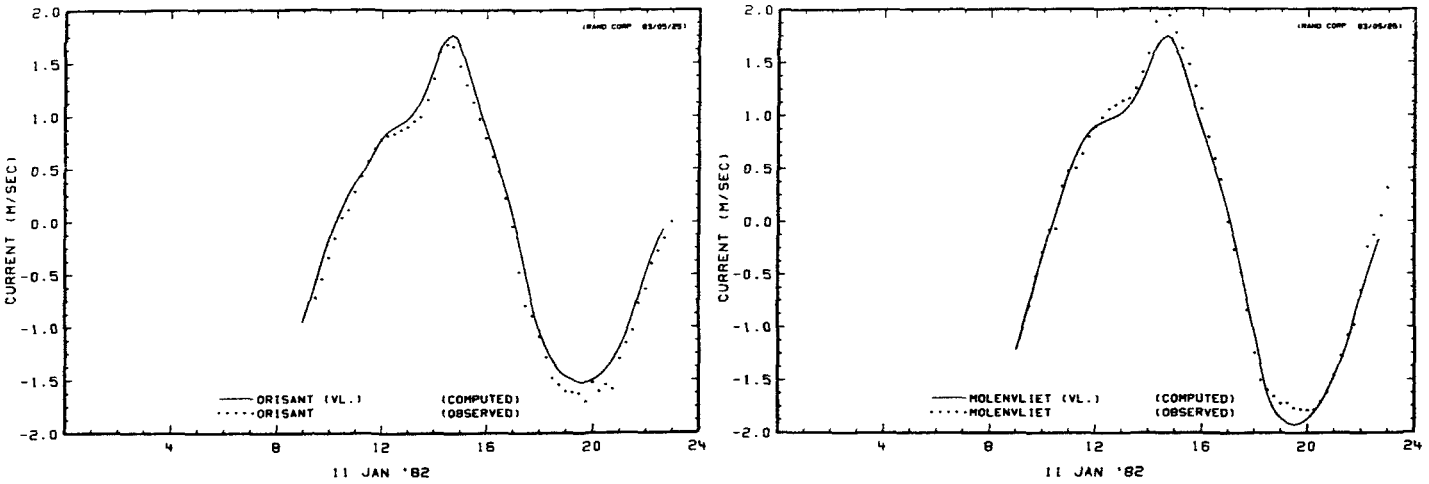

Figure 7.11 Comparison of measured and computed velocities in ROOMPOT model; tide 11-01-82

Also a comparison between these numerical models and the physical scale model M1001 had been made before the models were used by DELFT HYDRAULICS for the many computations reported in Sections 7.7 and 8.2.

7.7 Operational experience

7.7.1 Introduction

In the preceding paragraphs the calibration and verification of the models has been described for the initial situations without any narrowing of the three main channels. However, the models were to be used to compute the flow conditions for future situations with arbitrary building stages of the storm-surge barrier.

These building stages varied from the placing of the first pier until the placing of the last sill beam.
The good results of the calibration and verification were no guarantee for the accuracy of the computations for future situations. The following problems could arise:

- the total resistance of the storm-surge barriers in the three main channels might not be correct; giving errors in the prediction of the horizontal and vertical overall tidal movements (discharge, water level and head difference); particularly a problem for the overall models OOST3 and DOOS1
- the local resistance of the storm-surge barrier might not be correct, giving errors in the prediction of the discharge and velocity distributions at the axis of the barrier and therefore also errors in the distributions upstream and downstream of the barrier; particularly a problem for the detail models (grid size 45 and 90 m)

Both problems were mainly related to one central problem, namely the schematization of the storm-surge barrier. In all models the resistance of the barrier had to be introduced by using the 'BARRIER'-module of WAQUA (see also Section 7.3.2). The following sections will discuss:

- prediction of horizontal and vertical tidal movement at arbitrary building stages;
- prediction of discharge and velocity distributions in the vicinity of the barrier at arbitrary building stages;
- stability of the computations at arbitrary building stages.

7.7.2 Prediction of tidal movement

For the prediction of the tidal movement for an arbitrary building stage, the discharge characteristics of each compartment of the barrier had to be determined first. In a number of tables the cross-sectional profiles and the effective cross-sectional area (respectively A and $\mu_2 A$) were listed for each compartment and for ten building stages (from placed piers until placed sill beams). All these values were based on the studies on the discharge characteristics of the storm-surge barrier (M1644; see also Chapter 4); use was made of an interpolation in 'location' and in 'building stage'.

The tabulated values could, with some minor processing, be directly applied for the models with a grid size of 45 m, namely:

- discharge coefficient = $\mu_2 A/A$
- width = 39.5 m
- depth = A/width

In the other models with larger grid sizes the values of $\mu_2 A$ and A had to be added for two or more compartments (not always an integer number). These values were subsequently processed into the necessary figures in an identical way.

Application of the above-mentioned processing meant that in all the WAQUA-models μ_2-values were used as discharge coefficients.

However, at the start of the investigations the discharge coefficient for the

overall model OOST3 was corrected with a factor $\mu_3/\bar{\mu}_2$ (see also Section 4.2.2). This factor took into acount the three-dimensional effects, e.g. due to the presence of construction fronts. In the model OOST3 (with a grid size of 400 m) certain stages of a construction front, with discontinouities on a scale of 45 m, could hardly be represented; each 'barrier' unit in this model represents approximately eight to nine compartments of the real barrier. However, a number of computations with OOST3 for future situations clearly showed a stronger reduction in vertical and horizontal tidal movement than given by the hydraulic scale model M1000.
Though the reliability of the scale model was not known at that moment, it was decided not to use the correction factor $\mu_3/\bar{\mu}_2$ for future computations. This meant that in both the models M1000 and OOST3 in principle μ_2-values had been applied. With this approach both models gave almost the same prediction of the tidal movement for arbitrary building stages. Verification by prototype measurements later on confirmed the validity of this approach.

Finally, note that in connection with the first computations for the reproduction of velocity distributions at construction fronts (see also Section 4.2.4 and 7.7.3) it was decided to reduce the μ_2-value for compartments with a completed sill. The reduction was 20% and application of this reduction also gave better results with respect to the reproduction of the vertical and horizontal tidal movements. An explanation of the need of this reduction could not be found.

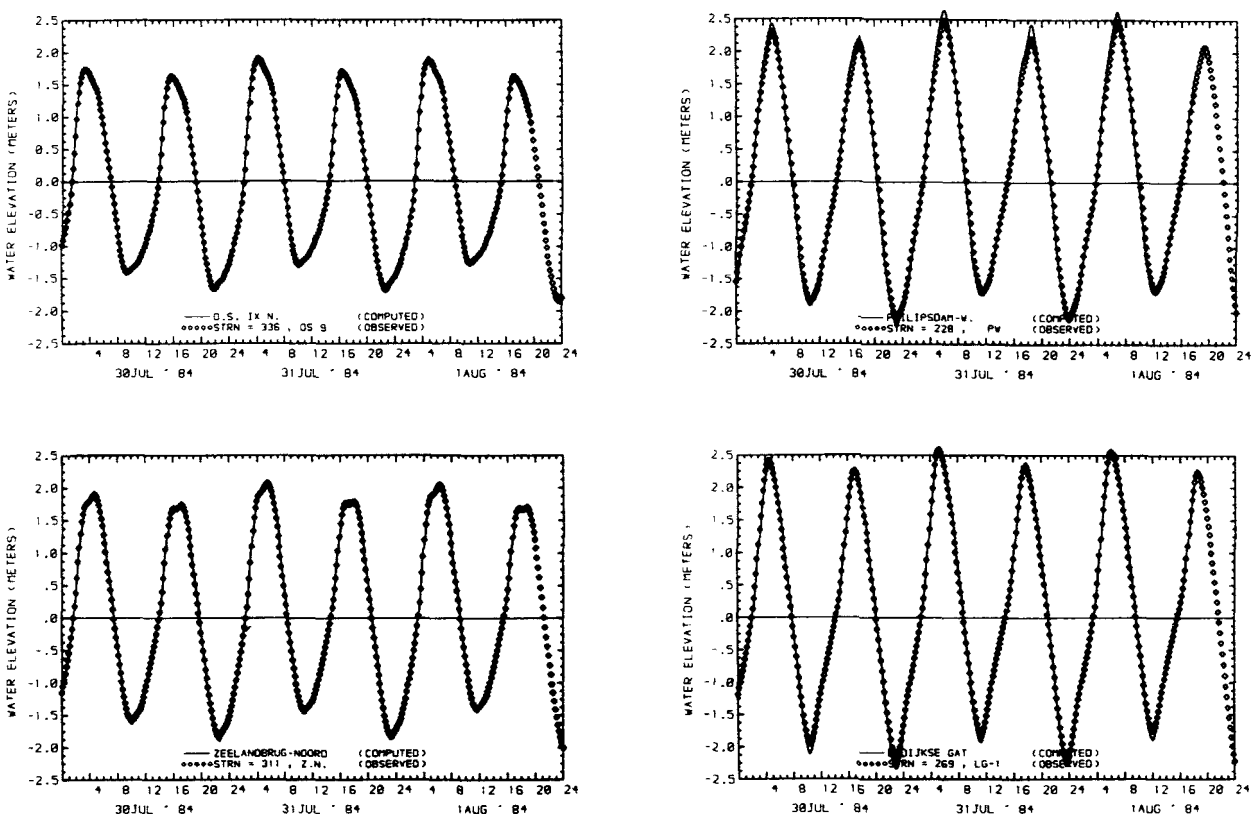

Figure 7.12 Results of reproduction of water levels, tide 30-07-84...01-08-84

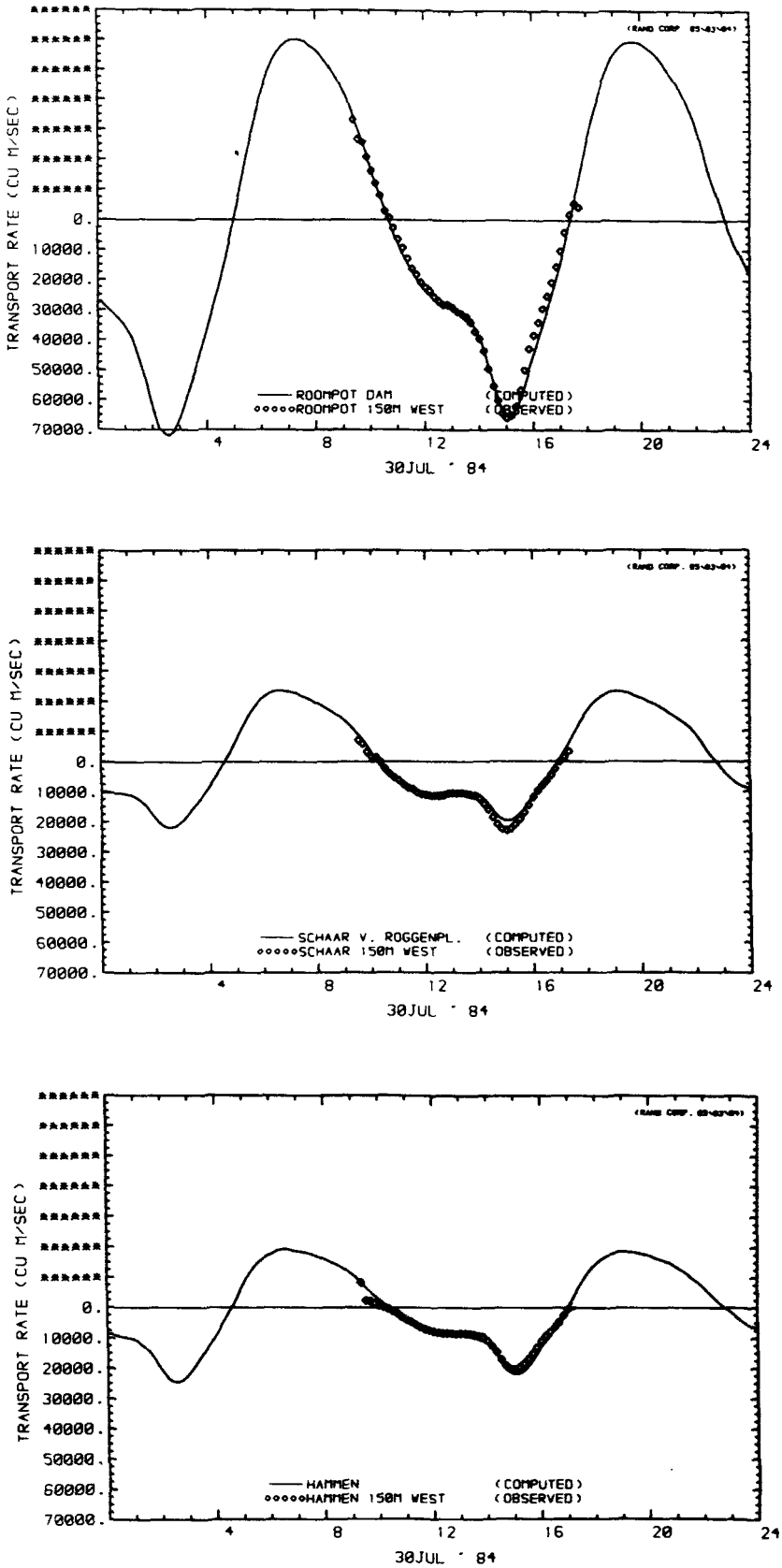

Figure 7.13 Results of reproduction of transport rates, tide 30-07-84

The preceding can be summarized as follows:

- all the WAQUA-models were using μ_2-values for the discharge coefficients (values were based on the flume test results);
- the μ_2-value of compartments with completed rubble sill was reduced by 20%.

Finally a limited number of results of verifications for building stages of the barrier are presented, see Figure 7.12 and 7.13. These are all related to the vertical and horizontal tidal movements. An extensive presentation is given in [7-15] and [7-16].

7.7.3 Prediction of discharge and velocity distributions

The flow pattern in the vicinity of the barrier at an arbitrary building stage depended, to a large extent, on the distribution of the 'resistance' along the axis of the barrier. In Section 7.7.2 it has been described in which way the discharge characteristics of each 'barrier' of the WAQUA-models could be determined.
A correct distribution of the resistance at the barrier was an essential (internal) boundary condition for the prediction of especially the downstream flow pattern. However, at advanced building stages with large vertical narrowing of the cross-section (placing of sill beams), three-dimensional effects would affect the results. Until then it was not known whether the two-dimensional models could calculate a realistic flow pattern.
Therefore the investigations started with the reproduction of a number of tests for the placing of sill beams which were carried out in the detail scale model M1001. The computations were carried out in a special WAQUA-model of the Roompot in which the depths of the scale model were simulated (which were based on earlier (predicted) sounding charts, with as result some local depth differences). Additionally, a steady-state flow was simulated instead of a tidal cycle, just as in the scale model (see also [7-19]).

Essential for these computations was the reproduction of the following characteristic properties of the flow pattern:

- (steep) gradients in the velocity distributions downstream of a construction front
- concentrated flow from the less narrowed part of the barrier
- large scale eddies on both sides of the main current
- a rather flat velocity distribution upstream of the barrier

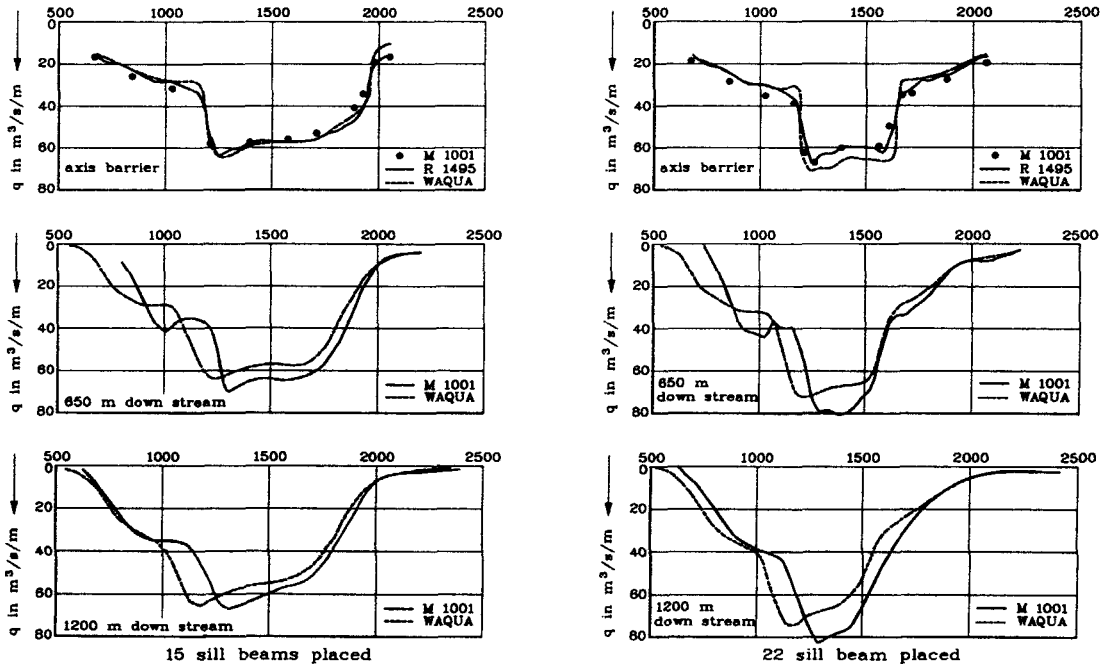

Figure 7.14 Results of reproduction of discharge distributions

Figure 7.14 gives a comparison of the computed velocity distributions and the velocity distributions measured in the scale model. At the barrier axis results of R1495 are presented as well.
The results show that the reproduction of steep gradients in the velocity and discharge distributions was rather good. However, the reproduction of large eddies on both sides of the main current and to a lesser extent the position of the main current was moderate. These results were achieved by using the following adjustments:

- viscosity coefficient ν =1.0 m²/s (prior to this investigation a value of ν =6.0 to 10.0 m²/s was used);
- μ_2-value of completed rubble sill reduced by 20%.

Using these adjustments, the flow patterns for a great number of building stages of the barrier were computed. The results of these computations with emphasis on the downstream flow pattern, are presented in [7-19].

As the building of the barrier proceeded, more field measurements of the velocity distributions in the vicinity of the barrier became available. Up to the completion of the rubble sill, the measurements were usually carried out in cross-sections upstream of the barrier. However, during the placing of the sill beams, also the downstream velocity distributions were determined.

In order to judge the quality of the computations, most of the available prototype measurements were reproduced (=hindcasted) with the WAQUA-models. This was partly done during the building of the barrier and partly after the completion of the works. From this it turned out that the upstream velocity distributions were reproduced in a proper way (see Figure 7.15 for results of the reproduction of velocity distributions upstream of the barrier). The downstream velocity distributions, however, clearly showed the following differences with the prototype:

- absence of large eddies on both sides of the main current in the model,
- location and steepness of velocity gradients.

Some supplementary computations showed that a far better reproduction could be achieved by modifying the barrier-formulation. In Section 8.2 the results of this exercise will be presented.

Extensive presentations of the computations related to velocity distributions are given in [7-15], [7-16], [7-17], [7-18] and [7-19].

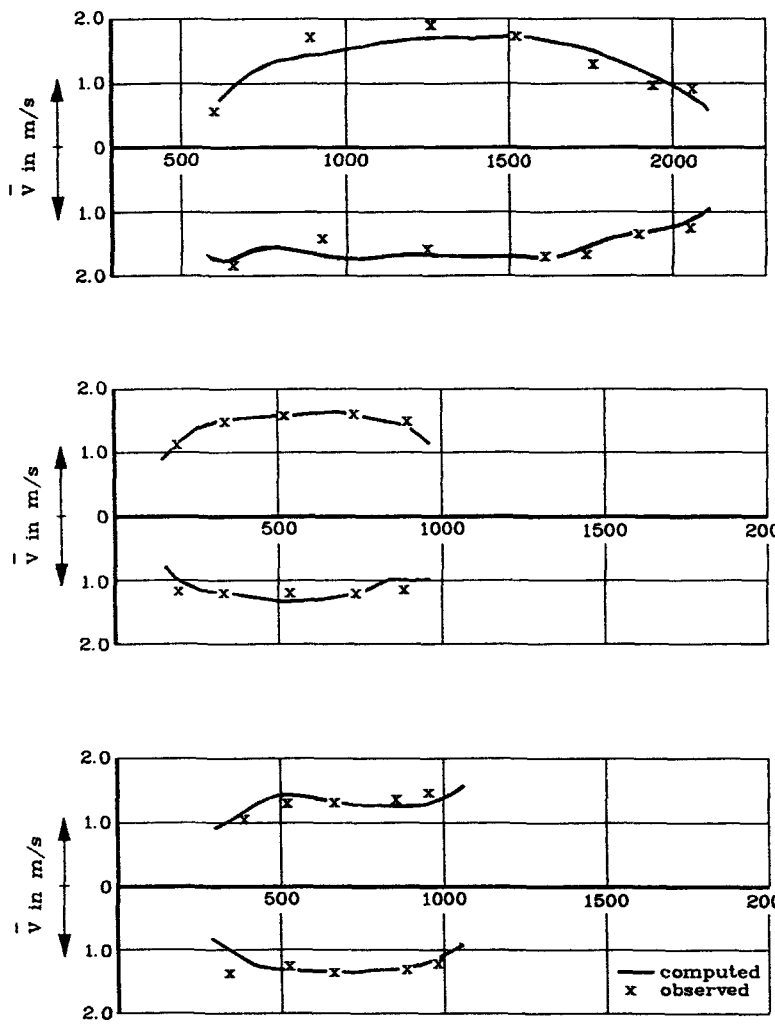

Figure 7.15 Results of reproduction of velocity distributions, 150 m upstream of barrier, tide 30-07-84(flood) and 01-08-84 (ebb)

7.7.4 Stability of the computations

In the preceding sections a description is given in what way the viscosity coefficient had changed and in what way the resistance of the barrier was schematized in order to get a good reproduction of tidal movement and flow patterns. In first instance, the other parameters of the WAQUA models remained unchanged, meaning that the values obtained during the calibration were maintained.
In the computations for a large number of building stages it appeared that sometimes spurious oscillations occurred. The presence of these oscillations depended somewhat on the number of placed sill beams. The oscillations showed up most clearly in the detail models (gridsize 45 m), whereby the models ROOMPOT and HAMMEN reacted in the most sensitive way.

For two situations with the most extreme oscillations extensive tests were carried out in order to reach a new adjustment. These were a situation in the Roompot with 18 placed sill beams and a situation in the Hammen with the rubble sill completed. At these tests the following parameters were varied:

- Δt = time-step
- ν = viscosity coefficient
- α = reflection coefficient for the boundaries

Ultimately it turned out that in the detail models non-oscillating computations could be achieved by using the following values for the relevant parameters:

Δt	= 15.0 s	(was: 30.0 s)
ν	= 2.0 m^2/s	(was: 1.0 m^2/s)
α	= 0.0	(was: 35.0)

It should be noted that the above-mentioned adjustments were a compromise between acceptable computer time and acceptable reproduction of gradients due to

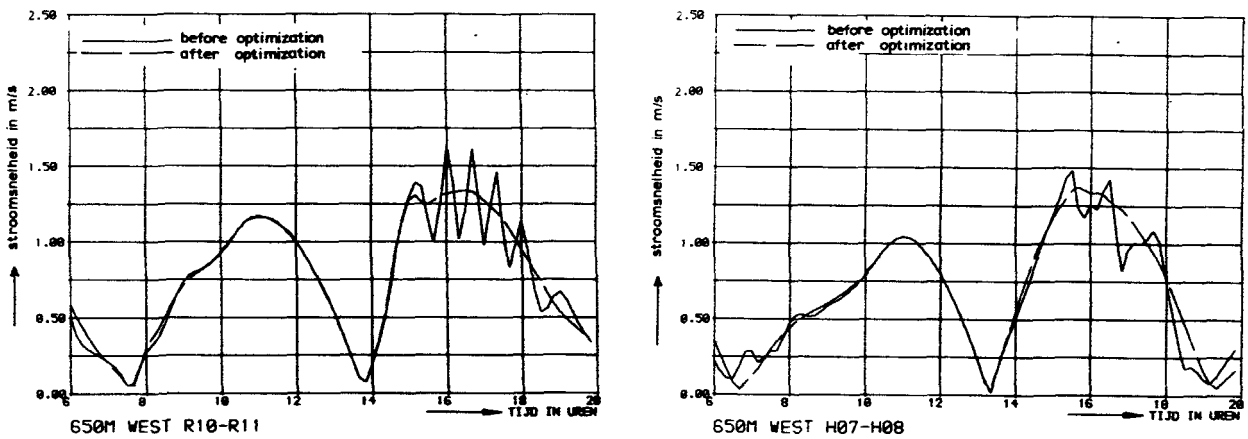

Figure 7.16 Examples of appeared oscillations and results after optimization

the construction fronts. The gradients were better reproduced using $\nu=1.0$, but this meant also a further reduction of the time-step. However, the total computer time would become unpractically long (one computation had to be performed during several nights).

This paragraph ends with the presentation of some examples of the oscillations and the results after above-described optimization of the adjustment. Both examples show results of computed velocities before and after the new adjustment, see Figure 7.16. An extensive presentation is given in [7-20].

References of Chapter 7

[7-1] RAND Corporation and Leendertse J.J.
Aspects of a computational model for long-period water wave propagation, Memorandum RM-5294-PR, Santa Monica, May 1967

[7-2] Rijkswaterstaat and Stelling G.S.
On the construction of computational methods for shallow water flow problems, Communications no. 35, The Hague, 1984

[7-3] Rijkswaterstaat and Roos A., van Dijk R.P. and Vincent J.
Review on available WAQUA-models at the Delta Department and District Coast and Sea, Nota WWKZ 85.G005, The Hague, 1985 (in Dutch)

[7-4] RAND Corporation and Leendertse J.J.
Verification of a model of the Eastern Scheldt, Report R-3108-NETH, Santa Monica, April 1984

[7-5] Rijkswaterstaat and de Ras M.A.M.
Test of the barrier facilities in WAQUA, Nota DDWT 80.017, The Hague, 1980 (in Dutch)

[7-6] Rijkswaterstaat and Bosselaar G.J.
OOST-3, Nota (in preparation)

[7-7] Leendertse J.J., Langerak A.,de Ras M.A.M.
Two-dimensional Tidal models for the Delta Works, In Hugo B.Fischer (ed.), "Transport Models for Inland and Coastal Waters", Proceedings of a Symposium on Predictive Ability, Academic Press, Inc., New York, 1981, pp. 408-450

[7-8] Voogt J.,Roos A.
Effects on tidal regime "Hydraulic aspects of Coastal structures", Part I, Delft University Press, Delft, 1980

[7-9] RAND Corporation and Leendertse J.J.
A summary of experiments with a model of the Eastern Scheldt, Report R-3611-NETH, Santa Monica, June 1988

[7-10] RAND Corporation and Leendertse J.J.
Influence of the advection term approximation on computed tidal propagation and circulation, Report N-2700-NETH, Santa Monica, June 1988

[7-11] RAND Corporation and Leendertse J.J. and Ritter S.L.
Sensitivity of the major system parameters of an Eastern Scheldt model, Report N-2701-NETH, Santa Monica, June 1988

[7-12] RAND Corporation and Leendertse J.J.
The computed relation between the semi-diurnal tidal in the Eastern Scheldt and its overtides, Report N-2702-NETH, Santa Monica, June 1988

[7-13] RAND Corporation and Leendertse J.J. and Ritter S.L.
The effect of different hydrodynamic formulations on computed tidal propagation and circulation in the Eastern Scheldt, Report N-2703-NETH, Sante Monica, June 1988

[7-14] RAND Corporation and Leendertse J.J., Roos A. and Dijkzeul J.C.M.
Nesting of two-dimensional model, Report WD-4260-NETH/RC, Santa Monica, February 1988

[7-15] DELFT HYDRAULICS and Hartsuiker, G.,
Storm surge barrier Eastern Scheldt, Two-dimensional models of the mouth of the Eastern Scheldt, Computation of flow pattern for prototype measurements at tide 6-11-1983 and tide 29-12-1983, R2053, May 1984 (in Dutch)

[7-16] DELFT HYDRAULICS and Hartsuiker, G.,
Storm surge barrier Eastern Scheldt, Two-dimensional models of the mouth of the Eastern Scheldt, Verification of flow pattern for prototype measurements at tide 30-4-1984 and tide 1-8-1984, R2093-01, January 1986 (in Dutch)

[7-17] DELFT HYDRAULICS and Hartsuiker, G.,
Storm surge barrier Eastern Scheldt, Two-dimensional models of the mouth of the Eastern Scheldt, Reproduction of flow pattern during installation of sill beams (Ametek-measurements), R2093-02, November 1986 (in Dutch)

[7-18] DELFT HYDRAULICS and Hartsuiker, G.,
Storm surge barrier Eastern Scheldt, Two dimensional models of the mouth of the Eastern Scheldt, Reproduction of flow pattern at final situations (Ametek-measurements), R2093-20, October 1987 (in Dutch)

[7-19] DELFT HYDRAULICS and Hartsuiker, G.,
Storm surge barrier Eastern Scheldt, Two-dimensional models of the mouth of the Eastern Scheldt, Reproduction of flow pattern for three construction fronts of placed sill beams, R2094-01/02, April 1985 (in Dutch)

[7-20] DELFT HYDRAULICS and Hartsuiker, G.,
Storm surge barrier Eastern Scheldt, Two-dimensional models of the mouth of the Eastern Scheldt, Investigation on instabilities in the computations, R2094-03/05, June 1986 (in Dutch).

8. Results and comparison with field data

8.1 Verification of the models; IMPLIC-R1495 and M1000-M1001

8.1.1 Introduction

In this section the results are given of the verification of the one-dimensional models that were used for the Eastern Scheldt storm-surge barrier. These models are described in Chapter 6. The verification was of major importance since the basic design parameters for the barrier were determined with these models. These basic parameters were (see also Chapter 2):

- the discharge through the main channels, Q
- the lateral distribution along the barrier, expressed by q/A
- the head difference over the barrier, Δh

The forecast system for these parameters is described in Chapter 3. The method of the verification is described in Section 8.1.2 and the results of the verification are presented in Section 8.1.3. The main purpose of the verification, as presented in the following sections, is to determine, in general, the overall accuracy and performance of the models that were used and not to discuss the results of specific construction stages of the storm-surge barrier.

The accuracy of the model IMPLIC-R1495 was governed by the input from the scale models M1000-M1001 such as:

- coefficients for the discharge relation μ_2 and μ_3 (see Section 6.2.3),
- calibration of the R1495 model by the coefficient B (see Section 6.3).

Verification of the models M1000-M1001 for Q, q/A and Δh is discussed in Section 8.1.4.

8.1.2 Systematic verification procedure

The verification procedure was set up in such a way, that each step in the forecast procedure was checked systematically. In this way not only the final results of the forecast were evaluated, but also the models as individual elements in the forecast system. The verifications took place on the basis of result of measurement campaigns.

During these campaigns all following basic hydraulic parameters were determined simultaneously in one of the main channels:

- The water levels on both sides of the barrier.
- The head difference over the barrier, Δh.
- The discharge through the channel, Q.

- The lateral distribution of the discharge, q/A.
- Local velocities.

Water levels and head difference were obtained from the permanent field stations.
The discharge was determined by measuring the velocity profiles upstream of the barrier with a number of vessels (at least four) anchored at fixed positions.
The q/A distribution could not be determined directly. It was derived from velocity measurements in the axis of the barrier. The instruments were placed in such positions, that the relation between the measured velocity and q/A was similar for each instrument. Thus the lateral distribution of q/A was the same as the lateral distribution of the actual measured velocities, except for a coefficient. With the discharge known from the measurements upstream, this coefficient could then be eliminated and the values of q/A could be determined, see Figure 8.1.

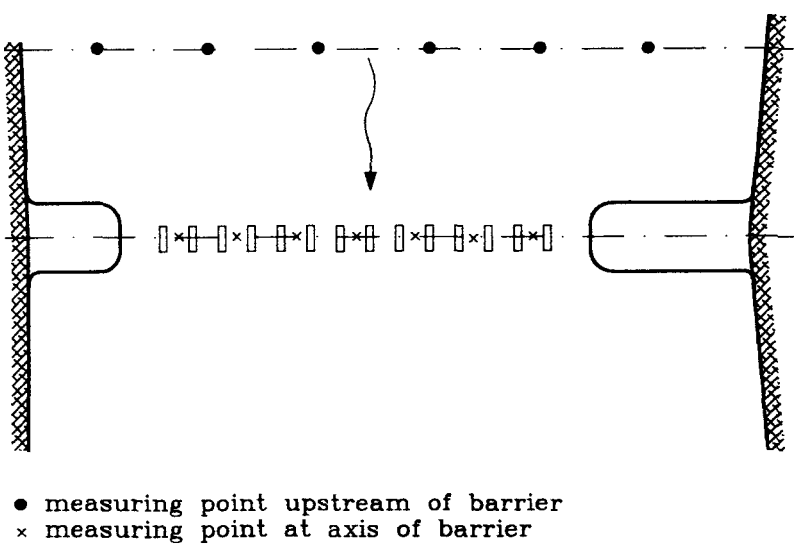

Figure 8.1 Location of flow measurement during measurement campaigns

In principle the purpose of the verification was two-fold:
- verification of the individual models of the forecast system.
- verification of the predicted design parameters.

Re-calibration of the models, based on the verifications, will lead to improvement of future forecasts. Verification of the forecasts of the design parameters was very important for the contractors building the barrier. The quality of the prediction of the design parameters determined to a consider-

able degree the extent of risks during the execution of the works. Therefore the accuracy of the predicted design values of q/A was guaranteed by contract by the Public Works Department [8-1].

To verify a model, a hindcast of it can be compared with measurements. This is a fairly simple procedure. The verification of the predicted design parameters is more difficult: In practice the conditions during the verification measurements will never be equal to the conditions for which the design parameters had been derived. These were: average tidal conditions and extreme tidal conditions with one-year return period. Since most of the verification measurements would take place under more or less average tidal conditions, all measured data were transformed to these conditions. This transformation was performed by using the computed relation between the tidal range at OS4 and the maximum transport rate Q_{max} (Figure 8.2).
When the ratio between the measured Q and Q at average tidal conditions is computed, the measured values of q/A are transformed to average tidal conditions using the same ratio.
The verification of the head difference over the barrier, Δh, was not done systematically for all measurement campaigns, since Δh became important as a governing parameter, only during the final construction stages of the barrier.

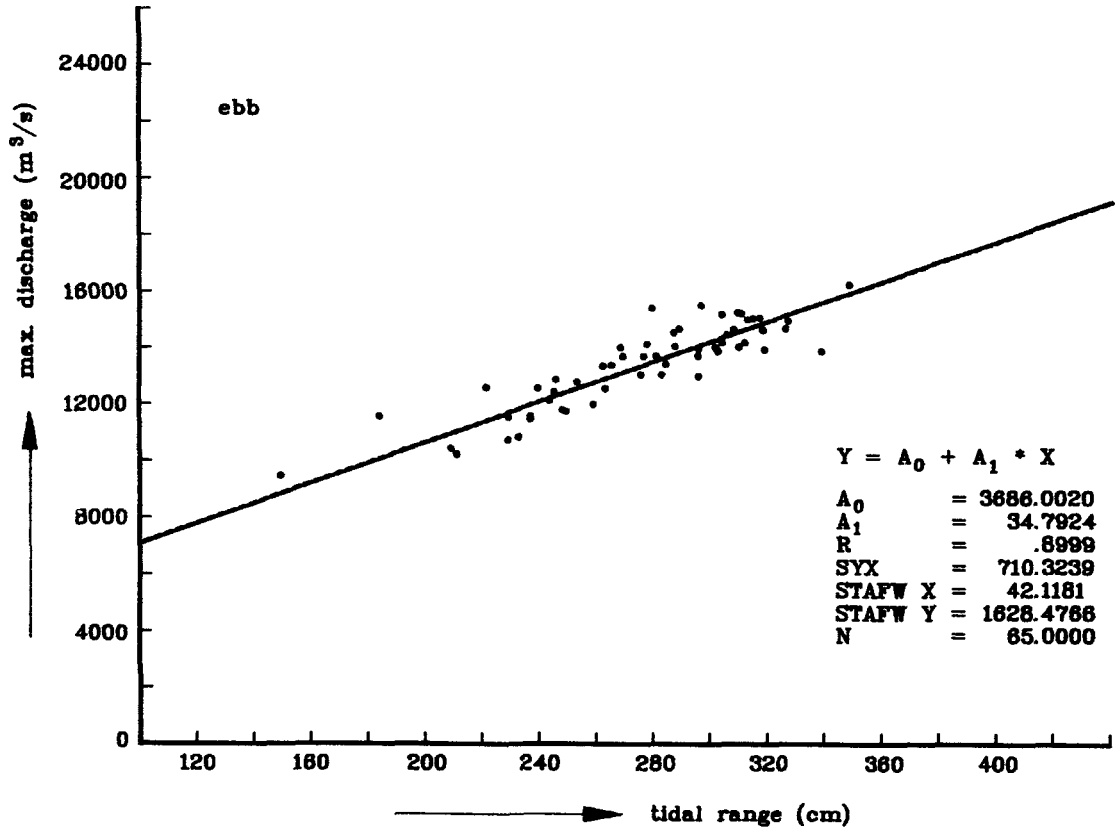

Figure 8.2 Linear regression maximum ebb discharge through Hammen channel and tidal range at station OS4

8.1.3 Results of the verification of IMPLIC-R1495

Verification campaigns, as described in the previous section, were performed completely for seventeen construction stages of the barrier (one construction stage represents a verification for one main channel for both ebb and flood flow). Additionally, a limited campaign without verification of q/A has been performed for eight construction stages, see Table 8.1.

date	in channel	construction stage of the barrier			sort of campaign
		Hammen	Schaar	Roompot	
29-12-83	Hammen	all piers	mats	mats	with q/A
31-03-84	Hammen	1/2rubble sill	15 piers	mats	no q/A
11-04-84	Schaar	rubble sill	piers	mats	with q/A
30-07-84	Hammen	rubble sill	2/3rubble sill	18 piers	no q/A
30-07-84	Schaar	rubble sill	2/3rubble sill	18 piers	no q/A
1-08-84	Roompot	rubble sill	2/3rubble sill	18 piers	no q/A
27-09-84	Roompot	rubble sill	rubble sill	piers	with q/A
26-10-84	Schaar	rubble sill	rubble sill	1/4rubble sill	no q/A
7-02-85	Roompot	rubble sill	rubble sill	1/2rubble sill	with q/A
20-06-85	Hammen	rubble sill	rubble sill	rubble sill	with q/A
20-06-85	Schaar	rubble sill	rubble sill	rubble sill	with q/A
20-06-85	Roompot	rubble sill	rubble sill	rubble sill	with q/A
23-07-85	Schaar	7 sill beams	1 sill beam	rubble sill	with q/A
26-07-85	Hammen	7 sill beams	1 sill beam	rubble sill	with q/A
9-09-85	Schaar	9 sill beams	9 sill beams	rubble sill	with q/A
14-09-85	Hammen	14 sill beams	9 sill beams	rubble sill	with q/A
16-09-85	Schaar	14 sill beams	9 sill beams	rubble sill	no q/A
26-09-85	Roompot	sill beams	sill beams	rubble sill	with q/A
27-09-85	Schaar	sill beams	sill beams	1 sill beam	no q/A
1-10-85	Hammen	sill beams	sill beams	3 sill beams	no q/A
21-11-85	Schaar	sill beams	sill beams	9 sill beams	with q/A
27-11-85	Roompot	sill beams	sill beams	9 sill beams	with q/A
10-12-85	Hammen	sill beams	sill beams	9 sill beams	with q/A
12-04-86	Roompot	sill beams	sill beams	21 sill beams	with q/A
26-04-86	Roompot	sill beams	sill beams	sill beams	with q/A

Table 8.1 Verification campaigns.

In this report the results of the verifications will not be presented integrally. Only a summary of the results is given for the following items:

- Discharge in the main channel, Q.
- Lateral discharge distribution, expressed by q/A.
- Effect of corrections.
- Head difference over the barrier, Δh.

Discharge in the main channel, Q.

The measured discharges were compared with hindcasts of the tidal motion during the respective day of the measurements. The results of this comparison were used to determine the need of a re-calibration of the IMPLIC model, especially for the discharge coefficients of the barrier. Such a calibration could improve the forecasts for the following construction stages. Examples are given in Figures 8.3 and 8.4.

The experience gained by the verifications was that, as the construction of the barrier progressed, the discharge characteristics of the barrier more and more dominated the tidal flow in the estuary. The influence of the discharge coefficient μ_3 became more important than the schematization of the Eastern Scheldt estuary itself.

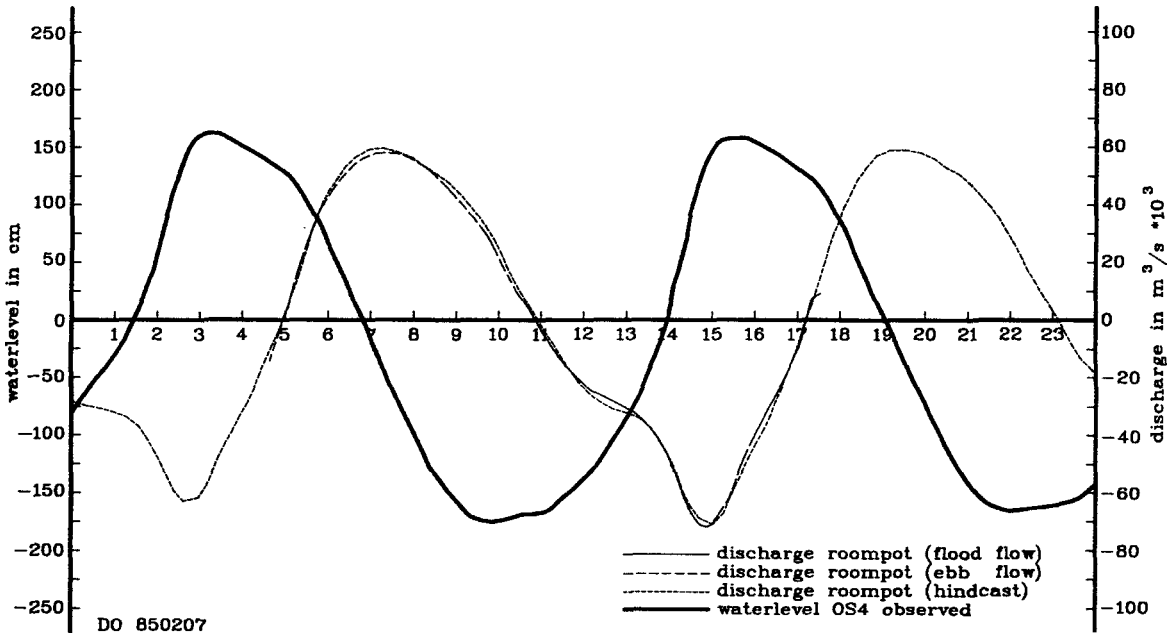

Figure 8.3 Hindcast Roompot discharge (IMPLIC), rubble sill completed

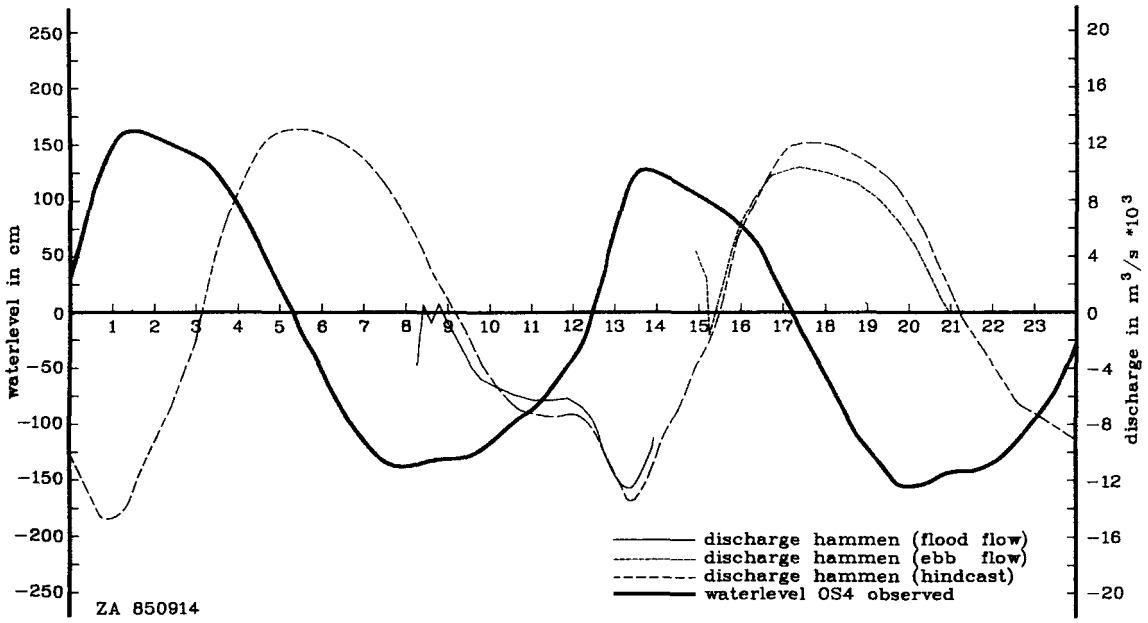

Figure 8.4 Hindcast Hammen discharge (IMPLIC), 14 sill beams installed

Additionally a verification was performed of the predicted design values of the discharge at maximum (ebb/flood)flow, Q_{max}. This was done by transforming the measured Q_{max} to the corresponding value at average tidal conditions. The results were compared with the predicted values. Figures 8.5 and 8.6 give the results of the verification. The presented values of Q_{max} are given relative to the situation without the barrier.

The results of the verifications, both for design values and hindcasts of the discharge at maximum flow, are summarized in Table 8.2. The table gives the average and standard deviation of the difference between measurement and forecast. All values are given as a percentage of the forecast:

$$\frac{Q_{max}\text{measured} - Q_{max}\text{ forecast}}{Q_{max}\text{ forecast}} \times 100\%$$

The deviations are given per main channel, Roompot, Schaar and Hammen, for maximum ebb flow and for maximum flood flow. Also the overall results are given; for each flow direction and separately for both directions.
All values in Table 8.2 are relative values, given as percentages. Negative values indicate a measurement less than the forecast.

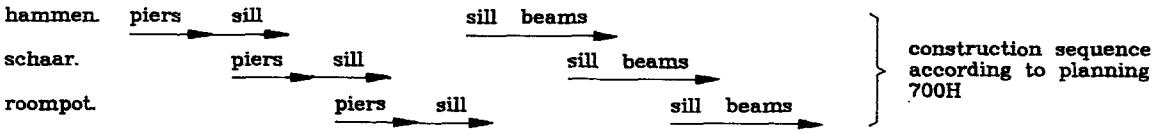

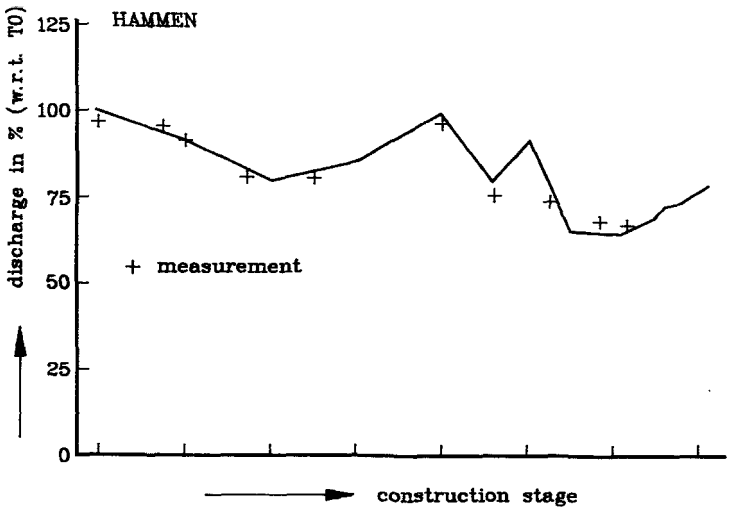

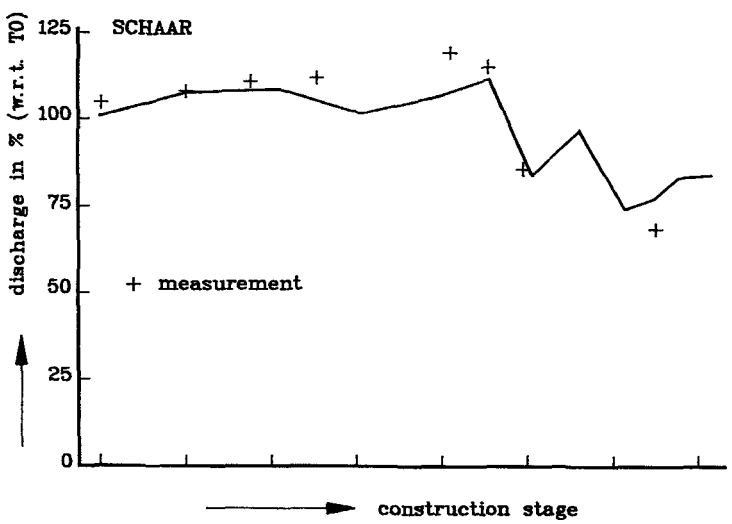

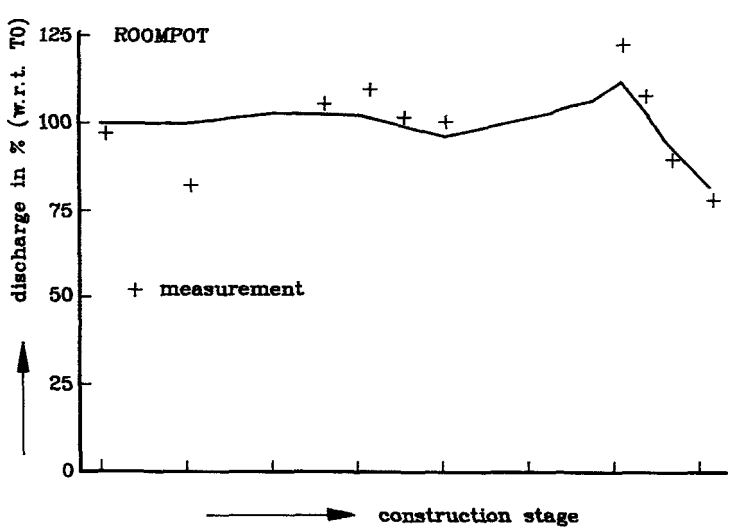

Figure 8.5 Verification predicted discharge at maximum flood

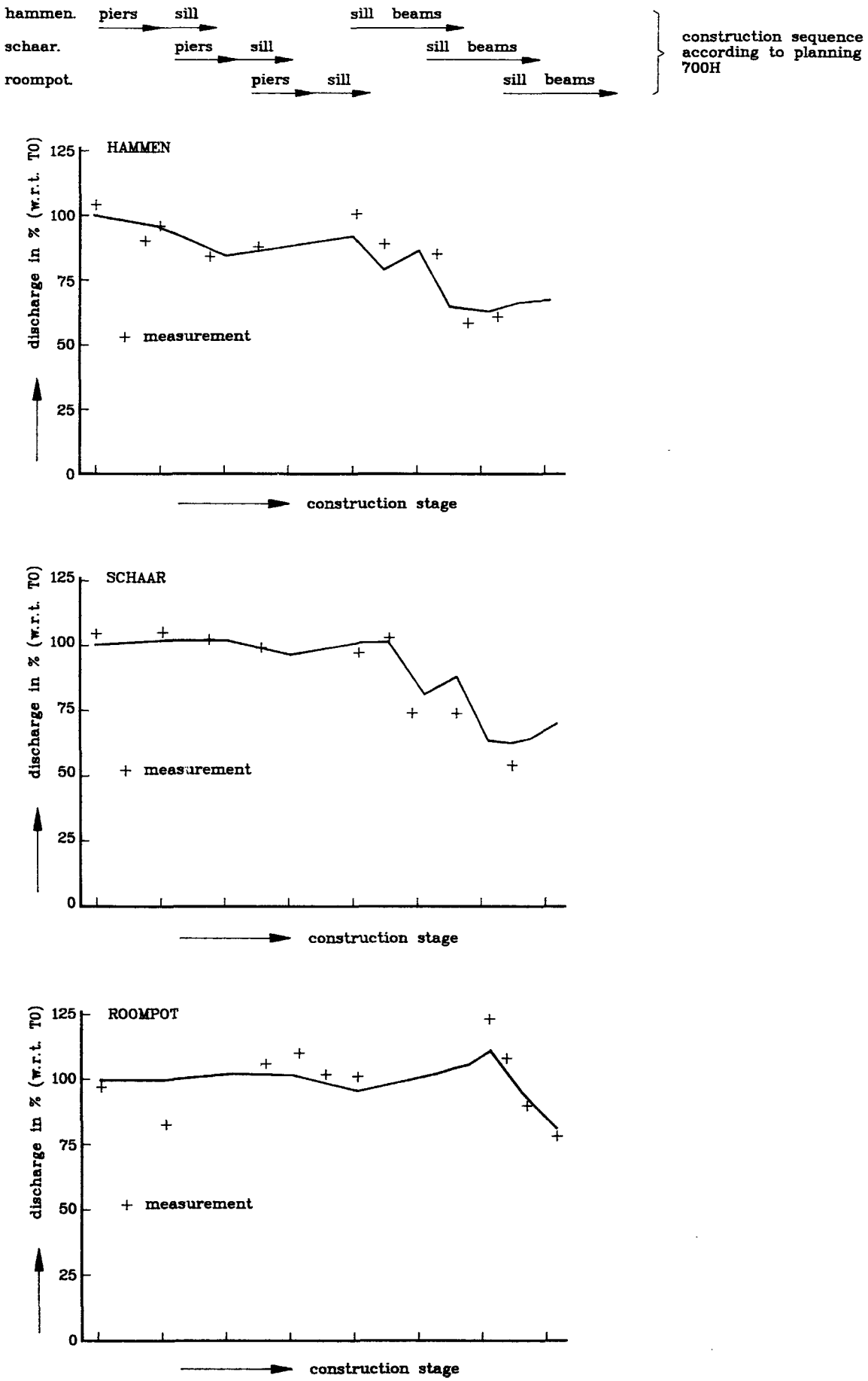

Figure 8.6 Verification predicted discharge at maximum ebb

relative deviation [%]	design values Q_{max}				hindcast Q_{max}			
	max. ebb		max. flood		max. ebb		max. flood	
	mean	σ	mean	σ	mean	σ	mean	σ
Roompot	-1.5	6.2	4.1	4.8	1.5	5.4	3.1	4.7
Schaar	-5.3	10.2	2.5	11.3	-2.7	3.9	4.4	5.0
Hammen	2.6	9.6	3.8	5.6	-2.4	6.4	-2.4	3.3
Total	-1.6	8.9	3.5	7.5	-2.1	5.1	1.7	5.2
Overall	mean = 0.9%, σ = 8.5%				mean = -0.2%, σ = 5.4%			

Table 8.2 Results of verification Q_{max} IMPLIC.

The conclusions from the results presented in Table 8.2 are:

- The model errors mostly had a random character, even when the individual channels were considered. The μ values of the errors were always much smaller than the σ values.
- The errors in the hindcasts were less than in the design values. The same also applies to the differences between the different channels.
- The accuracy of the initial calibration of 10% (maximum error, see 6.2.5) had also been achieved with the hindcasts (maximum deviations ≈ 2 σ ≈ 10%).

Lateral distribution of the transport rate, q/A.

The measured prototype values of q/A have been compared with the design values at maximum flow. This has been done to determine the overall accuracy of the prediciton of q/A as a design parameter. Examples of the results of these checks are given by Figures 8.7 through 8.9. In addition to the overall inaccuracy of q/A from IMPLIC-R1495, the inaccuracy of R1495 was determined separately, by excluding the error in the predicted discharge as computed by IMPLIC.

All results are collected in Table 8.3. The deviations are given as in Table 8.2 divided per main channel (Roompot, Schaar and Hammen), for maximum ebb flow and for maximum flood flow. Also the overall results are given; seperate for each flow direction and for both directions.

All values in Table 8.3 are relative values, given as a percentage. Negative values indicate a measurement less than the forecast.

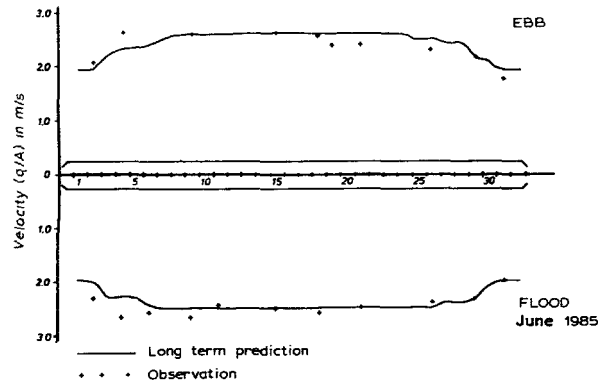

Figure 8.7 Verification predicted lateral q/A distribution at maximum flow, Roompot rubble sill completed

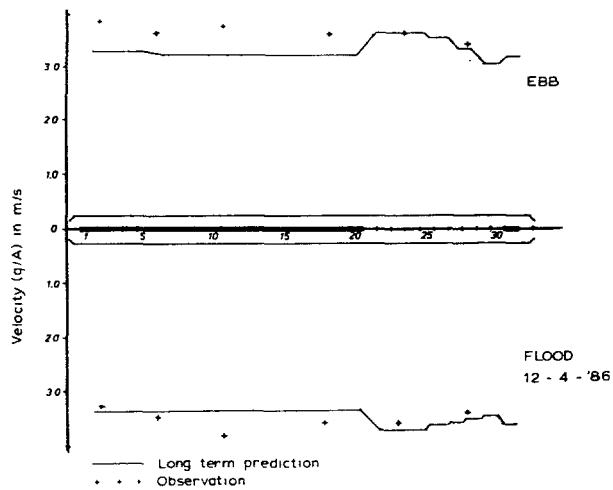

Figure 8.8 Verification predicted lateral q/A distribution at maximum flow, Roompot 21 sill beams installed

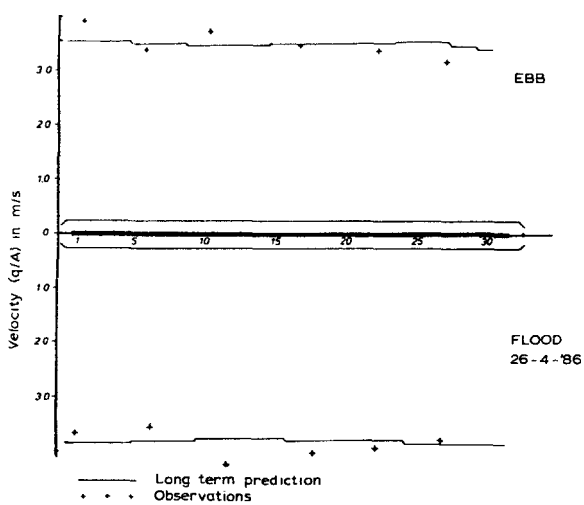

Figure 8.9 Verification predicted lateral q/A distribution at maximum flow, Roompot all sill beams installed

relative deviation [%]	overall error $(q/A)_{max}$ (IMPLIC + R1495)				excluding error in Q_{max} (R1495 only)			
	max. ebb		max. flood		max. ebb		max. flood	
	mean	σ	mean	σ	mean	σ	mean	σ
Roompot	0.4	11.8	6.1	9.1	2.2	9.9	1.2	8.4
Schaar	-10.9	7.6	-3.8	15.3	-5.1	6.2	-1.4	9.2
Hammen	2.9	11.0	1.5	12.2	2.1	9.5	-0.1	10.7
Total	-2.1	11.9	2.0	12.6	0.1	9.4	0.2	9.2
Overall	mean = 0.0%		σ = 12.4%		mean = 0.1%		σ = 9.3%	

Table 8.3. Results of verification $(q/A)_{max}$

Conclusions from Table 8.3. are:

- The errors in R1495 have a random character, even when individual channels are considered.
- When the errors of the discharge are included the overall error in the q/A forecasts is 12.4% (σ/μ), against 15% that was assessed beforehand.
- When the error of the forecast of the discharge was excluded, the overall error in the lateral distribution of q/A, as computed with R1495, was 9.3%.

To assess the consequences of the inaccuracy of the forecasts, it is important besides the mean error and its standard deviation also to determine the probability distribution. Initially the distribution function was assumed to be normal one [8-1]. The actual distribution of the overall errors in the forecast of q/A at maximum flow is given by Figure 8.10. Its distribution is indeed approximately a normal distribution.

The deviations given in Figure 8.10 were averaged over all construction stages of the barrier. It was also of interest to learn how the errors were distributed over the construction stages. In Figure 8.11 the predicted design values of q/A have been plotted against the measured values. Here low velocities correspond to early construction stages and high velocities to later stages. The figure shows that the deviations are equally distributed over low and high velocities, and thus over all construction stages.

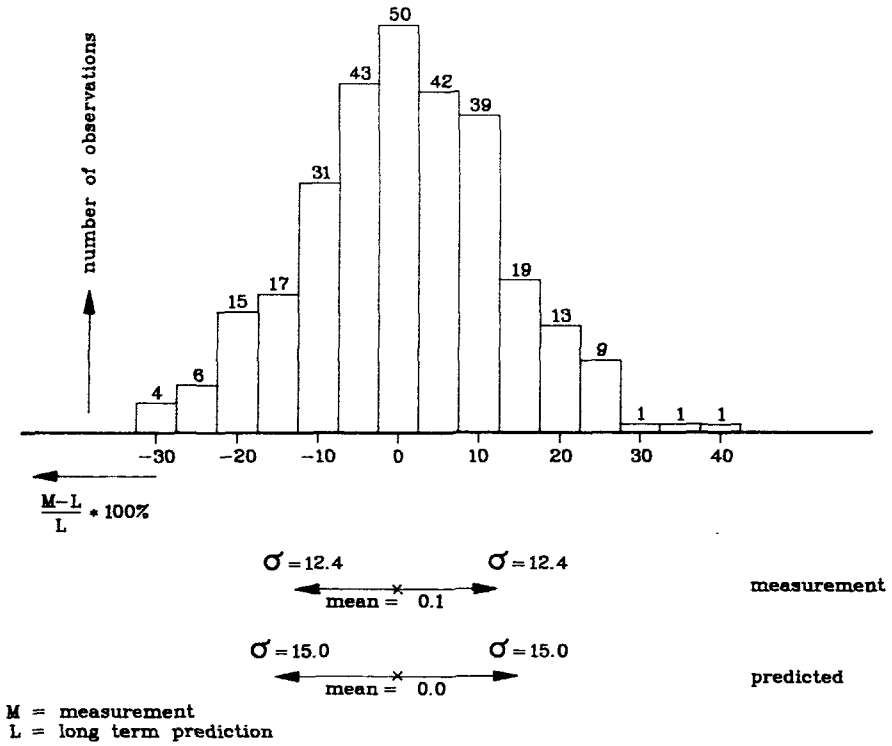

Figure 8.10 Distribution of the deviations between predicted and measured q/A

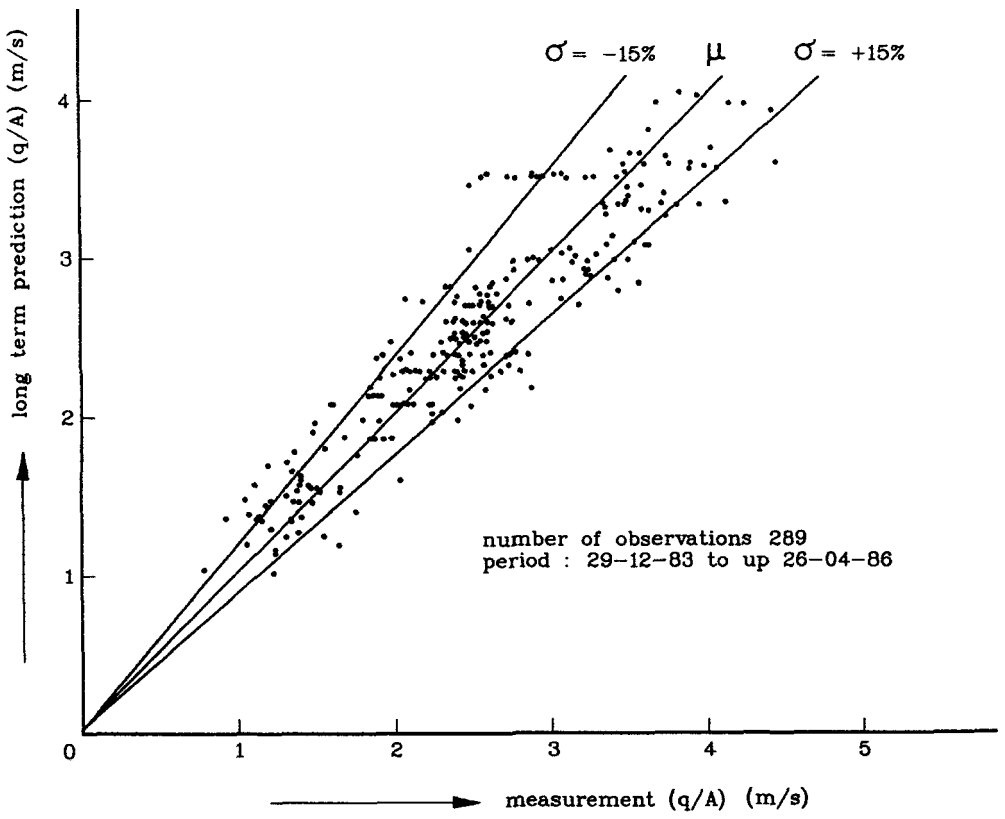

Figure 8.11 Measured q/A plotted against predicted q/A

Effect of corrections, operational control

The most critical operations, such as the placing of the sill beams, were controlled by on-line velocity measurements. With the help of these measurements the short-term operational forecasts could be improved. The short-term forecasts were computed with the IMPLIC/R1495 system, six hours ahead, based on astronomical tide data and meteorological effects. By a relatively simple manual correction the deviations in the forecast one to two hours ahead, could be reduced to half the value achieved without the input of the on-line measurements [8-2].

Head difference over the barrier, Δh

An overall check of the accuracy of the Δh forecasts was not useful, since the accuracy of the measurement of Δh in the prototype strongly depended on the narrowing of the channel, and thus on the construction stage of the barrrier. Roughly speaking three regimes could be discerned:

- narrowing less than 50%; construction stages until the rubble sill was completed:
  The value of Δh was small, less than 0.25 m. The discharge was only slightly affected by the barrier; less than 10%. The accuracy of Δh was mainly governed by the accuracy of the discharge coefficient μ_3 which was rather inaccurate for these construction stages. A prototype evaluation was not possible because of the relatively large errors in the measured (small) head differences.

- narrowing between 50% and 75%; positioning of the sill beams:
  The accuracy of the prediction of Δh was better than with previous construction stages. The barrier formula that was used is correct here. The discharge coefficients could be determined with an error less than 10%. The error in the predicted Δh could consequently be estimated as less than 20%*, since $\Delta h \sim \mu^{-2}$. Field experience shows that this estimate was correct [8-3].

- narrowing more than 75%; all sill beams installed with a number of gates closed:
  Δh was large and could be measured accurately. However, the discharge was small and could not be measured accurately, especially in field situations. Because of this, the overall discharge coefficient of the barrier in a channel could not be determined accurately. With the discharge coefficients

predicted beforehand, the error in the predicted Δh turned out to be 10% to 20%*. Once experience was gained with a specific geometry of the barrier, re-calibration diminished the errors in Δh computation with 5% to 10%*.

* accuracy of the models determined from hindcasts.

8.1.4 Accuracy of the scale models, M1000-M1001

A direct verification of the scale models M1000-M1001 with the field data from the measurement campaigns given in Table 8.1 was not possible without hindcast tests. As a result of the numerous changes in the construction scheme of the barrier, hardly any construction stage from these campaigns matched an available scale model test. However, conducting hindcast tests was very expensive, and thus was decided against.
Because the models IMPLIC and R1495 were calibrated on base of the results of the scale models, the results of the verification of IMPLIC and R1495 could be used as an indirect verification of the scale models for discharge Q, lateral discharge distribution, q/A and head difference Δh.

Discharge, Q, and head difference, Δh

Except for early construction stages, both Q and Δh were mostly determined by the discharge coefficient μ_3. The value of μ_3 was derived from M1000-M1001. The accuracy of Q and Δh from the scale models would thus be the same as from IMPLIC.

Lateral distribution of the transport rate, q/A

The R1495 model was calibrated on the basis of the M1001 results. Because an exact fit of the results was not possible with the R1495 model, R1495 would thus be less accurate than M1001. Therefore, the error in q/A from M1001 would be less than 9% (σ/μ). The exact value of the error could not be given; the error in M1001 was estimated at 5% (σ/μ).

Conclusion

The accuracy of Q, q/A and Δh, determined through the scale models M1000-M1001, was slightly better than those determined with IMPLIC-R1495.
However, the flexibility of the scale models was considerably less than the numerical models. Because of continuous changes in the planning of the construction, the results from the scale models had to be "translated" to different construction stages. In practice the errors of this translation were

larger than the errors made by using IMPLIC-R1495. Because of this, the scale models were not used directly. Note however, that scale models were indispensible for the calibration of IMPLIC-R1495.

8.2 Reproduction of downstream flow pattern

8.2.1 Introduction

In this section the reproduction of the flow pattern directly downstream of the barrier will be discussed. This flow pattern is an essential parameter for the prediction of local scour downstream of the bed protection works on both sides of the barrier. The development of scour holes was in first instance predicted through scour tests in the hydraulic scale model of the mouth of the Eastern Scheldt (see Chapter 5; detail model M1001). During the study period it was concluded that the scour could be calculated if a reliable prediction of the velocity distribution at the end of the bed protection was available.
The most interesting phase (related to scour problems) during the construction is the installation of the sill beams. It causes an abrupt change in the flow pattern (steep velocity gradients, strong eddies). The reproduction of the flow pattern had been carried out for a number of construction stages for which extensive field data were available. For these construction stages the flow pattern in the vicinity of the barrier had been computed with the WAQUA-models of the Eastern Scheldt (see Chapter 7) and the results were compared with the observed flow.
In addition, results of tests in the scale model were available and have also been compared with the field data. In this way a preference could be given whether physical scale models or numerical models should be used to determine (predict) the flow pattern in the vicinity of a structure as the storm-surge barrier.

8.2.2 Setup of the reproduction

For a number of building stages related to the installation of sill beams extensive field data were available. These data consisted of water levels, head differences, discharges, flow velocities and flow directions upstream, downstream and at the site of the barrier.
A special type of measurements was the so-named 'Ametek'-measurements: the downstream velocity distribution at the end of the bed protection was measured by a set of special equipment ('Ametek'= acoustic measuring system for determination of velocity profiles). The following list shows the building stages (grouped by main channel) for which 'Ametek'-measurements were available:

Roompot: rubble sill completed
9 sill beams placed
21 sill beams placed
barrier completed
Schaar : 1 sill beam placed
9 sill beams placed
16 sill beams placed
barrier completed
Hammen : rubble sill completed
7 sill beams placed
9 sill beams placed
14 sill beams placed
15 sill beams placed
barrier completed

For all these building stages the flow pattern was computed with the WAQUA-models. The schematization of the barrier in the numerical models was in first instance according to the original approach for incorporation of energy losses. At the barrier site the long-wave equations were replaced by the following barrier equation (see also Section 7):

$$Q_b = \mu_2 B (d_b+a) \sqrt{2g (h_1-h_3)} \qquad (8.1)$$

where:

Q_b	=	discharge per barrier opening	(m^3/s)
μ_2	=	discharge coefficient	(-)
B	=	width of barrier	(m)
d_b	=	depth of barrier w.r.t reference plane	(m)
a	=	water level w.r.t reference plane	(m)
g	=	acceleration due to gravity	(m/s^2)
h_1	=	upstream water level	(m)
h_3	=	downstream water level	(m)

It turned out that with this schematization the downstream flow pattern was not reproduced correctly. The implementation of the barrier equation in the computational scheme seemed to be the cause of the problems and so supplementary computations were carried out with a different approach to the energy losses at the barrier.
In these supplementary computations the building stages of the barrier were schematized by merely adjusting the local water depth and/or the local rough-

ness. With respect to the local water depth two alternatives were used, namely: the local depth equal to the original water depth in the channel or the local depth adjusted in such a way that the cross-sectional area equals the area at the throat of the barrier. The schematization had to be made in such a way that the discharge characteristics did not change. At the barrier site an adapted fixed value of the Chézy coefficient had been calculated by equating the Chézy equation to Equation 1.
This results in the following equation:

$$C = \frac{\mu_2 \, B(d_b+a) \sqrt{2gL}}{\Delta x \, (d+a)^{1.5}} \qquad (8.2)$$

where:

C	= adapted Chézy coefficient	($m^{\frac{1}{2}}/s$)
μ_2	= discharge coefficient	(-)
B	= width of barrier section	(m)
d_b	= depth of barrier w.r.t reference plane	(m)
a	= water level w.r.t reference plane	(m)
g	= acceleration due to gravity	(m/s^2)
L	= length of adjustment (1 or 2 grids)	(m)
Δx	= width of grid	(m)
d	= depth of bottom w.r.t. reference plane	(m)

The calculation of the adapted Chézy value was carried out for a water level at the reference plane (N.A.P.), which is very close to mean sea level. Because of the fixed value of C the resulting discharge characteristics of the barrier showed some deviation as a function of the downstream water level. For the reproduction of the flow pattern this was considered to be of minor importance.

8.2.3 Results of the reproduction

The flow patterns were computed for all the building stages for which 'Ametek'-measurements were available; for the schematization of the energy losses at the barrier site three methods were applied (see Section 8.2.2). These methods are:

- Method 1: Substitution of the long-wave equations by a barrier equation (= original method)
- Method 2: Adjustment of local water depth and roughness
- Method 3: Adjustment of roughness only

An extensive presentation of the results is given in [8-4] en [8-5]. For two more or less representative situations the results are discussed below, these situations are (see also Figure 8.12):

- The Roompot: 21 of the 31 sill beams installed; ebb flow.
- The Hammen: all 15 sill beams installed; flood flow.

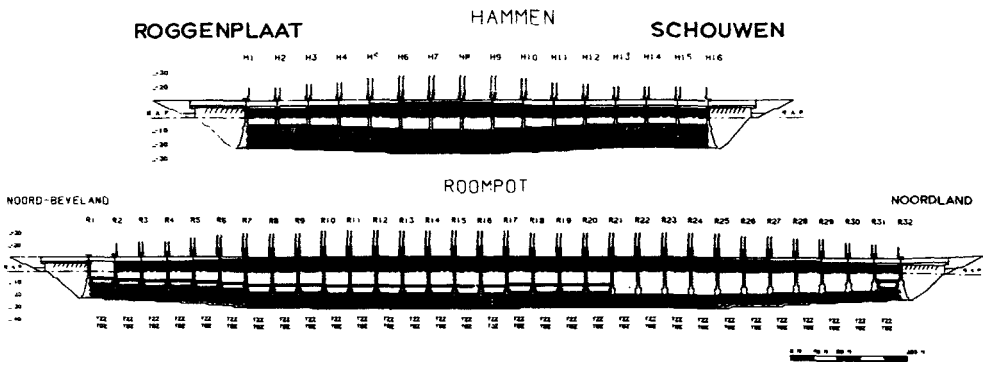

Figure 8.12 Cross-section of the barrier under construction in the Roompot and the Hammen channel

In these situations the flow was dominated by three-dimensional effects:

- The Roompot: At the transition between the barrier section with rubble sill and the adjacent one with the concrete sill beams, there was a sharp discontinuity in the barrier, in the cross-sectional opening and in the discharge coefficient. Downstream this discontinuity a mixing zone with a sharp velocity gradient developed.
- The Hammen: Downstream the barrier large eddies were formed behind the abutments of the dam.

Most of the results presented below, have been computed according to Method 2, except for one example which shows the effect of Method 1 and Method 3. In addition, results are presented from tests in the hydraulic scale model M1001. The results for both the Roompot and Hammen flow situations are presented in Figures 8.13 through 8.21:

- The computed flow pattern in the Roompot has been plotted in Figure 8.13 for maximum ebb flow.
- In Figure 8.14 the observed and computed discharge in the Roompot are given for both ebb flow and flood flow.
- The observed and computed flow velocities and flow directions at 350 m upstream and 630 m downstream of the barrier, are presented in Figure 8.15 (maximum ebb flow). The discharge per opening has also been plotted in Figure 8.15.

- The discharge in the Hammen is presented in Figure 8.16.
- In Figures 8.17 through 8.19 the computed flow pattern in the Hammen during maximum flood flow, has been plotted for Method 1, 2 and 3 respectively.
- Figure 8.20 shows for the three methods of schematization a comparison of the computed velocities at 630 m downstream of the barrier.
- Figure 8.21 finally gives the observed and computed velocities at 400 m upstream and 630 m downstream of the barrier and the discharge per barrier section (maximum flood flow). Additional to the field data and computed velocities, the measured flow velocities in the scale model are also given at 630 m downstream of the barrier.

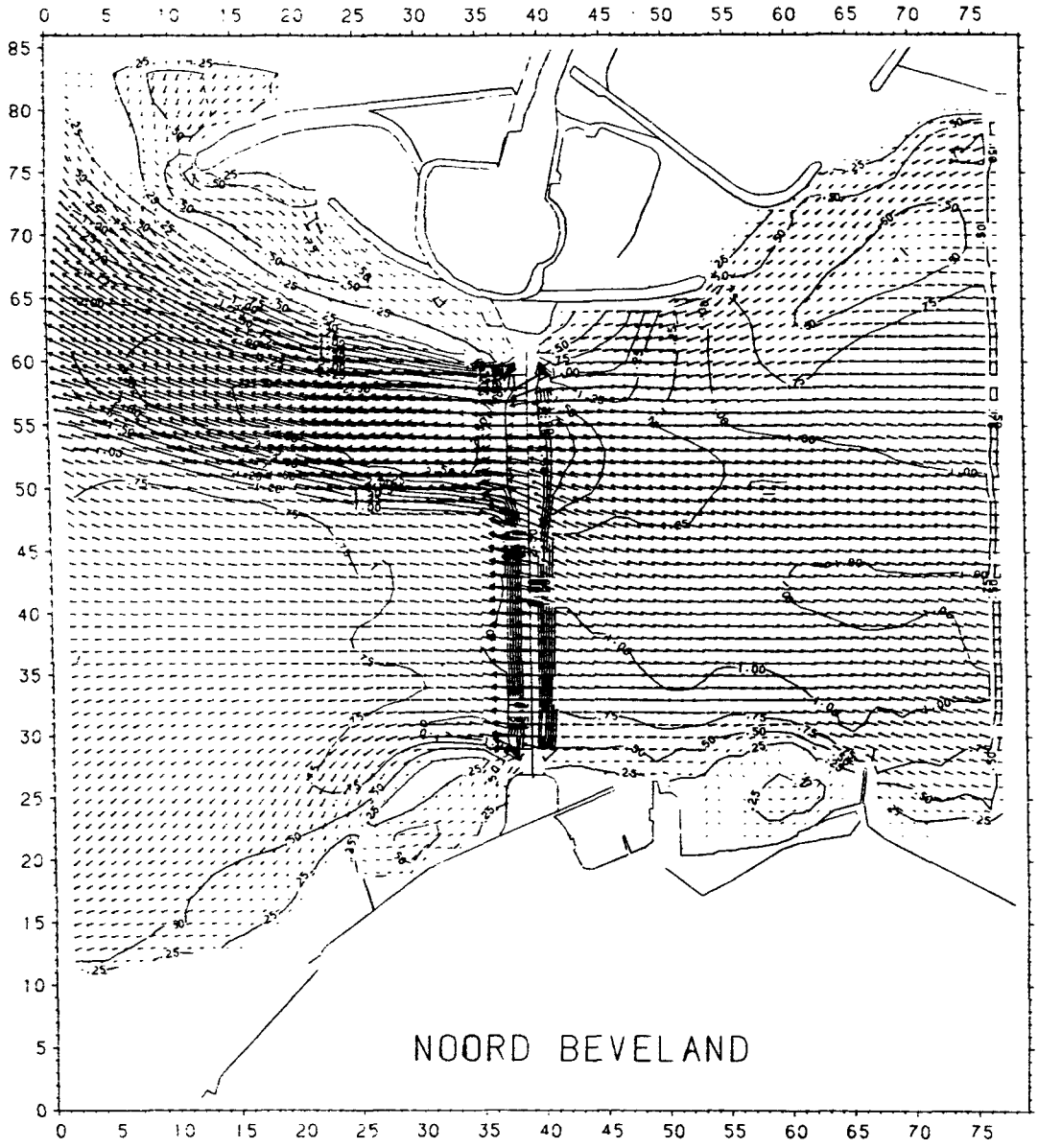

Figure 8.13 Roompot channel, flow patterns maximum ebb flow (Method 2)

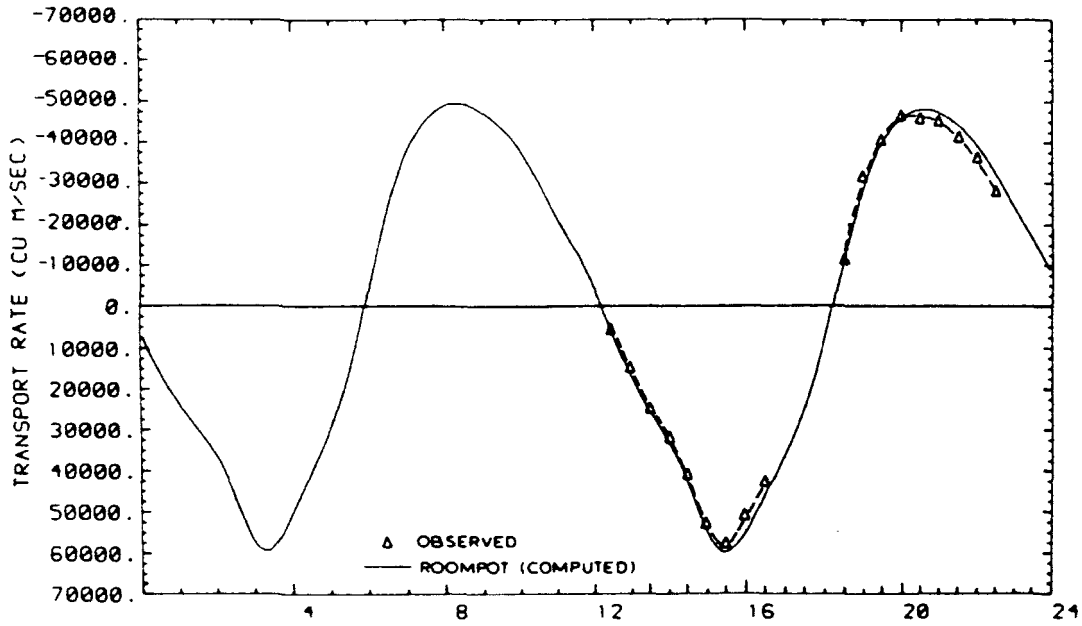

Figure 8.14 Roompot channel, transport rates

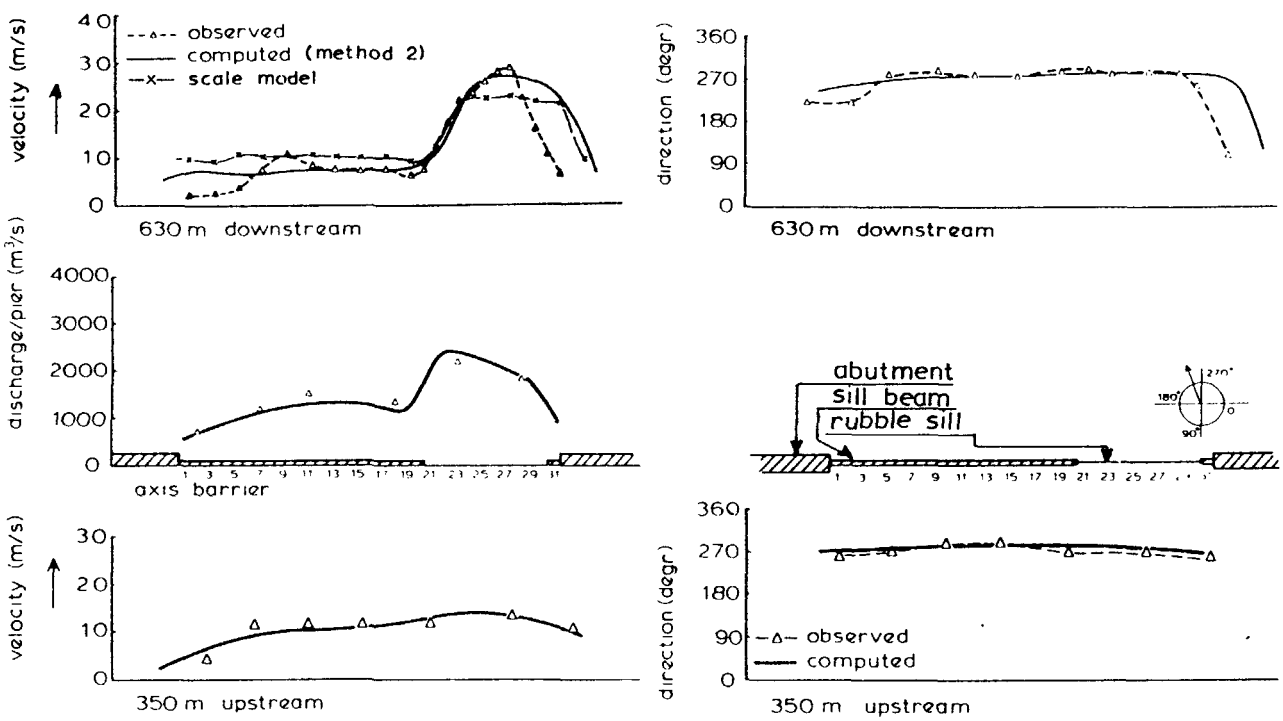

Figure 8.15 Roompot channel, flow velocities and directions, maximum ebb flow

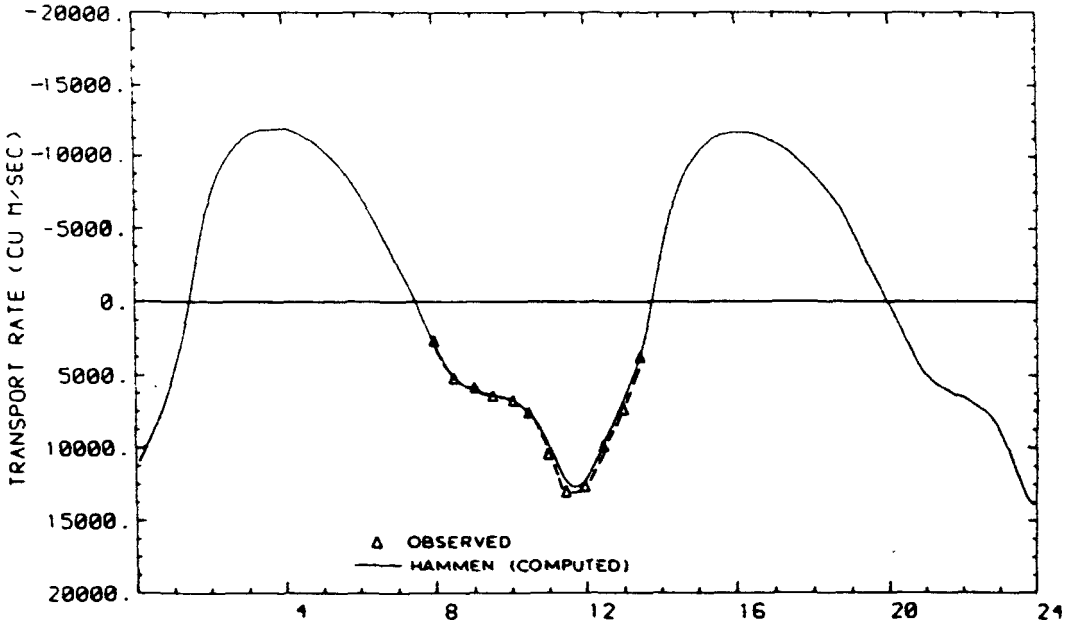

Figure 8.16 Hammen channel, transport rates

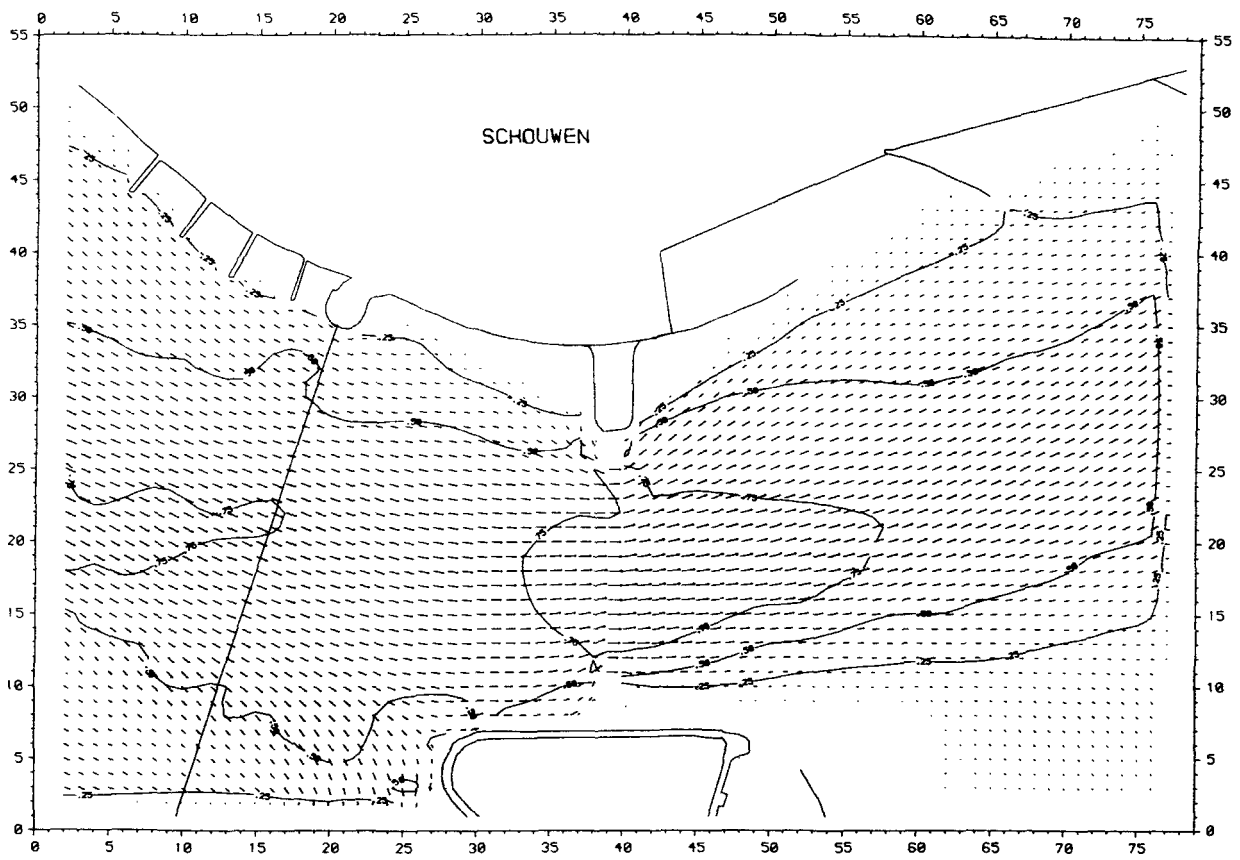

Figure 8.17 Hammen channel, flow pattern maximum flood (Method 1)

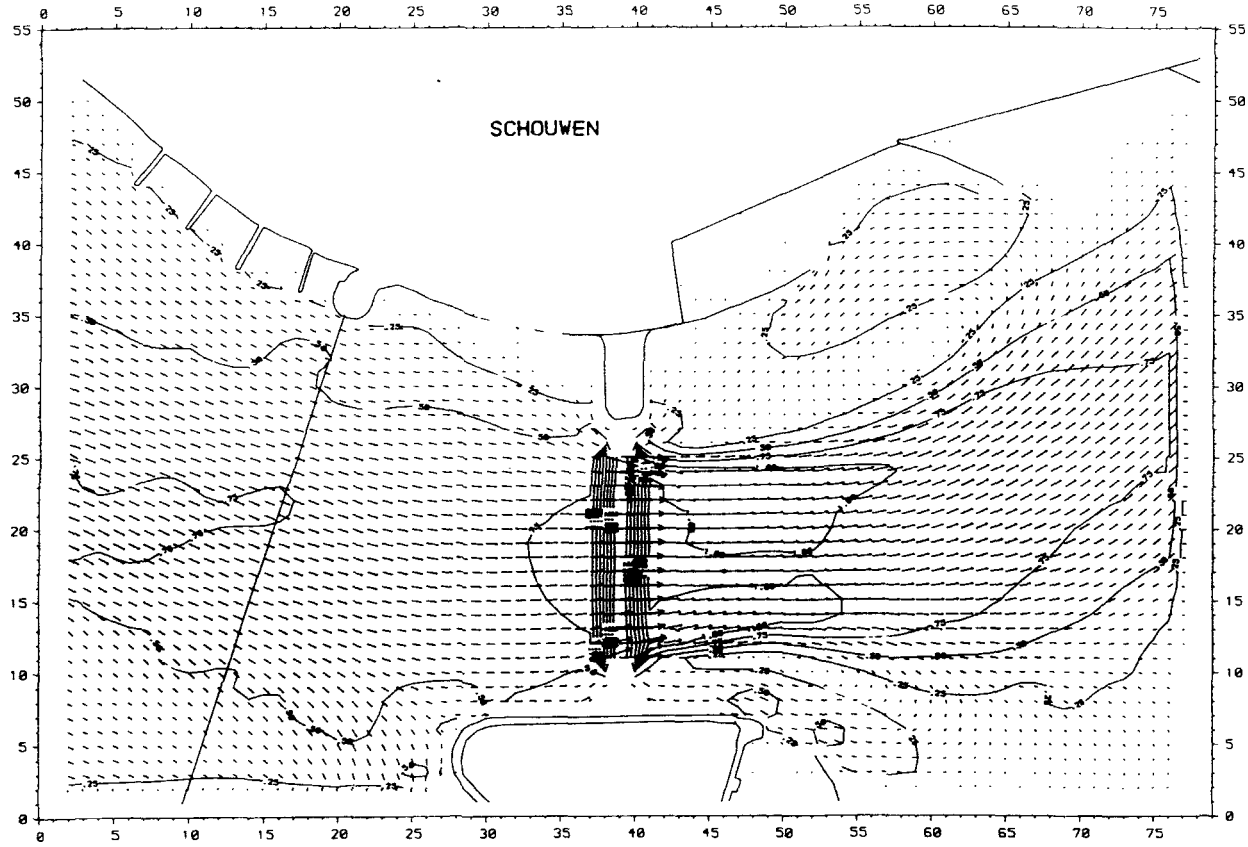

Figure 8.18 Hammen channel, flow pattern maximum flood (Method 2)

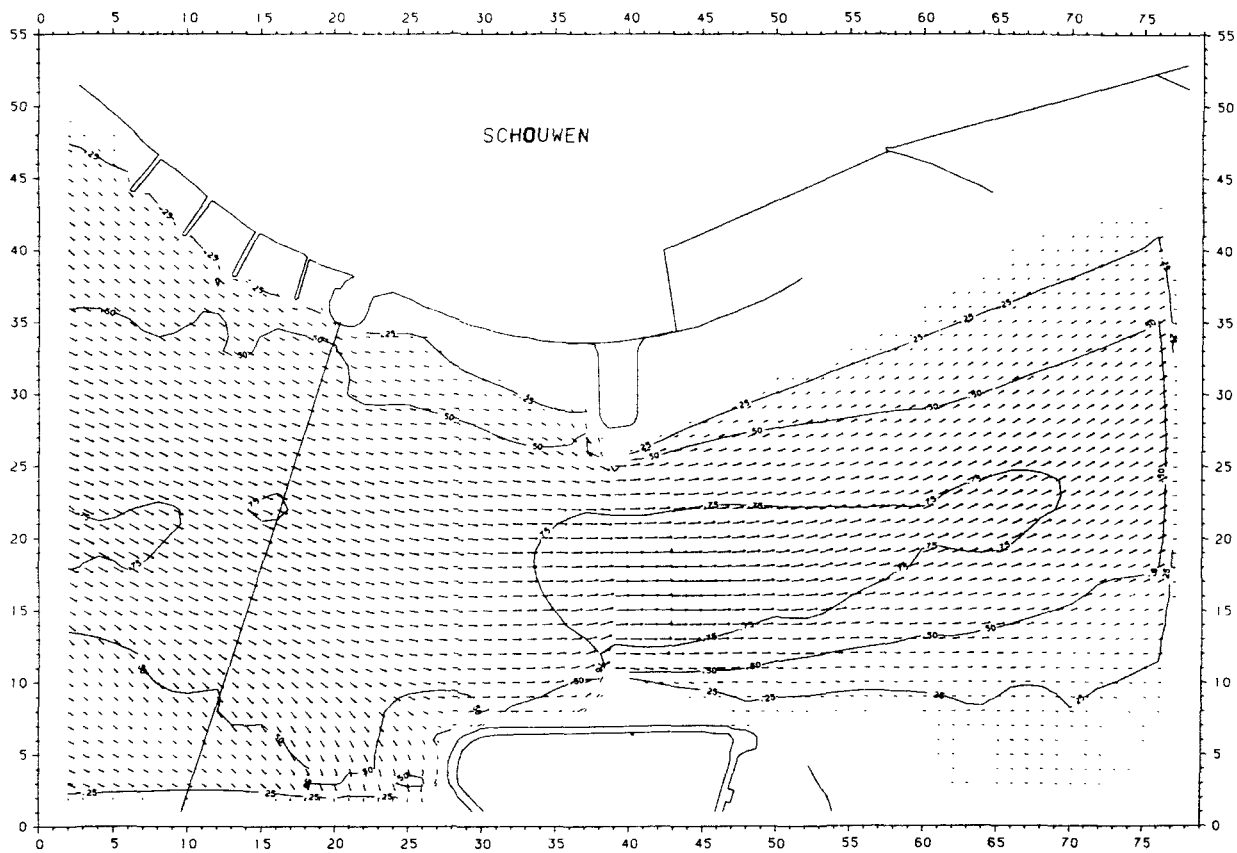

Figure 8.19 Hammen channel, flow pattern maximum flood (Method 3)

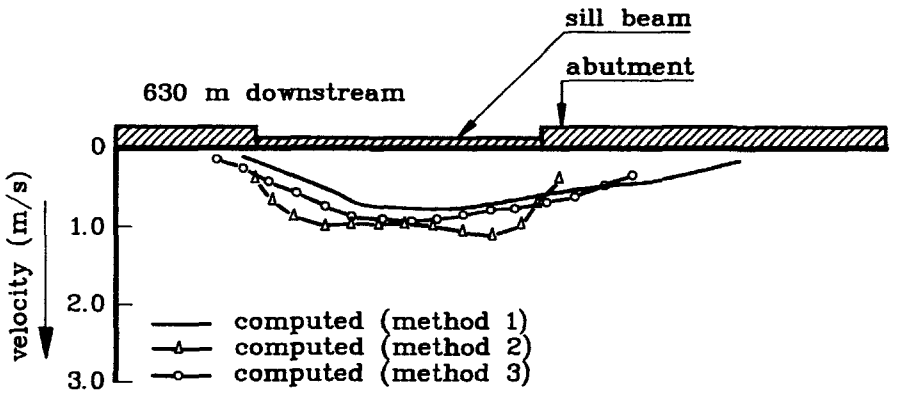

Figure 8.20 Hammen channel, flow velocities maximum ebb flow

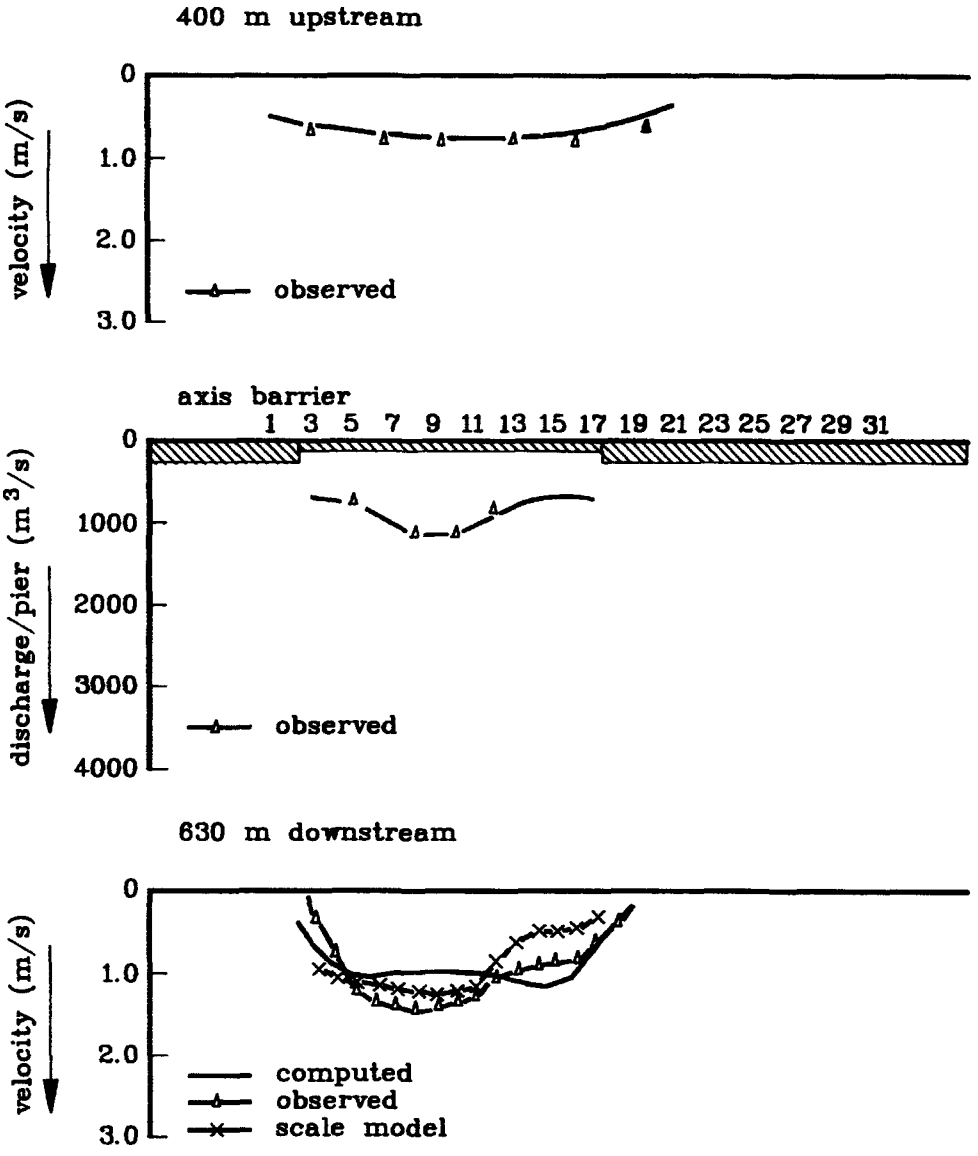

Figure 8.21 Hammen channel, flow velocities maximum ebb flow

Based on these and other [8-4] and [8-5] results, the performance of the three numerical methods for representation of the barrier is briefly discussed:

- Method 1: Substitution of the long-wave equations by a barrier equation.
  The flow pattern directly downstream of the barrier (which in this method formed an internal boundary in the model) was incorrect. The dispersion of the main flow was much stronger than in the prototype, downstream the barrier the absence of large eddies was obvious. The computed discharge and head difference agreed well with observations.
- Method 2: Adapted fixed roughness and adjustment of local depth.
  The downstream flow pattern gave a fairly good reproduction of the prototype; the barrier is no longer an internal boundary in the model. The dispersion of the flow and the velocity gradients were nearly equal to the prototype values and large eddies were present downstream the abutments. A disadvantage of this method is the rough approximation of the resistance; because an averaged roughness was used, it was not possible to account for the influence of different flow directions and different flow conditions. This resulted in a less accurate reproduction of the discharge and the head difference than with Method 1. A modification in the program to account for above variability is feasible and has already started (see Section 8.2.4).
- Method 3: Adapted fixed roughness.
  The downstream flow pattern was, more or less, half-way between the results of Method 1 and Method 2. The dispersion of the flow varies from a little stronger to much stronger than the dispersion according to Method 2. Downstream the abutments eddies are, however, practically absent.

The tests in the hydraulic scale model show a similarity with the prototype more or less equivalent to 'Method 2' of the numerical models. However, it should be pointed out here, that in the scale model no specific tests were carried out to investigate the reproduction of the 'Ametek'- measurements. Results were used from tests which had the best resemblance in geometry with the actual building stage. For some building stages the number of placed sill beams in the model differed slightly from the prototype.

8.2.4 Conclusions

Comparison of the results of the numerical models with the field data showed that, in general, the agreement between the model and the field data was good:

- Computed discharges agree well with field data
- The agreement between the computed flow pattern and the field data is very

good upstream of the barrier and at the site of the barrier
- Downstream of the barrier the agreement between the computations (method 2) and the field data was acceptable. The computed maximum velocities have an inaccuracy of 5 to 10% for construction stages without large discontinuities and 10 to 20% for construction stages with large discontinuities.
- The steepness of the velocity gradients downstream of the barrier were simulated rather well. However, the location where these gradients occured, had an inaccuracy of 50 to 100 m (channel width 1 to 2 km). For engineering applications, for example the calculation of scour holes, this difference was acceptable.

The depth-averaged flow pattern computed by the numerical models is as accurate as that obtained from the hydraulic scale model. The method to deal with the energy losses at the barrier site largely influences the quality of the results of the numerical models.

On the basis of these results it was decided to develop a new method for the introduction of energy loss at the barrier:
- Method 4: Dynamically adapted roughness
  This is a mixed version of Method 1 and 2 (or 3). At the barrier site the roughness coefficient is continuously adapted as given by Equation (8.2) so that the discharge and head loss satisfy Equation (8.1) for a given value of the discharge coefficient .

Thus a new Chézy value is continuously calculated during the computation and this makes it possible to use different coefficients for different flow directions and different flow conditions.

8.3 Coefficient of discharge

8.3.1 Model and field data and their accuracy

Theoretical aspects and the (scale and numerical) model investigations on the coefficient of discharge of the barrier (μ_3) at various construction stages have been described in Chapter 4.
In Section 4.2.3 the inaccuracy of reproduction of μ_3 in the scale models has been estimated at ± 7%. For determination of μ_3 from observations (of Q and Δh) in these models, measurement inaccuracies of these two quantities add to increase the inaccuracy of μ_3. At early stages of construction, Q is large and Δh is small, meaning a small inaccuracy of Q and a large inaccuracy of Δh. At final stages of the construction, the opposite is true. The

"average" measurement error of Q is estimated at ± 5% and that of Δh also at ± 5%. Assuming again that all errors are mutually independent, the inaccuracy range of μ_3 determined in the scale model, becomes ± 10%.

For the numerical models, μ_3 is an input value in the case of the one-dimensional model (IMPLIC). In the case of the two-dimensional models, the inaccuracy in the computed μ_3 is made up of two components: inaccuracy in the values of μ_2 as determined through the flume tests (estimated at ± 5%, see Section 4.2.2) and inaccuracies related to spatial schematization and resolution power of the model. The contribution of the latter component is difficult to estimate. One tends to estimate the combined inaccuracy lower than the corresponding scale model value. However, the (not yet clarified) need to reduce the values of μ_2 for the construction stage "sill completed" by 20% in the WAQAU models (see Section 4.2.4) urges caution. As long as a satisfactory explanation has not yet been found, it will be safer to take the inaccuracy range in the numerical models equal to that of the scale models, namely ± 10%.

In the course of the construction period (1984-1986), several major field campaigns were carried out. In these compaingns, extensive water level and current velocity (discharge) measurements were carried out, each campaign covering at least one (semi-diurnal) tidal period.
The measurements included the water level in the work harbours and discharge cross-sections adjacent to the barrier site, thus providing data to compute the discharge coefficient μ_3. The results of the measurement campaigns listed in Table 8.4 have been used to verify the μ_3-results of the various models as discussed further in Section 8.3.2.
These campaigns are the same (but not all of them) as those used in other verifications, see Table 8.1.
Discharge measurements in large tidal channels as those of the Eastern Scheldt have an inaccuracy range of about ± 10%. Taking errors of Δh-measurements into consideration, the inaccuracy of μ_3 determined in the field can thus be expected to range between ± 10% (at high Δh) and ± 15% or larger (at low Δh).

Date	Extensive discharge measurement in	Construction stage in relevant channel
27-09-84	Roompot	all piers placed
26-10-84	Schaar	sill completed
07-02-85	Roompot	mid-height of sill crest reached
20-06-85	Hammen	sill completed
20-06-85	Schaar	sill completed
26-06-85	Roompot	sill completed
23-07-85	Schaar	sill completed
26-07-85	Hammen	sill completed
09-09-85	Schaar	9 sill beams placed
14-09-85	Hammen	14 sill beams placed
16-09-85	Schaar	9 sill beams placed
26-09-85	Roompot	sill completed
27-09-85	Schaar	all sill beams placed
01-10-85	Hammen	all sill beams placed
21-11-85	Schaar	all sill beams placed
27-11-85	Roompot	9 sill beams placed
10-12-85	Hammen	all sill beams placed
12-04-86	Roompot	21 sill beams placed
26-04-86	Roompot	all sill beams placed
21-05-86	Hammen	all sill beams + rubble side-fill
26-05-86	Schaar	
21-09-86	Roompot	

Table 8.4 Summary of field campaigns used for μ_3-verification

8.3.2 Verification of the results of the models

From the data of the measurements listed in Table 8.4, the discharge coefficient of the structure μ_3 was computed for the relevant channel and construction stage. For this the average computed value in a period of two hours around maximum ebb flow and a period of two hours around maximum flood flow were taken as μ_3-ebb and μ_3-flood, respectively.
Inspection of the instantaneous values of μ_3 showed no systematic variation, either as a function of Q or as a function of the water level, during the said two hours.

The results have been plotted in the figures presented earlier in Chapter 4, giving model-computed or measured μ_3 als a function of $\bar{\mu}_2$ A (Figures 4.14 through 4.16). To facilitate comparison, model results are given a small points with a band enveloping all model results given in faint print, whereas the field results are given as large bold printed dots, see Figures 8.22 through 8.24.

In these above figures, the points representing construction stage "all sill beams + rubble side-fill" are excluded; they are presented in Table 8.5. The presence of the side-fills, meaning that the construction of the barrier is completed, causes μ_3 to increase significantly, particularly during ebb flow.

Source	Ebb flow			Flood flow		
	Roompot	Schaar	Hammen	Roompot	Schaar	Hammen
Detail scale model	1.00	0.98	1.02	1.00	1.02	0.99
Prototype*	1.05	1.01	1.01-1.04	0.99	0.97	0.96-0.99
* from lower part of Table 8.4						

Table 8.5 Discharge coefficients construction stage "all sill beams + rubble side-fill"

Inspection of Figures 8.22 through 8.24 and Table 8.5 shows that:

1. The band enveloping all scale and numerical model results has an average width equal to or less than ± 10% (see Section 8.3.1), in some cases with a smaller width at low $\bar{\mu}_2$ A values and a larger width at large $\bar{\mu}_2$ A values. Due to the very low magnitude of Δh at large $\bar{\mu}_2$ A values, the accuracy of μ_3 can, indeed, deteriorate significantly.
2. The differences between the results of the various models are not systematic and can be described as random or erratic.
3. Judging from the point of view of the relation μ_3 versus $\bar{\mu}_2$ A, the prototype results are significantly more erratic than those of the models. This is partly due to the larger determination inaccuracies in the field.
4. Taking points 2 and 3 above into consideration, Figures 8.22 through 8.23 indicate a reasonable agreement between prototype and the models. There seems to be a tendency of the models to overestimate μ_3-flood in de Roompot and Hammen channels.
5. The agreement between the detail scale model and prototype results for the completed storm-surge barrier (Table 8.5) is good.

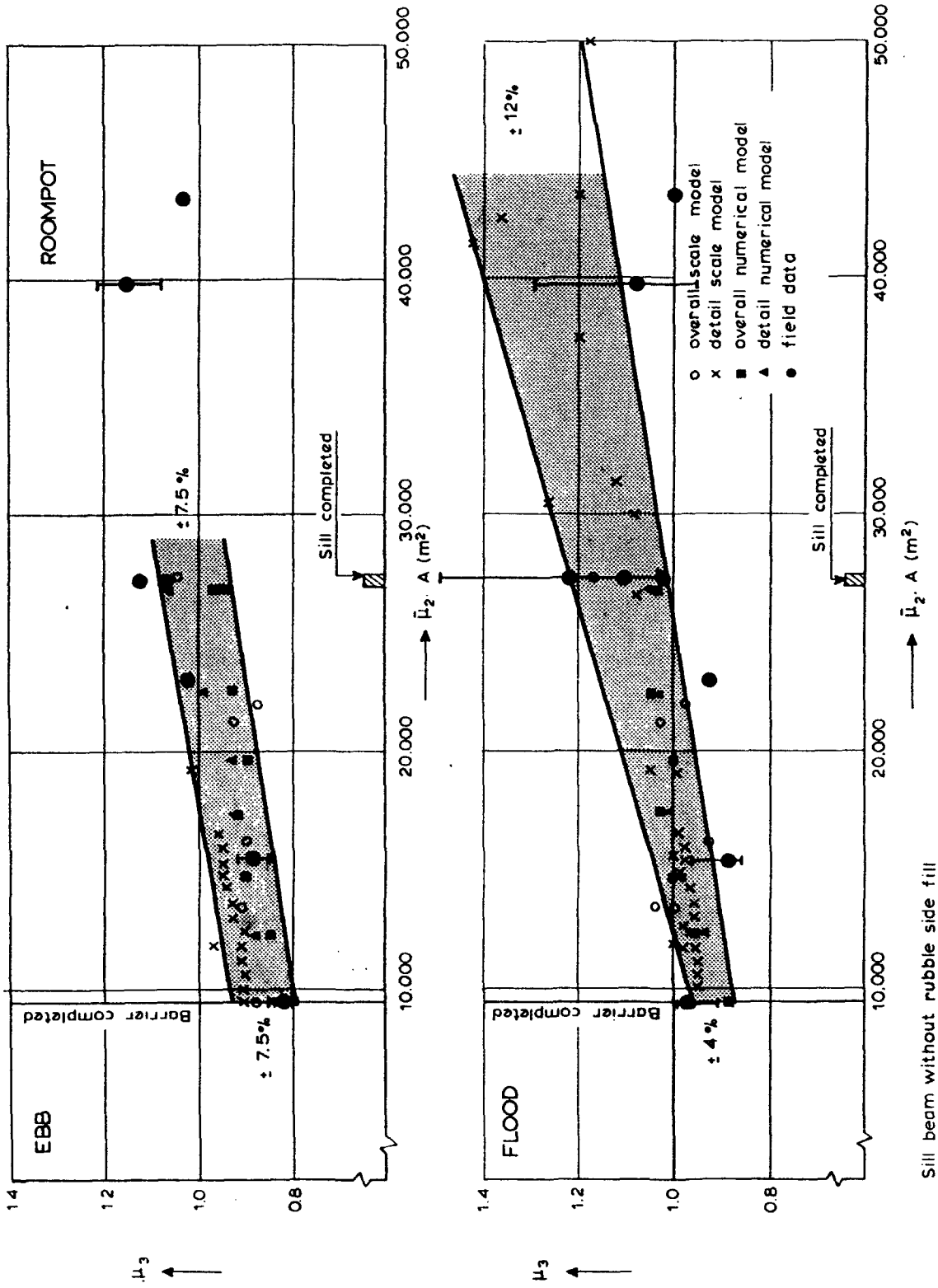

Figure 8.22 Verification of μ_3 results of the models, Roompot channel

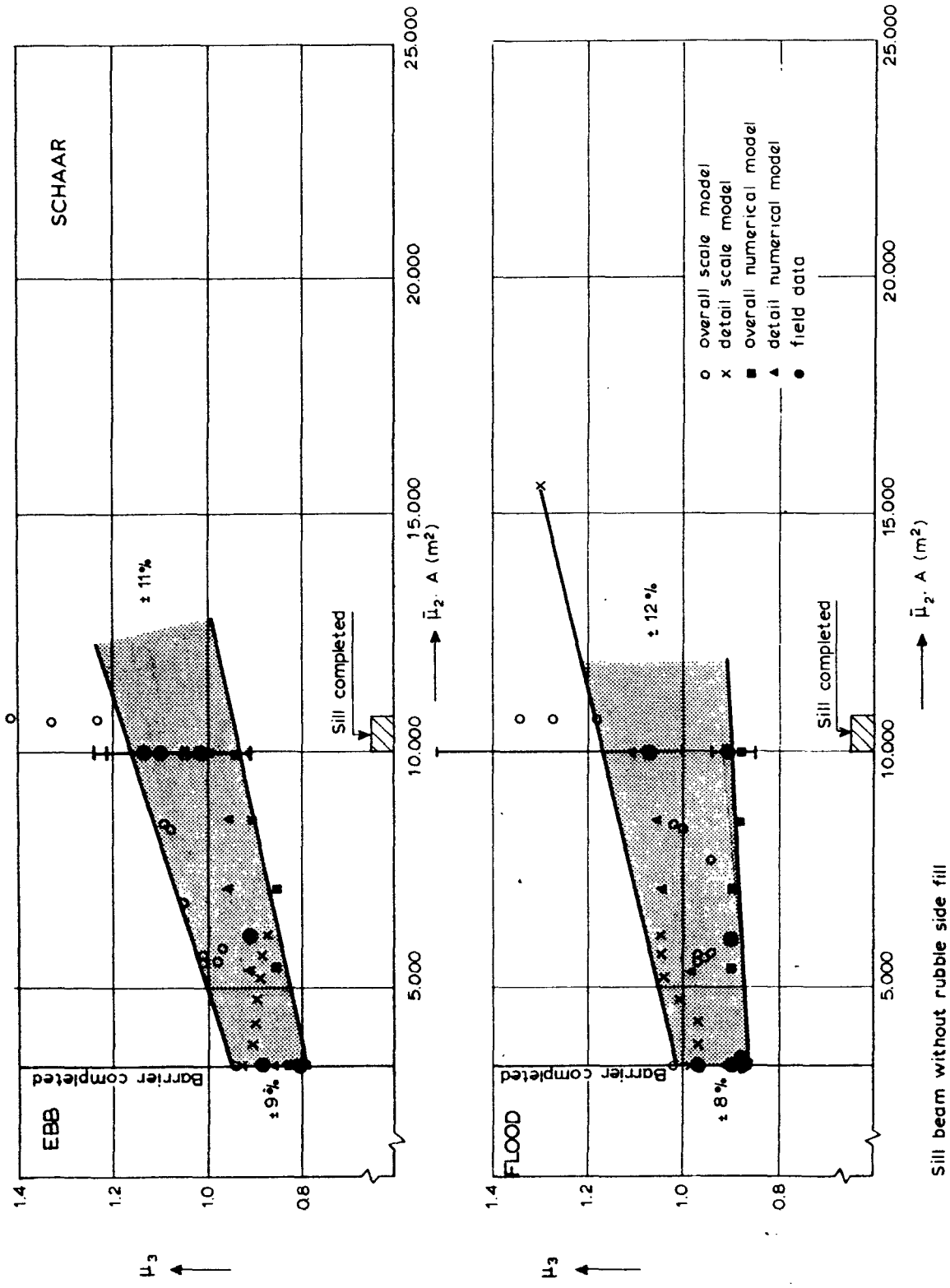

Figure 8.23 Verification of μ_3 results of the models, Schaar channel

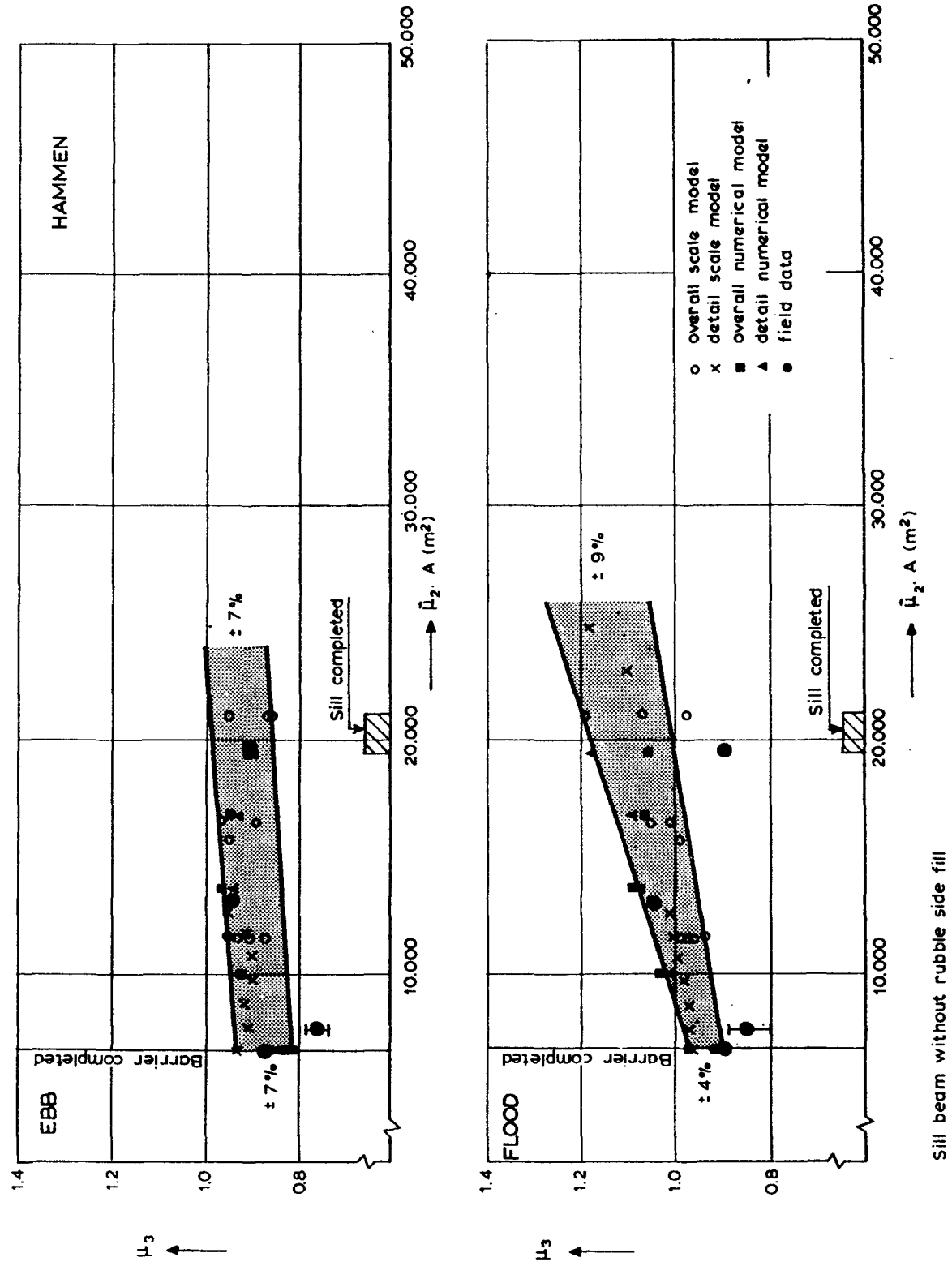

Figure 8.24 Verification of μ_3 results of the models, Hammen channel

References of Chapter 8

[8-1] Rijkswaterstaat
Flow information for the final construction stages of the storm surge barrier, BESTRO-M-84.338/SOOCOO-M-84.508, December 1984 (in Dutch)

[8-2] Rijkswaterstaat
Evaluation Installing of the sill beams, October 1986, 5PROBU-M-86006 (in Dutch).

[8-3] Rijkswaterstaat
Verification of head differences in the channels Hammen, Schaar and Roompot, March 1986, DDWTZ 86.257 (in Dutch).

[8-4] DELFT HYDRAULICS and Hartsuiker, G.,
Storm surge barrier Eastern Scheldt, Two-dimensional models of the mouth of the Eastern Scheldt, Reproduction of flow pattern during installation of sill beams (Ametek-measurement) R2093-02, November 1986 (in Dutch)

[8-5] DELFT HYDRAULICS and Hartsuiker, G.,
Storm surge barrier Eastern Scheldt, Two-dimensional models of the Eastern Scheldt, Reproduction of flow pattern final situation (Ametek-measurements), R2093-20, October 1988 (in Dutch)

9. Summary and Conclusions

9.1 Hydraulic boundary conditions

Because of the type of structure of the storm-surge barrier in the Eastern Scheldt as well as its construction method, the hydraulic boundary conditions were of major importance for both the design of the barrier and the construction phase.
Forecasts of the hydraulic conditions were used:

- as design parameters
- for planning of the construction activities
- for operational control of the construction activities

An accurate forecast system was needed, that had to function during the entire construction period, which was over four years long. Further, the system had to be highly flexible because of the numerous changes in the planned construction order of the barrier.

A restricted number of hydraulic parameters were forecasted, the selected parameters were:

Q = discharge through a main channel
q/A = average velocity per pier section
Δh = head difference over the barrier

These parameters can be regarded as the "governing parameters" for the hydraulic problems to be solved, such as stability of rubble stone layers, local scour, etc. The forecast system was dedicated to these governing parameters. The right choice of the basic parameters was the key to succes of the forecast system.

9.2 Modelling tidal flow

Following simulation techniques were used for modelling the tidal flow in the Eastern Scheldt estuary:

- hydraulic scale models
- numerical models

The hydraulic scale models use the same laws of physics for the simulation of the water motion which govern the water motion in nature. The scaled phenomena are correctly reproduced by the model if the relevant scale laws are adhered to.

The numerical models simulate the water motion by the numerical solution of the equations which describe the water motion (Navier-Stokes).
Three types of numerical models, can be distinguished i.e. one-, two- or three-dimensional models. Integration of the basic equations in vertical and horizontal direction, yields the two- and one-dimensional long-wave equations respectively.

In the studies for the storm-surge barrier three simulation techniques were applied, following the historical development:
- hydraulic scale models
- one-dimensional numerical models
- two-dimensional numerical models.

At the start of the hydraulic research (1969) only scale models were used. Available were: an overall tidal model, a steady-state detail model and several detail models of sections of the barrier.

During the research period more and more numerical models were being used. Both one-dimensional and two-dimensional models were developed.

Two-dimensional depth-averaged numerical models gradualy replaced the scale models for 2-DH applications. The overall tidal model was replaced entirely. The detail model was partially replaced by two-dimensional numerical models; but particularly for three-dimensional aspects, the scale model was still indispensible.

The one-dimensional numerical models were mostly used additional to the scale models, and not as a replacement of the scale models. Extensive operational forecasts were only possible with the one-dimensional models. The scale models and two-dimensional numerical models served as a check and for the calibration of the one-dimensional models.

9.3 **Simulation of storm-surge barrier**

The resistance to flow caused by the storm-surge barrier can modify the tidal motion in the entire estuary. Therefore it was essential that the hydraulic characteristics of the barrier were correctly simulated in the models.
The hydraulic characteristics of a structure can be expressed by the coefficient of discharge describing the emperical relationship between the discharge through the structure and the head difference across it.

When considering the coefficient of discharge of a structure as the storm-surge barrier, one has to distinguish between:

- μ_2 : the coefficient of a uniform, infinitely wide (Section of the) structure;
- μ_3 : the coefficient of the entire structure in its surroundings and depending on the definitions used of Δh and downstream water level.

In principle:

$$\mu_3 \neq \bar{\mu}_2$$

where:

$$\bar{\mu}_2 = [\sum_{i=1}^{n} \mu_{2,i} \cdot A_i]/A$$

$\bar{\mu}_2$ can be computed for an arbitrary construction stage from known (flume tests) data on μ_2 for the various sections of that structure.
μ_3 can only be predicted through a model; the Eastern Scheldt studies showed that both a scale model and a two-dimensional numerical (detail) model can be used for that purpose. In the numerical model, μ_2 values have to be used to describe the resistance at the various grids of the structure.

9.4 Applied tidal models

9.4.1 Hydraulic scale models

Two hydraulic scale models of the Eastern Scheldt were available:

- a distorted overall tidal model of the entire estuary, vertical scale 1:100 and horizontal scale 1:400
- a steady-state detail model of the mouth of the estuary with the three main channels, undistorted scale 1:80.

From the investigations in the overall tidal model information was obtained on the tidal movement (water levels and discharges), mutual influence of closure gaps and flow patterns.
Investigations in the detail model gave detailed results on flow pattern, current-velocities and -directions in the vicinity of the barrier and the effective cross-sectional area of the barrier. In addition, the detail model was used to investigate local scour and stability of materials.

The overall model was in operation until 1983. From that time on it was replaced by numerical models. The detail model could not be completely replaced by numerical models.

Before the actual investigations started, an extensive calibration for the initial situation was carried out. Later, several verifications were made for different tides and different situations (related to bathymetry and constructed dam sections). As a result of the calibration and the verifications, the following accuracy of the model could be achieved:

- water levels: amplitude ±2% and phase ±5 minutes
- discharge: amplitude ±5% and phase ±10 minutes
- velocity distribution ±0.15 m/s

9.4.2 One-dimensional numerical models

A one-dimensional model of the Eastern Scheldt, based on the IMPLIC-system, was available. The main function of the model was to compute the water levels in the Eastern Scheldt, the head differences over the barrier and the discharges through the three main channels. Because of its short running time, this model was suitable for operational forecasts. The hydraulic characteristics of the storm-surge barrier were derived from the scale models.

For the computation of the lateral distribution of the discharge along the barrier, a quasi two-dimensional model was available. The discharge through a main channel and the water level on both sides of the barrier were derived from the results of the one-dimensional tidal model. The quasi two-dimensional model was calibrated with the results of the scale model tests.

From an accuracy analysis the following inaccuracy ranges were estimated for the prediction of design values of the hydraulic parameters:

- Q : discharge per main channel, standard deviation of the errors is 10%.
- q/A: average velocity per barrier section, standard deviation of the errors is 15% (overall error, including errors in predicted discharge, Q).

9.4.3 Two-dimensional numerical models

For the Eastern Scheldt a series of off-line nested two-dimensional numerical models was available. The models were based on the WAQUA-system for the depth-averaged simulation of hydrodynamics and water quality for well-mixed flow. The grid size of the models ranged from 400 m for the overall model of the en-

tire estuary, to 45 m for the most detailed models of the three main channels. Moreover, models with intermediate grid sizes of 100 m and 90 m were in operation.

The computations with these models provided information on tidal movements, mutual influence of building stages, flow pattern, current-velocities in the vicinity of the barrier. Naturally, the amount of detail of the computed flow pattern is dependent on the applied grid size.
This means that the coarse-grid model was mainly used to provide the information on the overall tidal movement, whereas the most detailed model gave the information on the velocities in the vicinity of the barrier.

In 1983 after an extensive testing period, it was decided to use these models instead of the overall tidal scale model.
As a result of the calibration of the models and several verifications the following accuracy of the results related to the reproduction of the overall tidal flow was achieved:
- water levels: amplitude ±2% and phase ±5 minutes
- discharges: amplitude ±5% and phase ±10 minutes

The numerous computations for arbitrary building stages of the storm-surge barrier showed that the schematization of the barrier (with concentrated head-losses) in the computational scheme was very important. The way of schematization does influence the tidal movement and the discharge- and velocity-distrubutions in the vicinity of the barrier.

9.5 Comparison with field data

9.5.1 Verification of the one-dimensional numerical models

Systematic measurement campaigns were carried out for the verification of:
- Individual models of the forecast system:
  Here the accuracy of the models was determined by a hindcast of the measurements.
- Prediction of the design values of the hydraulic parameters:
  For this the measurements had first to be translated to design conditions before they could be compared with the predictions.

For the transport rate through the main channels, Q, and the average velocity per pier section, q/A, a systematic verification was performed throughout all construction stages of the barrier. The general conclusions from this verification were:

- The hindcast accuracy of Q was hardly influenced by construction progress of the storm-surge barrier. The maximum error in the initial calibration was 10%; this resulted in a standard deviation of about 5%.
- The error in the predicted design values of q/A turned out to be less than the inaccuracy range of 15%, assessed beforehand.

An overall verification of the forecasts of the head-difference over the barrier, Δh, was not performed directly. From the results of the verification of the discharges and the coefficient of discharge, the hindcast-error in Δh was estimated to be between 10% and 20% (standard deviation).

9.5.2 Reproduction of downstream flow pattern

The downstream flow pattern is an essential parameter for the prediction of local scour downstream of the bed-protection works. The prediction of scour was in first instance made through scour tests in the detail scale model. During the study period it was concluded that scour could be calculated if a reliable prediction of the velocity distribution at the end part of the bed protection was available.

For a number of building stages related to the placing of the sill beams, a reproduction of the downstream-velocity distribution was executed in the two-dimensional numerical models. With these building stages the following characteristic events in the flow pattern were present:

- large eddies behind the abutments of the dam
- steep velocity gradients downstream of discontinuities at the axis of the barrier.

In the two-dimensional numerical models the energy loss at the barrier site was schematized in three different ways:

1. substitution of long-wave equation by a barrier equation
2. adjustment of local water depth and roughness
3. adjustment of roughness only

From the results of the reproduction the next conclusions were derived:

- The agreement between the computation (Method 2) and the field data was acceptable; the inaccuracy in the computed velocities for construction stages without and with large discontinuities was ±5 to ±10% and ±10 to ±20% respectively;
- The steepness of the velocity gradients was nearly correct, only the location of the gradients could shift to some extent;
- The flow pattern computed by the numerical models was as accurate as that obtained from the physical scale model. However, the method to deal with the energy losses greatly influenced the quality of the results form the numerical models.

9.5.3 Coefficient of discharge

The inspection of the values of μ_3 as function of $\bar{u}_2$ A, determined from the various models and in the field, shows that:

- The band enveloping all model results, had an average width ≤ ±10%, which was the predicted inaccuracy range for determining μ_3 in these models. At large $\bar{u}_2$ A values, the accuracy of μ_3 could deteriorate significantly.
- The differences between the results of the various models are not systematic and can be described as random or erratic.
- Judging from the point of view of the relation μ_3 versus $\bar{u}_2$ A, the prototype results were significantly more erratic than those of the models. This is partly due to the larger determination inaccuracies in the field.
- The agreement between prototype and the models was reasonable. There seemed to be a tendency of the models to overestimate μ_3-flood in the Roompot and Hammen channels.
- The agreement between the detail scale model and prototype results is good for the completed storm-surge barrier.

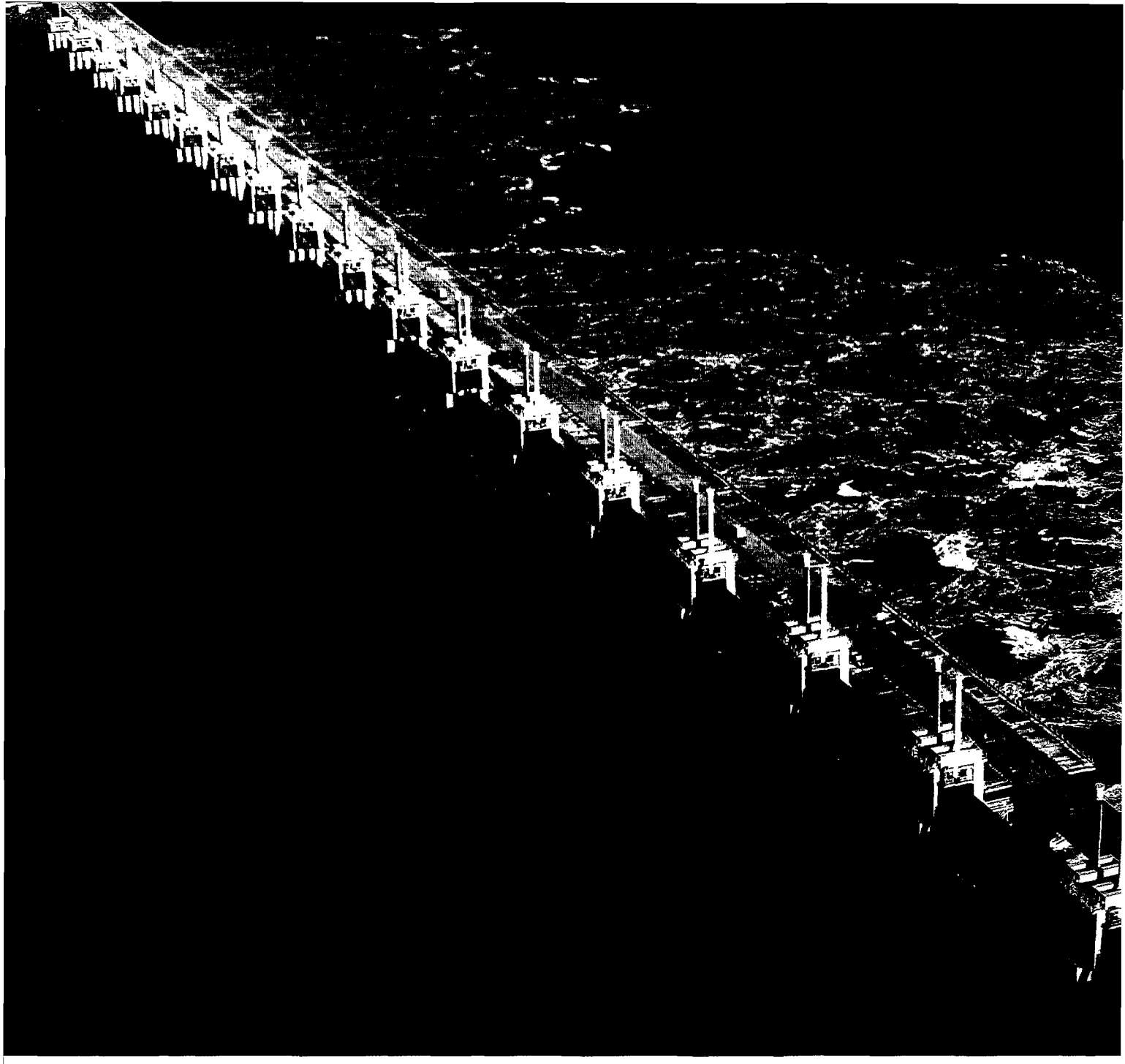

DELFT HYDRAULICS
p.o. box 152
8300 AD Emmeloord
The Netherlands

Rijkswaterstaat
p.o. box 5014
4330 KA Middelburg
The Netherlands